

School of Earth and Planetary Sciences

Sedimentology of Passive Margin Sequences in the Northern Carnarvon  
Basin and Implications for Variations in Seismic Velocity

Mulky Winata

ORCID iD: 0000-0002-5124-1037



This thesis is presented for international collaborative doctoral research degrees  
between Curtin University and University of Aberdeen

May 2024

## Declaration

---

To the best of my knowledge and belief this thesis contains no material previously published by any other person except where due acknowledgement has been made.

This thesis contains no material which has been accepted for the award of any other degree or diploma in any university.

Mulky Winata

A handwritten signature in black ink, appearing to read 'Mulky Winata', with a stylized flourish at the end.

Perth, 30 November 2023

## Abstract

---

*The Northern Carnarvon Basin, part of the Northwest Shelf of Australia, contains a post-rift passive margin succession, which has generally been considered as a simple and homogenous deposit, recording a transition from siliciclastic to carbonate sedimentation. Seismic data shows that this view is an oversimplification of a much more complex depositional history. To gain a better understanding of the depositional processes that have operated in this area, as well as the spatial and temporal variation in sedimentary environments, an interpretation was carried out that integrates 2D and 3D seismic data with information from exploration wells across the basin. This study shows that sedimentary sequences above the Valanginian breakup unconformity (~138 Ma) exhibit a wide array of seismic facies, each associated with different marine depositional settings. The most significant lateral variations occur during the Turonian (~95 Ma) to Rupelian (~30 Ma) and during the Tortonian (~7 Ma) to Present. In the former interval, three dominant seismic facies are identified, including polygonally faulted, incised, and parallel bedded. These suggest a transition from a system dominated by fine-grained hemipelagic deposition to one shaped by energetic bottom currents, resulting in both depositional and erosional features. The bottom currents primarily affected the central region of the Exmouth Plateau. A merged 3D seismic dataset was created to highlight the evolution of bottom current deposits. The Turonian to Rupelian sequence contains sediment mounds, moats, complex moat fills in the southeast of the study area, and intricate stacked deep incisions, as well as conical depressions in the northeast. In the Tortonian to Present sequence, sigmoidal and laterally continuous reflections transition into more chaotic reflection patterns and are interpreted as clinoforms and mass-transport complexes (MTCs). Understanding these lateral facies variation is instrumental in accurately predicting the seismic velocity model for these subsurface formations. Furthermore, this research sheds light on the breakup of Gondwana and the early stages of oceanic basin formation. The initial deposition corresponds to a time when a vast, open ocean existed to the north. The growth of sediment mounds coincided with the accelerated separation of Greater India and Australia, potentially altering westward-flowing ocean currents. The cessation of bottom current activity corresponds to the swift separation of Australia from Antarctica, likely leading to changes in circulation patterns. The presence of MTCs may signify increased seismic activity and slope instability, likely resulting from the development of collisional plate boundaries.*

## Acknowledgements

---

This doctoral research was an immensely exciting journey, enriched with invaluable experiences and made possible through the unwavering support of numerous excellent individuals and esteemed institutions. I consider myself fortunate to have crossed paths with them, as without their backing, this research endeavour would have remained a dream.

First and foremost, I wish to express my heartfelt gratitude to my supervisor, Professor Chris Elders, for not only accepting my application for PhD research but also affording me the incredible opportunity to embark on this project. His unwavering support, profound academic insights, and wealth of experience have been instrumental in shaping the trajectory of my work. Professor Elders' guidance has been a beacon, ensuring that I remained on the right path throughout this academic journey. Additionally, I would like to extend my appreciation to him for providing technical and non-technical support especially for facilitating online meetings and discussions during the challenging period of COVID-19 restrictions.

Secondly, I extend my sincere gratitude to my co-supervisor, Professor Randell Stephenson, for graciously offering his invaluable supervision to this project. His extensive academic experience and diverse perspectives have provided me with a wealth of advice and insights that have greatly enriched my work. Professor Stephenson's guidance has been instrumental in ensuring that I maintained the right course throughout my research journey. Furthermore, I would like to acknowledge the non-technical support he provided during my research tenure at the University of Aberdeen in Scotland, particularly during the challenging period of COVID-19 restrictions. His unwavering support outside the academic realm has been truly appreciated. I would also like to express my appreciation to my other co-supervisor Associate Professor Vittorio Maselli from Dalhousie University in Canada for his valuable contributions to my research. His insightful discussions and constructive comments have played a significant role in shaping my work, particularly in drawing attention to the intricacies of deep-water sedimentary processes. His scientific guidance and advice have been a true inspiration, influencing the direction and methods of my research.

Thirdly, I would like to extend my sincere gratitude to Geoscience Australia for generously providing the invaluable dataset, including seismic and well data, which formed the bedrock of this research. Accessible through the Western Australian Petroleum and



Geothermal Information Management System (WAPIMS) and National Offshore Petroleum Information Management System (NOPIMS) websites, these data sources were instrumental in this study. Moreover, my appreciation extends to Schlumberger, CEGAL, and ELIIS for their software tools, including Petrel, Blueback Toolbox, and Paleoscan, respectively. These software packages were instrumental in facilitating the interpretation of seismic facies and geomorphology, enabling the creation of detailed maps and comprehensive analyses that underpin the findings of this research.

Fourthly, I wish to extend my gratitude to the Aberdeen – Curtin Alliance 2018 for facilitating this exceptional international collaborative doctoral research, bringing together two distinguished universities, Curtin University and the University of Aberdeen. This opportunity was instrumental in making my PhD research possible and fostering a unique academic exchange. Through this experience, I had the privilege of expanding my professional network and forming lasting friendships with fellow researchers. The Alliance not only supported my academic journey but also enriched my personal and professional life.

Lastly, I want to express my deep appreciation to my beloved family and friends in both Perth, Australia, and Jakarta, Indonesia, for providing me with precious moments of relaxation, unwavering support, and understanding throughout my PhD journey. Their presence in my life during this time in Perth has added great value and will forever remain a remarkable chapter in my life.

## Primary Publications

---

This thesis consists of three manuscripts that are either published, submitted for publication or are ready to be submitted for publication. The publications contained in chapters 2 to 4 are listed below.

### **Chapter 2**

Winata, M., Elders, C., Maselli, V., Stephenson, R. A., 2023. Regional seismic stratigraphic framework and depositional history of the post-Valanginian passive margin sequences in the Northern Carnarvon Basin, North West Shelf of Australia, *Marine and Petroleum Geology*, Volume 156, 106418, ISSN 0264-8172, <https://doi.org/10.1016/j.marpetgeo.2023.106418>, impact factor 4.2.

### **Chapter 3**

Winata, M., Elders, C., Maselli, V., Stephenson, R. A., Cretaceous – Paleogene Evolution of Bottom Currents in the Northern Carnarvon Basin, Northwest Shelf of Australia, submitted in Nov 2023, *Marine and Petroleum Geology*, impact factor 4.2.

### **Chapter 4**

Winata, M., Elders, C., Maselli, V., Stephenson, R. A., Velocity Variations Associated with Seismic Facies and Seismic Stratigraphic in the post – Valanginian Passive Margin Sequences of the Northern Carnarvon Basin, Northwest Shelf of Australia, ready for submission to *Petroleum Geoscience* in Dec 2023, impact factor 2.3.

## Secondary Publications

---

The following abstracts were submitted based on the results of this PhD project.

### ***Conference abstracts***

Winata, M., Elders, C., Maselli, V., Stephenson, R. A., Anomalous Cretaceous shelf sediments in the Northern Carnarvon Basin. Basins Workshop 2020, Perth and online, December 2020, oral presentation.

Winata, M., Elders, C., Maselli, V., Stephenson, R. A., The Cretaceous-Paleogene evolution of bottom current activity in the Northern Carnarvon Basin, Northwest Shelf of Australia. AAPG European Region – Mixed / Hybrid Systems (Turbidite, MTDs and Contourites) on Continental Margins, Lisbon - Portugal, June 2023, oral presentation (Elders, C.).

Winata, M., Elders, C., Maselli, V., Stephenson, R. A., Contourites looking for a contour. Basins Workshop 2023, Perth, December 2023, oral presentation.

# Table of Contents

---

Research Title .....	i
Declaration .....	ii
Abstract .....	iii
Acknowledgements .....	iv
Primary publications .....	vi
Secondary publications .....	vii
Table of Contents .....	viii
List of Figures .....	xiii
List of Tables.....	xxi
<b>Chapter One: Introduction and Overview .....</b>	<b>1</b>
1. Introduction .....	1
2. Geological background.....	2
2.1. Regional tectonic and structural framework.....	2
2.1.1. The inboard rift sub-basins.....	2
2.1.2. The outboard Exmouth Plateau .....	3
2.2. Regional basin evolution and stratigraphy .....	3
2.2.1. Triassic Post-Permian rift or Pre-Mesozoic rift.....	3
2.2.2. Jurassic and Earliest Cretaceous syn-rift .....	4
2.2.3. Cretaceous – Cenozoic passive margin .....	5
2.2.4. Bottom current in the Northern Carnarvon Basin.....	8
2.2.5. Slumps and mass transport complexes .....	9
2.3. A brief history of bottom currents.....	9
3. Aims and objectives .....	11
4. Data and methodology.....	13
References.....	13

**Chapter Two: Regional Seismic Stratigraphic Framework and Depositional History of the Post-Valanginian Passive Margin Sequences in the Northern Carnarvon Basin, Northwest Shelf of Australia..... 30**

Research highlights.....	30
Abstract .....	30
1. Introduction .....	31
2. Tectono-stratigraphic setting.....	32
3. Data and methodology.....	35
4. Regional seismic stratigraphic framework .....	36
4.1. Unit 1 – Horizons K1-K3 (~123.3 Ma Aptian – ~95 Ma Turonian) .....	37
4.2. Unit 2 – Horizons K3-T4 (~95 Ma Turonian – ~30 Ma Rupelian) .....	38
4.3. Unit 3 – Horizons T4-T6 (~30 Ma Rupelian – ~7Ma Tortonian).....	40
4.4. Unit 4 – Horizons T6-T10 (~7Ma Tortonian – 0 Ma Present).....	41
5. Evolution of the Post-Valanginian Sequence in the NCB.....	42
5.1. Valanginian to Turonian: Post Breakup Subsidence .....	42
5.2. Turonian to Early Oligocene: Bottom Current Activity .....	43
5.3. Late Oligocene to Late Miocene: Carbonate Shelf .....	45
5.4. Late Miocene to Present: Mass Transport Complexes .....	45
6. Summary and conclusions.....	46
Conflicts of Interest .....	47
Acknowledgements .....	48
References.....	48

**Chapter Three: Cretaceous – Paleogene Evolution of Bottom Currents in the Northern Carnarvon Basin, Northwest Shelf of Australia..... 79**

Research highlights.....	79
Abstract .....	79
1. Introduction .....	80
2. Regional setting.....	81

2.1. Geological background .....	81
2.2. Oceanographic circulation.....	82
3. Data and methodology.....	84
3.1. Dataset .....	84
3.2. Methodology .....	85
4. Major morphosedimentary features.....	86
4.1. Seismic stratigraphic framework .....	86
4.2. Unit 1: Early Aptian (~123 Ma, horizon K1) – Cenomanian (~94 Ma, horizon K3) .....	87
4.3. Units 2a and b: Turonian (~94 Ma, horizon K3) – Maastrichtian (~66 Ma, horizon K5) .....	88
4.4. Units 2c and d: Danian (~66 Ma, horizon K5) – Lutetian (~45 Ma, horizon T2)	89
4.5. Units 2e and f: Lutetian (~45 Ma, horizon T2) – Rupelian (~30 Ma, horizon T4) .....	89
5. Bottom current evolution .....	90
5.1. Initiation and development of large-scale bathymetric relief .....	90
5.2. Large scale mounds and moats .....	90
5.3. Moat filling processes.....	91
5.4. Basin floor infill.....	92
5.5. Conical depressions.....	93
6. Discussion.....	94
6.1. Bathymetric setting .....	94
6.2. Plate separation and thermohaline circulation .....	95
7. Summary and conclusions.....	96
Conflicts of Interest .....	97
Acknowledgements .....	97
References.....	98

**Chapter Four: Velocity Variations Associated with Seismic Facies and Seismic Stratigraphic in the post-Valanginian Passive Margin Sequences of the Northern Carnarvon Basin, Northwest Shelf of Australia..... 125**

Research highlights.....	125
Abstract .....	125
1. Introduction .....	126
2. Geological background.....	127
3. Data and methodology.....	127
3.1. Dataset .....	127
3.2. Methodology .....	128
4. Seismic facies and stratigraphic framework.....	129
5. Velocity distribution .....	131
6. Discussion.....	133
6.1. Velocity trend in correlation to compaction, lithology, and sedimentary structures .....	133
6.2. Implications for velocity prediction and well planning.....	135
7. Summary and conclusions.....	135
Conflicts of Interest .....	136
Acknowledgements .....	135
References.....	137

**Chapter Five: Summary, Discussion, and Implications ..... 154**

1. Summary .....	154
1.1. Early post-rift sequence (Valanginian – Aptian) .....	154
1.2. Unit 1 (Aptian – Turonian).....	154
1.3. Unit 2 (Turonian – Rupelian) .....	155
1.4. Unit 3 (Rupelian – Tortonian) .....	155
1.5. Unit 4 (Tortonian – Present).....	156
1.6. Seismic velocity in complex structures.....	156
2. Discussion.....	157
2.1. Lithostratigraphic versus seismic stratigraphic correlations .....	157
2.2. The onset of bottom current activity .....	158
2.3. Bathymetric setting of bottom current deposits.....	159

2.4. Oceanic circulation around Australia between the Valanginian and Present Day	163
2.5. Bottom current deposits in clastic versus carbonate	165
3. Conclusion	165
4. Future work	166
References	167



## List of Figures

---

### **Chapter One**

- Fig. 1. a) The basin outline and location. b) Seismic and well datasets that were utilised in this research* ..... 26
- Fig. 2. Simplified stratigraphic diagram of the NCB*..... 27
- Fig. 3. Regional seismic profiles from the Exmouth Plateau showing pre- and passive margin sequences* ..... 28
- Fig. 4. The evolution of conceptual models for bottom current depositional systems* . 29

### **Chapter Two**

- Fig. 1. a-c) Location map illustrating the geological provinces and structural elements of the NCB, including the location of 2D & 3D seismic and wells data* ..... 60
- Fig. 2. a-b) Generalised tectono-stratigraphic chart for the NCB* ..... 61
- Fig. 3. Stratigraphic ages for the key seismic markers assembled from the Cygnus-1, Guilford-1, Yellowglen-1 and Orthrus-1 wells* ..... 62
- Fig. 4. Seismic stratigraphic interpretation of the NCB showing sixteen seismic horizons that correspond to the tops of sixteen formations* ..... 63
- Fig. 5. A summary chronostratigraphic chart of the post-Valanginian sequences based on regional seismic sections* ..... 64
- Fig. 6. Well cross-section showing the four main seismic stratigraphic units from west to east in the middle of the Exmouth Plateau* ..... 65

*Fig. 7. a) Thickness map of the Early Post-rift sequence that was created from horizons K0 and K1. b) Seismic facies map showing that Early Post-rift is mostly characterised by polygonal faulting and parallel to subparallel facies ..... 66*

*Fig. 8. a) Thickness map of Unit 1 that was created from horizons K3 and K1. b) Seismic facies map showing that Unit 1 is mostly characterised by parallel and subparallel facies ..... 67*

*Fig. 9. Detail of regional seismic lines C and I displaying prominent unconformities and corresponding to horizons K1, K2 and K3 can be seen within the depocentre ..... 68*

*Fig. 10. a) Thickness map of Unit 2 that was made from horizons T4 and K3. b), c), d) Seismic facies maps of Units 2a-2b, Units 2c-2d and Units 2e-2f, showing the dominant seismic facies e.g., polygonal faulting, stacked incisions, and parallel and subparallel ..... 69*

*Fig. 11. Depth structure maps of horizons K3 and T4 showing the erosional features associated with bottom current activity ..... 70*

*Fig. 12. Detail of regional seismic sections C and D showing polygonal faults, and disrupting horizons K4, K5, T1, T2, T3 and T4 from Unit 2 ..... 71*

*Fig. 13. Detail of regional seismic sections C and J showing erosive boundaries corresponding to Horizons K4, K5, T1, T2, T3 and T4 ..... 72*

*Fig. 14. Detail of regional seismic sections A and B showing major downlap surfaces, and corresponding to horizons T2, T3 and T4 in the northeast of the study area ..... 73*

*Fig. 15. a) Sediment drifts, sediment mounds and contourite channels on regional seismic section E. b) Highly eroded beds and simple to complex scours on regional seismic section J ..... 74*

*Fig. 16. a) Thickness map of Unit 3 with sediment depocentre D that was derived from horizons T6 and T5. b) Seismic facies maps of Unit 3, which contains sub-units 3a and 3b showing the distribution of several seismic facies ..... 75*

*Fig. 17. a) Thickness map of Unit 4 with sediment depocentre E that was generated from horizon T10 and the merger of horizons T6 of Unit 3 and T4 of Unit 2. b-d) Seismic facies map of sub-units 4a-c and 4d, showing widespread occurrence of chaotic seismic facies and parallel and subparallel beds ..... 76*

*Fig. 18. a, b). Regional seismic section A illustrating the seismic facies present in Units 3 and 4 and are dominated by progradational patterns ..... 77*

*Fig. 19. a, b). Regional seismic sections A and B highlighting the presence of slumps and MTCs in Unit 4 on the NW side of the Rankin Platform ..... 78*

### **Chapter Three**

*Fig. 1. Location map showing basin outline of the NCB, regional present-day bathymetry, and the location of 2D/3D seismic and wells data ..... 107*

*Fig. 2. Present day ocean current pathways modified from Wijeratne et al. (2018) and Australian Government - DCCEEW (2007) ..... 108*

*Fig. 3. Generalised stratigraphic chart for the NCB showing correlation to seismic-stratigraphy and ties to wells (Satyr-1, Archilles-1, Guildford-1, GR: Gamma-ray) ..... 109*

*Fig. 4. A composite regional seismic cross-section illustrating the Triassic – Recent sequences in the Exmouth Plateau ..... 110*

*Fig. 5. a, b) Two seismic profiles illustrating the characteristics of Aptian – Lutetian sequences in the study area ..... 111*

*Fig. 6. a-f). Time structure maps showing the evolution of the Valanginian – Maastrichtian surfaces between horizons K0 and K5..... 112*

*Fig. 7. a-f). Maps showing the time thickness of sediments during the post-rift phase from the Valanginian (horizon K0) to the Rupelian (horizon T4) ..... 113*

*Fig. 8. a-d). Time structure maps showing the evolution of Thanetian – Tortonian (horizons T1-T6) ..... 114*

*Fig. 9. a-d) Interpreted seismic profile showing the development of moats as well as aggradational sediment mounds developed during Aptian – Rupelian in the southwest ..... 115*

*Fig. 10. a, b) RMS stratal slices illustrating the establishment of polygonal faults and parallel gullies on the crest of the westerly sediment mound between horizons K3 and K5 in the Turonian – Maastrichtian..... 116*

*Fig. 11. a) RMS stratal slices showing the hook-shaped and irregular incisions developed between horizons K4b and K5. b) Time structure map of horizon K4a showing the location of southerly moat, which infilled with small-scale mounds and segmented incisions. c) Three seismic profiles showing the nature of the infill from horizons K3 to K5..... 117*

*Fig. 12. a, b) Time structure map of horizon K5 illustrating widespread polygonal faults, large parallel incisions and deep incisions. c) Two seismic profiles showing the variation in sediment thickness and sedimentary structures between horizons K3 and K5 ..... 118*

*Fig. 13. a) RMS map of horizon T1a showing curved gullies in the infill of the westerly moat. b) Time structure map of horizon T1a showing the location of the curved gullies. c) Two interpreted seismic profiles illustrating the variation in sedimentary structures between horizons T1a and T1b ..... 119*

*Fig. 14. a, b) Time structure map of horizon T1b illustrating parallel gullies in the infill of the westerly moat. c) Seismic profile showing the contrast between curved gullies below the flattened horizon and parallel gullies above it as shown by Fig. 14d ..... 120*

*Fig. 15. a) Time structure map of horizon T1 showing the location of complex sedimentary features developed on the slope at the edge of the basin floor. b, c, d) RMS maps above horizon T1 illustrating the complex interrelationship between sediment waves, parallel gullies and deep incisions. e) Two seismic profiles illustrating these sedimentary features developed at horizons T1, T3 and T4 in the northeast of the area ..... 121*

*Fig. 16. a, b) Time structure maps of horizons T3 and T4 showing conical depressions indicative of large pockmarks or deepwater carbonate dissolution. c) Seismic section showing channels infilled by young MTCs..... 122*

*Fig. 17. a-h) Reconstruction of bottom currents activity from the Aptian to Rupelian inferred from the development of sediment mounds, moats, complex incisions in the southwest and northeastern areas ..... 123*

*Fig. 18. a-d) Plate reconstruction compiled from Müller et al., 2019 and potential ocean circulation pathways with location of bottom current deposits and inferred local currents. .... 124*

**Chapter Four**

*Fig. 1. Map showing the basin outline of the NCB and the main structural elements within it, regional present-day bathymetry, the location of the 3D seismic datasets used in this study and the location of a WNW–ESE regional seismic line..... 140*

*Fig. 2. Generalised stratigraphic chart for the NCB correlated to the seismic stratigraphic scheme and to formation tops in three wells (Satyr-1, Archilles-1, Guildford-1, GR: Gamma-ray) ..... 141*

*Fig. 3. A composite regional seismic cross section illustrating the Triassic – Earliest Cretaceous pre- and syn-extensional sequence. Horizon K0 corresponds to the end of rifting and Cretaceous – Recent passive margin sequences in the Exmouth Plateau ..... 142*

*Fig. 4. SW-NE (a) and SE-NW (b) seismic sections illustrating the different seismic facies each of the seismic-stratigraphic units that comprise the Valanginian – Present day passive margin sequence. .... 143*

*Fig. 5. a, b) Interval velocity cross plots classified according to seismic stratigraphic units (a) and seismic facies (b) ..... 144*

*Fig. 6. Maps illustrating time thickness (left side) and interval velocity (right side) from Early Post-rift to Unit 2cd. The interval velocity maps are overlain on the thickness maps ... 146*

*Fig. 7. Maps illustrating time thickness (left side) and interval velocity (right side) from Unit 2ef to Unit 4. The interval velocity maps are overlain on the thickness maps..... 147*

*Fig. 8. Interval velocity cross plots as a function of lithology. Clastic sediments are shown in blue and carbonate sediments in yellow ..... 148*

*Fig. 9. Seismic profile overlies with wells section showing seismic facies (SF) and interval velocity (IV) variation between the main seismic stratigraphic boundaries ..... 149*

*Fig. 10. NE-SW oriented seismic section showing seismic facies (SF) and interval velocity (IV) variation between wells and within the main seismic stratigraphic sequences in the SE of the study area ..... 150*

*Fig. 11. NE-SW oriented seismic section showing seismic facies (SF) and interval velocity (IV) variation between wells and within the main seismic stratigraphic sequences in the NW of the study area ..... 151*

*Fig. 12. E-W oriented seismic section showing seismic facies (SF) and interval velocity (IV) variation between wells and within the main seismic stratigraphic sequences in the south of the study area ..... 152*

*Fig. 13. NW-SE oriented seismic section showing seismic facies (SF) and interval velocity (IV) variation between wells and within the main seismic stratigraphic sequences in the south of the study area ..... 153*

## **Chapter Five**

*Fig. 1. Generalised lithostratigraphic chart of the NCB correlated to the seismic-stratigraphy and showing the tie with the lithostratigraphic formations in the Achilles-1 well ..... 172*

*Fig. 2. a), b) Maps showing tectonic reconstructions for the Valanginian (a) and the Aptian (b), also showing the development of a narrow ocean basin between Australia and Greater India. c) Seismic facies map for the Valanginian - Aptian interval..... 173*

*Fig. 3. a), b) Maps showing reconstructions for the Aptian (a) and Turonian (b). During this period, Greater India continued to drift northward, potentially allowing for improved ocean circulation on the western margin. c), d) Seismic facies and thickness maps showing that this is associated with the initial development of bottom current deposits in the centre Exmouth Plateau ..... 174*

*Fig. 4. a), b) Maps showing tectonic reconstructions for the Turonian (a) and Rupelian (b), also showing increased separation of Greater India from Australia, the development of a wide ocean between Australia and Africa, as well as the initial stages of separation of Australia from Antarctica. c) to f) Seismic facies and thickness maps showing that this period was dominated by mounds, moats, and moat fills (c-d, e-f), and deep incisions and conical depression, as well as a shift in the location of sediment accumulation to the northeast (g-h) ..... 175*

*Fig. 5. a), b) Maps showing tectonic reconstructions for the Rupelian (a) and Tortonian (b), also showing that Australia fully separated from Antarctica and drifted to the north, associated with subduction beneath Eurasia. c), d) Seismic facies and thickness maps showing that this corresponds to the development of prograding carbonate ramps and the deposition of chaotic slumps and MTCs in the Exmouth Plateau ..... 176*

*Fig. 6. a), b) Maps showing tectonic reconstructions for the Tortonian (a) and the present day (b), also showing increased convergence between Australia and Eurasia. c), d) Seismic facies and thickness maps showing that this resulted in widespread slumps and MTCs in the Exmouth Plateau ..... 177*

*Fig. 7. a), d) Paleoenvironmental maps from Bradshaw et al. (1988) and b), c) from Apthorpe (1988) and their relationship to paleoenvironmental maps generated in this study ..... 178*

*Fig. 8. a) Bathymetric map of the Northern Carnarvon Basin. b), c) A comparison of Present day and Aptian-Rupelian bathymetric profiles of the NCB. In the Aptian-Rupelian a c. 500 km wide gently sloping ramp-style margin (sensu Van Wagoner et al., 1988) was present ..... 179*

*Fig. 9. a) Schematic diagram showing interaction between currents to form different scales of sedimentary structure by reworking of hemipelagic suspended sediment on a gently sloping ramp-style margin. b) The proximal low gradient slopes in contourite-dominated mixed systems (Rodrigues et al., 2022)..... 180*

*Fig. 10. a-f) Ocean currents and plate reconstructions, which refer to the paleogeographic reconstructions of Scotese and Wright (2018) and the climate model simulations of Valdes et al. (2021) ..... 183*



## List of Tables

---

### **Chapter Two**

*Table. 1. a-c) Details of the 2D and 3D seismic surveys that were used to construct the regional composite lines. The information was compiled from the WAPIMS website.. 57*

*Table. 2. Summary of the seismic facies in the post-rift sequence in the NCB ..... 59*

### **Chapter Three**

*Table. 1. Public domain 3D seismic datasets used in this study provided by Geoscience Australia ..... 107*

### **Chapter Four**

*Table. 1. 3D seismic datasets that were used in this study that are provided by NOPIMS ..... 140*

*Table. 2. V0-K functions for each of the stratigraphic units (a) and seismic facies (b) . 145*

---

*Chapter One:*  
*Introduction and Overview*

---

# Chapter One: Introduction and Overview

---

## 1. Introduction

The Northern Carnarvon Basin (NCB) is situated in the south-westernmost part of Australia's Northwest Shelf (NWS), which also encompasses three other basins, namely the Roebuck, Browse and Bonaparte basins (Fig. 1a; Longley et al., 2002). These basins constitute what is known as the Westralian Superbasin (Fig. 1a; Yeates et al., 1987). The NWS reaches widths of up to 900 kilometres and extends approximately 2800 kilometres in length, containing Mesozoic and more recent strata, with thicknesses exceeding 10 kilometres (Marshall and Lang, 2013). The NCB was established during the Late Palaeozoic to Cenozoic and experienced an extended series of geological events. These include Carboniferous to Permian rifting, Late Permian to Triassic post-rift subsidence, Jurassic rifting, Valanginian breakup, and the subsequent post-rift phase, which ultimately led to the development of a passive continental margin (Fig. 2 and 3). During this final phase, the NCB witnessed the deposition of intricate and diverse sedimentary sequences, exhibiting a mix of siliciclastic sediments intercalated with carbonates.

The investigation of passive margin sequences within the NCB has been limited, primarily due to their perceived lack of economic prospectivity and lack of data availability. From a regional perspective, this interval has only been described in general terms, often extrapolated from onshore outcrops (Riera et al., 2019, 2021). However, seismic data shows that further offshore the margin exhibits complex sedimentary structures, with significant lateral facies changes, some of which are indicative of bottom current sedimentary processes. Hence onshore sequences may not be a complete guide to the variety of sediments offshore. These deposits have not been widely discussed and only a few authors have recognised their presence (Romine and Durrant, 1996; Belde et al., 2017 and Nugraha et al., 2019). Their observations are mostly based on 2D seismic data and analysis of 3D seismic data from a limited area. However, the existing simplified lithostratigraphic nomenclature commonly applied to these sequences makes correlation between areas with different sedimentary styles difficult, and leaves open many questions about how bottom current processes operate and develop through time, as well as their association with evolving oceanic conditions associated with the progressive separation of Gondwanan continents. The resulting complexity of sedimentary structures may give rise to anomalous velocity characteristics

which can affect seismic imaging and processing and may also be associated with changes in drilling conditions. Understanding the nature of the sedimentary processes, the type of deposit that results and their distribution in the NCB may help with future well planning and prognoses.

## 2. Geological background

### 2.1. Regional tectonic and structural framework

The NCB is a significant sedimentary basin located on Australia's NWS. It covers an area of approximately 535,000 square kilometres and consists of four inboard Mesozoic rift sub-basins separated from an outboard Mesozoic-Cenozoic marginal plateau (the Exmouth Plateau) by the Kangaroo Syncline and Rankin Platform (Fig. 1a). The basin contains Phanerozoic to present day sediments, including deltaic to marine siliciclastic and shelfal to deep water carbonate deposits, the majority of which accumulated during the Mesozoic-Cenozoic.

#### 2.1.1. The inboard rift sub-basins

The inboard rift sub-basins are elongated and NNE-trending, comprising of Triassic to Early Cretaceous sediments. The thickness of Jurassic and Cretaceous sequences varies from over 10 kilometres in the Exmouth and Dampier sub-basins, up to 12 kilometres in the Beagle sub-basin and up to 15 kilometres in the Barrow sub-basin. Fine-grained marine claystone was deposited in the Dampier sub-basin during the Late Jurassic and Early Cretaceous, while the Exmouth and Barrow sub-basins contain the Early Cretaceous Barrow Delta succession (Tindale et al., 1998). Structural highs such as the De Grey Nose, Sultan Nose, and Alpha Arch are associated with NE-trending oblique faulting, uplift and rotation, and separate these sub-basins (Fig. 1a; Romine et al., 1997). Extensional fault systems, such as the Sholl Island and Flinders fault systems, divide the sub-basins from the Peedamullah and Lambert shelves to the south and east. The Rankin fault system separates the Rankin Platform from the Dampier sub-basin (Fig. 1a; Stagg and Colwell, 1994). The North Turtle and Bruce terraces in the Beagle sub-basin, as well as the Enderby Terrace in the Dampier sub-basin, are covered by mainly Triassic-Cenozoic sediments, deposited over rotated blocks or down-faulted margins.

### *2.1.2. The outboard Exmouth Plateau*

The Exmouth Plateau covers an area of approximately 400 by 600 kilometres and includes key structural components like the Kangaroo Syncline, Investigator sub-basin, Wombat Plateau, and Rankin Platform (Fig. 1a; Tindale et al., 1998; Stagg et al., 2004). The plateau primarily comprises Triassic sediments with generally thin or absent Jurassic sediments. It is surrounded by three oceanic abyssal plains with water depths exceeding 4 kilometres, namely the Jurassic Argo abyssal plain to the northeast, the Cretaceous Gascoyne abyssal plain to the northwest, and the Cretaceous Curvier abyssal plain to the southwest (Fig. 1a). The plateau features an N-S trending structural high, the Exmouth Plateau Arch, the shallowest part of which is at around 0.8 kilometres water depth. The plateau displays a system of domino-like normal faults, primarily oriented north-south to north-northeast to south-southwest, related to Late Triassic-Jurassic rifting.

## *2.2. Regional basin evolution and stratigraphy*

### *2.2.1. Triassic Post-Permian rift or Pre-Mesozoic rift*

Following an extended phase of Permian rifting, the NCB transitioned into a shallow marine environment during the late Permian post-rift, with deposition primarily in northern depocenters (Longley et al., 2002). A marine transgression in the earliest Triassic led to the deposition of the Locker Shale (Fig. 2), which coarsens upwards until the Middle Triassic. This formation consists mainly of marine siltstone and claystone with some limestone and sandstone interbeds. During the Late Triassic, the Mungaroo Formation (Fig. 2) was deposited by the Mungaroo Delta and extended northwestward offshore, resulting in fluvial sandstone, shoreline sandstone, marine claystone, minor coal, and limestone. The Middle Triassic Cossigny Member encompasses interbedded siltstone, claystone, and limestone. The basin continued to subside rapidly in the latest Triassic, leading to the deposition of the Brigadier Formation, characterised by bedded shelfal claystone, sandstone, and marl, which are largely found in the Kangaroo and Victoria troughs on the eastern Exmouth Plateau (Bussell et al, 2001; Jablonski et al, 2013).

### *2.2.2. Jurassic and Earliest Cretaceous syn-rift*

The basin started rifting in the earliest Jurassic, resulting in a thin sandstone of the North Rankin Formation (Fig. 2) on horst blocks in the Rankin Platform, the Dampier, Beagle, and Barrow sub-basins (Seggie et al, 2007). Subsequently, during the Pliensbachian, the Murat Siltstone formed thin beds of shelfal claystone, siltstone, and marl that passed laterally into the Learmonth Sandstone Formation. Deposition continued in the Exmouth sub-basin until the Middle Jurassic characterised by the Athol Claystone and Siltstone Formations. The Pliensbachian rifting phase established major border faults like the Rosemary, Flinders, and Rankin faults which define the Rankin Platform, Lambert and Peedamullah shelves, as well as the inboard sub-basins. The oblique extensional system influenced structural fragments and deposition styles in the inboard sub-basins by reactivation of pre-existing NE trending faults under a WNW extension regime that also created new NNE oriented faults (Barber, 1988; Romine et al, 1997).

In the Toarcian – earliest Callovian, the Athol Formation and Legendre Formation were characterised by marine sediment and deltaic sandstone, respectively. The Legendre Delta was mainly deposited in the Beagle sub-basin and extended westward into the Rankin Platform and the Dampier sub-basin. In the Callovian – Oxfordian, Argo Land separated from the Australian plate, establishing the Argo Abyssal Plain and creating the Callovian and Oxfordian unconformities (Jablonski, 1997). During this period, transgressive sandstone and claystone of the Calypso Formation was deposited in various sub-basins and shelves. The uplift in the Late Jurassic rotated several fault blocks, promoting sediment supply to depocenters in the Rankin Platform and Exmouth Plateau. The thick Dingo Claystone of this age encompasses deep marine deposits, accumulated rapidly due to thermal subsidence, particularly around the flanks of the Dampier, Barrow, and Exmouth sub-basins (Tindale et al, 1998).

In the Late Jurassic, shallow marine sandstones formed in restricted depocenters on the Exmouth Plateau. Extensional reactivation of Triassic fault blocks on the Rankin Platform led to the establishment of the Kangaroo Syncline during. The Mungaroo Formation was eroded, and sediments accumulated in the Kangaroo Syncline forming coarse clastic units including the Late Jurassic Jansz Sandstone, along with turbiditic sandstones in the Eliassen, Angel, Biggada and Dupuy formations (Jenkins et al, 2003; Moss et al, 2003). Deposition concluded

in the early Berriasian due to subsequent uplift and erosion during the rifting of Greater India and Australia.

The Lower Barrow Group was deposited during the late syn-rift phase in the Berriasian – Valanginian, reaching up to 2.5 km in thickness (Geoscience Australia, 2022). Originally, sediments came from the south, depositing into the Exmouth sub-basin. It then expanded northward, creating a thick lower lobe (the Malouet Formation) to the west of Barrow Island and across the Exmouth Plateau (Ross and Vail, 1994). In the late Berriasian, an upper lobe (the Flacourt Formation) developed ~250 km to the east of the earlier lobe in the Dampier and Barrow sub-basins. The primary sedimentary facies are basin-floor fan sandstones, pro-delta to foreset claystones, and topset sandstones. Based on sedimentary facies and clinoform geometries, Paumard et al. (2018) interpreted the Lower Barrow Group as a moderately deep water progradational shelf-slope margin, with variation in shelf margin geometry resulting from changes in subsidence and uplift during the late syn-rift and early post-rift phases of basin evolution that caused significant variation in accommodation and sediment supply. In contrast, Mantilla et al. (2022) argued that the scale of the clinoforms, along with evidence for opposing dips in the topsets, suggests that the Lower Barrow Group is better interpreted as a modified sediment drift developed entirely in deep water. Sediment supply to the Lower Barrow Group ceased in the Valanginian, marked by breakup in the southwest of the Exmouth Plateau (Hocking, 1990) and the lower lobe was subsequently eroded in the Exmouth sub-basin.

### *2.2.3. Cretaceous – Cenozoic passive margin*

The continental breakup between Greater India and Australian plates resulted in the Valanginian unconformity which was associated with the onset of seafloor spreading and creation of the Curvier and Gascoyne abyssal plains (Gibbons et al., 2012; Heine and Müller, 2005; Longley et al., 2002). The breakup event marked the onset of the post-rift phase (Longley et al., 2002). During the breakup, there was an extensive area of uplift and erosion in the northern Exmouth Sub-basin which is known as the Ningaloo Arch (Fig. 1a; Tindale et al., 1998). The product of that erosion was the deposition of a deltaic sequence, known as the Upper Barrow Group, which comprises the Zeepaard Formation, the Flag Sandstone, and the overlying Birdrong Sandstone (Arditto, 1993). Progradational topsets of the Zeepaard

Formation were extensively developed on the Rankin Platform as well as in the Exmouth and Barrow sub-basins while the Flag Sandstone formed as a basin-floor fan in the northeast part of the Barrow sub-basin. Following this, rapid crustal subsidence and relative sea level rise associated with the onset of seafloor spreading caused regional marine flooding, resulting in deposition of a condensed transgressive glauconitic sandstone (the Mardie Greensand) and an extensive marine transgression, resulting in deposition of the Muderong Shale over the whole of the NCB (Barber, 1988; Romine and Durrant, 1996; Longley et al., 2002; Marshall and Lang, 2013). The formation also contains glauconitic sandstones such as the M. australis Sandstone Member, which is also known as the Stag Sandstone, and the Windalia Sandstone in the Dampier and Barrow Sub-basins, respectively.

Between the Valanginian Unconformity and the Barremian, the Muderong Shale was deposited in a partially restricted marine embayment (Longley et al., 2002). Deposition continued until the Aptian in open marine environment (Romine and Durrant, 1996). During the Barremian, India drifted northward and subsequent subsidence occurred over the entire Northwest Shelf of Australia (Jablonski and Saitta, 2004). By the Aptian, the separation of India as well as the breakup from Antarctica established open or unrestricted oceanic circulation around the Indian plate (Longley et al., 2002; Jablonski and Saitta, 2004).

The open marine system resulted in deposition of the Windalia Radiolarite (Bradshaw et al., 1988) as a result of increased circulation which resulted in upwelling of deep oceanic water and the development of more oxygenated waters (Ellis, 1987). Deposition of the Windalia Radiolarite was followed by aggradation of siltstones and shales of the Lower Gearle Siltstone which is laterally equivalent to marls of the Haycock Formation. The formations were deposited in an outer-shelf environment (Romine and Durrant, 1996). Deposition ceased between of the late Cenomanian and early Turonian resulting in an unconformity, coincident with the onset of Australia – Antarctica breakup (Longley et al., 2002).

Continental breakup between Antarctica and Australia developed along the southern rift margin of Australia from the Turonian to Campanian (Romine and Durrant, 1996). From the Santonian, sedimentary systems on the Northwest Shelf changed from siliciclastic to carbonate. There was widespread deposition of transgressive carbonates in the Toolonga Calcilutite and Withnell Formation. The brake away phase between Antarctica and the southern margin of Australia was responsible for compression and transpression in the NCB, which resulted in uplift of the hinterland and structural inversion in the Exmouth Sub-basin



further west, causing development of the Novara Arch in the early Santonian and the Resolution Arch during the Campanian (Tindale et al, 1998). Sediment influx from the uplift of these structures resulted in the final phase of siliciclastic deposition in the Upper Gearle Siltstone. In addition, rapid inversion and fault reactivation created slope instability, also caused erosion in the Toolonga Calcilutite and Withnell Formation (Tindale et al., 1998; Bradshaw et al., 1998). The transpressional phase reactivated structures in the pre-existing rift within the Dampier and Barrow sub-basins, and subsequently formed Barrow Island.

In Cenozoic, sedimentation in the Northern Carnarvon Basin was dominated by carbonates which progressively developed in warmer conditions (Apthorpe, 1988; Romine et al., 1997). This allowed a widespread prograding carbonate bank to form, and it has continued until the present day. In contrast, a shallow marine environment associated with cool-water carbonates resulted in deposition of the Dockrell Formation during the Palaeocene (Norvick, 2002). The carbonates passed seawards through slope facies into condensed, deep-water carbonates and marls (Norvick, 2002).

In the earliest Eocene, a brief clastic influx occurred parts of northwestern Australia. Subsequently, the sedimentation was followed by several phases of shallow marine carbonate bank progradation which formed the Giralia Calcarenite and Walcott Formation (Norvick, 2002). The development of carbonates continued with progradation of the Oligocene to Middle Miocene Mandu Limestone and the Middle Miocene Trealla Limestone on the inner parts of the margin (Heath and Apthorpe, 1984; Tindale et al., 1998). In the Miocene, further deformation was caused by the collision of the Australia, Indian and Eurasian plates, resulting in significant compression (Longley et al., 2002). This led to inversion in the Late Miocene causing deformation and unconformities in the Trealla Limestone and Bare Formation. Carbonate growth in the Trealla Limestone was interrupted by dolomitic siliciclastic sands of the Bare Formation which was fed by a delta system (Sanchez et al., 2012; Cathro et al., 2003). Apart from the continued growth of the Exmouth Arch, Miocene inversion was the latest phase of tectonism (Paumard et al., 2018 after Jablonski, 1997; Müller et al., 1998; Longley et al., 2002; Cathro and Karner, 2006; Gibbons et al., 2012; Marshall and Lang, 2013; McCormack and McClay, 2013; Gartrell et al., 2016). Subsequent sedimentation resulted in deposition of the Delambre Formation from the Pliocene to Recent (Heath and Apthorpe, 1984; Butcher, 1989), although the widespread development of mass transport

complexes within this sequence (Hengesh et al., 2012, Nugraha et al., 2019 and Scarselli et al., 2013, 2020) suggests continued tectonic activity.

#### *2.2.4. Bottom current in the Northern Carnarvon Basin*

The preceding account of the tectono-stratigraphic evolution of the NCB highlights how little attention has been paid to bottom current activity in the past, and how the use of lithostratigraphic nomenclature lends itself to a relatively simple description of the continental margin. However, Romine and Durrant (1996) initially recognized middle to Late Cretaceous contourites and scours in the region, but there was no further work on these deposits until 2017 when Belde et al. (2017) identified large-scale Quaternary sediment waves in shallow water carbonate sand deposits in the Barrow sub-basin and the Rankin Platform. Nugraha et al. (2019) provided a more detailed description of various bottom current features in the Exmouth Plateau near the Rankin Platform, including Late Cretaceous contourite drifts and channels, large Eocene sediment waves and scours, and minor Late Miocene to Recent furrows, while Mantilla et al. (2022) provided a controversial reinterpretation of the Lower Barrow Group delta as a large asymmetric bottom current mounded deposit. Thus, there are only four pre-existing accounts of bottom current activity in the NCB, although they include deposits that cover an extensive period from the Early Cretaceous onwards. In addition, both Young (2001), and Imbert and Ho (2012) have recognised unique erosive features in Paleogene sequences that might be interpreted as a series of canyons and erosional channels or as a funnel-shaped, large scale pockmarks.

Most of these studies have utilised 2D seismic data or spatially restricted 3D seismic data sets from different areas. Nugraha et al. (2019) suggest that the increasing separation between continents associated with the rapid north-westwards drift of India after the Albian (Veevers, 2000), and the rapid movement of Australia northwards away from Antarctica from the Eocene (Müller et al., 2000; Seton et al., 2012), allowed the establishment of oceanic circulation around the north-western, western, and southern margins of Australia, resulting in the development of bottom currents that impinged on the depositional and erosional systems on the Northwest Shelf. However, the limited use of 3D seismic data means that information regarding the spatial and temporal distribution of bottom current activity is

limited, as is information about current patterns, and their implications for broader oceanic circulation during the breakup of Gondwana.

#### *2.2.5. Slumps and mass transport complexes*

Hengesh et al. (2012), Nugraha et al. (2019) and Scarselli et al. (2013, 2020) have identified sediment collapses in the Neogene – Recent sediments in the Exmouth Plateau that were interpreted as slumps and mass transport complexes. Seismic data suggests that such submarine landslide events have affected a wider area and have been active over a longer period of time than suggested by these studies which were focussed mainly on seabed features in areas around the Exmouth Arch. This implies widespread instability along the margin over an extended period of time, but the precise extent, duration and causes of this instability are unknown.

#### *2.3. A brief history of bottom currents*

Contourite research initially received relatively little attention in comparison to turbidite studies (Heezen and Hollister, 1964). Contourites are now recognized as diverse deposits formed by various currents in deep oceans, continental slopes, shallow margins, and even lakes, marking a broadening understanding of their formation (Ceramicola et al., 2001; Gilli et al., 2005; Verdicchio and Trincardi, 2008; Vandorpe et al., 2011; Campbell and Deptuck, 2012; Heirman et al., 2012; Preu et al., 2012; Roque et al., 2012; Uenzelmann-Neben and Gohl, 2012; Li et al., 2013). Since the International Geoscience Correlation Programme 432 (Contourites, Bottom Currents and Palaeocirculation), which ran from 1998 to 2001, advances in technology have led to improved data quality, revealing contourite drifts in a variety of settings and deepening knowledge of the processes responsible for their formation. This progress has introduced terms like Contourite Depositional Systems and Contourite Depositional Complexes (Hernández-Molina et al., 2004, 2008; Rebesco and Camerlenghi, 2008). A significant body of research has focused on the Mediterranean Outflow Water (MOW). This has played a pivotal role as a natural laboratory for the study of contourites (Gonthier et al., 1984; Nelson et al., 1993; Llave et al., 2001; Mulder et al., 2003; Hernandez-Molina et al., 2006; Marchès et al., 2007; Llave et al., 2011; Roque et al., 2012; Brackenridge et al., 2013) and has been the focus of studies in the Gulf of Cádiz, as well as contributing to

studies in other areas like the Bay of Biscay and the Porcupine Seabight (Ercilla et al., 2008; Van Rooij et al., 2003, 2009, 2010; Hernandez-Molina et al., 2011). Extensive research efforts have enhanced understanding of the interaction between bottom currents and deep-water environments. Simultaneously, many countries have investigated continental margins to determine the Base of Slope (BOS) following United Nations Convention on the Law of the Sea (UNCLOS) guidelines. This work has underscored the prevalence of contourites in deep water environments and their significant role in shaping continental slope and rise morphology (Hernández-Molina et al., 2009, 2010).

Most of these studies are based on seabed and near seabed investigations, focusing on recent to sub-recent drift settings, and in many cases relate to mud dominated systems (Hollister and Heezen, 1972; Carter and McCave, 1994; Stow et al., 2002; Hanquiez, 2006; Wynn and Masson, 2008; Mulder et al., 2013). More recently, the importance mixed depositional systems which involve the interaction of sediment gravity flows and bottom currents has been recognised. These result in key features like mounded drifts and submarine channels that are recognizable in various continental margin settings (Fig. 4; Heezen et al., 1966; Mountain and Tucholke, 1985; Rebesco et al., 1996, 2002, 2007; Faugères et al., 1999; Rebesco and Stow, 2001; Knutz and Cartwright, 2003; Hernández-Molina et al., 2006; Mulder et al., 2008; Deptuck et al., 2012; Brackenridge et al., 2013; Gong et al., 2013; Alonso et al., 2016; Sansom, 2018). Although contourites are typically made up of fine-grained sediments and not considered significant prospects for exploration, bottom currents that develop in mixed systems, reworking gravity flows that include coarser clastic sediments, significantly boost the potential development reservoirs in deep marine settings (e.g., sand-rich deposits in the Gulf of Cadiz in the Iberian Peninsula: Mulder et al., 2006; Brackenridge et al., 2013; Stow et al., 2013; Alonso et al., 2016; Hernández-Molina et al., 2014). This led to the recognition of contourite deposits on conventional seismic data and in the older rock record (from the Cretaceous onwards), with initial discoveries of oil fields in extreme deep water on the Brazilian Atlantic margin, in the Gulf of Mexico, and in the North Sea (Mutti et al., 1980, 2014; Viana and Faugères, 1998; Mutti and Carminatti, 2011; Shanmugam et al., 1990, 1993; Enjolras et al., 1986). The discovery of substantial gas reserves in Paleogene mixed system deposits in Mozambique has particularly rekindled academic and research interest, highlighting their exceptional reservoir quality (Fonnesu, 2013; Fonnesu et al., 2020). This has driven an expansion of research into mixed systems in recent years with the discovery of

many notable examples of such deposits, primarily on commercial seismic data. Combined with lab experiments, this has resulted in significant advances in concepts as illustrated in Fig. 4 (Creaser et al., 2017; Fonnesu et al., 2020; Batchelor et al., 2021; Miramontes et al., 2021; Rodrigues et al., 2021, 2022).

### 3. Aims and objectives

The previous account has identified the following issues, both in terms of understanding the tectonostratigraphic evolution of the NCB, and in terms of the current state of knowledge of bottom current deposits. It has revealed the following knowledge gaps:

- Given the limited previous work on passive margin sequences in the NCB, and on bottom current deposits in particular the spatial and temporal distribution of these deposits is not fully known.
- As most previous studies have used mainly 2D data, or limited 3D data, details of the way in which sedimentary processes have evolved, and the currents responsible for them are not completely understood.
- These two points together result in a limited understanding of the way in which thermohaline circulation might have evolved during and following the break-up of Gondwana, and how these currents might have impinged on the NW shelf.
- Most models for bottom currents show deposition adjacent to distinct topographic slopes (contourites). However, the NCB formed a broad, gently sloping margin thorough much of its evolution. This provides the opportunity to study bottom current activity in a different setting to many studies.
- Most studies of bottom current deposits relate to clastic sediments of Cenozoic, and particularly of Quaternary age. The NCB deposits span Mesozoic and Cenozoic sediments and include deposits found in both clastic and carbonate sequences. This provides the opportunity to determine if either of these factors have any bearing on the evolution of bottom current deposits.
- Anecdotally, accurate well prognoses and the prediction of drilling conditions is challenging in parts of the NCB. This is likely a consequence of highly variable lithologies, and associated variations in seismic velocities. Understanding the

sedimentary processes responsible for the formation of bottom current deposits, and their spatial distribution, may improve pre-drill well prognoses.

In the light of this, the specific aims of this research are:

- To create a seismic stratigraphic framework which defines the different depositional sequences that comprise the passive margin sequence in the NCB and to determine the vertical and lateral facies changes that show where bottom current related sedimentary structures are located across the basin, and how they change through time.
- To carry out a detailed 3D seismic interpretation, on a semi-regional scale using a combination of seismic facies mapping and seismic geomorphology to understand details of the sedimentary processes and how they have evolved through time.
- To relate the evolution of the structures to current patterns and to place them in their plate tectonic context to understand how increasing separation between continents may have influenced oceanic circulation patterns.
- To quantify the relationships between the different sequences and their velocity properties to develop a predictive velocity description based on facies variations.

This dissertation has three main chapters, which are presented as separate manuscripts. Each chapter is self-contained and includes background and references relevant to the topic. Chapter 2 was published in *Marine and Petroleum Geology (MPG)*, Volume 156 in October 2023, and describes the regional seismic stratigraphic framework and depositional history of the post-Valanginian passive margin sequences. Chapter 3 has been submitted and is under review with *Marine and Petroleum Geology*. This incorporates the interpretation of bottom current sedimentary structures in the Late Cretaceous to Paleogene sequences in the central part of the central Exmouth Plateau. Chapter 4 (to be submitted) investigates the facies and stratigraphic controls on velocity variations in the post-Valanginian passive margin sequences. An integration of seismic imaging and seismic velocities derived from wells gives a better prediction and analysis. Chapter 5 provides a synthesis of this research, summarises its significance and identifies areas for potential future research.

#### 4. Data and methodology

We utilise a public domain dataset including seismic and well data for this research. The data can be accessed online via the National Offshore Petroleum Information Management System (NOPIMS) and the Western Australian Petroleum and Geothermal Information Management System (WAPIMS). 2D seismic lines cover most of NCB, an area of about 140,000 square kilometres, whereas 3D seismic data is mainly located in the centre of the Exmouth Plateau (Fig. 1b). The 2D and 3D seismic data are Pre-stack Time Migrated (PSTM) and are of high data quality in the shallower passive margin sequences. Hundreds of wells have been drilled within the basin, but they are mainly in the inboard sub-basin areas. There are approximately 100 wells in the Exmouth Plateau. However, as the objectives of most well lies in deeper pre- and syn-rift sequences, information from the passive margin sequence is often lacking. 60 wells which contain sufficient velocity and biostratigraphic information from the shallow parts of the holes were selected and are used in this research (Fig. 1b). Combined 2D-3D seismic and well datasets provide continuous coverage over large parts of the basin and enable the detailed mapping of sedimentary structures and a wide variety of bedforms related to bottom current activity across various stratigraphic levels. Details of the data used and methods that have been applied are fully explained in each chapter (Chapter 2, 3 and 4).

#### References

- Apthorpe, M., 1988. Cainozoic depositional history of the North West Shelf. In: Purcell, P.G., Purcell, R.R. (Eds.), *The North West Shelf, Australia. Proceedings of the Petroleum Exploration Society of Australia Symposium*, Perth, WA, 55–84.
- Alonso, B., Ercilla, G., Casas, D., Stow, D.A., Rodríguez-Tovar, F.J., Dorador, J., Hernández-Molina, F.J., 2016. Contourite vs gravity-flow deposits of the Pleistocene Faro drift (Gulf of Cadiz): sedimentological and mineralogical approaches. *Mar. Geol.* 377, 77–94. <https://doi.org/10.1016/j.margeo.2015.12.016>.
- Arditto, P.A., 1993. Depositional sequence model for the post-Barrow Group Neocomian succession, Barrow and Exmouth Sub-basins, Western Australia. *APEA J.* 33, 151–160.
- Barber, P. M., 1988. The Exmouth Plateau deep water frontier: A case history. In: Purcell, P. G., Purcell, R. R., (Eds.). *The North West Shelf, Australia: Proceedings of Petroleum Exploration Society Australia Symposium*. Perth: WA, 173-187.

- Batchelor, C.L., Bellwald, B., Planke, S., Ottesen, D., Henriksen, S., Myklebust, R., Johansen, S.E., Dowdeswell, J.A., 2021. Glacial, fluvial and contour-current-derived sedimentation along the northern North Sea margin through the Quaternary. *Earth Planet. Sci.* 566, 116966 <https://doi.org/10.1016/j.epsl.2021.116966>.
- Belde, J., Back, S., Bourget, J., Reuning, L., 2017. Oligocene and Miocene carbonate platform development in the Browse Basin, Australian northwest shelf. *J. Sediment. Res.* 87, 795–816. <https://doi.org/10.2110/jsr.2017.44>.
- Brackenridge, R.A., Hernández-Molina, F.J., Stow, D.A.V., Llave, R., 2013. A Pliocene mixed contourite–turbidite system offshore the Algarve Margin, Gulf of Cadiz: seismic response, margin evolution and reservoir implications. *Marine and Petroleum Geology* 46, 36–50. <https://doi.org/10.1016/j.marpetgeo.2013.05.015>.
- Bradshaw, M.T., Yeates, A.N., Beynon, R.M., Brakel, A.T., Langford, R.P., Totterdell, J.M., Yeung, M., 1988. Palaeogeographic evolution of the North West Shelf region. In: Purcell, P.G., Purcell, R.R. (Eds.), *The North West Shelf, Australia. Proceedings of the Petroleum Exploration Society of Australia Symposium*, 29–54.
- Bussell, M.R., Jablonski, D., Enman, T., Wilson, M.J., Bint, A.N., 2001. Deepwater exploration: northern Western Australia compared with Gulf of Mexico and Mauritania. *The APPEA Journal*, 41(1), 289–319.
- Butcher, B.P., 1989. Northwest Shelf of Australia. *AAPG Mem.* 48, 81-115.
- Campbell, D.C., Deptuck, M.E., 2012. Alternating bottom-current-dominated and gravity flow-dominated deposition in a lower slope and rise setting—insights from the seismic geomorphology of the Western Scotian Margin, Eastern Canada. In: Prather, B.E., Deptuck, M.E., Mohrig, D., Van Hoorn, B., Wynn, R.B. (Eds.), *Application of the Principles of Seismic Geomorphology to Continental-slope and Base-of-slope Systems: Case Studies from Seafloor and Near-seafloor Analogues. SEPM Special Publication*, 99, 329–346. <http://dx.doi.org/10.2110/pec.12.99.0329>.
- Cathro, D. L., Austin, J. A. Jr., Moss, G. D., 2003. Progradation along a deeply submerged Oligocene-Miocene Heterozoan carbonate shelf; how sensitive are clinofolds to sea level variations? *AAPG Bull.*, 87, 1547–1574. <https://doi.org/10.1306/05210300177>.
- Cathro, D.L., Karner, G.D., 2006. Cretaceous–tertiary inversion history of the Dampier Sub-basin, Northwest Australia: insights from quantitative basin modeling. *Mar. Petrol. Geol.* 23 (4), 503–526. <http://dx.doi.org/10.1016/j.marpetgeo.2006.02.005>.



- Carter, L., McCave, I.N., 1994. Development of sediment drifts approaching an active plate margin under the SW Pacific Deep Western boundary undercurrent. *Paleoceanography* 9, 1061–1085. <http://dx.doi.org/10.1029/94PA01444>.
- Ceramicola, S., Rebesco, M., De Batist, M., Khlystov, O., 2001. Seismic evidence of small scale lacustrine drifts in Lake Baikal (Russia). *Marine Geophysical Research* 22, 445–464. <https://doi.org/10.1023/A:1016351700435>.
- Creaser, A., Hernández-Molina, F., Badalini, G., Thompson, P., Walker, R., Soto, M., Conti, B., 2017. A late cretaceous mixed (turbidite-contourite) system along the Uruguayan margin: Sedimentary and paleoceanographic implications. *Mar. Geol.* 390, 234–253. <https://doi.org/10.1016/j.margeo.2017.07.004>.
- Deptuck, M.E., Mohrig, D., Van Hoorn, B., Wynn, R.B., 2012. In: Prather, B.E., Deptuck, M.E., Mohrig, D.C., van Hoorn, B., Wynn, R.B. (Eds.), *Application of the Principles of Seismic Geomorphology to Continental Slope and Base-Of-Slope Systems: Case Studies from Seafloor and Near-Seafloor Analogues*. Society for Sedimentary Geology, London.
- Ellis, G., 1987. Lower Cretaceous radiolarian biostratigraphy and depositional environment of the Windalia Radiolarite, Carnarvon Basin, Western Australia. Honours Thesis, University of Western Australia, unpublished.
- Enjolras, J.M., Goudain, J., Mutti, E., Pizon, J., 1986. New turbiditic model for the lower tertiary sands in the south Viking graben. In: Spencer, A.M., Holter, E., Campbell, C.J., Hanslein, S.H., Nystherm, E., Ormaasen, E.G. (Eds.), *Habitat of Hydrocarbons on the Norwegian Continental Shelf*. Graham and Trotman, London, 171–178.
- Ercilla, G., Casas, D., Estrada, F., Vázquez, J.T., Iglesias, J., García, M., Gómez, M., Acosta, J., Gallart, J., Maestro-González, A., 2008. Morphosedimentary features and recent depositional architectural model of the Cantabrian continental margin. *Marine Geology* 247, 61–83. <https://doi.org/10.1016/j.margeo.2007.08.007>.
- Etheridge, M. A., O'Brien, G.W., 1994. Structural and tectonic evolution of the Western Australian margin basin system. *PESA J.* 22: 45-64.
- Faugères, J.-C., Stow, D.A., Imbert, P., Viana, A., 1999. Seismic features diagnostic of contourite drifts. *Mar. Geol.* 162 (1), 1–38. [https://doi.org/10.1016/S0025-3227\(99\)00068-7](https://doi.org/10.1016/S0025-3227(99)00068-7).

- Fonnesu, F., 2013. The Mamba Complex Supergiant Gas Discovery (Mozambique): an Example of Turbidite Fans Modified by Deepwater Tractive Bottom Currents. In: The 12th PESGB/HGS Conference on African E&P, London.
- Fonnesu, M., Palermo, D., Galbiati, M., Marchesini, M., Bonamini, E., Bendias, D., 2020. A new world-class deep-water play-type, deposited by the syndepositional interaction of turbidity flows and bottom currents: The giant Eocene Coral Field in northern Mozambique, *Marine and Petroleum Geology*, Volume 111, 179-201, <https://doi.org/10.1016/j.marpetgeo.2019.07.047>.
- Gartrell, A.P., 2000. Rheological controls on extensional styles and the structural evolution of the Northern Carnarvon Basin, North West Shelf, Australia. *Aust. J. Earth Sci.* 47, 231–244. <https://doi.org/10.1046/j.1440-0952.2000.00776.x>.
- Gartrell, A., Torres, J., Dixon, M., Keep, M., 2016. Mesozoic rift onset and its impact on the sequence stratigraphic architecture of the Northern Carnarvon Basin. *APPEA J.* 56, 143–158. <https://doi.org/10.1071/AJ15012>.
- Geoscience Australia, 2022. Regional Geology of the Northern Carnarvon Basin [WWW Document]. Offshore Pet. Explor. Acreage Release.
- Gibbons, A.D., Barckhausen, U., Van Den Bogaard, P., Hoernle, K., Werner, R., Whittaker, J.M., Müller, R.D., 2012. Constraining the Jurassic extent of Greater India: tectonic evolution of the West Australian margin. *Geochem. Geophys. Geosyst.* 13, 1–25. <https://doi.org/10.1029/2011GC003919>.
- Gilli, A., Anselmetti, F.S., Ariztegui, D., Beres, M., McKenzie, J.A., Markgraf, V., 2005. Seismic stratigraphy, buried beach ridges and contourite drifts: the Late Quaternary history of the closed Lago Cardiel basin, Argentina (49 degrees S). *Sedimentology* 52, 1–23. <https://doi.org/10.1111/j.1365-3091.2004.00677.x>.
- Gong, C., Wang, Y., Zhu, W., Li, W., Xu, Q., 2013. Upper Miocene to quaternary unidirectionally migrating deep-water channels in the Pearl River Mouth basin, northern south China sea, 2013. *AAPG Bull.* 97 (2), 285–308. <http://dx.doi.org/10.1306/07121211159>.
- Gonthier, E., Faugères, J.-C., Stow, D.A.V., 1984. Contourite facies of the Faro Drift, Gulf of Cadiz. In: Stow, D.A.V., Piper, D.J.W. (Eds.), *Fine Grained Sediments, Deepwater Processes and Facies*. Geological Society, London, Special Publication, 15, 275–291.
- Hanquiez, V., 2006. Processus sédimentaires et évolution récente (Quaternaire terminal) du Golfe de Cadix, vol. 1 *Sédimentologie Thesis*, Bordeaux.

- Heath, R.S., Apthorpe, M.C., 1984. New formation names for the Late Cretaceous and Tertiary sequence of the southern North West Shelf. *GSWA, Record*, 1984/7, 35.
- Heezen, B.C., Hollister, C.D., 1964. Deep sea current evidence from abyssal sediments. *Marine Geology* 1, 141–174. [https://doi.org/10.1016/0025-3227\(64\)90012-X](https://doi.org/10.1016/0025-3227(64)90012-X).
- Heezen, B.C., Hollister, C.D., Ruddiman, W.F., 1966. Shaping of the continental rise by deep geostrophic contour currents. *Science* 152 (3721), 502–508. <https://doi.org/10.1126/science.152.3721.502>.
- Heine, C., Müller, R.D., 2005. Late Jurassic rifting along the Australian North West Shelf: margin geometry and spreading ridge configuration. *Aust. J. Earth Sci.* 52, 27–39. <https://doi.org/10.1080/08120090500100077>.
- Heirman, K., De Batist, M., Arnaud, F., De Beaulieu, J.L., 2012. Seismic stratigraphy of the late Quaternary sedimentary infill of Lac d'Armor (Kerguelen archipelago): a record of glacier retreat, sedimentary mass wasting and southern Westerly intensification. *Antarctic Science* 24, 608–618. <http://dx.doi.org/10.1017/S0954102012000466>.
- Hengesh, J., Dirstein, J., Stanley, A., 2012. Seafloor geomorphology and submarine landslide hazards along the continental slope in the Carnarvon Basin, Exmouth Plateau, North West Shelf, Australia, *The APPEA Journal*, 52, 493–511. <https://doi.org/10.1071/AJ11039>.
- Hernández-Molina, F.J., Larter, R.D., Rebesco, M., Maldonado, A., 2004. Miocene changes in bottom current regime recorded in continental rise sediments on the Pacific margin of the Antarctic Peninsula. *Geophysical Research Letters* 31, L22606. <https://doi.org/10.1029/2004GL020298>.
- Hernandez-Molina, F.J., Llave, E., Stow, D.A.V., Garcia, M., Somoza, L., Vazquez, J.T., Lobo, F.J., Maestro, A., del Rio, V.D., Leon, R., Medialdea, T., Gardner, J., 2006. The contourite depositional system of the Gulf of Cadiz: a sedimentary model related to the bottom current activity of the Mediterranean outflow water and its interaction with the continental margin. *Deep-Sea Research Part II: Topical Studies in Oceanography* 53, 1420–1463. <https://doi.org/10.1016/j.dsr2.2006.04.016>.
- Hernández-Molina, F.J., Stow, D.A.V., Llave, 2008. Continental slope contourites. In: Rebesco, M., Camerlenghi, A. (Eds.), *Contourites. Developments in Sedimentology*, 60. Elsevier, Amsterdam, pp. 379–408. [https://doi.org/10.1016/S0070-4571\(08\)10019-X](https://doi.org/10.1016/S0070-4571(08)10019-X).

- Hernández-Molina, F.J., Paterlini, M., Violante, R., Marshall, P., de Isasi, M., Somoza, L., Rebesco, M., 2009. Contourite depositional system on the Argentine slope: an exceptional record of the influence of Antarctic water masses. *Geology* 37, 507–510. <https://doi.org/10.1130/G25578A.1>.
- Hernández-Molina, F.J., Paterlini, M., Somoza, L., Violante, R., Arecco, M.A., de Isasi, M., Rebesco, M., Uenzelmann-Neben, G., Neben, S., Marshall, P., 2010. Giant mounded drifts in the Argentine Continental Margin: origins, and global implications for the history of thermohaline circulation. *Marine and Petroleum Geology* 27, 1508–1530. <https://doi.org/10.1016/j.marpetgeo.2010.04.003>.
- Hernandez-Molina, F.J., Serra, N., Stow, D.A.V., Llave, E., Ercilla, G., Van Rooij, D., 2011. Along-slope oceanographic processes and sedimentary products around the Iberian margin. *Geo-Marine Letters* 31, 315–341. <https://doi.org/10.1007/s00367-011-0242-2>.
- Hernández-Molina, F.J., Llave, E., Preu, B., Ercilla, G., Fontan, A., Bruno, M., Serra, N., Gomiz, J.J., Brackenridge, R.E., Sierro, F.J., Stow, D.A.V., Garcia, M., Juan, C., Sandoval, N., Arnaiz, A., 2014. Contourite processes associated with the Mediterranean outflow water after its exit from the strait of Gibraltar: global and conceptual implications. *Geology* 42 (3), 227–230. <https://doi.org/10.1130/G35083.1>
- Hocking, R.M., 1990. Carnarvon Basin. In: *Geology and Mineral Resources of Western Australia*. Western Australia Geological Survey, Memoir 3, 457–495.
- Hollister, C.D., Heezen, B.C., 1972. Geological effects of ocean bottom currents: western North Atlantic. In: In: Gordon, A.L. (Ed.), *Studies in Physical Oceanography*, vol. 2. Gordon and Breach, New York, 37–66.
- Imbert, P., Ho, S., 2012. Seismic-Scale Funnel-Shaped Collapse Features from the Paleocene - Eocene of the North West Shelf of Australia. *Marine Geology*, 332, 198-221. <https://doi.org/10.1016/j.margeo.2012.10.010>.
- Jablonski, D., 1997. Recent advances in the sequence stratigraphy of the Triassic to Lower Cretaceous succession in the Northern Carnarvon Basin, Australia. *APPEA J.* 37, 429–454. <https://doi.org/10.1071/AJ96026>.
- Jablonski, D., Saitta, A. J., 2004. Permian to Lower Cretaceous plate tectonics and its impact on the tectono-stratigraphic development of the western Australian margin. *The APPEA Journal*, 44(1), 287–327. <https://doi.org/10.1071/AJ03011>.

- Jablonski, D., Preston, J., Westlake, S., Gumley, C.M., 2013. Unlocking the origin of hydrocarbons in the central part of the Rankin Trend, Northern Carnarvon Basin, Australia. In: Keep, M. and Moss, S.J. (eds), *The Sedimentary Basins of Western Australia 4. Proceedings of the Petroleum Exploration Society of Australia Symposium*, Perth, 2013, 31pp.
- Jenkins, C.C., Maughan, D.M., Acton, J.H., Duckett, A., Korn, B.E., Teakle, R.P., 2003. The Jansz gas field, Carnarvon Basin, Australia. *The APPEA Journal*, 43(1), 303–324.
- Knutz, P.C., Cartwright, J., 2003. 3D anatomy of late Neogene contourite drifts and associated mass flows in the Faeroe-Shetland Channel. In: Davies, R.J., Cartwright, J.A., Stewart, S., Lappin, M., Underhill, J.R. (Eds.), *3D Seismic Technology: Applications to the Exploration of Sedimentary Basins*, vol. 29. Mem. Geol. Soc., London, 63–72. <https://doi.org/10.1144/GSL.MEM.2004.029.01.07>.
- Li, H., Wang, Y., Zhu, W., Xu, Q., He, Y., Tang, W., Zhuo, H., Wang, D., Wu, J., Li, D., 2013. Seismic characteristics and processes of the Plio-Quaternary unidirectionally migrating channels and contourites in the northern slope of the South China Sea. *Marine and Petroleum Geology* 43, 370–380. <http://dx.doi.org/10.1016/j.marpetgeo.2012.12.010>.
- Llave, E., Hernandez-Molina, F.J., Somoza, L., Diaz-del Rio, V., Stow, D.A.V., Maestro, A., Alveirinho Dias, J.M., 2001. Seismic stacking pattern of the Faro-Albufeira contourite system (Gulf of Cadiz): a Quaternary record of paleoceanographic and tectonic influences. *Marine Geophysical Research* 22, 487–508. <https://doi.org/10.1023/A:1016355801344>.
- Llave, E., Matias, H., Hernandez-Molina, F.J., Ercilla, G., Stow, D.A.V., Medialdea, T., 2011. Pliocene–Quaternary contourites along the northern Gulf of Cadiz margin: sedimentary stacking pattern and regional distribution. *Geo-Marine Letters* 31, 377–390. <http://dx.doi.org/10.1007/s00367-011-0241-3>.
- Longley, I.M., Buessenschuett, C., Clydsdale, L., Cubitt, C.J., Davis, R.C., Johnson, M.K., Marshall, N.M., Murray, A.P., Somerville, R., Spry, T.B., Thompson, N.B., 2002. The North West Shelf of Australia - a Woodside perspective. In: Keep, M., Moss, S. (Eds.), *The Sedimentary Basins of Western Australia 3. Proceedings of the Petroleum Exploration Society of Australia Symposium*, 27–88.
- Mantilla, O., Hernández-Molina, F.J., Scarselli, N., 2022. Can deepwater bottom currents generate clinothems? An example of a large, asymmetric mounded drift in Upper

- Jurassic to Lower Cretaceous sediments from northwestern Australia. *Geology* 2022; 50 (6): 741–745. <https://doi.org/10.1130/G50068.1>.
- Marchès, E., Mulder, T., Cremer, M., Bonnel, C., Hanquiez, V., Gonthier, E., Lecroart, P., 2007. Contourite drift construction influenced by capture of Mediterranean Outflow Water deep-sea current by the Portimao submarine canyon (Gulf of Cadiz, South Portugal). *Marine Geology* 242, 247–260. <https://doi.org/10.1016/j.margeo.2007.03.013>.
- Marshall, N.G., Lang, S.C., 2013. A new sequence stratigraphic framework for the North West Shelf, Australia. In: Keep, M., Moss, S.J. (Eds.), *The Sedimentary Basins of Western Australia 4. Proceedings of the Petroleum Exploration Society of Australia Symposium*, 1–32.
- McCormack, K., McClay, K., 2013. Structural architecture of the gorgon platform, North West Shelf, Australia. In: Keep, M., Moss, S.J. (Eds.), *The Sedimentary Basins of Western Australia IV: Proceedings of the Petroleum Exploration Society of Australia Symposium*. Perth, WA, 2013.
- Moss, S., Barr, D., Kneale, R., Clews, P., Cruse, T., 2003. Mid to Late Jurassic shallow marine sequences of the eastern Barrow Sub-basin: the role of low-stand deposition in new exploration concepts. *The APPEA Journal*, 43(1), 231–255.
- Mountain, G.S., Tucholke, B.E., 1985. Mesozoic and Cenozoic geology of the U.S. Atlantic continental slope and rise. In: Poag, C.W. (Ed.), *Geologic Evolution of the United States Atlantic Margin*. Van Nostrand Reinhold, New York, 292–341.
- Mulder, T., Lecroart, P., Hanquiez, V., Marches, E., Gonthier, E., Guedes, J.C., Thiebot, E., Jaaidi, B., Kenyon, N., Voisset, M., Perez, C., Sayago, M., Fuchey, Y., Bujan, S., 2006. The western part of the Gulf of Cadiz: contour currents and turbidity currents interactions. *Geo Mar. Lett.* 26 (1), 31–41. <https://doi.org/10.1007/s00367-005-0013-z>
- Mulder, T., Faugères, J.C., Gonthier, E., 2008. Mixed turbidite-contourite systems. In: Rebesco, M., Camerlenghi, A. (Eds.), *Contourites Developments in Sedimentology* 60. Elsevier, Amsterdam, 435–456. [https://doi.org/10.1016/S0070-4571\(08\)10021-8](https://doi.org/10.1016/S0070-4571(08)10021-8).
- Mulder, T., Hassan, R., Ducassou, E., Zaragosi, S., Gonthier, E., Hanquiez, V., Marchès, E., Toucanne, S., 2013. Contourites in the Gulf of Cadiz: a cautionary note on the potentially ambiguous indicators of bottom current velocity. *Geo Mar. Lett.* 33, 357–367. <https://doi.org/10.1007/s00367-013-0332-4>.

- Müller, R.D., Mihut, D., Baldwin, S., 1998. A new kinematic model for the formation and evolution of the West and Northwest Australian Margin. In: Purcell, P.G., Purcell, R.R. (Eds.), *The Sedimentary Basins of Western Australia 2. Proceedings of the Petroleum Exploration Society of Australia Symposium*, Perth, WA, 56–72.
- Müller, D., Gaina, C., Clark, S., 2000. *Seafloor Spreading Around Australia*, vol. 24.
- Mutti, E., Barros, M., Possato, S., Rumenos, L., 1980. Deep-sea Fan Turbidite Sediments Winnowed by Bottom-Currents in the Eocene of the Campos Basin, Brazilian Offshore. 1st IAS Eur. Meet. Abstr., 114.
- Mutti, E., Carminatti, M., 2011. Deep-water Sands in the Brazilian Offshore Basins: AAPG Search and Discovery.
- Nelson, C.H., Baraza, J., Maldonado, A., 1993. Mediterranean undercurrent sandy contourites, Gulf of Cadiz, Spain. *Sedimentary Geology* 82, 103–131.
- Nugraha, H.D., Jackson, C.A.-L., Johnson, H.D., Hodgson D.M., Reeve M.T., 2019. Tectonic and oceanographic process interactions archived in the Late Cretaceous to Present deep-marine stratigraphy on the Exmouth Plateau, offshore NW Australia. *Basin Res*, vol 31, 405–430. <https://doi-org.dbgw.lis.curtin.edu.au/10.1111/bre.12328>.
- Norvick, M. S., 2002. Palaeogeographic maps of the northern margins of the Australian plates: initial report. Unpublished report for Geoscience Australia.
- Paumard, V., Bourget J., Payenberg T., Ainsworth R. B., George A. D., Lang S., Posamentier H. W., Peyrot D., 2018. Controls on shelf-margin architecture and sediment partitioning during a syn-rift to post-rift transition: Insights from the Barrow Group (Northern Carnarvon Basin, North West Shelf, Australia). *Earth-Science Reviews* Volume 177, February 2018, 643–677. <https://doi.org/10.1016/j.earscirev.2017.11.026>.
- Preu, B., Schwenk, T., Hernández-Molina, F.J., Violante, R., Paterlini, M., Krastel, S., Tomasini, J., Spieß, V., 2012. Sedimentary growth pattern on the northern Argentine slope: the impact of North Atlantic Deep Water on southern hemisphere slope architecture. *Marine Geology* 329–331, 113–125. <https://doi.org/10.1016/j.margeo.2012.09.009>.
- Rebesco, M., Larter, R.D., Camerlenghi, A., Barker, P.F., 1996. Giant sediment drifts on the continental rise west of the Antarctic Peninsula. *Geo Mar. Lett.* 16 (2), 65–75. <https://doi.org/10.1007/BF02202600>.

- Rebesco, M., Stow, D.A.V., 2001. Seismic expression of contourites and related deposits: a preface. *Marine Geophysical Research* 22, 303–308. <https://doi.org/10.1023/A:1016316913639>.
- Rebesco, M., Pudsey, C.J., Canals, M., Camerlenghi, A., Barker, P.F., Estrada, F., Giorgetti, A., 2002. Sediment drifts and deep-sea channel systems, Antarctic Peninsula Pacific margin. *Geol. J. Soc. Mem.* 22 (1), 353–371. <https://doi.org/10.1144/GSL.MEM.2002.022.01.25>.
- Rebesco, M., Camerlenghi, A., Volpi, V., Neagu, C., Accettella, D., Lindberg, B., Cova, A., Zgur, F., 2007. Interaction of processes and importance of contourites: insights from the detailed morphology of sediment Drift 7, Antarctica. *Geol. Soc. Spec. Publ.* 276, 95–110. <https://doi.org/10.1144/GSL.SP.2007.276.01.05>.
- Contourites. In: Rebesco, M., Camerlenghi, A. (Eds.), 2008. *Developments in Sedimentology*, 60. Elsevier, Amsterdam.
- Rebesco, M., Hernández-Molina, F.J., Van Rooij, D., Wåhlin, A., 2014. Contourites and associated sediments controlled by deep-water circulation processes: state-of-the-art and future considerations. *Mar. Geol.* 352, 111–154. <https://doi.org/10.1016/j.margeo.2014.03.011>.
- Riera, R., Bourget, J., Paumard, V., Wilson, M., Shragge, J., George, A.D., Borgomano, J., Wilson, T., 2019. Discovery of a 400 km<sup>2</sup> honeycomb structure mimicking a regional unconformity on 3-D seismic data. *Geology* 47 (12), 1181–1184. <https://doi.org/10.1130/G46484.1>.
- Riera, R., Bourget, J., Hakansson, E., Paumard, V., Wilson, M.E.J., 2021. Outcrops of a Middle Miocene tropical oligotrophic lagoon deposit sheds new light on the origin of the Western Australian coral reef province. *Palaeogeography, Palaeoclimatology, Palaeoecology* 576, 110501. <https://doi.org/10.1016/j.palaeo.2021.110501>.
- Rodrigues, S., Hernández-Molina, F.J., Kirby, A., 2021. A late cretaceous mixed (turbidite-contourite) system along the argentine margin: paleoceanographic and conceptual implications. *Mar. Pet. Geol.* 123, 104768 <https://doi.org/10.1016/j.marpetgeo.2020.104768>.
- Rodrigues, S., Hernández-Molina, F.J., Fonnesu, M., Miramontes, E., Rebesco, M., Campbell, D.C., 2022. A new classification system for mixed (turbidite-contourite) depositional systems: Examples, conceptual models and diagnostic criteria for modern and ancient



- records, *Earth-Science Reviews*, Volume 230, 104030, ISSN 0012-8252, <https://doi.org/10.1016/j.earscirev.2022.104030>.
- Romine, K.K., Durrant, J. 1996. Carnarvon Cretaceous-Tertiary Tie Report. Record 1996/036. Geoscience Australia, Canberra. <https://pid.geoscience.gov.au/dataset/ga/25187>.
- Romine, K.K., Durrant, J.M., Cathro, D.L., Bernardel, G., 1997. Petroleum play element prediction for the Cretaceous-Tertiary basin phase, Northern Carnarvon Basin. *APPEA J.* 37, 315–339. <https://doi.org/10.1071/AJ96020>.
- Ross, M.I. and Vail, P.R., 1994. Sequence stratigraphy of the lower Neocomian Barrow Delta, Exmouth Plateau, northwestern Australia. In: Purcell, P.G. and Purcell, R.R. (eds), *The Sedimentary Basins of Western Australia 1. Proceedings of the Petroleum Exploration Society of Australia Symposium*, Perth, 1994, 435–447.
- Roque, C., Duarte, H., Terrinha, P., Valadares, V., Noiva, J., Cachão, M., Ferreira, J., Legoinha, P., Zitellini, N., 2012. Pliocene and Quaternary depositional model of the Algarve margin contourite drifts (Gulf of Cadiz, SW Iberia): seismic architecture, tectonic control and paleoceanographic insights. *Marine Geology* 303–306, 42–62. <https://doi.org/10.1016/j.margeo.2011.11.001>.
- Sanchez, M. C., Fulthorpe S. C., Steel, J. R., 2012. Middle Miocene–Pliocene siliciclastic influx across a carbonate shelf and influence of deltaic sedimentation on shelf construction, Northern Carnarvon Basin, Northwest Shelf of Australia. *Basin Research*, Blackwell Publishing Ltd, European Association of Geoscientists & Engineers and International Association of Sedimentologists, vol. 24, 1–19. <https://doi.org/10.1111/j.1365-2117.2012.00546.x>.
- Sansom, P., 2018. Hybrid turbidite-contourite systems of the Tanzanian margin. *Pet. Geosci.* 24, 258–276. <https://doi.org/10.1144/petgeo2018-044>
- Scarselli, N., McClay, K., Elders, C. 2013. Submarine Slide and Slump Complexes, Exmouth Plateau, NW Shelf of Australia, in Keep, M. and Moss, S.J (Eds.), *Western Australian Basins Symposium 2013*, Aug 18-21 2013. Perth: Petroleum Exploration Society of Australia. <https://doi.org/10.1002/9781119500513.ch16>.
- Scarselli, N., McClay, K.R., Elders, C. 2020. Seismic examples of composite slope failures (Offshore North West Shelf, Australia). In: Ogata, K, Pini, G.A., & Festa, A. (eds.) *Submarine landslides: subaqueous mass transport deposits from outcrops to seismic*

- profiles. AGU Geophysical Monograph Series 246. <https://doi.org/10.1002/9781119500513.ch16>.
- Seggie, R.J., Lang, S.C., Marshall, N.M., Cubitt, C.J., Alsop, D., Kirk, R., Twartz, S., 2007. Integrated multi-disciplinary analysis of the Rankin Trend gas reservoirs, North West Shelf, Australia. *The APPEA Journal*, 47(1), 55–67.
- Seton, M., Müller, R.D., Zahirovic, S., Gaina, C., Torsvik, T., Shephard, G., Talsma, A., Gurnis, M., Turner, M., Maus, S., Chandler, M., 2012. Global continental and ocean basin reconstructions since 200Ma. *Earth Sci. Rev.* 113 (3–4), 212–270. <https://doi.org/10.1016/j.earscirev.2012.03.002>.
- Shanmugam, G., Spalding, T.D., Kolb, R.A., Lockrem, T.M., 1990. Deep-water bottom current reworked sand: their recognition and reservoir potential, northern Gulf of Mexico (abs.). *AAPG Bull.* 74, 762.
- Shanmugam, G., Spalding, T.D., Rofheart, D.H.M., 1993. Process sedimentology and reservoir quality of deep-marine bottom-current reworked sands (sandy contourites): an example from the Gulf of Mexico. *AAPG Bull.* 77, 1241–1259.
- Stagg, H.M.J.G.J., Colwell, J.B., 1994. The structural foundations of the Northern Carnarvon Basin. *Sediment. Basins West. Aust. Proc. Pet. Explor. Soc. Aust. Symp.* 349–364. Perth 1994.
- Stagg, H.M.J., Alcock, M.B., Bernardel, G., Moore, A.M.G., Symonds, P.A., Exon, N.F., 2004. Geological framework of the Outer Exmouth Plateau and adjacent ocean basins. *Geoscience Australia Record*, 2004/13, 160.
- Stow, D.A.V., Faugères, J.-C., Howe, J., Pudsey, C.J., Viana, A.R., 2002. Bottom currents, contourites and deep-sea sediment drifts: current state-of-art. In: In: Stow, D.A.V., Pudsey, C.J., Howe, J., Faugères, J.-C., Viana, A.R. (Eds.), *Deep-water Contourite Systems: Modern Drifts and Ancient Series, Seismic and Sedimentary Characteristics*, vol. 22. Geological Society, London, Memoir, 7–20. <https://doi.org/10.1144/GSL.MEM.2002.022.01.02>.
- Stow, D.A.V., Brackenridge, R., Hernandez-Molina, F.J., 2011. Contourite Sheet Sands: New Deepwater Exploration Target, *Search and Discovery Article #30182*.
- Tindale, K., Newell, N., Keall, J., Smith, N., 1998. Structural evolution and charge history of the Exmouth Sub-basin, Northern Carnarvon Basin, Western Australia. In: Purcell, P.G.,

- Purcell, R.R. (Eds.), *The Sedimentary Basins of Western Australia 2. Proceedings of the Petroleum Exploration Society of Australia Symposium*, 447–472.
- Uenzelmann-Neben, G., Gohl, K., 2012. Amundsen Sea sediment drifts: archives of modifications in oceanographic and climatic conditions. *Marine Geology* 299–302, 51–62. <http://dx.doi.org/10.1016/j.margeo.2011.12.007>.
- Van Rooij, D., De Mol, B., Huvenne, V., Ivanov, M.K., Henriët, J. P., 2003. Seismic evidence of current-controlled sedimentation in the Belgica mound province, upper Porcupine slope, southwest of Ireland. *Marine Geology* 195, 31–53. [https://doi.org/10.1016/S0025-3227\(02\)00681-3](https://doi.org/10.1016/S0025-3227(02)00681-3).
- Vandorpe, T., Van Rooij, D., Stow, D.A.V., Henriët, J. P., 2011. Pliocene to recent shallow water contourite deposits on the shelf and shelf edge off south-western Mallorca, Spain. *Geo-Marine Letters* 31, 391–403. <http://dx.doi.org/10.1007/s00367-011-0248-9>.
- Veevers, J.J., 2000. Change of tectono-stratigraphic regime in the Australian plate during the 99 Ma (mid-Cretaceous) and 43 Ma (mid-Eocene) swerves of the Pacific. *Geology*, 28 (1), 47-50. [https://doi.org/10.1130/0091-7613\(2000\)28%3C47:COTRIT%3E2.0.CO;2](https://doi.org/10.1130/0091-7613(2000)28%3C47:COTRIT%3E2.0.CO;2).
- Verdicchio, G., Trincardi, F., 2008. Mediterranean shelf-edge muddy contourites: examples from the Gela and South Adriatic basins. *Geo-Marine Letters* 28, 137–151. <http://dx.doi.org/10.1007/s00367-007-0096-9>.
- Viana, A.R., Faugères, J.C., Stow, D.A.V., 1998. Bottom-current-controlled sand deposits — a review of modern shallow- to deep-water environments. *Sediment. Geol.* 115 (1–4), 53–80. [https://doi.org/10.1016/S0037-0738\(97\)00087-0](https://doi.org/10.1016/S0037-0738(97)00087-0)
- Wynn, R.B., Masson, D.G., 2008. Sediment waves and bedforms. In: In: Rebesco, M., Camerlenghi, A. (Eds.), *Contourites, Developments in Sedimentology*, vol. 60. Elsevier, Amsterdam, 289–300. [https://doi.org/10.1016/S0070-4571\(08\)10015-2](https://doi.org/10.1016/S0070-4571(08)10015-2).
- Yeates, A.N., et al., 1987. The Westralian Superbasin: an Australian link with Tethys. In: McKenzie, K.G. (Ed.), *Shallow Tethys*, vol. 2. A. A. Balkema, Rotterdam, Netherlands, 199 – 213.
- Young, H.C., Lemon, N.M., Hull, J., 2001. The middle cretaceous to recent sequence stratigraphic evolution of the exmouth-barrow margin, Western Australia. *The APPEA Journal*, 41, 381–413. <https://doi.org/10.1071/AJ00018>.



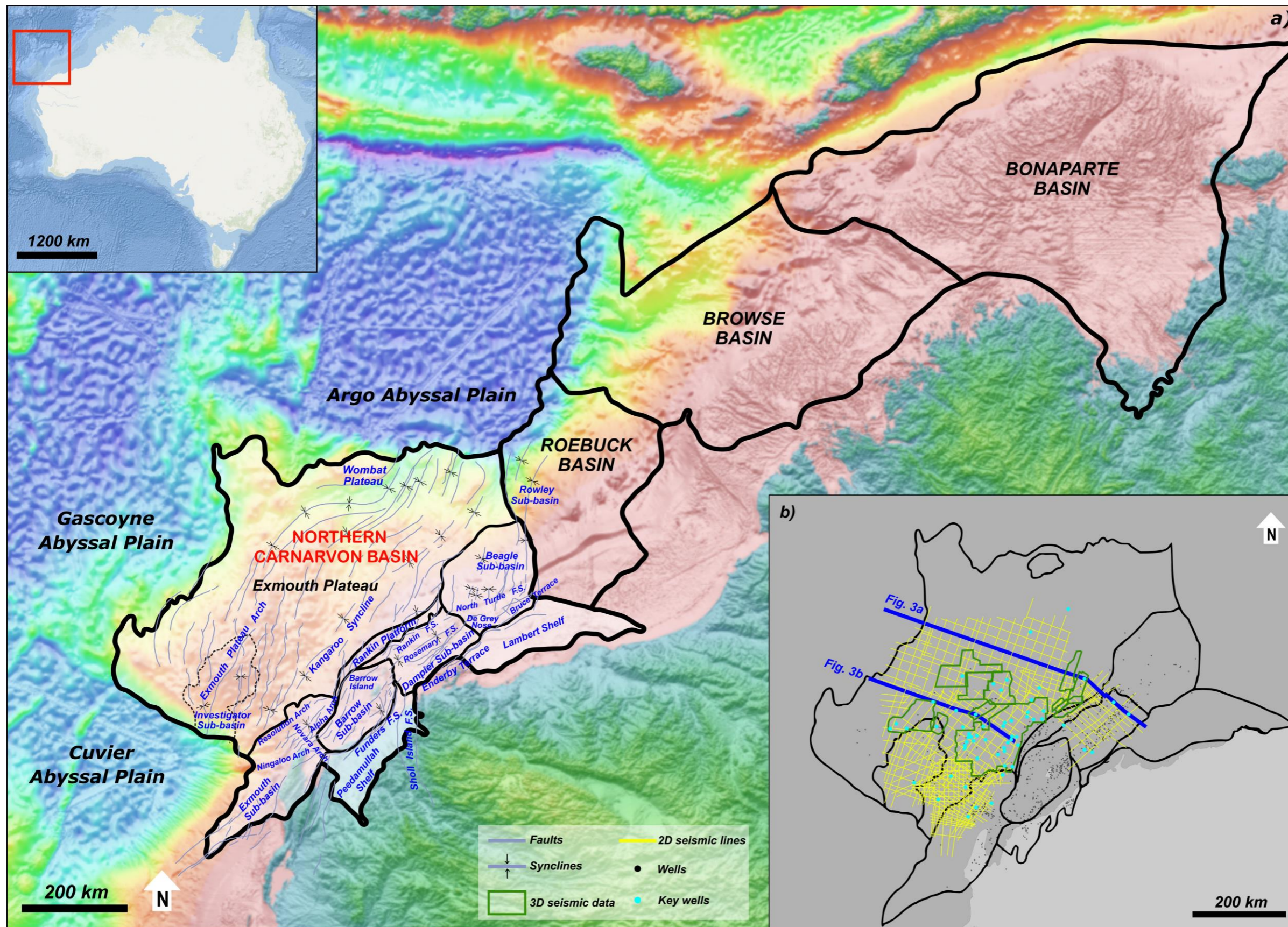


Fig. 1. a) Digital elevation and bathymetric map (Geoscience Australia, 2022) of Northwest Australia, showing the extent of the Northwest Shelf and the boundaries (black lines) that separate basins, sub-basins and other structural components. The trends of major faults and folds in the Northern Carnarvon Basin are shown in light blue. b) Seismic and well datasets that were utilised in this research. 2D lines are shown in yellow, the outlines of 3D surveys in green and the location of wells in blue.



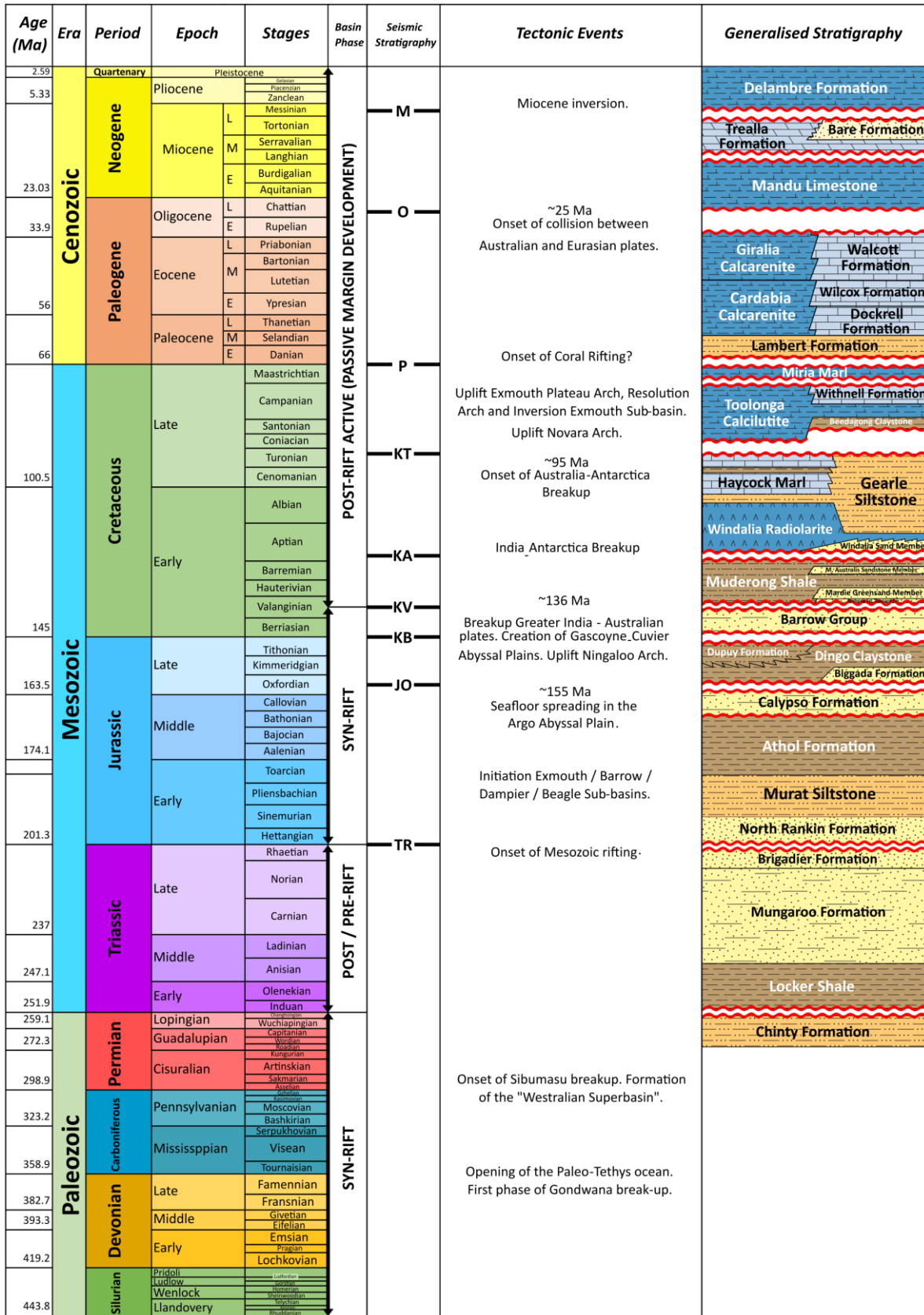


Fig. 2. Simplified stratigraphic diagram of the NCB compiled from Romine et al. (1997), Jablonski (1997), Longley et al. (2002), Cathro and Karner (2006), Gibbons et al. (2012), Marshall and Lang (2013), Gartrell et al. (2016), Paumard et al. (2018) and Geoscience Australia (2022) showing the relationship between unconformity bounded sequences and tectonic events. Sandstone formations shown in yellow, siltstones in orange, mudstones in brown, shelfal carbonates in light blue and deep marine carbonates in dark blue.

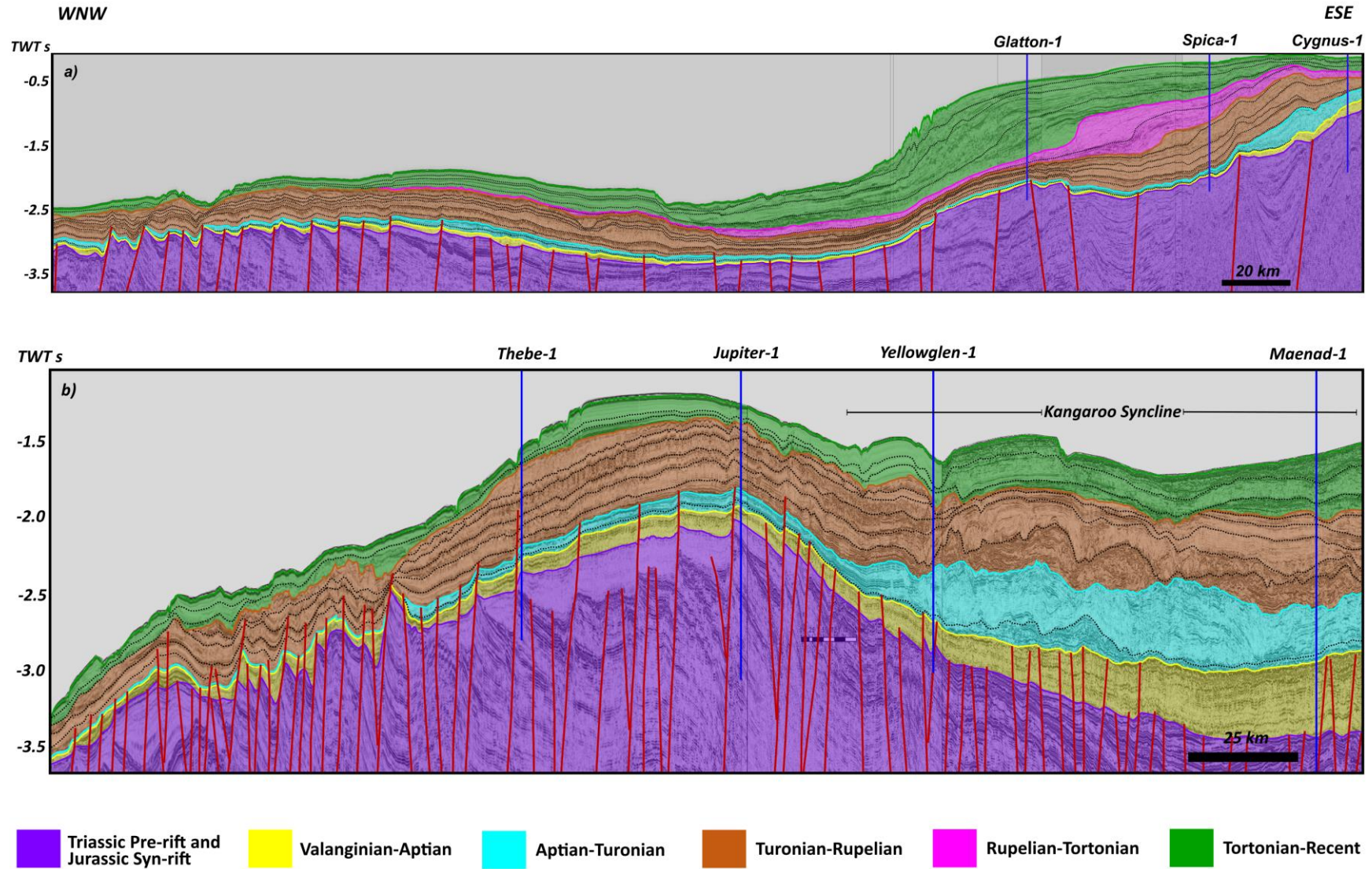


Fig. 3. WNW–ESE oriented regional seismic profiles from the Exmouth Plateau showing the Triassic – Earliest Cretaceous pre- and syn-extensional sequences in purple and the main seismic stratigraphic sequences that comprise the Cretaceous – Recent passive margin described in Chapter 2. See Figure 1a for the location of the seismic sections.



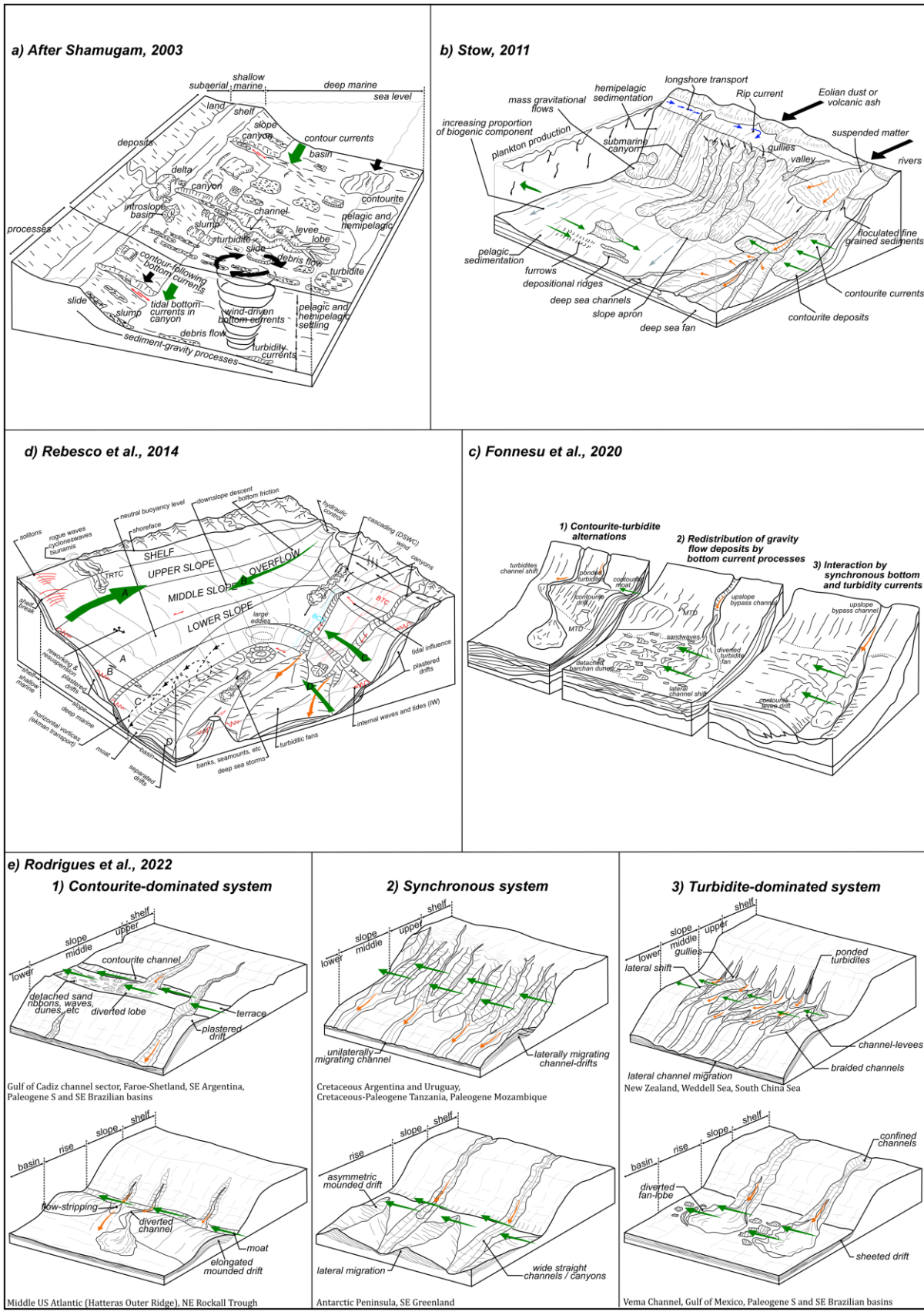


Fig. 4. The evolution of conceptual models for bottom current depositional systems showing the increasing emphasis placed on mixed depositional systems and a shift from the consideration of continental margins to a wider variety of slope settings.

---

*Chapter Two:*

*Regional Seismic Stratigraphic  
Framework and Depositional History of  
the Post-Valanginian Passive Margin  
Sequences in the Northern Carnarvon  
Basin, Northwest Shelf of Australia*

---



# Chapter Two: Regional Seismic Stratigraphic Framework and Depositional History of the Post-Valanginian Passive Margin Sequences in the Northern Carnarvon Basin, Northwest Shelf of Australia

---

## Research highlights

1. We provide a detailed seismic-stratigraphic framework for sequences above the Valanginian breakup unconformity on the Northwest Shelf of Australia.
2. We identify key depositional sequences and their constituent packages and interpret their associated environments of deposition.
3. A stable shelf environment existed from the Valanginian up to the Turonian.
4. From the Turonian until the Rupelian, deposition was influenced by high energy bottom currents which created incisions and sediment drifts.
5. From the Rupelian, the influence of bottom currents decreased and the progradation of clinoforms, combined with increased tectonic activity, resulted in widespread sediment instability and the development of mass-transport complexes.

## Abstract

The post-rift succession of the Northern Carnarvon Basin (north-western Australia) has commonly been interpreted as a relatively simple and uniform sequence that records a transition from siliciclastic to carbonate sedimentation deposited on a passive margin. However, given the significant vertical and lateral variation in seismic facies visible on seismic data, this interpretation likely oversimplifies the depositional history of the margin. Regional composite seismic lines that cross most of the basin, integrated with lithological and biostratigraphic information from exploration wells, provide the context for a better understanding of the depositional processes and environments that characterize the post-rift continental margin succession. We show that the sedimentary sequences deposited above the Valanginian breakup unconformity contain a wide variety of seismic facies that can be linked to a number of different marine depositional environments, with the greatest lateral variation occurring in the Turonian – Rupelian and in the Tortonian – Present. The former interval consists of three dominant seismic facies, namely polygonally faulted, incised, and

parallel bedded, which we interpret to indicate a lateral transition from an environment primarily dominated by fine-grained pelagic/hemipelagic deposition to one dominated by energetic bottom currents that created both depositional and erosional features, such as contourite drifts and associated moats. The latter interval is expressed by sigmoidal and continuous reflections which pass laterally into more chaotic reflection packages, which we interpret as clinoforms and mass-transport complexes (MTCs). The development of bottom currents may be connected to changes in circulation associated with the opening of oceans adjacent to the northwest margin of Australia, while the MTCs may indicate increased regional seismic activity and slope instability resulting from the development of collisional plate boundaries. Definition of these sequences highlights the significant changes that have occurred in the sedimentary processes that operated on the margin, and their potential link to its tectonic evolution.

## 1. Introduction

The Northern Carnarvon Basin (NCB) is a large sedimentary basin located in the southernmost part of the Northwest Shelf (NWS) of Australia (Fig. 1a and 1c). It is a prolific hydrocarbon basin with most of the plays, including source rocks and reservoirs, deposited during different phases of rifting between the Triassic and the Early Cretaceous (Geoscience Australia, 2015). Consequently, a large number of studies have investigated the syn-rift geological history of the basin (Romine and Durrant, 1996; Longley et al., 2002; Norvick, 2002; Jablonski and Saitta, 2004; Marshall and Lang, 2013). By comparison, relatively little is known about the post-rift sedimentary sequences deposited in Late Mesozoic and Cenozoic times. This knowledge gap is due to several factors that include: 1) limited and non-economic hydrocarbon prospectivity of the post-rift sequence, 2) limited availability of scientific and commercial boreholes with recovery in post-rift sequences, and 3) uncertainties in the regional correlation of depositional sequences due to variable local lithostratigraphic schemes and the presence of a large number of unconformities. Although regionally correlatable sequence stratigraphic boundaries have been identified (Marshall and Lang, 2013), this still leaves open many questions regarding the post-rift depositional history of the basin and the main processes driving sediment accumulation on the passive margin.

Recently acquired seismic data reveal the complexity of the post-rift interval, which is in contrast with existing, and often relatively simple, lithostratigraphic schemes (Geoscience Australia, 2015; well reports). Utilising regional 2D and 3D seismic reflection surveys integrated with well data, we investigate the lateral and vertical variation in seismic facies within and between previously recognised sequence stratigraphic boundaries to propose a seismic stratigraphic framework that accounts for the depositional environments and their spatial and temporal changes across the margin. The widespread availability of high quality seismic data and the variability of seismic facies makes the Northwest Shelf an excellent location to investigate the complexity of the sedimentary processes that operated on the deeper part of the continental margin and insights gained from this margin may be applied to other continental margins in similar settings.

## 2. Tectono-stratigraphic setting

The NCB lies at the southwest end of the NWS of Australia. It covers an area that encompasses the present-day shelf to the deep-water segment of the Exmouth Plateau (Fig. 1a), as far as the limit between the continental slope and the abyssal plain. The basin is divided into several sub-basins including the Exmouth, Barrow, Dampier and Beagle sub-basins (Fig. 1a), which contain Mesozoic and Cenozoic sequences that are more than 15 km thick (Bradshaw et al., 1988; Gartrell, 2000; Longley et al., 2002). The Exmouth Plateau is an area of distributed extensional faults that developed from the basin flanks to the edge of the abyssal plain (Fig.1a; Falvey and Veevers, 1974; Exon and Willcox, 1978; Barber, 1988; Scarselli et al., 2013). The NWS underwent a complicated tectono-stratigraphic evolution from the Late Paleozoic to Cenozoic associated with the breakup and separation of Gondwana (Audley-Charles et al., 1988; Bradshaw et al., 1988; Stagg and Colwell, 1994; Driscoll and Karner, 1998; Borel and Stampfli, 2002; Metcalfe, 2013; Reeve et al., 2016; Paumard et al., 2018). In the Late Permian to Triassic, following Permian extension, a large part of the basin was in the post-rift phase, predominantly characterised by thermal subsidence. The first phase of Mesozoic rifting occurred during the Late Triassic to Early Jurassic, resulting in the formation of sub-basins (Barber, 1988; Marshall and Lang, 2013; Paumard et al., 2018). During the middle Jurassic, the basin moved into the main rifting phase (Jablonski, 1997), which in some

places extended into the late Jurassic, culminating in Valanginian breakup between India and Australia (Etheridge and O'Brien, 1994).

The breakup led to the formation of a regionally recognised unconformity and correlative disconformity (the Valanginian Unconformity (Fig. 2), or K20.0 SB of Marshall and Lang, 2013) which is only locally associated with uplift and erosion (Tindale et al., 1998), such as that which formed the Ningaloo Arch (Fig. 1a; Tindale et al., 1998; Longley et al., 2002; Heine and Müller, 2005; Gibbons et al., 2012). A product of the erosion was the deposition of a deltaic sequence, identified as the Birdrong Sandstone or Upper Barrow Group (Arditto, 1993). Following this, rapid subsidence and sea level rise coinciding with the onset of seafloor spreading caused regional marine flooding, resulting in deposition of a condensed transgressive glauconitic sandstone (the Mardie Greensand) as well as an extensive marine transgression, which resulted in deposition of the Muderong Shale over most of the Northern Carnarvon Basin (Barber, 1988; Romine and Durrant, 1996; Longley et al., 2002; Norvick, 2002; Marshall and Lang, 2013). Between the Valanginian Unconformity and the Barremian, the Muderong Shale was initially deposited in a partially restricted marine embayment (Longley et al., 2002). During the Barremian, India drifted northward creating more open seaways. This, combined with continued subsidence over the entire Northwest Shelf (Jablonski and Saitta, 2004) resulted in ongoing deposition of the Muderong Shale until the Aptian in an open marine environment (Romine and Durrant, 1996).

By the Aptian, the separation of India, as well as the onset of the separation of Antarctica from Australia, established unrestricted oceanic circulation around the Indian plate (Longley et al., 2002; Jablonski and Saitta, 2004). This caused upwelling and enhanced the productivity of radiolaria (Ellis, 1987; Longley et al., 2002), leading to deposition of the Windalia Radiolarite (Fig. 2; Bradshaw et al., 1988). From the Turonian to Campanian, Antarctica – Australia breakup continued to develop along the southern margin of Australia (Romine and Durrant, 1996). This has been linked to compression in the NCB (Longley et al., 2002; Norvick, 2002; Jablonski and Saitta, 2004), resulting in uplift and structural inversion in the Exmouth sub-basin expressed by the initiation of the Novara Arch in the early Santonian and the Resolution Arch in the earliest Campanian (Fig. 1a and 2; Tindale et al., 1998). In addition, transpression reactivated pre-existing rift structures and created features such as Barrow Island (Fig. 1b; Bradshaw et al., 1998; Tindale et al., 1998).

During the Cenozoic, sedimentation in the NCB was dominated by progradation of carbonate systems along the length of the margin, which developed in warmer water conditions (Apthorpe, 1988; Romine et al., 1997; Longley et al., 2002; Keep et al., 2007). This allowed the formation of an extensive carbonate shelf which continued to develop until the present day, interrupted during the Paleocene by a period of cool-water carbonate deposition in a shallow marine environment, which resulted in the deposition of the Dockrell Formation (Norvick, 2002). The shelf carbonates pass seawards through slope facies into condensed, deep-water carbonates and marls (Norvick, 2002).

In the earliest Eocene, a brief clastic influx occurred in some areas of northwestern Australia (Pattillo and Nicholls, 1990; Whittam et al., 1996). This was followed by further phases of shallow marine carbonate shelf progradation which formed the Giralia Calcarenite and Walcott Formation (Norvick, 2002). The progradation of carbonates continued with deposition of the Oligocene to Middle Miocene Mandu Limestone and the Middle Miocene Trealla Limestone (Heath and Apthorpe, 1984; Tindale et al., 1998). In the Miocene, collision of the Australia – India and Eurasia plates contributed to a major compressional event (Longley et al., 2002). This led to inversion in the Late Miocene causing unconformities in the Trealla Limestone and Bare Formation. Carbonate growth in the Trealla Limestone was interrupted by deposition of dolomitic siliciclastic sands of the Bare Formation, which were fed by a delta system (Sanchez et al., 2012; Cathro et al., 2003). The margin remains tectonically active, expressed by the development of the Exmouth Plateau Arch and extensive slope instability, as demonstrated by the widespread development of slides, slumps, mass flows, turbidity currents and debris flows (Jablonski, 1997; Müller et al., 1998; Longley et al., 2002; Cathro and Karner, 2006; Gibbons et al., 2012; Marshall and Lang, 2013; McCormack and McClay, 2013; Scarselli et al., 2013; Gartrell et al., 2016; Paumard et al., 2018). Seismically, these events are clearly captured by contorted and chaotic seismic facies, and some grooves or incisions (Hengesh et al., 2012; Scarselli et al., 2013; Paumard et al., 2019). Widespread mass-transport deposits occur within the Delambre Formation, which was deposited from the Pliocene to Recent (Heath and Apthorpe, 1984; Butcher, 1989).

### 3. Data and methodology

This research uses public domain 2D and 3D seismic reflection and well data that are available from the NOPIMS (National Offshore Petroleum Information Management System) and WAPIMS (Western Australian Petroleum and Geothermal Information Management System) databases (Fig. 1b). Seismic data acquired for petroleum assessment cover almost all the NCB, an area of approximately 139,960 km<sup>2</sup>. 19 2D and 21 3D seismic surveys of different vintages were used for seismic interpretation. The acquisition and processing history of the seismic surveys is summarised in Table 1. In general, pre-stack time-migrated seismic sections provide high-quality images, typically with a 4 ms sampling interval. A mistie correction was applied to each survey by applying a vertical correction factor using the 3D data as a reference. Approximately 40 wells were selected close to seismic lines to provide stratigraphic and lithological constraints on seismic interpretation. It is important to note that the wells mostly targeted Jurassic and Triassic intervals. Consequently, lithological, well log and biostratigraphic data is sparse in the post-Valanginian sequences.

Seismic stratigraphic interpretation was carried out following the principles of Mitchum et al. (1977a, 1977b). Sixteen horizons were selected based on the recognition of unconformities, reflection terminations, prominent seismic characteristics, and lateral continuity. In addition, seismic facies analysis allowed characterisation of their associated units, based on internal reflector geometries, amplitude, and stacking patterns of reflection sets (Table 2). The interpretation was also controlled by closing loops within the seismic grid to eliminate misties. The horizons were tied to four wells (Cygnus- 1, Guilford-1, Yellowglen-1 and Orthrus-1; Fig. 1b and 3). In addition, thirty-six other wells lying up to 20 km from the lines were used to further constrain the correlation (see well cross-section in Fig. 6). A combination of micropaleontological and palynological reports from the four wells were used to assign biostratigraphic ages to the interpreted horizons. The horizons are named K0-K5 and T1-T10 using a simple alphanumeric nomenclature, with K corresponding to Cretaceous, T to Cenozoic, and the numbers representing the age, from old to young (Fig. 2, 3 and 4). The majority of these horizons are equivalent to the boundaries given by Longley et al. (2002), Marshall and Lang (2013) and Geoscience Australia (2015), but additional surfaces were also interpreted where significant changes in sedimentary style were observed.

The regionally correlatable seismic markers were used to define units based on the similarity of dominant seismic facies and hence do not always correspond to the play-based

sequences of Marshall and Lang (2013). K0 represents the Valanginian Unconformity which marks the beginning of post-rift sedimentation and the development of a widespread transgressive unit that can be easily correlated over large parts of the NW Shelf resulting in the establishment of a widespread fully marine shelf (Barber, 1988; Romine and Durrant, 1996; Longley et al., 2002; Norvick, 2002; Marshall and Lang, 2013). The top of the Muderong Shale (Horizon K1) marks the onset of much more variable seismic facies. Consequently, the sequence above this is divided into four primary units which are Unit 1: Aptian – Turonian  $\approx$  K40.0 SB – K50.0 SB (Early to Late Cretaceous), Unit 2: Turonian – Rupelian  $\approx$  K50.0 SB – T30.0 SB (Late Cretaceous to Early Oligocene), Unit 3: Rupelian – Tortonian  $\approx$  T30.0 SB – T40.0 SB (early Oligocene to late Miocene) and Unit 4: Tortonian – Present  $\approx$  T40.0 SB – Recent SB (late Miocene to Present) (Fig. 2, 3 and 4).

The main surfaces were depth converted using the average interval velocity of each unit compiled from checkshot and vertical seismic profile (VSP) data from 10 wells. The interval velocities used range from 1712.06 m/s for Unit 1 (the oldest unit), through 1639.99 m/s for Unit 2 and 1571.87 m/s for Unit 3 to 1515.80 m/s for Unit 4 (the youngest unit). The velocity of seawater is between 1490-1500 m/s. Isopach maps for each unit were derived from the maps of the main surfaces. Seismic facies maps of the primary units illustrate the distribution of different facies. The facies maps combined with well data (GR, cores, lithology, biostratigraphy and palynology) were used to determine depositional environment. Together these are utilised to describe the post-Valanginian evolution of the passive margin.

#### 4. Regional seismic stratigraphic framework

The sequence between the Valanginian Unconformity and the base of Unit 2 mainly comprises fine-grained clastic sediments, while Units 2 to 4 are predominantly composed of fine-grained carbonates (Cathro, 2002; Moss et al., 2004; Chongzhi et al., 2013; and ditch cuttings from wells in the Exmouth Plateau), but also include siliciclastic sediments of early Paleocene and late Miocene age (Fig. 2, 3, 4, and 6).

K0 to K1 (Early post-rift) represents the Valanginian to Aptian stratigraphic interval, equivalent to K20.0SB to K40.0 SB (Fig. 2b and 3) of Marshall and Lang (2013). Over large parts of the Exmouth Plateau this interval is only a few metres thick (Fig. 7a), and thins and onlaps onto the remnant paleobathymetric expression of rotated fault blocks to the north and west

(seismic line A and C on Fig. 4). Significant depocentres with up to 650m of sediment are present in the Dampier sub-basin and in a bathymetric low in front of the Lower Barrow Shelf Edge (Fig. 7a). A more subtle depositional lobe associated with the Upper Barrow shelf is present on the NW margin of the Exmouth sub-basin. Over almost the entire area this interval is characterised by parallel to subparallel reflections (PrSp) and polygonal faults (Pf), with low angle progradational and aggradational clinoforms (Pg/Ag) present in the lower part of the sequence in the vicinity of Upper Barrow Shelf (Fig. 7b). Lithologically this interval corresponds to the Muderong Shale, with the lower parts laterally equivalent in the southeast to the Zeepard and Birdrong Formations of the Upper Barrow Group and to the Mardie Greensand Formations.

#### 4.1. Unit 1 – Horizons K1-K3 (~123.3 Ma Aptian – ~95 Ma Turonian)

Unit 1 conformably overlies the Muderong Shale. It is bounded at its base by horizon K1 (K40.0 SB of Marshall and Lang, 2013), and its top by horizon K3 (K50.0 SB of Marshall and Lang, 2013). It is divided into two sub-units (1a and 1b) by horizon K2. It is less than 150 m thick over most of the Exmouth Plateau (Fig. 8a). A distinct sediment accumulation in the southeast of the NCB, centred over the Exmouth sub-basin, and running over the basin flank to the northwest, is up to 700 m in thickness (Fig. 8a).

Horizon K1 is mostly a high amplitude, laterally continuous reflection that also locally onlaps onto rotated fault blocks in the northwest of the Exmouth Plateau (seismic line A and C on Fig. 4). Horizon K3 is a medium amplitude reflection that is generally conformable but forms a prominent unconformity in the southeast in the vicinity of the depocentre (Fig. 9). Horizon K2, which marks the boundary between sub-units 1a and 1b, is a low amplitude, conformable reflection that onlaps and downlaps onto horizon K1 at the edge of the depocentre (Fig. 9).

The dominant seismic facies of Unit 1 within the depocentre is characterised by subparallel to wavy (SpWv), medium to high amplitude reflections (Fig. 8b), indicating the presence of subtle bedforms, which combined with the increased sediment thickness, may correspond to sediment mounds. Subparallel reflections mostly appear in sub-unit 1a (horizons K1-K2) and wavy reflections are more developed in sub-unit 1b (horizons K2-K3). Away from the depocentre Unit 1 consists of parallel to subparallel (PrSp) seismic reflections



(Fig. 8b), with a zone of parallel (Pr) reflections (Fig. 8b) in the southern part of the study area, showing more uniform deposition.

In wells, horizon K1 corresponds to the top of the Muderong Shale Formation (Fig. 5 and 6). K1 is the most laterally consistent reflector and is present over the whole basin. Deposition of the Muderong Shale terminated in the Aptian (Romine and Durrant, 1996; Longley et al., 2002; Norvick 2002; well reports), and the top of this unit (K1) is also referred to as the Intra-Aptian Unconformity. However, for the most part it is conformable, apart from where it onlaps rotated fault blocks, or where there is a time gap generated by the onlap of sub-unit 1a.

Sub-unit 1a coincides with radiolarian-rich sediment in most wells (Fig. 3, 5 and 6), corresponding to the Windalia Radiolarite (Ellis, 1987; Bradshaw et al., 1988; Longley et al., 2002). This formation developed regionally until the latest Aptian or earliest Albian (Longley et al., 2002; Jablonski and Saitta, 2004). The top of this sub-unit corresponds to horizon K2. Horizon K3 is the top of sub-unit 1b and ties to wells at the top of the Lower Gearle Siltstone and the Haycock Marl intervals (Fig. 3, 5 and 6). These formations were deposited during the Turonian. The Lower Gearle Siltstone generally consists of siltstones and shales but passes laterally into marls in the Haycock Marl (Romine and Durrant, 1996).

#### 4.2. Unit 2 – Horizons K3-T4 (~95 Ma Turonian – ~30 Ma Rupelian)

Unit 2 is separated from Unit 1 by horizon K3 at the base and is bound by horizon T4 (T30.0 SB of Marshall and Lang, 2013) at the top. It encompasses six seismic sequences and contains up to 550 m of sediment over most of the NCB (Fig. 10a). Specific depocentres in the centre of the Exmouth Plateau, and at the northern margin of the Dampier sub-basin contain sediments up to 800 m in thickness (Fig. 10a) and may in part correspond to large scale sediment drifts (Fig. 11a).

The six seismic sequences in Unit 2 are bounded by horizons K4, K5, T1 (K60.0 SB, T10.0 SB, T20.0 SB of Marshall and Lang, 2013, respectively), and by horizons T2, T3 and T4 (T30.0 SB). In general, the seismic horizons are characterised by relatively constant amplitude reflections in the northwest and northern area of the Exmouth Plateau and in the area surrounding the Investigator sub-basin (Fig. 1a), where they are correlated using consistent stratigraphic markers from wells. In these areas, the sequences are characterised by

conformable, laterally continuous reflections of medium-high amplitude that are disrupted by a series of small offset faults (Fig. 12). In contrast, in the southeast of the area, near the Exmouth sub-basin and Rankin Platform, the equivalent surfaces are marked by complex stacked erosional truncations. The sequences within this area are also characterised by irregularly stacked incisions (Fig. 13). In addition, horizons T2, T3 and T4 represent downlap surfaces of low amplitude in the northeast area near the Dampier sub-basin (Fig. 14).

Unit 2 contains a great variety of seismic facies. The most common acoustic facies are the semi-continuous or parallel disrupted reflections with small offset faults, similar to those described as polygonal faults (Cartwright, 1994; Watterson et al., 2000). The polygonal faults (Pf) show a variation of styles with different degrees of rotation and disruption of the beds (Fig. 12). The faults are present in all six seismic sequences over a large part of the NCB but are mainly seen in the north and west (Fig. 10b, c, d). However, the polygonal faulted facies is less prominent in the older sequences in the south. Polygonal faults typically form in fine-grained sediments, indicating that this is the dominant lithology in these areas. The second most common acoustic facies is incised (IncErs) reflections (Fig. 10b, c, d, and Fig. 13). The reflections are characterised by simple incisions and complex stacked erosional truncations, which overlie and crosscut one another. The erosional surfaces are associated with mounded reflections (Fig. 15), representing a composite of both erosional and depositional features, comparable to similar features described by Hernández-Molina et al., 2003, 2006 from Gulf of Cadiz. The incised reflections are progressively replaced by parallel (Pr) and parallel to subparallel (PrSp) reflections, going up sequence from sub-units 2c to 2f (Fig. 10b, c, d). In addition, parallel and parallel to subparallel reflections also appear in the Dampier sub-basin, Rankin Platform, and in the northwest at the edge of the Exmouth Plateau. The parallel reflections change laterally into the subparallel to wavy (SpWv) reflections in sub-units 2e and 2f (Fig. 10d). In the northeast of the Exmouth Plateau near the Dampier sub-basin, seismic reflectivity in sub-units 2e and 2f is expressed by downlapping reflections that show the initial growth of clinofolds which are more significantly developed in Unit 3 and 4.

Horizon K4 at the top of sub-unit 2a is close to the top of the Upper Gearle Siltstone and the Toolonga Calcilutite in most available wells (Fig. 3, 5 and 6). These formations were deposited during the latter part of the Turonian and the Campanian. The lithology of the Upper Gearle Siltstone is similar to the Lower Gearle Siltstone, but it is more widespread and typically unconformably overlies the Lower Gearle Siltstone. In the northern part of the NCB,

the Gearle Siltstone is generally thin, and it is replaced by the Toolonga Calcilutite. Lithologically, the Toolonga Calcilutite contains carbonate-rich sediments. The top of sub-unit 2b at horizon K5 is assigned to the top of the Withnell Formation and the Miria Marl, which together developed during the latter part of the Campanian and the Maastrichtian (Fig. 3, 5 and 6). The Withnell Formation primarily consists of fine-grained limestones but corresponds to marls in the Miria Marl. The Miria Marl interval is thin, and sometimes it is not differentiated from the Withnell Formation. The top of sub-unit 2b (K5) is referred to as the Base Tertiary Unconformity.

In most wells, the top of sub-unit 2c (T1) corresponds to the top of the Lambert and Dockrell Formations, which developed in the Paleocene (Fig. 3, 5 and 6; Romine and Durrant, 1996; Cathro, 2002; Payenberg et al., 2013; Geoscience Australia, 2015; well reports). The Lambert Formation mainly contains claystone, but the Dockrell Formation is more marly (Romine and Durrant, 1996; Alrefaee et al., 2018; Cathro, 2002; well reports). Meanwhile, the top of sub-unit 2d at horizon T2 corresponds to the top of the Wilcox and Cardabia Formations that were deposited in the early and middle Eocene (Fig. 3, 5 and 6; Romine and Durrant, 1996; Cathro, 2002; Payenberg et al., 2013; Geoscience Australia, 2015; well reports). The Wilcox Formation consists of marls, and the Cardabia Formation contains relatively condensed fine-grained carbonates. Sub-units 2e (with its top at T3) and 2f (with its top at T4) are correlated to the Giralia Formation but in the northern and southwestern parts of the NCB they correspond to the laterally equivalent Lower Walcott Formation in sub-unit 2e which can be distinguished from the Upper Walcott Formation in sub-unit 2f. These formations were deposited in the middle Eocene and the early Oligocene. Lithologically, the Giralia Formation is similar to the Cardabia Formation, while the Walcott Formation consists of foraminiferal limestones and calcareous siltstone. The top of sub-unit 2f (T4) is referred to as the Oligocene Unconformity.

#### 4.3. Unit 3 – Horizons T4-T6 (~30 Ma Rupelian – ~7Ma Tortonian)

The third seismic stratigraphic unit downlaps onto horizon T4 at the top of Unit 2 and is bounded by horizon T6 (T40.0 SB of Marshall and Lang, 2013) at its top (Fig. 18a). It is subdivided by horizon T5 into two seismic sequences (sub-units 3a and 3b). Overall, Unit 3 is less than 100 m thick, and it is mostly confined to the northeast of the NCB (Fig. 16a). A

significant depocentre occurs in the northern part of the Dampier sub-basin and the Rankin Platform, containing sediments up to 550 m in thickness (Fig. 16a).

Horizons T5 and T6 are unconformable reflections of medium-high amplitude that form downlap surfaces. Seismic reflectivity in sub-unit 3a is characterised by steeply downlapping simple sigmoid reflections (Fig. 18a), while sub-unit 3b presents more complex sigmoid geometries with gentle to high angle downlapping reflections (Fig. 18a). In general, the clinofolds in Unit 3 show strongly progradational (Pg) stacking patterns (Fig. 18a) and appear primarily in the area of the Rankin Platform and the Dampier sub-basin (Fig. 16b). This acoustic facies passes laterally into parallel to subparallel (PrSp) reflections in more distal areas (Fig. 16b), and then into semi-chaotic (SmCh) reflections that downlap onto horizon T4 (Fig. 16b). These seismic characteristics are evidence of submarine mass failure events.

In most wells, sub-unit 3a correlates to the Mandu Formation of late Oligocene and early Miocene age (Fig. 3, 5 and 6). This deposit consists of both coarse and fine-grained carbonate sediment including some reef facies (Tortopoglu, 2015; Alrefaee et al., 2018). Sub-unit 3b corresponds to the Trealla and Bare Formations, which were deposited during the Middle and Late Miocene (Fig. 3, 5 and 6). The uppermost part of the Trealla Limestone passes laterally into sands of the Bare Formation.

#### 4.4. Unit 4 – Horizons T6-T10 (~7Ma Tortonian – 0 Ma Present)

Unit 4 is the youngest seismic stratigraphic unit and it unconformably overlies horizon T6 of Unit 3 in the northeast and horizon T4 of Unit 2 in the remainder of the NCB. Its top is horizon T10 (seabed). Unit 4 comprises four seismic sequences, which contain sediment up to 350 m thick over most of the area (Fig. 17a). A distinct depocentre in the northeast part of the Rankin Platform has more than 650 m of sediment (Fig. 17a).

Horizons T7, T8, T9 are unconformable reflections of medium-high amplitude, expressed by downlap surfaces in the northeast (Fig. 18b). Here, the surfaces separate four sub-units (4a-4d) characterised by downlapping reflections (Pg in Fig. 17b, c) with complex sigmoidal geometries. In contrast, in the northern and southern part of the area all the horizons are semi-continuous and continuous reflections of low-medium amplitude (Fig. 18b), and the main acoustic facies of all the sub-units comprise chaotic reflections (Ch: Chaotic, SmCh: Semi Chaotic and PrCh: Parallel to Chaotic in Fig. 17b, c), parallel (Pr) and parallel to

subparallel (PrSp) reflections (Fig. 17b, c). The clinoforms in Unit 4 are mainly progradational and slightly aggradational. In the shelf break areas, the clinoforms are overlain and crosscut by gullies or channels on slopes (Fig. 19). The chaotic acoustic facies is more widespread in sub-units 4a to 4c (Ch: Chaotic, SmCh: Semi Chaotic and PrCh: Parallel to Chaotic in Figure 17b) and much less extensive in sub-unit 4d (Fig. 17c). This wide distribution of chaotic facies shows multiple mass failure events that happened at the time of deposition. Besides, sub-unit 4d is characterised by parallel (Pr) and parallel to subparallel (PrSp) reflections (Fig. 17b, c). However, on the northwest at the edge of the Exmouth Plateau, it is expressed by subparallel to wavy (SpWv) reflections that developed from sub-units 4a to 4d (Fig. 17b, c).

Unit 4 corresponds to the Delambre Formation in most available wells (Fig. 3, 5 and 6). This formation was deposited during the late Miocene to Recent. Lithologically, the Delambre Formation is similar to the Mandu Formation (Tellez, 2015; Alrefaee et al., 2018).

## 5. Evolution of the Post-Valanginian Sequence in the NCB

From the integration of seismic and well data, we are able to demonstrate four distinct phases in the post-rift evolution of the Northern Carnarvon Basin: an initial phase of subsidence from the Valanginian to the Turonian, a period from the Turonian to the Early Oligocene dominated by bottom current activity in parts of the basin, the establishment of prograding carbonate shelves in the Late Oligocene to Late Miocene and the widespread development of mass transport complexes from the Late Miocene to Present.

### 5.1. *Valanginian to Turonian: Post Breakup Subsidence*

During the Berriasian, prior to breakup, the NCB was characterised by the Lower Barrow Group which comprises a clastic shelf located in the south east portion of the basin, turbidite fans fed by southerly derived turbidity currents and laterally equivalent distal muds which accumulated in deeper water settings to the northwest (Paumard et al., 2018).

As a consequence of Valanginian breakup, sediment supply from the south was terminated marking the end of deposition of the Lower Barrow Group. However, uplift and erosion in the Exmouth sub-basin resulted in the deposition of a separate deltaic sequence referred to as the Upper Barrow Group (Arditto, 1993). This is succeeded in the Hauterivian by the glauconitic Mardie Greensand Member which represents a significant phase of transgression as relative sea level begun to rise on the subsiding continental margin

(Geoscience Australia, 2015). The transgression continued during the Aptian, resulting in the deposition of the Muderong Shale (Romine and Durrant, 1996; Longley et al., 2002; Norvick, 2002; Marshall and Lang, 2013), which is clearly imaged on seismic sections, showing generally continuous reflections with high to medium amplitudes. Further marine transgression continued through the deposition of Unit 1 in the Aptian – Turonian, where deposition of the Windalia Radiolarite occurred during the Aptian (Bradshaw et al., 1988). This unit resulted in widespread deposition of fine-grained sediment represented by parallel and subparallel seismic facies. However, the development of mounded features characterised by wavy seismic facies in the southeast part of the basin suggests the initiation of bottom current activity and the development of large scale mounds in this part of the shelf (Stow et al., 2009; Rebesco et al., 2014).

#### *5.2. Turonian to Early Oligocene: Bottom Current Activity*

Horizon K3 (or K50.0 SB) marks a significant change in the style of deposition, characterised by stacked incisions and sediment mounds which are laterally equivalent to more uniform beds (polygonally faulted sequences) elsewhere in the basin. The complex stacked incision seismic facies is likely evidence of energetic bottom currents while the polygonally faulted sequences generally form in fine-grained sediments (Cartwright et al., 2003) and represent a continuation of a low energy environment. This bimodal distribution of facies continues through the whole of the Turonian – Rupelian stratigraphic interval represented by Unit 2.

Ocean bottom currents promote the formation of erosional surfaces as well as depositional features, such sediment drifts and bedforms, with different geometries and dimensions (Stow et al., 2002; Rebesco et al., 2014; Ercilla et al., 2016) depending on the velocity of the currents and the availability of sediments (Masson et al., 2004; Hernández-Molina et al., 2006; Stow et al., 2009). During the Late Cretaceous (sub-unit 2ab), large scours and sediment mounds as well as numerous smaller irregular scours were developed in the southeast of the Exmouth Plateau near the Rankin Platform and Exmouth sub-basin (Fig. 10b, 11a, 13). The largest depressions are visible on the basal surface of Unit 2 (horizon K3, Fig. 11a) and dissect the large-scale mounds developed towards the top of Unit 1. The largest depression is 221 km long and up to 67 km wide. The base of these depressions are partially

erosional, and partially depositional (Fig. 11a) implying that the currents redistributed and transported fine-grained sediments on either side of the depression to form smaller scale sediment mounds (Rebesco and Stow, 2001; Stow et al., 2002; Rebesco 2005; Hernández-Molina et al., 2008).

These depressions are filled by multiple stacked sediment bodies which are characterised by parallel and subparallel beds (Fig. 10b, c, d, and Fig. 15a). They are also cut by multiple irregular scours which become increasingly common in the younger sequences and further down slope towards the north-east. The scours comprise multiple and cross cutting V and/or U-shaped incisions typically 2.5 km in width and 25 km in length, the largest of which are up to 6.5 km in width (horizons K4-K5, Fig. 15). We interpret these as sediment waves and contourite channels, indicating the presence of energetic bottom currents. These structures have also been recognised and similarly interpreted by Nugraha et al. (2019).

Erosive currents persisted into the Paleogene, particularly in the north of the area near the Rankin Platform. In addition, circular features are also visible on the base Paleogene surface (horizon T3, Fig. 15b and horizon T4 Fig. 11b) in the areas covered by 3D data. In cross section, the features are similar to the elongate V-shaped incisions described above (Fig. 15b), but are conical in shape and are similar to those described by Imbert and Ho (2012). These structures are common in part of the Exmouth Plateau near the Rankin Platform, and they are variable in size. The largest are 5 km in diameter and are filled by chaotic sediment packages. They lack the sediment drifts associated with erosive incisions and we interpret these features either as large pockmarks caused by fluid escape or the result of deep water carbonate dissolution.

The erosive current activity is much more pronounced in the southeast of the Exmouth Plateau near the Rankin Platform and represents significantly different conditions to those in the remainder of the Exmouth Plateau where uniform polygonal faulted sediments were deposited. The reason for this is unclear, but one possible explanation might relate to the development of currents associated with the increasing separation of India from Australia. The onset of high energy current activity occurs in the Turonian, following a dramatic increase in the north-westward drift of India that began in the Albian (Veevers, 2000). This potentially enlarged oceanic circulation along the north-western margin of Australia, creating the potential for significant current activity on the NWS. Changes in relative sea level may also have influenced sedimentary processes but increases in the rate of tectonic subsidence in the

Late Cretaceous (around 95 Ma and 65 Ma; Müller et al., 1998) and in the Paleogene (Romine and Durrant, 1996) are not coincident with any of the changes in sedimentary processes observed on the NWS. Similarly, there is no clear evidence that the Oligocene dissolution features formed at a time when there was a global sea level fall (Miller et al., 1991; Romine and Durrant, 1996).

### 5.3. *Late Oligocene to Late Miocene: Carbonate Shelf*

Another significant change occurs at horizon T4 (or T30.0 SB), which marks the cessation of bottom current activity and the onset of clinoform sequences during the Oligocene and Miocene, the dominant seismic facies of Unit 3. Full separation between Australia and Antarctica along the southeastern margin developed at this time (Gibbons et al., 2015) and may have further modified circulation with the development of new currents around the Southern Ocean. The clinoforms are mainly progradational and are consistent with the deposition of carbonates during subsidence which occurred during the Rupelian – Tortonian interval (Romine and Durrant, 1996; Longley et al., 2002; Marshall and Lang, 2013). In addition, slope instability associated with more steeply dipping clinoforms resulted in slumps or mass-transport complexes (MTCs) in more distal areas. These features are clearly seen on seismic data, illustrated by semi-chaotic seismic facies within Unit 3 (Fig. 16b and 18a). However, the limited extent of Unit 3 is probably associated with the limited extent of shelf deposition, causing the sediments to downlap and onlap onto the top of Unit 2.

### 5.4. *Late Miocene to Present: Mass Transport Complexes*

The development of clinoforms, slumps and MTCs is much more widespread in Unit 4, starting from the late Miocene horizon T6 (or T40.0 SB) and particularly well developed in sub-units 4a-4c. Like Unit 3, clinoforms mainly occur in the northeast of the Rankin Platform, are mostly progradational and slightly aggradational.

Slope failures in the Exmouth Plateau are particularly common and are found in areas around the Kangaroo Syncline, the Resolution Arch and the Exmouth Plateau Arch (Fig. 17a, d). Hengesh et al. (2012) and Scarselli et al. (2013, 2020) studied the sediment collapses within the Neogene – Recent section on the SE and NW flanks of the Exmouth Plateau Arch e.g., the Glencoe and Chadon complexes of Hengesh et al. (2012), and the Thebe and Bonaventure



complexes of Scarselli et al. (2013), as well as along the shelf break on the inboard margin of the Exmouth Plateau (e.g. Willem and Gorgon complexes, Fig. 17d). Slope failures in the Exmouth Plateau occurred in water depths ranging from 200-300 m at the shelf edge and adjacent to the deeper water parts of the NCB in water depths of more than 1500 m (Hengesh et al., 2012).

MTCs are associated with slope instability associated with the development of large clinoforms at the shelf slope break, and by increasing slope gradients in areas around the Resolution and Exmouth Plateau arches as a result of Miocene to Recent compression (Hengesh et al., 2012; Scarselli et al., 2013). The Exmouth Plateau Arch only becomes visible on sediment thickness maps in Unit 4 (Figs. 7, 8 and 17) suggesting that it only developed from the Late Miocene onwards. Earthquake activity and increased slope angles caused instability in poorly consolidated sediments (i.e., fine-grained sediment of the Delambre Formation), while increased lateral loads and decreased stability develop in the shelf break and upper slope domain (Hengesh et al., 2012; Scarselli et al., 2013), as evidenced in other margin settings (Maselli et al., 2020). As a result, multiple stacked MTCs were generated with different sizes ranging in extent from ~20 to ~60 km. In the northern area on seismic line A (Fig. 19a), slumps and MTCs are mainly produced by sediment collapse from a topographic high near the NE flank of the Exmouth Plateau Arch. In addition, on seismic line B (Fig. 19b) the transported deposits are derived from the steep shelf slope breaks and extensive clinoforms in the east. On the southern side of the Exmouth Plateau, the shelf edge is above the Resolution Arch. Here, the slope gradient is gentle with much less volume represented by clinoforms. Submarine failures are also present, but the MTCs form single or double stacks less than 20 km in extent.

## 6. Summary and conclusions

This paper presents a regional seismic stratigraphic framework for the Northern Carnarvon Basin that highlights the evolution of sedimentary processes on the continental margin following Valanginian breakup. Detailed observations of the seismic characteristics of ten regional seismic sections that are tied to wells have been used to define the major seismic stratigraphic units. The units are defined by regionally correlatable boundaries, and are associated with distinct sedimentary facies and depositional sequences.

The four main stratigraphic units contain heterogeneous and complex sequences separated by multiple unconformities. Following widespread transgression from the Valanginian to the Aptian, the Aptian – Turonian succession of Unit 1 is generally thin with parallel bedding in the northwest of the Exmouth Plateau. The beds represent a uniform depositional environment. In the southeast, subparallel and wavy beds imply an increased influence of submarine currents and the initial development of sediment mounds in an outer shelf setting. In the Turonian – Rupelian succession of Unit 2, polygonal faulting occurring mainly in the north and west of the Exmouth Plateau shows a continuation of low energy depositional processes. Conversely, the southeast of the study area is dominated by multiple stacked incisions and sediment drifts, more widespread and varied than previously recognised, which indicate the presence of more active bottom currents. In the younger sequences, incisions are replaced by parallel and subparallel beds indicative of decreasing current energy. The Rupelian – Tortonian succession of Unit 3 marks the development of progradational clinoforms. The clinoforms formed at the shelf edge were subject to slope instability resulting in chaotic deposits. Sedimentary units terminate, onlap and downlap onto Unit 2. Chaotic sedimentary units are more extensively developed in the Tortonian – Recent succession of Unit 4. In addition to slope instability, the widespread distribution of chaotic sediments is also associated with the evolution of the Exmouth Plateau Arch and related seismic activity, and the accumulation of fine-grained sediments.

In conclusion, the interpretation of seismic reflection data in combination with well data reveals the complex stratigraphic evolution of the post-rift margin sequences in the Northern Carnarvon Basin. The variation in seismic facies is primarily controlled by the establishment of energetic bottom currents, from the Turonian to the Early Oligocene, and the emplacement of MTCs, since the Late Miocene, testifying to the dynamic interaction of oceanographic and tectonic processes during the infill of the NCB. This study illustrates the complexity of the depositional and erosional processes that operate on a passive continental margin and demonstrates the need for further study to unravel the complex interplay of processes that give rise to such deposits in the basin.

#### Conflicts of Interest

The authors declare no conflict of interests.

## Acknowledgements

We would like to express our gratitude to Geoscience Australia for the provision of public domain seismic and well log data. All available datasets used in this research are open source, can be accessed through the National Offshore Petroleum Information Management System (NOPIMS; <https://nopims.dmp.wa.gov.au/nopims>). Schlumberger are thanked for the provision of Petrel software. Mulky Winata is supported by a collaborative PhD scholarship under the Aberdeen – Curtin Alliance (<http://aberdeencurtinalliance.org/>) namely between Curtin University (Perth, Australia) and the University of Aberdeen (Aberdeen, Scotland). Diego Kietzmann, Victorian Paumard, Marina Rabineau and two anonymous referees are thanked for their thoughtful reviews of earlier versions of this manuscript.

## References

- Apthorpe, M., 1988. Cainozoic depositional history of the North West Shelf. In: Purcell, P.G., Purcell, R.R. (Eds.), *The North West Shelf, Australia. Proceedings of the Petroleum Exploration Society of Australia Symposium*, Perth, WA, 55–84.
- Alrefaee, H., Ghosh S., Abdel-Fattah, M., 2018. 3D seismic characterization of the polygonal fault systems and its impact on fluid flow migration: An example from the Northern Carnarvon Basin, Australia. *Journal of Petroleum Science and Engineering* 167, 120–130. <https://doi.org/10.1016/j.petrol.2018.04.009>.
- Arditto, P.A., 1993. Depositional sequence model for the post-Barrow Group Neocomian succession, Barrow and Exmouth Sub-basins, Western Australia. *APEA J.* 33, 151–160.
- Audley-Charles, M.G., Ballantyne, P.D., Hall, R., 1988. Mesozoic-Cenozoic rift-drift sequence of Asian fragments from Gondwanaland. *Tectonophysics* 155, 317–330. [https://doi.org/10.1016/0040-1951\(88\)90272-7](https://doi.org/10.1016/0040-1951(88)90272-7).
- Barber, P. M., 1988. The Exmouth Plateau deep water frontier: A case history. In: Purcell, P. G., Purcell, R. R., (Eds.). *The North West Shelf, Australia: Proceedings of Petroleum Exploration Society Australia Symposium*. Perth: WA, 173-187.
- Borel, G.D., Stampfli, G.M., 2002. Geohistory of the North West Shelf: a tool to assess the Palaeozoic and Mesozoic motion of the Australian Plate. In: Keep, M., Moss, S.J. (Eds.), *The Sedimentary Basins of Western Australia 3. Proceedings of the Petroleum Exploration Society of Australia Symposium*, 119–128.

- Bradshaw, M.T., Yeates, A.N., Beynon, R.M., Brakel, A.T., Langford, R.P., Totterdell, J.M., Yeung, M., 1988. Palaeogeographic evolution of the North West Shelf region. In: Purcell, P.G., Purcell, R.R. (Eds.), *The North West Shelf, Australia. Proceedings of the Petroleum Exploration Society of Australia Symposium*, 29–54.
- Bradshaw, J., Sayers, J., Bradshaw, M., Kneale, R., Ford, C., Spencer, L., Lisk, M., 1998. Palaeogeography and its impact on the petroleum systems of the North West Shelf, Australia. In: Purcell, P.G., Purcell, R.R. (Eds.), *The Sedimentary Basins of Western Australia 2. Proceedings of the Petroleum Exploration Society of Australia Symposium*, 95–121.
- Butcher, B.P., 1989. Northwest Shelf of Australia. *AAPG Mem.* 48, 81-115.
- Cathro, D.L., 2002. Three-Dimensional Stratal Development of a Carbonate-siliciclastic Sedimentary Regime, Northern Carnarvon basin, Northwest Australia. PhD dissertation. The University of Texas at Austin, Austin, Texas, 490.
- Cathro, D. L., Austin, J. A. Jr., Moss, G. D., 2003. Progradation along a deeply submerged Oligocene-Miocene Heterozoan carbonate shelf; how sensitive are clinoforms to sea level variations? *AAPG Bull.*, 87, 1547–1574. <https://doi.org/10.1306/05210300177>.
- Cathro, D.L., Karner, G.D., 2006. Cretaceous–tertiary inversion history of the Dampier Sub-basin, Northwest Australia: insights from quantitative basin modeling. *Mar. Petrol. Geol.* 23 (4), 503–526. <http://dx.doi.org/10.1016/j.marpetgeo.2006.02.005>.
- Cartwright, J.A., 1994. Episodic basin-wide hydrofracturing of overpressured early cenozoic mudrock sequences in the North Sea Basin. *Mar. Petroleum Geol.* 11, 587–607. [https://doi.org/10.1016/0264-8172\(94\)90070-1](https://doi.org/10.1016/0264-8172(94)90070-1).
- Cartwright, J.A., James, D.M.D., Bolton, A.J., 2003. The genesis of polygonal fault systems: a review. In: Van Rensbergen, P., Hillis, R., Morley, C. (Eds.), *Subsurface Sediment Mobilisation*, vol. 216. Geological Society of London, Special Publication, 223–242. <https://doi.org/10.1144/GSL.SP.2003.216.01.15>.
- Chongzhi, T., Guoping B., Junlan L., Chao D., Xiaoxin L., Houwu L., Dapeng W., 2013, Mesozoic lithofacies palaeogeography and petroleum prospectivity in North Carnarvon basin, Australia: *Journal of Palaeogeography*, 81-92. <https://doi.org/10.3724/SP.J.1261.2013.00019>.

- Driscoll, N.W., Karner, G.D., 1998. Lower crustal extension across the Northern Carnarvon Basin, Australia: evidence for an eastward dipping detachment. *J. Geophys. Res.* 103, 4975–4991. <https://doi.org/10.1029/97JB03295>.
- Ellis, G., 1987. Lower Cretaceous radiolarian biostratigraphy and depositional environment of the Windalia Radiolarite, Carnarvon Basin, Western Australia. Honours Thesis, University of Western Australia, unpublished.
- Ercilla, G., Juan, C., Hernandez-Molina, F.J., Bruno, M., Estrada, F., Alonso, B., Casas, D., Lı Farran, M., Llave, E., Garcia, M., 2016. Significance of Bottom Currents in Deep-Sea Morphodynamics: An Example from the Alboran Sea. *Marine Geology*, 378, 157-170. <https://doi.org/10.1016/j.margeo.2015.09.007>.
- Etheridge, M. A., O'Brien, G.W., 1994. Structural and tectonic evolution of the Western Australian margin basin system. *PESA J.* 22: 45-64.
- Exon, N.F., Willcox, J.B., 1978. Geology and petroleum potential of Exmouth Plateau area off Western Australia. *AAPG Bull.* 62, 10–72. <https://doi.org/10.1306/C1EA47F2-16C9-11D7-8645000102C1865D>.
- Falvey, D.A., Veevers, J.J., 1974. Physiography of the Exmouth and Scott Plateaus, Western Australia, and adjacent Northeast Wharton Basin. *Mar. Geol.* 17, 21–59. [https://doi.org/10.1016/0025-3227\(74\)90046-2](https://doi.org/10.1016/0025-3227(74)90046-2).
- Gartrell, A.P., 2000. Rheological controls on extensional styles and the structural evolution of the Northern Carnarvon Basin, North West Shelf, Australia. *Aust. J. Earth Sci.* 47, 231–244. <https://doi.org/10.1046/j.1440-0952.2000.00776.x>.
- Gartrell, A., Torres, J., Dixon, M., Keep, M., 2016. Mesozoic rift onset and its impact on the sequence stratigraphic architecture of the Northern Carnarvon Basin. *APPEA J.* 56, 143–158. <https://doi.org/10.1071/AJ15012>.
- Geoscience Australia, 2015. Regional Geology of the Northern Carnarvon Basin [WWW Document]. Offshore Pet. Explor. Acreage Release.
- Gibbons, A.D., Barckhausen, U., Van Den Bogaard, P., Hoernle, K., Werner, R., Whittaker, J.M., Müller, R.D., 2012. Constraining the Jurassic extent of Greater India: tectonic evolution of the West Australian margin. *Geochem. Geophys. Geosyst.* 13, 1–25. <https://doi.org/10.1029/2011GC003919>.
- Gibbons, A. D., Zahirovic, S., Müller, R. D., Whittaker, J. M., Yatheesh, V., 2015. A tectonic model reconciling evidence for the collisions between India, Eurasia and intra-oceanic

- arcs of the central-eastern Tethys. *Gondwana Research*. <https://doi.org/10.1016/j.gr.2015.01.001>.
- Heath, R.S., Apthorpe, M.C., 1984. New formation names for the Late Cretaceous and Tertiary sequence of the southern North West Shelf. *GSWA, Record*, 1984/7, 35.
- Heine, C., Müller, R.D., 2005. Late Jurassic rifting along the Australian North West Shelf: margin geometry and spreading ridge configuration. *Aust. J. Earth Sci.* 52, 27–39. <https://doi.org/10.1080/08120090500100077>.
- Hengesh, J., Dirstein, J., Stanley, A., 2012. Seafloor geomorphology and submarine landslide hazards along the continental slope in the Carnarvon Basin, Exmouth Plateau, North West Shelf, Australia, *The APPEA Journal*, 52, 493–511. <https://doi.org/10.1071/AJ11039>.
- Hernández-Molina, F.J., Llave, E., Somoza, L., Fernández-Puga, M.C., Maestro, A., León, R., Barnolas, A., Medialdea, T., García, M., Vázquez, J.T., Díaz del Río, V., Fernández-Salas, L.M., Lobo, F., Alveirinho Dias, J.M., Rodero, J., Gardner, J., 2003. Looking for clues to paleoceanographic imprints: a diagnosis of the gulf of Cadiz contourite depositional systems. *Geology* 31 (1), 19–22.
- Hernández-Molina, F.J., Larter, R.D., Rebesco, M., Maldonado, A., 2006. Miocene reversal of bottom water flow along the Pacific Margin of the Antarctic Peninsula: stratigraphic evidence from a contourite sedimentary tail. *Mar. Geol.* 228, 93–116. <https://doi.org/10.1016/j.margeo.2005.12.010>.
- Hernández-Molina, F.J., Stow, D.A.V., Llave, 2008. Continental slope contourites. In: Rebesco, M., Camerlenghi, A. (Eds.), *Contourites. Developments in Sedimentology*, 60. Elsevier, Amsterdam, pp. 379–408. [https://doi.org/10.1016/S0070-4571\(08\)10019-X](https://doi.org/10.1016/S0070-4571(08)10019-X).
- Imbert, P., Ho, S., 2012. Seismic-Scale Funnel-Shaped Collapse Features from the Paleocene - Eocene of the North West Shelf of Australia. *Marine Geology*, 332, 198-221. <https://doi.org/10.1016/j.margeo.2012.10.010>.
- Jablonski, D., 1997. Recent advances in the sequence stratigraphy of the Triassic to Lower Cretaceous succession in the Northern Carnarvon Basin, Australia. *APPEA J.* 37, 429–454. <https://doi.org/10.1071/AJ96026>.
- Jablonski, D., Saitta, A. J., 2004. Permian to Lower Cretaceous plate tectonics and its impact on the tectono-stratigraphic development of the western Australian margin. *The APPEA Journal*, 44(1), 287–327. <https://doi.org/10.1071/AJ03011>.

- Keep M., Harrowfield M., Crowe W., 2007. The Neogene tectonic history of the North West Shelf, Australia. *Exploration Geophysics* 38, 151–174.
- Longley, I.M., Buessenschuett, C., Clydsdale, L., Cubitt, C.J., Davis, R.C., Johnson, M.K., Marshall, N.M., Murray, A.P., Somerville, R., Spry, T.B., Thompson, N.B., 2002. The North West Shelf of Australia - a Woodside perspective. In: Keep, M., Moss, S. (Eds.), *The Sedimentary Basins of Western Australia 3. Proceedings of the Petroleum Exploration Society of Australia Symposium*, 27–88.
- Marshall, N.G., Lang, S.C., 2013. A new sequence stratigraphic framework for the North West Shelf, Australia. In: Keep, M., Moss, S.J. (Eds.), *The Sedimentary Basins of Western Australia 4. Proceedings of the Petroleum Exploration Society of Australia Symposium*, 1–32.
- Maselli, V., Iacopini, D., Ebinger, C.J., Tewari, S., de Haas, H., Wade, B.S., Pearson, P.N., Francis, M., van Vliet, A., Richards, B., Kroon., D., 2020. Large-scale mass wasting in the western Indian Ocean constrains onset of East African rifting. *Nature Communications* 11, 3456.
- Masson, D.G., Wynn, R.B., Bett, B.J., 2004. Sedimentary environment of the Faroe-Shetland and Faroe Bank channels, north-east Atlantic, and the use of bedforms as indicators of bottom current velocity in the deep ocean. *Sedimentology* 51, 1207–1241. <https://doi.org/10.1111/j.1365-3091.2004.00668.x>.
- McCormack, K., McClay, K., 2013. Structural architecture of the gorgon platform, North West Shelf, Australia. In: Keep, M., Moss, S.J. (Eds.), *The Sedimentary Basins of Western Australia IV: Proceedings of the Petroleum Exploration Society of Australia Symposium*. Perth, WA, 2013.
- Metcalfe, I., 2013. Gondwana dispersion and Asian accretion: tectonic and palaeogeographic evolution of eastern Tethys. *J. Asian Earth Sci.* 66, 1–33. <https://doi.org/10.1016/j.jseaes.2012.12.020>.
- Miller, K.G., Wright, J.D., Fairbanks, R.G., 1991. Unlocking the Ice House: Oligocene-Miocene 861 Oxygen Isotopes, Eustasy, and Margin Erosion. *Journal of Geophysical Research: Solid Earth*, 862 96, 6829-6848.
- Mitchum, R.M., Vail, P.R., Sangree, J.B., 1977a. Seismic stratigraphy and global changes of sea-level, part 6: stratigraphic interpretation of seismic reflection patterns in depositional sequences. In: Payton, C.E. (Ed.), *Seismic Stratigraphy - Applications to Hydrocarbon Exploration*. AAPG Memoir 26, 117–133.

- Mitchum, R.M., Vail, P.R., Thompson, S., 1977b. Seismic stratigraphy and global changes of sea-level, part 2: the depositional sequence as a basic unit for stratigraphic analysis. In: Payton, C.E. (Ed.), *Seismic Stratigraphy - Applications to Hydrocarbon Exploration*. AAPG Memoir 26, 53–62.
- Moss, G.D., Cathro, D.L., Austin Jr., J.A., 2004. Sequence biostratigraphy of prograding clinoforms, northern Carnarvon Basin, Western Australia: a proxy for variations in Oligocene to Pliocene global sea level? *Palaios* 19, 206–226. [https://doi.org/10.1669/0883-1351\(2004\)019<0206:SBOPCN>2.0.CO;2](https://doi.org/10.1669/0883-1351(2004)019<0206:SBOPCN>2.0.CO;2)
- Müller, R.D., Mihut, D., Baldwin, S., 1998. A new kinematic model for the formation and evolution of the West and Northwest Australian Margin. In: Purcell, P.G., Purcell, R.R. (Eds.), *The Sedimentary Basins of Western Australia 2. Proceedings of the Petroleum Exploration Society of Australia Symposium*, Perth, WA, 56–72.
- Nugraha, H.D., Jackson, C.A.-L., Johnson, H.D., Hodgson D.M., Reeve M.T., 2019. Tectonic and oceanographic process interactions archived in the Late Cretaceous to Present deep-marine stratigraphy on the Exmouth Plateau, offshore NW Australia. *Basin Res*, vol 31, 405–430. <https://doi-org.dbgw.lis.curtin.edu.au/10.1111/bre.12328>.
- Norvick, M. S., 2002. Palaeogeographic maps of the northern margins of the Australian plates: initial report. Unpublished report for Geoscience Australia.
- Pattillo, J., and Nichols, P.J., 1990. A tectonostratigraphic framework for the Vulcan graben, Timor Sea region. *APEA J.*, 30, 27-51.
- Paumard, V., Bourget J., Payenberg T., Ainsworth R. B., George A. D., Lang S., Posamentier H. W., Peyrot D., 2018. Controls on shelf-margin architecture and sediment partitioning during a syn-rift to post-rift transition: Insights from the Barrow Group (Northern Carnarvon Basin, North West Shelf, Australia). *Earth-Science Reviews* Volume 177, February 2018, 643–677. <https://doi.org/10.1016/j.earscirev.2017.11.026>.
- Paumard, V., Bourget, J., Lang, S., Wilson, T., Riera, R., Gartrell, A., Vakarelov, B., O’Leary, M., George, A.D., 2019. Imaging past depositional environments of the North West Shelf of Australia: Lessons from 3D seismic data, in: Keep, M., Moss, S.J. (Eds.), *The Sedimentary Basins of Western Australia V: Proceedings of the Petroleum Exploration Society of Western Australia Symposium*, Perth, WA, 2019, 30.
- Payenberg, T.H.D., Howe, H., Marsh, T., Sixsmith, P., Kowalik, W.S., Powell, A., Ratcliffe, K., Iasky, V., Allgoewer, A., Howe, R.W., Montgomery, P., Vonk, A., Croft, M., 2013—An



- integrated regional Triassic stratigraphic framework for the Carnarvon Basin, NWS, Australia. In: Keep, M. and Moss, S.J. (eds) The Sedimentary Basins of Western Australia IV: Proceedings of the Petroleum Exploration Society of Australia Symposium, Perth, WA, 2013.
- Rebesco, M., Stow, D.A.V., 2001. Seismic expression of contourites and related deposits: a preface. *Marine Geophysical Research* 22, 303–308. <https://doi.org/10.1023/A:1016316913639>.
- Rebesco, M., 2005. Contourites. In: Selley, R.C., Cocks, L.R.M., Plimer, I.R. (Eds.), *Encyclopedia of Geology*. Elsevier, Oxford, 513–527.
- Rebesco, M., Hernández-Molina, J., van Rooij, D., Wåhlin, A., 2014. Contourites and associated sediments controlled by deep-water circulation processes: state-of-the-art and future considerations. *Mar. Geol.* 352, 111–154. <https://doi.org/10.1016/j.margeo.2014.03.011>.
- Reeve, M.T., Jackson, C.A.L., Bell, R.E., Magee, C., Bastow, I.D., 2016. The stratigraphic record of prebreakup geodynamics: evidence from the Barrow Delta, offshore Northwest Australia. *Tectonics* 35, 1935–1968.
- Romine, K.K., Durrant, J., 1996. Carnarvon Cretaceous-Tertiary Tie Report. Record 1996/036. Geoscience Australia, Canberra. <https://pid.geoscience.gov.au/dataset/ga/25187>
- Romine, K.K., Durrant, J.M., Cathro, D.L., Bernardel, G., 1997. Petroleum play element prediction for the Cretaceous-Tertiary basin phase, Northern Carnarvon Basin. *APPEA J.* 37, 315–339. <https://doi.org/10.1071/AJ96020>.
- Sanchez, M. C., Fulthorpe S. C., Steel, J. R., 2012. Middle Miocene–Pliocene siliciclastic influx across a carbonate shelf and influence of deltaic sedimentation on shelf construction, Northern Carnarvon Basin, Northwest Shelf of Australia. *Basin Research*, Blackwell Publishing Ltd, European Association of Geoscientists & Engineers and International Association of Sedimentologists, vol. 24, 1–19. <https://doi.org/10.1111/j.1365-2117.2012.00546.x>.
- Scarselli, N., McClay, K., Elders, C., 2013. Submarine Slide and Slump Complexes, Exmouth Plateau, NW Shelf of Australia, in Keep, M. and Moss, S.J (Eds.), *Western Australian Basins Symposium 2013*, Aug 18-21, 2013. Perth: Petroleum Exploration Society of Australia. <https://doi.org/10.1002/9781119500513.ch16>.

- Scarselli, N., McClay, K.R., Elders, C., 2020. Seismic examples of composite slope failures (Offshore North West Shelf, Australia). In: Ogata, K, Pini, G.A., & Festa, A. (eds.) Submarine landslides: subaqueous mass transport deposits from outcrops to seismic profiles. AGU Geophysical Monograph Series 246. <https://doi.org/10.1002/9781119500513.ch16>.
- Stagg, H.M.J.G.J., Colwell, J.B., 1994. The structural foundations of the Northern Carnarvon Basin. Sediment. Basins West. Aust. Proc. Pet. Explor. Soc. Aust. Symp. 349–364. Perth 1994.
- Stow, D.A.V., Kahler, G., Reeder, M., 2002. Fossil contourites: type example from an Oligocene palaeoslope system, Cyprus. In: Stow, D.A.V., Pudsey, C.J., Howe, J.A., Faugères, J.-C., Viana, A.R. (Eds.), Deep-water Contourite Systems: Modern Drifts and Ancient Series, Seismic and Sedimentary Characteristics. Geological Society, London, Memoir, 22, 443–455. <https://doi.org/10.1144/GSL.MEM.2002.022.01.31>.
- Stow, D.A.V., Hernández-Molina, F.J., Llave, E., Sayago-Gil, M., Díaz-del Río, V., Branson, A., 2009. Bedform-velocity matrix: the estimation of bottom current velocity from bedform observations. *Geology* 37, 327–330. <https://doi.org/10.1130/G25259A.1>.
- Tindale, K., Newell, N., Keall, J., Smith, N., 1998. Structural evolution and charge history of the Exmouth Sub-basin, Northern Carnarvon Basin, Western Australia. In: Purcell, P.G., Purcell, R.R. (Eds.), The Sedimentary Basins of Western Australia 2. Proceedings of the Petroleum Exploration Society of Australia Symposium, 447–472.
- Tellez, J.J., 2015. Seismic Sequence Stratigraphy and Architectural Elements for Cenozoic Strata at the Rankin Platform Sub-Basin, North Carnarvon Basin, Australia. Master thesis. The University of Oklahoma, 108.
- Tortopoglu, B., 2015. The Structural Evolution of the Northern Carnarvon Basin, Northwest Australia. Master thesis. University of Colorado School of Mines, 170.
- Veevers, J.J., 2000. Change of tectono-stratigraphic regime in the Australian plate during the 99 Ma (mid-Cretaceous) and 43 Ma (mid-Eocene) swerves of the Pacific. *Geology*, 28 (1), 47-50.
- Watterson, J., Walsh, J.J., Nicol, A., Nell, R.R., Breatan, P.G., 2000. Geometry and origin of a polygonal fault system. *J. Geol. Soc. Lond.* 157, 151–162. <https://doi.org/10.1144/jgs.157.1.151>.

Whittam, D.B., Norvick, M.S. and McIntyre, C.L., 1996. Mesozoic and Cainozoic tectonostratigraphy of western ZOCA and adjacent areas. APPEA J., 36, 209-232.

a) Line	Seismic Survey	~ Total km in AOI	Direction
A	EX00-29, 98C-4143, 98C-4134, Xline 5047 Banambu 3D, PG93-1040, PG93-1009, GPDB95-03	588.667	WNW - ESE
B	EX00-15, Random line Centaur 3D, B02-35M, 98C-4083, 98C-4090, Xline 1209 Rosie 3D, Random line SW Rankin 3D, GPDB95-14	465.116	
C	EX00-01, EX00-28, B02-44M, JA95-115	327.144	
D	X79B-1129, X79B-1100, HE94-230, JA95-220, JA95-108E, EX08-010M, EX05-011	269.168	
E	EX05-023, EX05-065, HE94-150, HE96-22	252.547	
F	98J-4169, HE94-104, EX05-043	199.812	
G	OM08-602, OM08-501, EX05-050	318.508	SSW - NNE
H	EX00-26, JA95-209N, X95A-2148, X95A-2107, X95A-2127, JA95-209S, EX05-057	396.686	
I	SK56P-056, HE94-109, HE94-190, HE94-105, HE94-200, JA95-217, JA95-121, B02-65M, AMAGNAC2D-W08AM-0033, EX00-44, OM08-032, OM08-104	530.515	
J	EX00-60, OM08-111, 98C-4085, JA95-222, JA95-116, Inline 1928 Draeck 3D, WAS76-17, 98J-4155	547.539	

b) No	Survey name	Survey type	Line prefix	Start date	End date	Operator	Contractor	Line Length (km)
1	Scientific Investigation 10 SL	2D	WAS76	29/07/1976	30/09/1976	Geophysical Service Inc	GSI	7708
2	NA	2D	X78A	19/02/1978	2/01/1979	Esso Exploration & Production Aust Inc	GSI	17167
3	X79B	2D	X79B	7/07/1979	16/09/1979	Esso Exploration & Production Aust Inc	GSI	5570
4	Michelle	2D	PG93	12/11/1993	10/12/1993	Phillips Australian Oil Company	WesternGeco	3100.5
5	HE94	2D	HE94	20/06/1994	12/08/1994	BHP Petroleum (Australia) Pty Ltd	WesternGeco	6255.1
6	SPA 2SL/1994-95	2D	GPDB95	22/06/1995	27/08/1995	WesternGeco Australia Pty Ltd	WesternGeco	2523
7	X95A	2D	X95A	27/09/1995	27/10/1995	Esso Australia Pty Ltd	NA	2440.24
8	JA95	2D	JA95	13/10/1995	16/12/1995	Japan National Oil Corporation	AGSO	6691.2
9	NA	2D	EXS96	30/05/1996	15/06/1996	PGS Nopec Australia Pty Ltd	Nopec	1750
10	HE96	2D	HE96	1/06/1996	15/06/1996	BHP Petroleum (Australia) Pty Ltd	Digicon Inc	1766.4
11	Capri	2D	98C	31/01/1998	12/03/1998	Woodside Offshore Petroleum Pty Ltd	NA	4702.1
12	Jawa	2D	98J	12/03/1998	25/03/1998	Woodside Offshore Petroleum Pty Ltd	NA	1780.53
13	Exmouth North	2D	EX00	19/12/1999	15/06/2000	Australian Seismic Brokers Pty Ltd	Veritas	8446
14	Champagne / Wheatstone	2D	B02	20/03/2003	22/04/2003	Chevron Texaco Australia Pty Ltd	Veritas	847.6-2546
15	Klimt	2D	OM08	18/01/2008	29/04/2008	OMV Australia Pty Ltd	Gardline Marine	7407
16	Armagnac	2D	NA	24/06/2008	4/09/2008	Woodside Burrup Pty Ltd	Veritas	6399
17	NA	2D	EX08	NA	NA	NA	NA	NA
18	NA	2D	EX05	NA	NA	NA	NA	NA
19	NA	2D	SK	NA	NA	NA	NA	NA

Table. 1. a) Details of the individual 2D seismic sections that were used to construct the ten regional composite lines in the area of interest. Lines A-F trend WNW-ESE and lines G-J trend SSW-NNE. b) Details of the 2D seismic surveys acquired and processed in the 1990s and 2000s used for the regional seismic stratigraphic interpretation. The information was compiled from the WAPIMS website (Western Australian Petroleum and Geothermal Information Management System). NA means that information is not available.

c) No	Survey name	Survey type	Line prefix	Start date	End date	Operator	Contractor	Area (sqkm)	
1	South West Rankin	3D	R96	20/02/1996	30/04/1996	Woodside Offshore Petroleum Pty Ltd	Western Geophysical Company	783	
2	Rosie	3D	RO3	19/11/1996	18/02/1997	Western Mining Corporation Ltd	NA	1139	
3	Banambu	3D	NA	22/12/1997	02/02/1998	Woodside Offshore Petroleum Pty Ltd	NA	1164	
4	Chandon	3D	NA	19/02/2004	08/04/2004	Chevron Texaco Australia Pty Ltd	NA	1237	
5	Scarborough	3D	NA	20/03/2004	09/05/2004	BHP Billiton Petroleum (Australia) Pty Ltd	WesternGeco	1266.27	
6	Io-Jansz	3D	NA	12/04/2004	19/09/2004	Chevron Texaco Australia Pty Ltd	Veritas	2785.5	
7	Willem	3D	NA	15/01/2006	18/04/2006	Woodside Energy Ltd	Veritas	1832.56	
8	Duyfken	3D	NA	24/05/2006	02/09/2006	Chevron Australia Pty Ltd	Baker Atlas	3600.285	
9	Bonaventure	3D	NA	02/09/2006	15/12/2006	Chevron Australia Pty Ltd	WesternGeco	4143.743	
10	Charon	3D	NA	17/07/2007	27/08/2007	Chevron Australia Pty Ltd	Baker Atlas	1799	
11	Draeck	3D	DR07	17/12/2006	20/08/2007	Chevron Australia Pty Ltd	WesternGeco	1231	
				20/08/2007	20/08/2007			79.841	
12	Centaur	3D	NA	29/08/2007	10/11/2007	Chevron (TAPL) Pty Ltd	WesternGeco	2624	
13	Meo-NWS	3D	NA	13/12/2007	27/12/2007	MEO Australia Ltd	PGS	258.16	
14	Glencoe	3D	NA	03/12/2007	19/03/2008	Hess Exploration Australia Pty Ltd	CGG Veritas	4485.4	
15	Colombard	3D	NA	22/03/2008	07/08/2008	Woodside Energy Ltd	CGG Veritas	3172.68	
16	Rose	3D	NA	18/08/2008	30/09/2008	Oilex Ltd		1498.5075	
17	Aragon	3D	NA	11/08/2008	18/11/2008	WestenGeco Australia Pty Ltd	WesternGeco	2928.2566	
18	Artemis	3D	NA	10/03/2009	31/03/2009	NWS Exploration Pty Ltd	PGS	257.83	
19	Cazadores	3D	NA	30/12/2008	24/03/2009	Woodside Burrup Pty Ltd	WesternGeco	4551	
20	Eendracht	3D	NA	09/06/2009	27/09/2009	Fugro Multi Client Services Pty Ltd	NA	3223	
				27/01/2010	26/06/2010			NA	3630
				17/07/2010	27/10/2010			NA	7915

Table 1. c) Details of the 3D seismic surveys acquired and processed in the 1990s and 2000s and used in this study. The information was compiled from the WAPIMS website (Western Australian Petroleum and Geothermal Information Management System). NA means that information is not available.

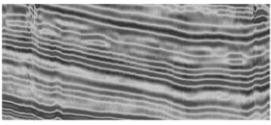

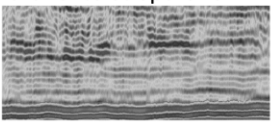

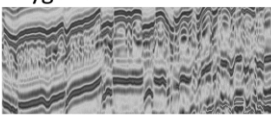

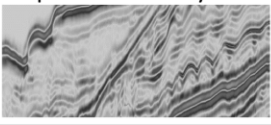

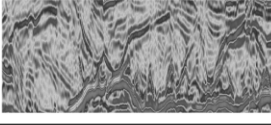

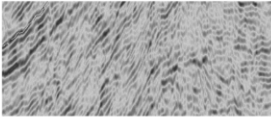

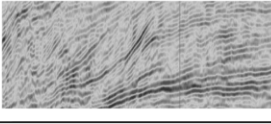

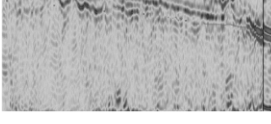

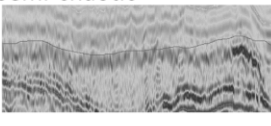

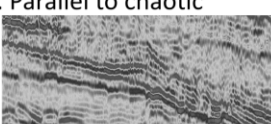

Example	Colour in seismic facies map	Seismic facies	Interpretation
1. Parallel 	Pr 	- Medium to high amplitude - Parallel and laterally continuous	- Laterally continuous deposit - Low energy condition - Distal setting
2. Parallel to subparallel 	PrSp 	- Low to medium amplitude - Parallel to subparallel	(Mitchum et al., 1977a and 1977b)
3. Polygonal fault 	Pf 	- Medium to high amplitude - Semi-continuous - Dissected by faults	- Polygonally faulted deposit - Fine-grained sediment - Low energy condition - Distal setting (Cartwright, 1994 and Watterson et al., 2000)
4. Subparallel to wavy 	SpWv 	- Medium amplitude - Subparallel to wavy	- Small scale bedforms - Moderate bottom current e.g., sediment waves (Stow et al., 2009 and Rebesco et al., 2014)
5. Incision or erosive 	IncErs 	- Low to medium amplitude - Individual to multiple incision(s)	- Erosional surfaces e.g., scours, grooves - Strong bottom current (Hernández-Molina et al., 2003, 2006)
6. Semi- to dis-continuous 	SmcDc 	- Low amplitude - Semi-continuous to discontinuous	- Disturbed deposit - In the inboard area (NCB) - Shelf setting (Mitchum et al., 1977a and 1977b)
7. Progradation/Aggradation 	Pg/Ag 	- Medium to high amplitude - Continuous - Simple to multiple stacked progradation/aggradation	- Clinofolds - Shelf edge to slope (Mitchum et al., 1977a and 1977b)
8. Chaotic to transparent 	Ch 	- Low to medium amplitude - Chaotic	- Slumps and mass transport complexes (MTCs)
9. Semi-chaotic 	SmCh 	- Low to medium amplitude - Semi-continuous to chaotic	- Slope to basinal area
10. Parallel to chaotic 	PrCh 	- Low to medium amplitude - Parallel to chaotic	(Mitchum et al., 1977a and 1977b)

Table. 2. Summary of the seismic facies recognised in the post-rift sequence in the NCB, explaining the acronyms and the colour legend used in the main text and in the seismic facies maps.



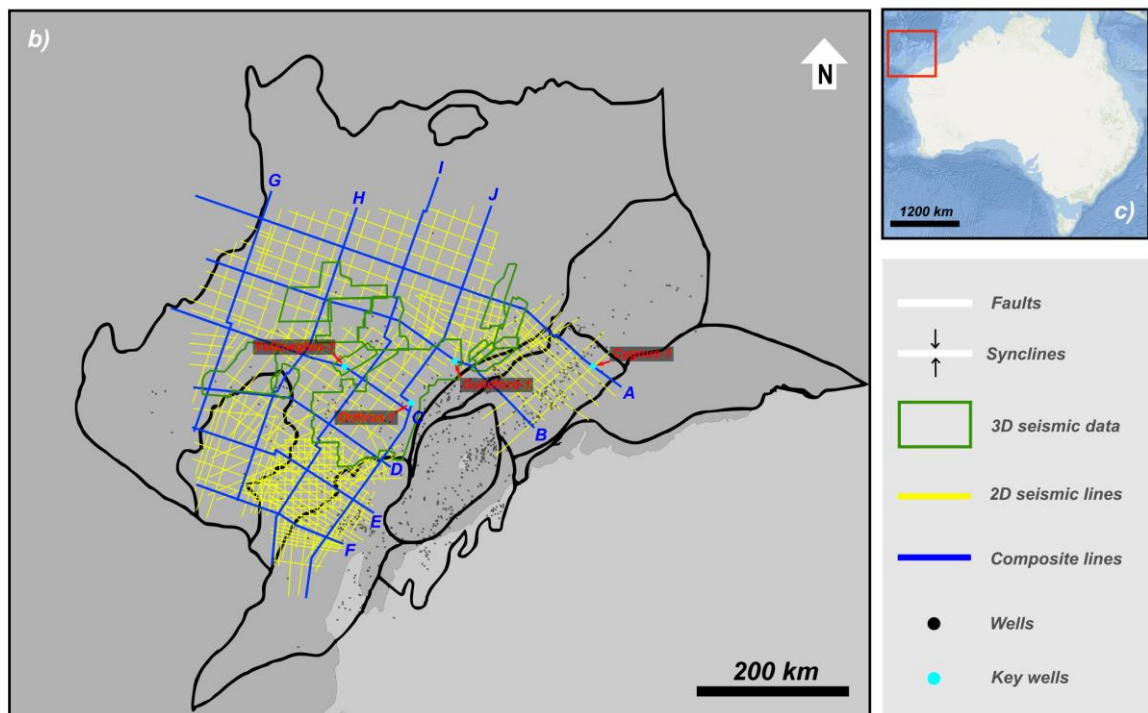
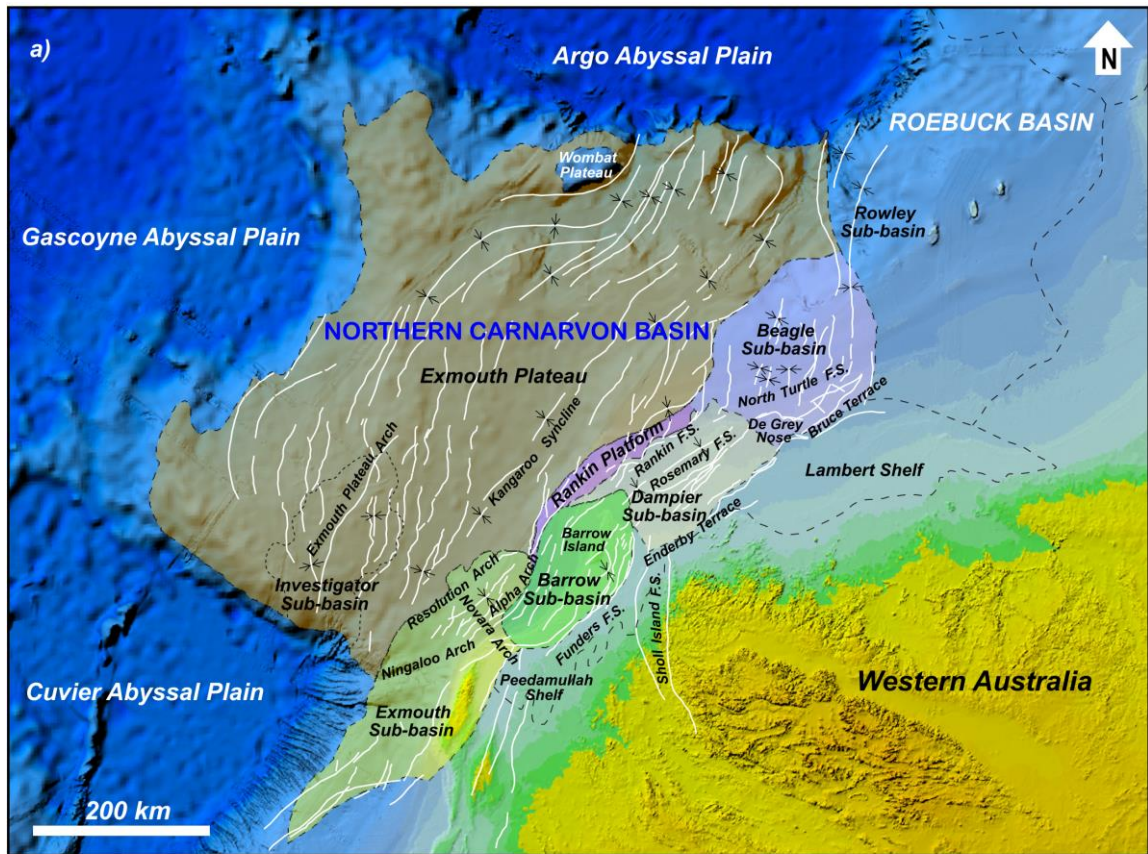


Fig. 1. a) Location map illustrating the geological provinces and structural elements of the Northern Carnarvon Basin (modified from Geoscience Australia, 2015). b) The location of ten regional lines (blue) that were constructed from 2D & 3D seismic data and tied to 40 wells distributed along and close to the lines. The interpreted horizons were tied to Cygnus-1, Guilford-1, Yellowglen-1 and Orthrus-1 to assign biostratigraphic ages. The additional 2D lines used in this study are shown in yellow, and the outlines of 3D surveys are shown in green. c) The location of the NCB (red square) on the Northwest Shelf of Australia.



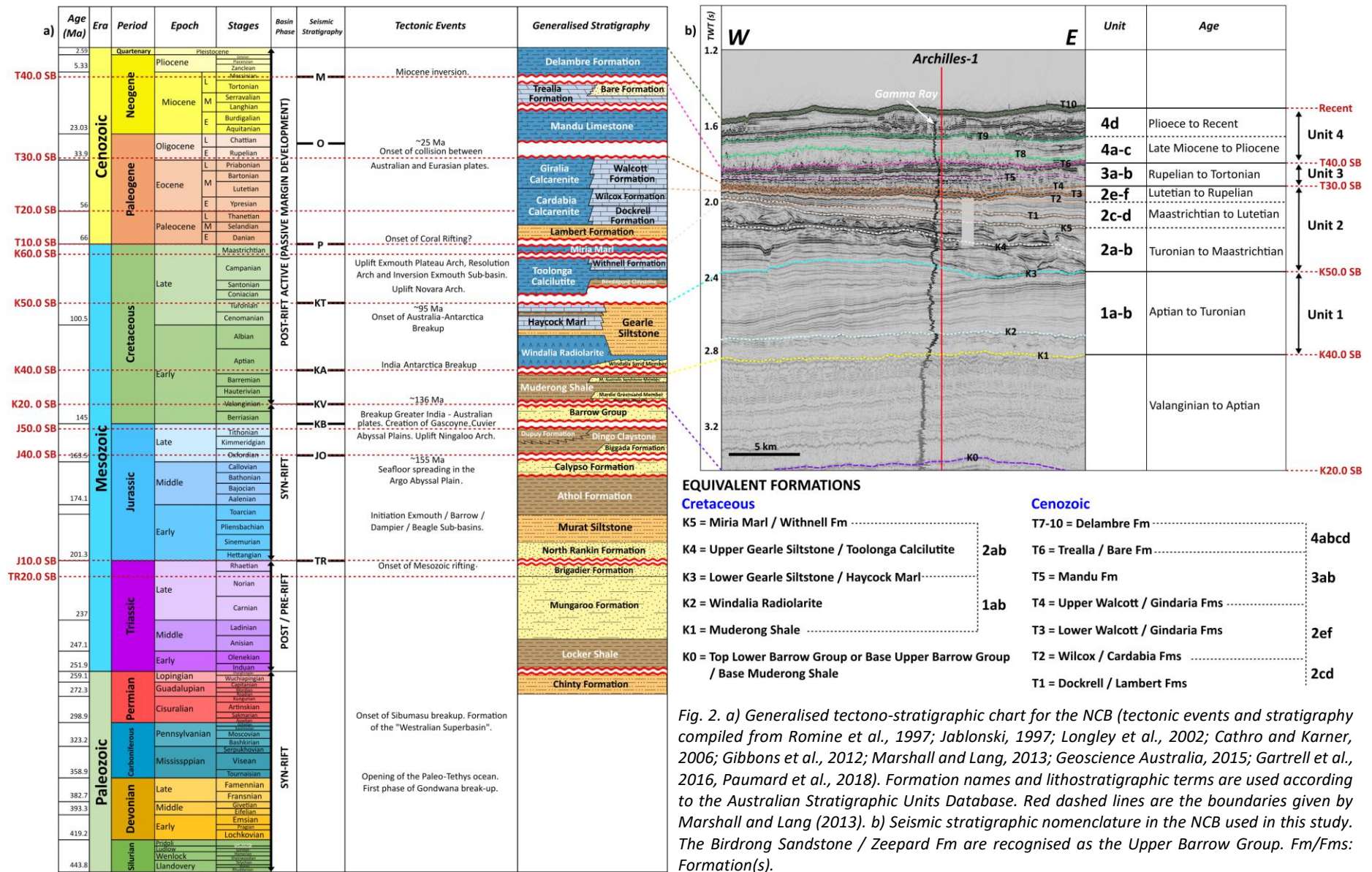


Fig. 2. a) Generalised tectono-stratigraphic chart for the NCB (tectonic events and stratigraphy compiled from Romine et al., 1997; Jablonski, 1997; Longley et al., 2002; Cathro and Karner, 2006; Gibbons et al., 2012; Marshall and Lang, 2013; Geoscience Australia, 2015; Gartrell et al., 2016; Paumard et al., 2018). Formation names and lithostratigraphic terms are used according to the Australian Stratigraphic Units Database. Red dashed lines are the boundaries given by Marshall and Lang (2013). b) Seismic stratigraphic nomenclature in the NCB used in this study. The Birdrong Sandstone / Zeepard Fm are recognised as the Upper Barrow Group. Fm/Fms: Formation(s).



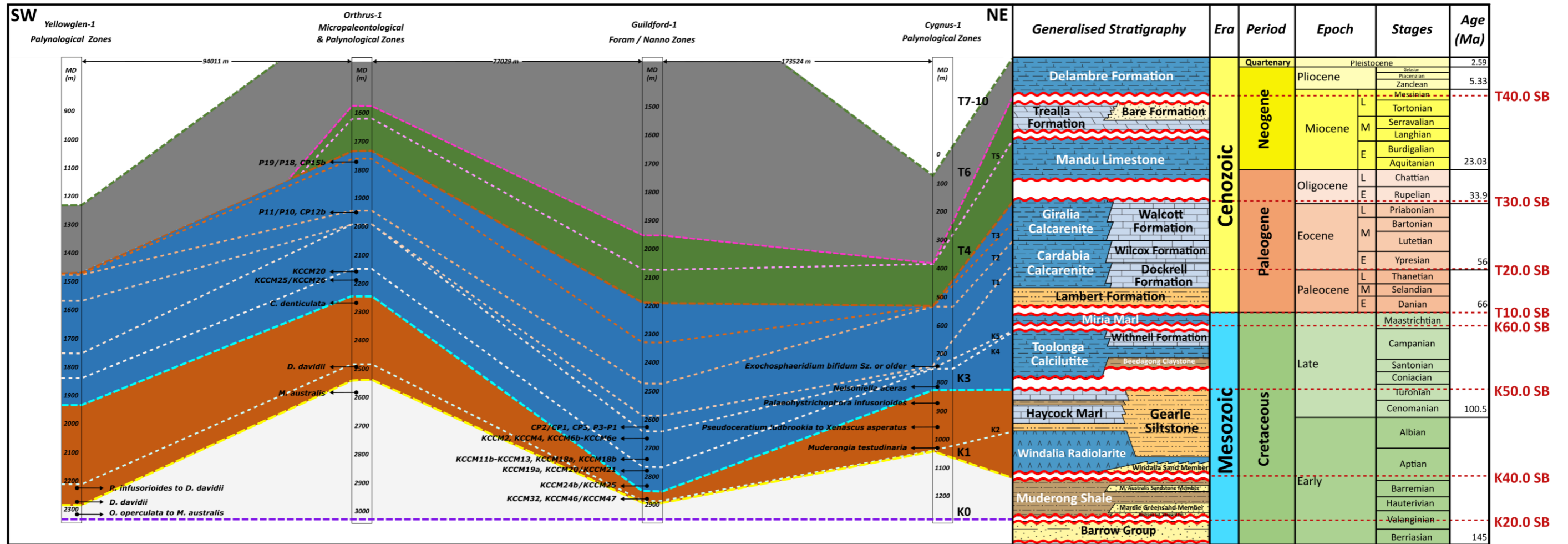
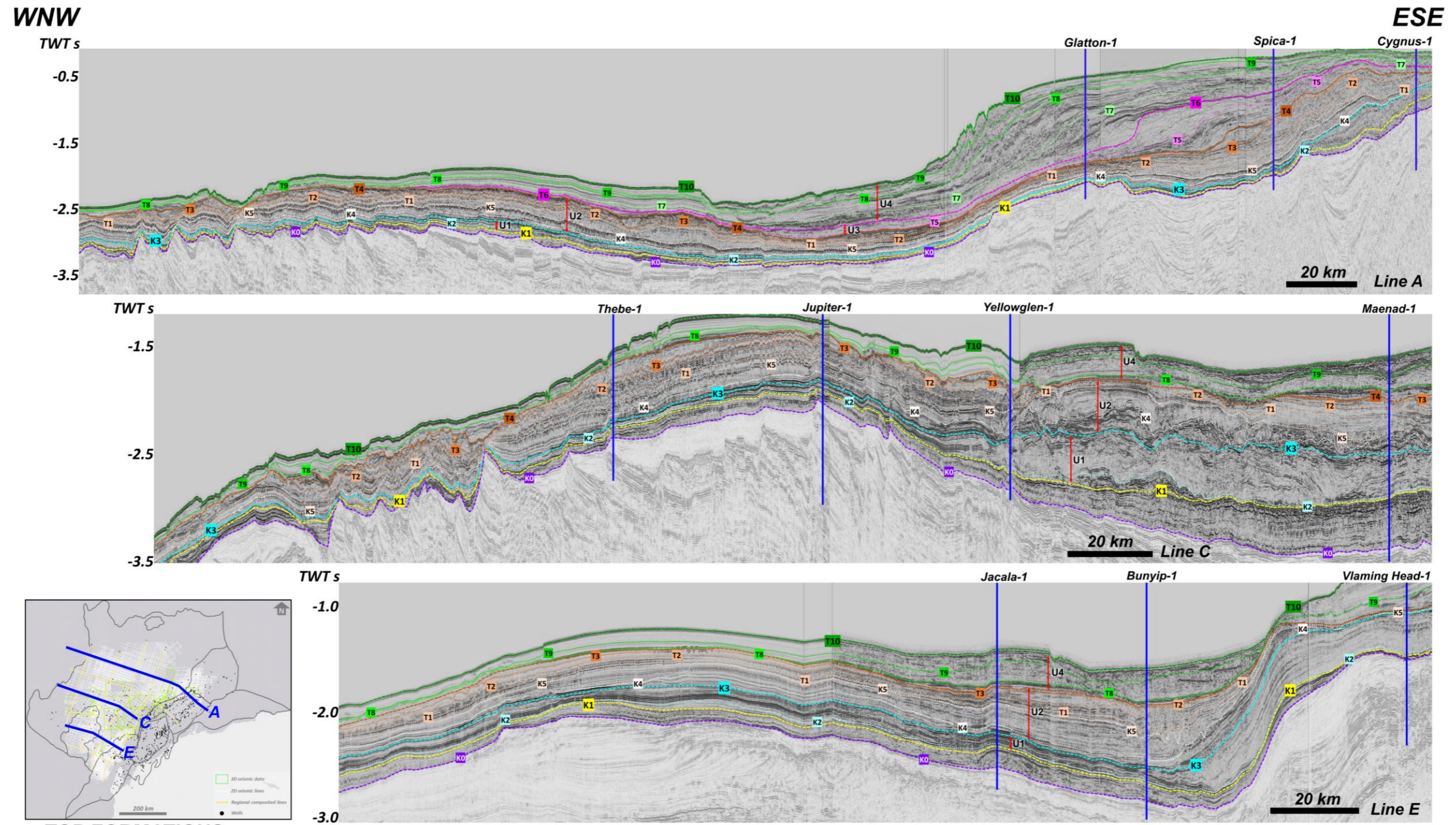


Fig. 3. Stratigraphic ages for the key seismic markers assembled from the Cygnus-1, Guildford-1, Yellowglen-1 and Orthrus-1 well completion reports (see location on Figure 1b). In addition, units and age intervals in the Neogene are defined and constrained by stratigraphic markers and ditch cuttings descriptions from 36 additional wells. Red dashed lines are the boundaries given by Marshall and Lang (2013).





**TOP FORMATIONS**

**Cretaceous**

- K5 ≈ Miria Marl / Withnell Formations
- K4 ≈ Upper Gearle Silstone / Toolonga Calcilutite
- K3 ≈ Lower Gearle Silstone / Haycock Marl
- K2 ≈ Windalia Radiolarite
- K1 ≈ Muderong Shale
- K0 ≈ Lower Barrow Group or Base Upper Barrow / Base Muderong Shale

Unit 2a-b

Unit 1a-b

**Cenozoic**

- T5 ≈ Mandu Formation
- T4 ≈ Upper Walcott / Gindaria Formations
- T3 ≈ Lower Walcott / Gindaria Formations
- T2 ≈ Wilcox / Cardabia Formations
- T1 ≈ Dockrell / Lambert Formations

Unit 3a

Unit 2e-f

Unit 2c-d

- T10 ≈ Upper Delambre Formation (Seabed)
- T9 ≈ Middle 2 Delambre Formation
- T8 ≈ Middle 1 Delambre Formation
- T7 ≈ Lower Delambre Formation
- T6 ≈ Trealla / Bare Formation

Unit 4d

Unit 4a-b-c

Unit 3b

Fig. 4. Seismic stratigraphic interpretation of the NCB shown on regional seismic lines A, C and E. Sixteen seismic horizons correspond to the tops of sixteen formations, which can be grouped into four primary units (Units 1-4), which are also shown in Figs 2 and 3.



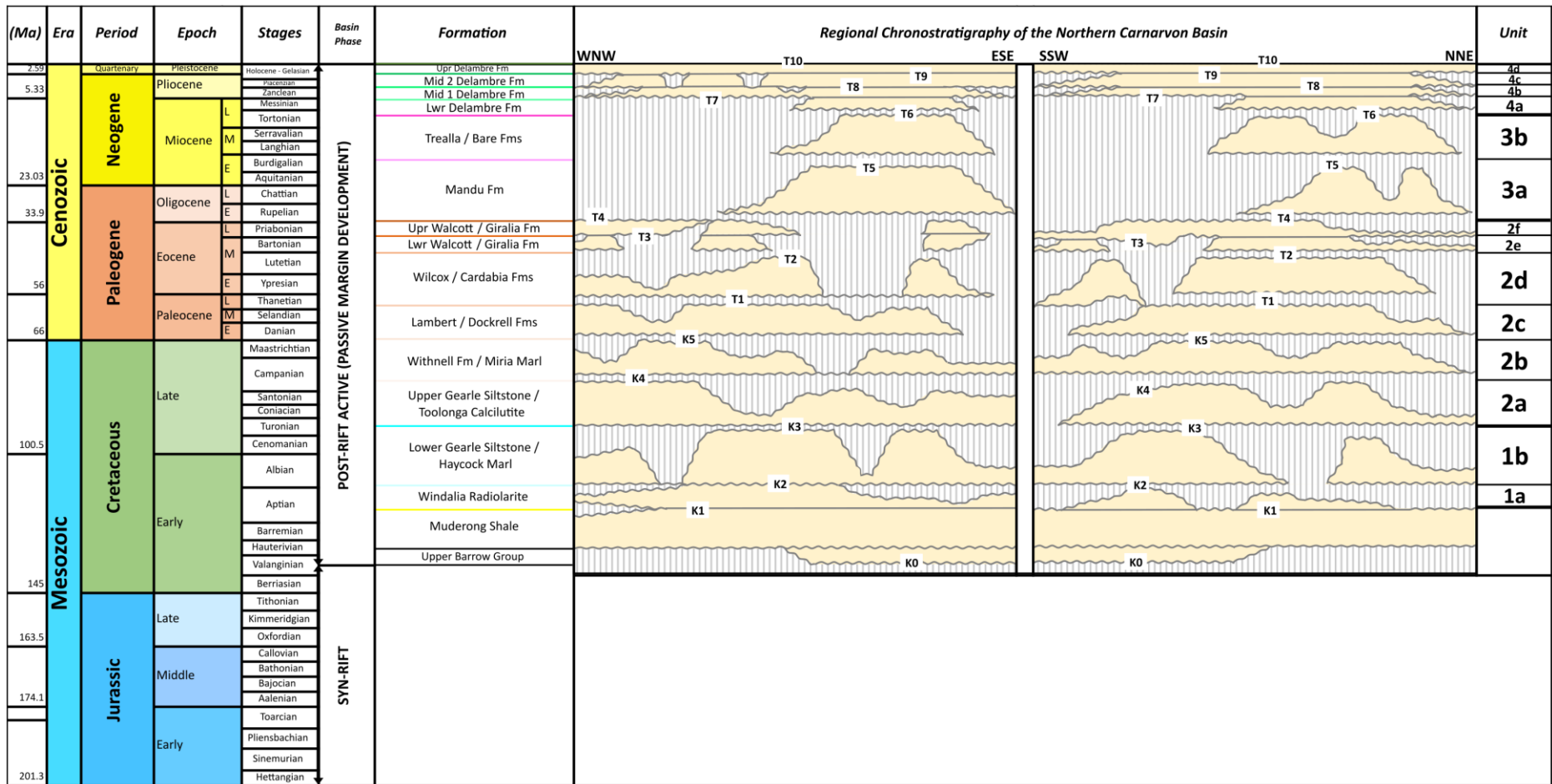


Fig. 5. A summary chronostratigraphic chart of the post-Valanginian sequences based on the seismic stratigraphic interpretation of WNW-ESE and SSW-NNE oriented regional seismic sections.

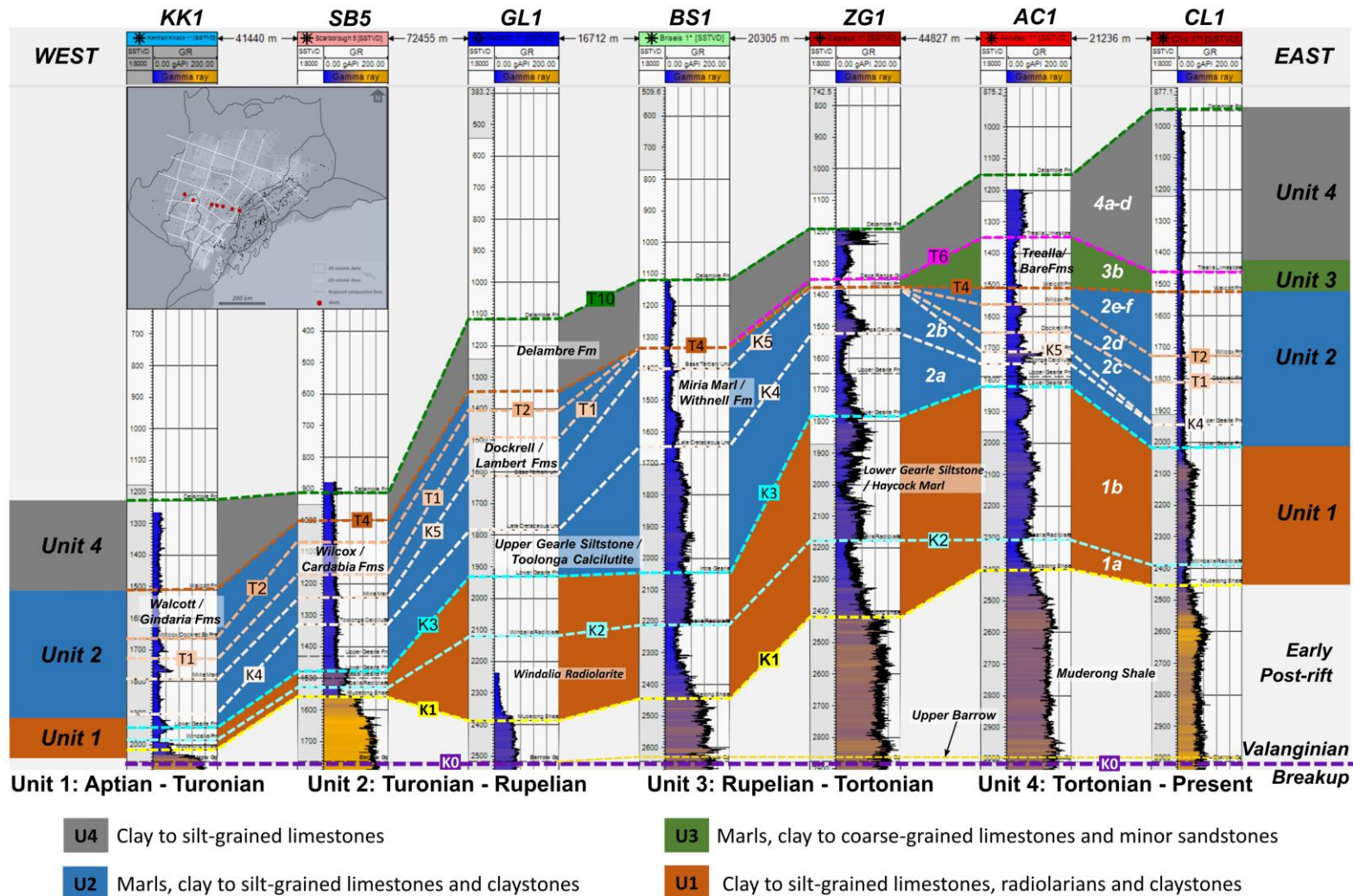
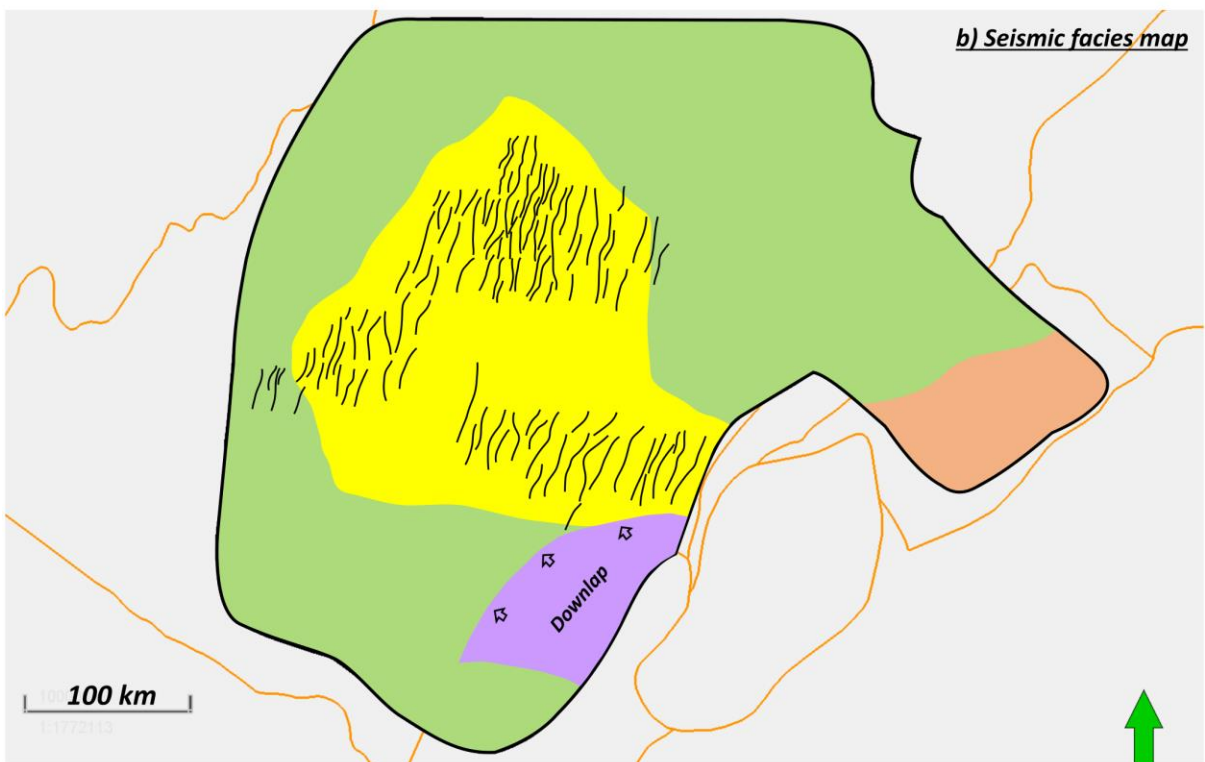
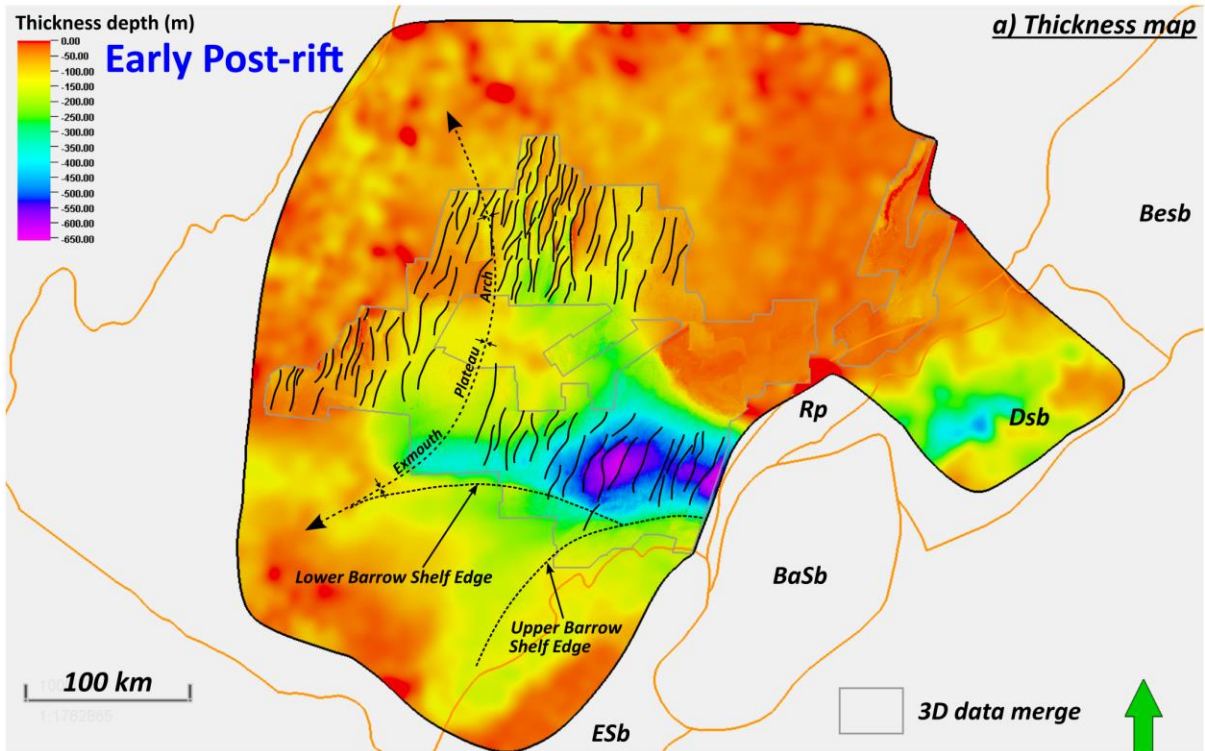


Fig. 6. Well cross-section showing the four main seismic stratigraphic units from west to east in the middle of the Exmouth Plateau. The basal dashed line marks the breakup unconformity and onset of deposition of the Muderong Shale during thermal subsidence. KK1: Kentish Knock-1, SB5: Scarborough-5, GL1: Glenloth-1, BS1: Briseis-1, ZG1: Zagreus-1, AC1: Achilles-1, CL1: Clio.



ESb : Exmouth sub-basin

Rp : Rankin Platform

Dsb : Dampier sub-basin

BaSb : Barrow sub-basin

Besb : Beagle sub-basin

Pf

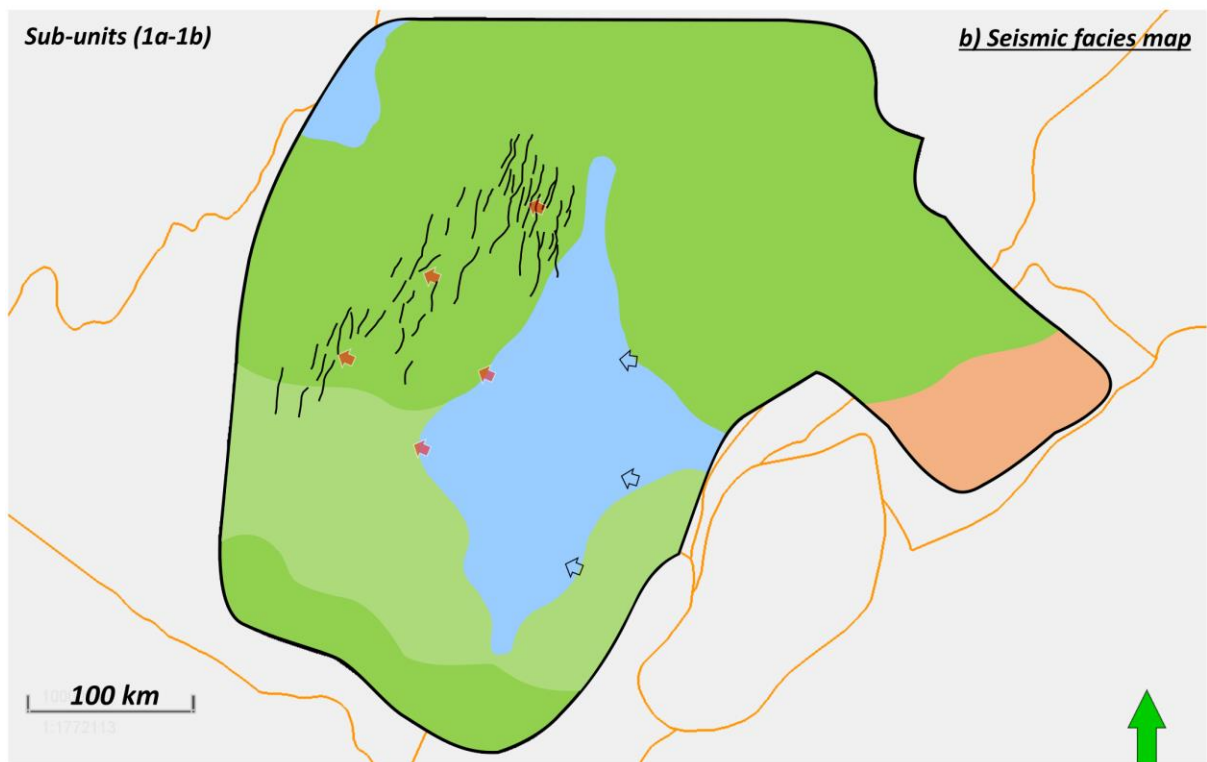
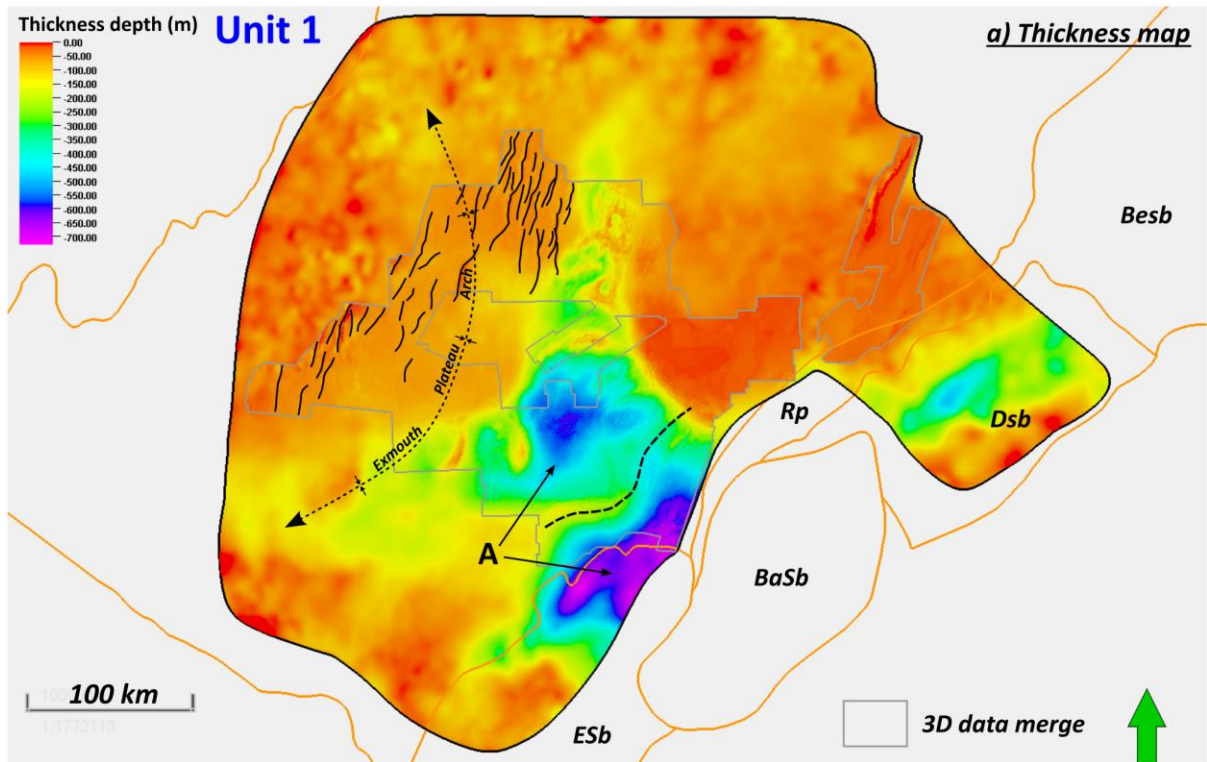
SmcDc

PrSp

Pg/Ag

Fig. 7. a) Thickness map of the Early Post-rift sequence with a sediment depocentre in the middle of the Exmouth Plateau. This map was created from horizons K0 and K1. Black lines indicate the crests of emergent underlying fault blocks. b) Seismic facies map showing that Early Post-rift is mostly characterised by polygonal faulting and parallel to subparallel facies (see Table 2 for colour legend). The Upper Barrow is included in the Early Post-rift interval. Pf (Polygonal fault), SmcDc (Semi-discontinuous), PrSp (Parallel to Subparallel), Pg/Ag (Progradation/Aggradation).





**ESb** : Exmouth sub-basin      **Rp** : Rankin Platform  
**BaSb** : Barrow sub-basin      **Besb** : Beagle sub-basin      **---** : Pseudo boundary for separate deponcentre  
**Dsb** : Dampier sub-basin      **A** : Depocentre

Fig. 8. Maps for Unit 1 which consists of sub-units 1a and 1b. a) Thickness map of Unit 1 with sediment depocentre A. This map was created from horizons K3 and K1. Black lines indicate the crests of emergent underlying fault blocks. b) Seismic facies map showing that Unit 1 is mostly characterised by parallel and subparallel facies (see Table 2 for colour legend). Red arrow: onlaps, black arrow: downlaps. Pr (Parallel), PrSp (Parallel to Subparallel), SpWv (Subparallel to Wavy), SmcDc (Semi- to discontinuous).

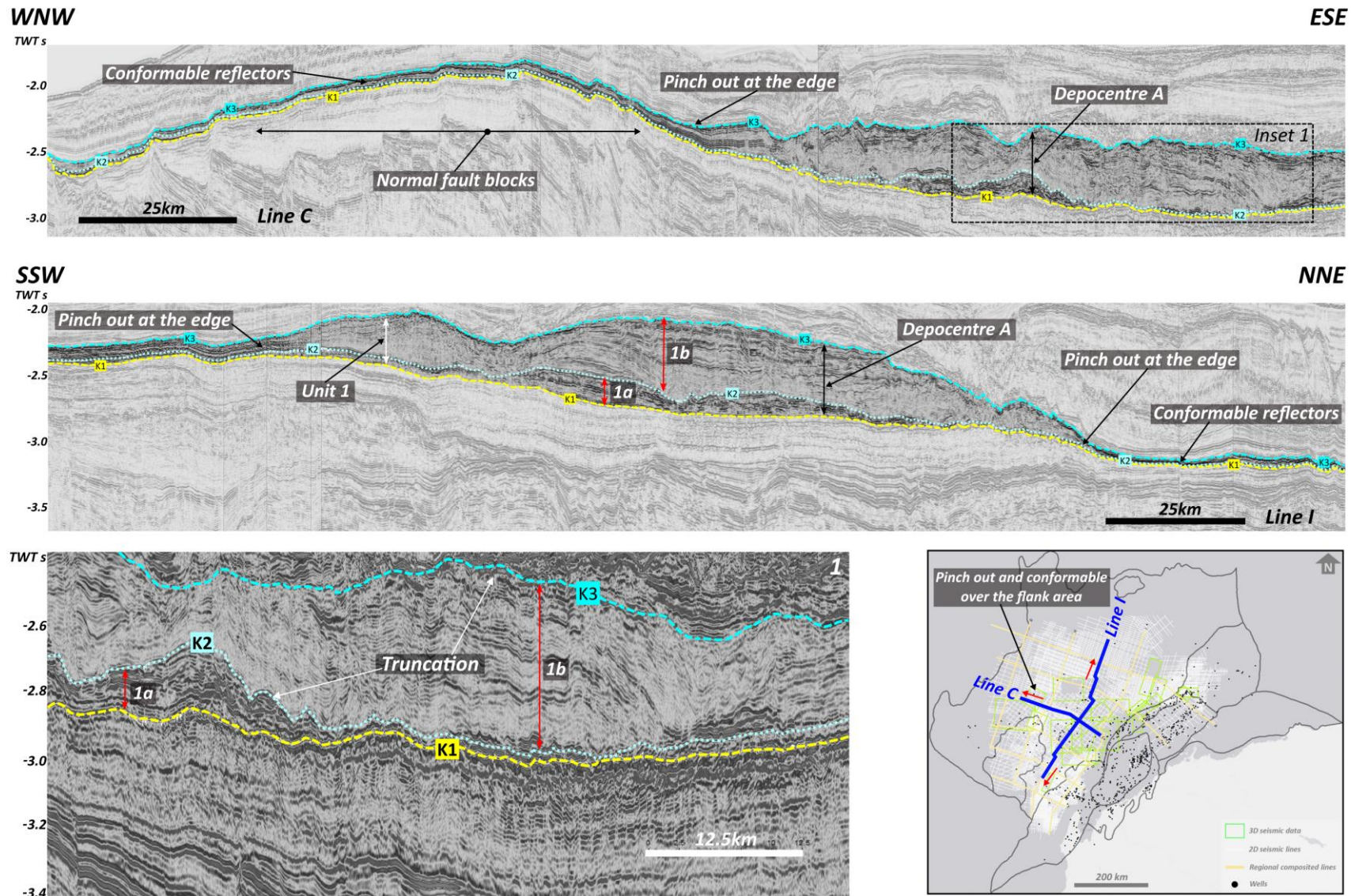


Fig. 9. Detail of regional seismic lines C and I displaying the nature of depocentre A. Sequences are thin and conformable on the flanks and at the edge of the depocentre. Prominent unconformities corresponding to horizons K1, K2 and K3 can be seen within the depocentre.



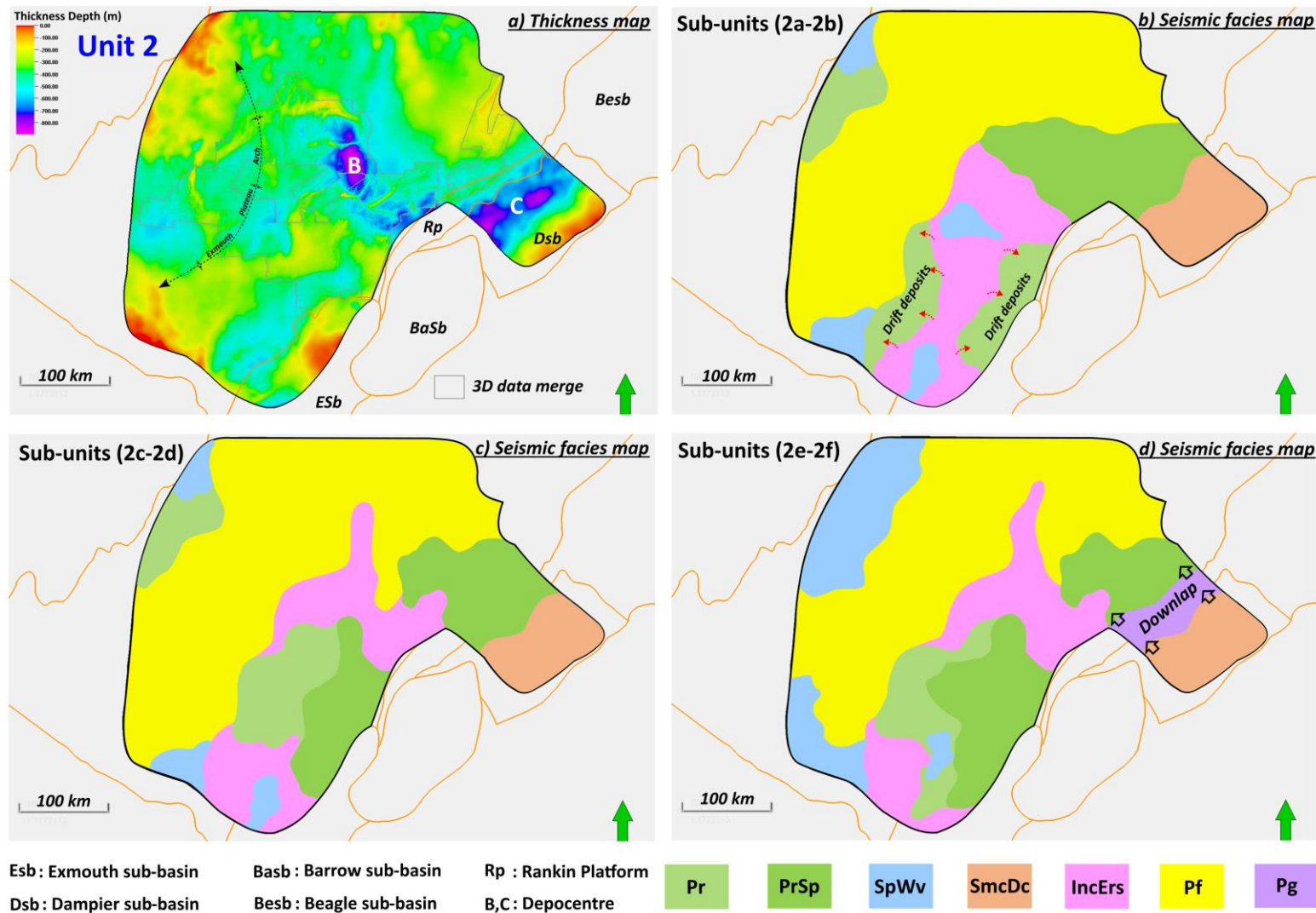
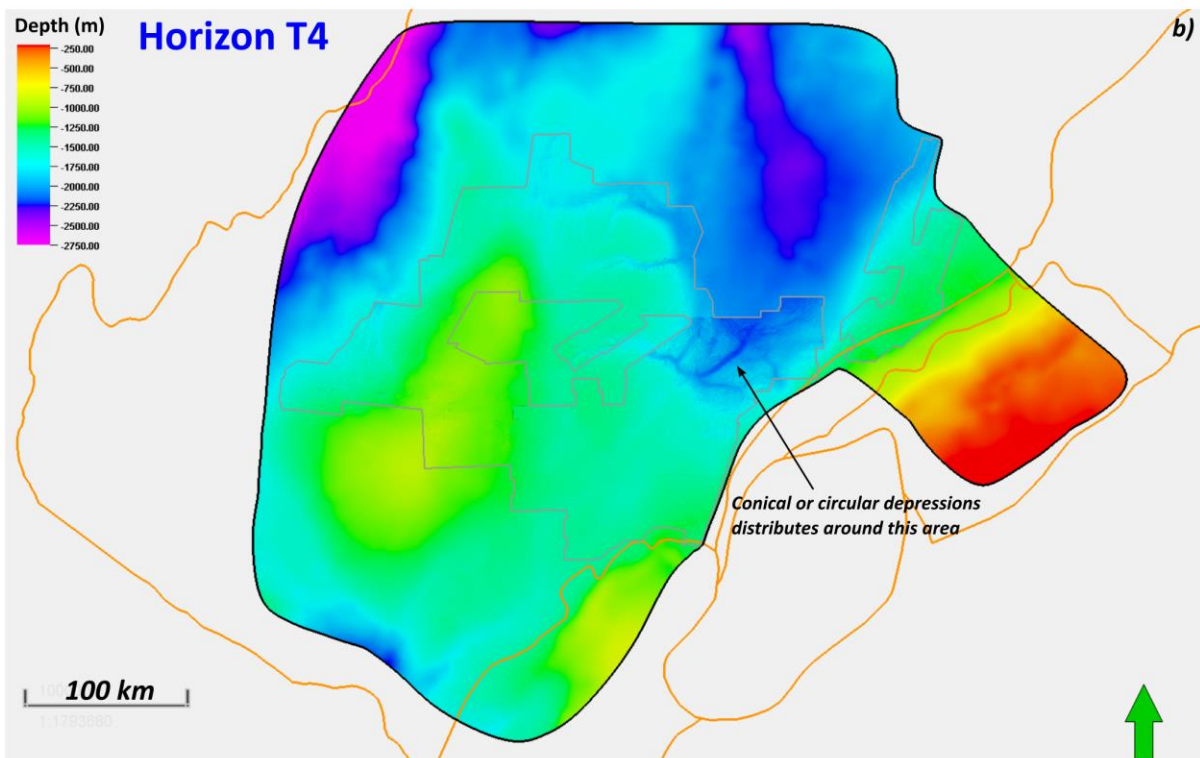
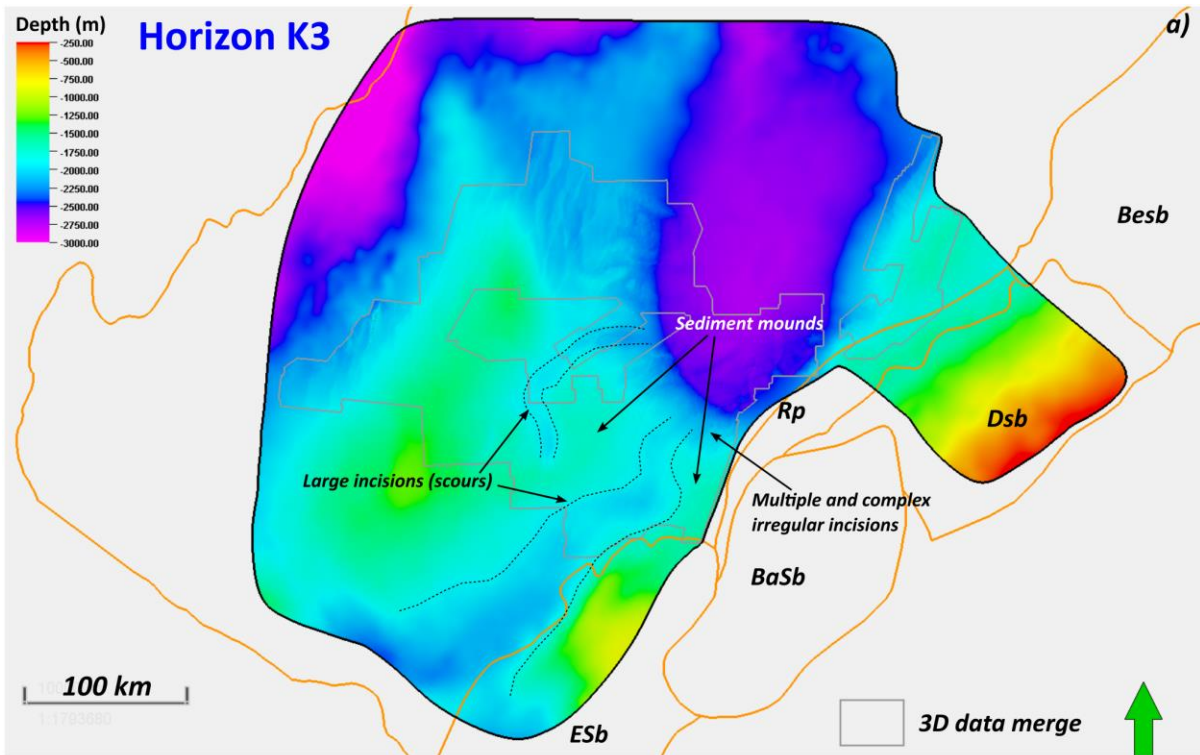


Fig. 10. Maps for Unit 2 which comprises 6 sub-units, namely 2a-2f. a) Thickness map of Unit 2 with sediment depocentres B and C. This map was made from horizons T4 and K3. b), c), d) Seismic facies maps of Units 2a-2b, Units 2c-2d and Units 2e-2f, respectively, showing the three dominant seismic facies in this interval: polygonal faulting, stacked incisions, and parallel and subparallel (see Table 2 for colour legend). Pr (Parallel), PrSp (Parallel to Subparallel), SpWv (Subparallel to Wavy), SmcDc (Semi- to discontinuous), IncErs (Incision or Erosive), Pf (Polygonal fault), Pg (Progradation).





Esb: Exmouth sub-basin    Basb: Barrow sub-basin    Rp: Rankin Platform    Dsb: Dampier sub-basin    Besb: Beagle sub-basin

Fig. 11. Depth structure maps of horizons K3 and T4 showing examples of the erosional features associated with bottom current activity during the Turonian to Early Oligocene.

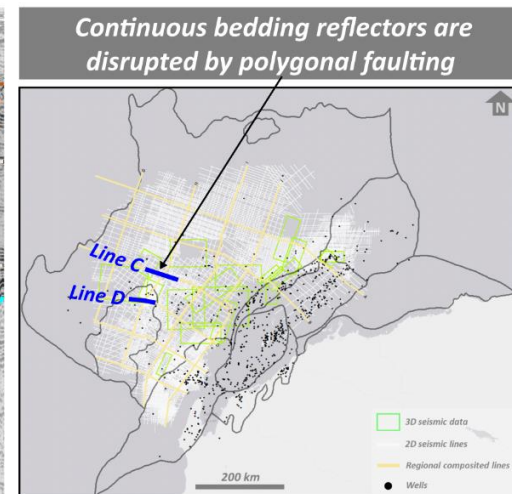
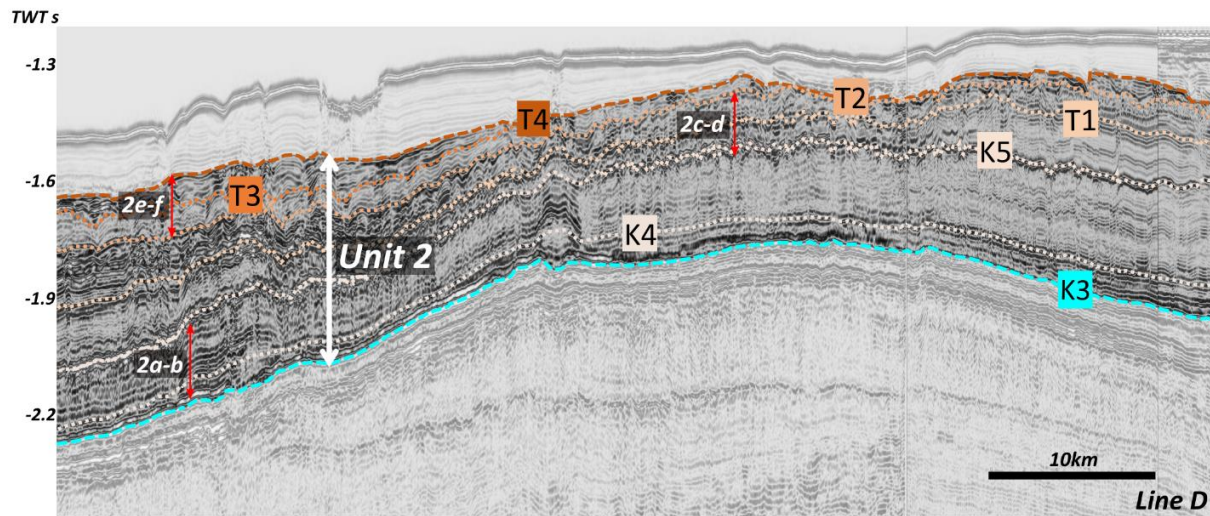
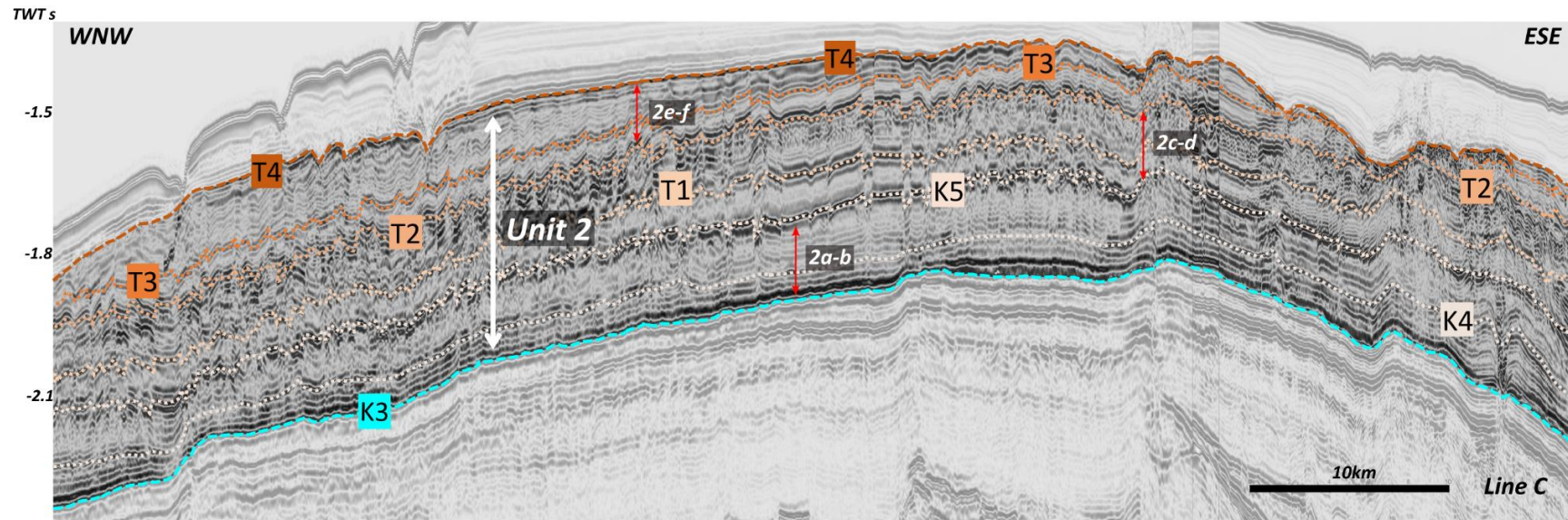


Fig. 12. Detail of regional seismic sections C and D showing polygonal faults, which are widespread across the most of the NCB, disrupting horizons K4, K5, T1, T2, T3 and T4 from Unit 2. The location is shown on the inset map.



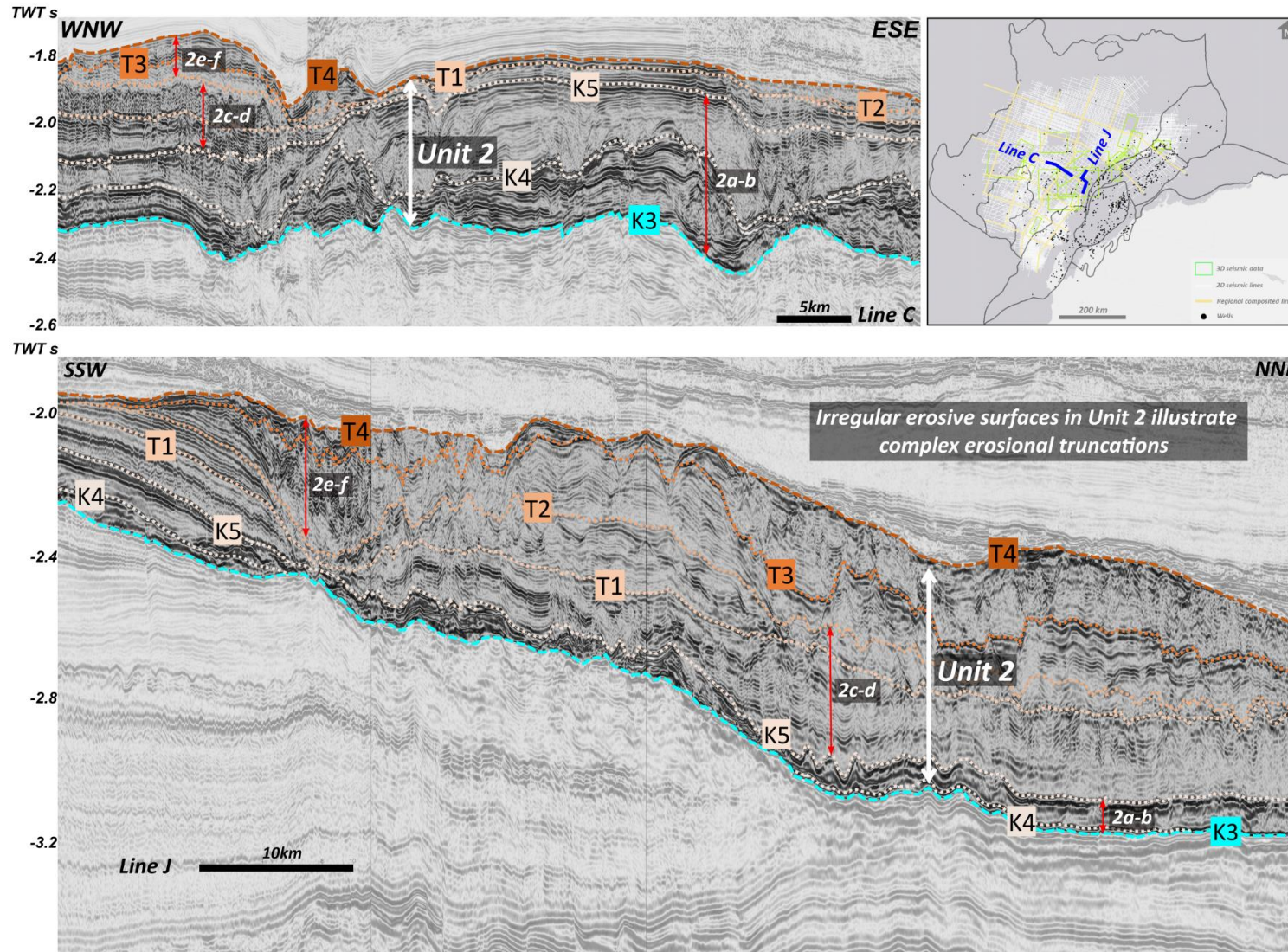


Fig. 13. Detail of regional seismic sections C and J showing erosive boundaries corresponding to Horizons K4, K5, T1, T2, T3 and T4. These define multiple stacked incisions. The location of the sections is shown on the inset map.



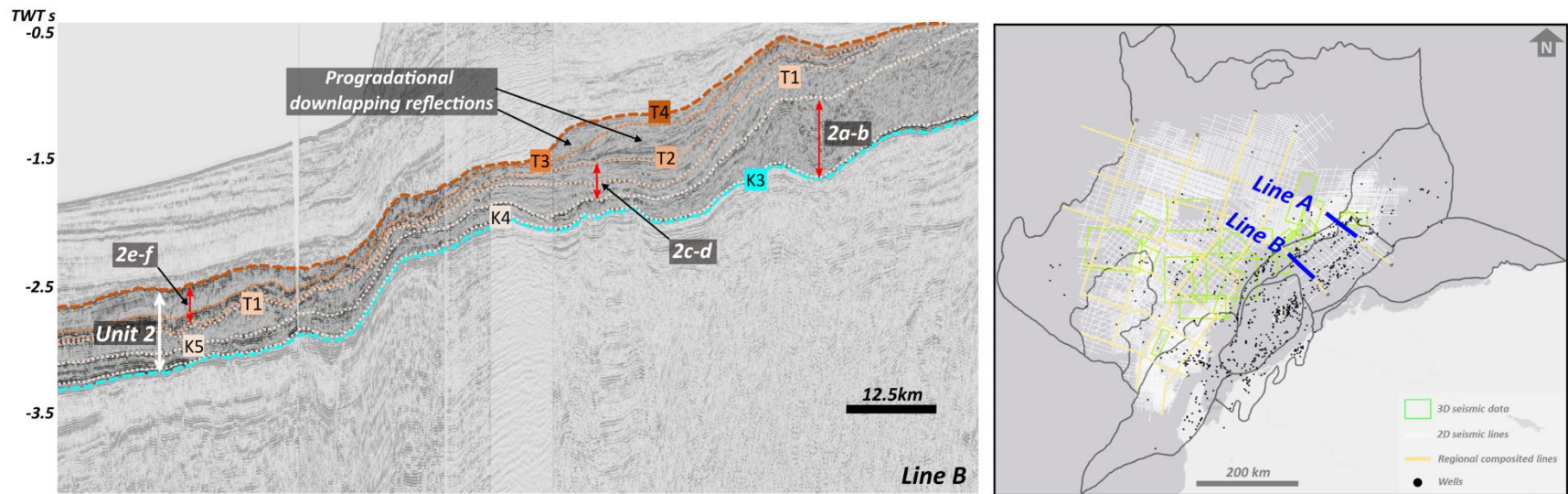
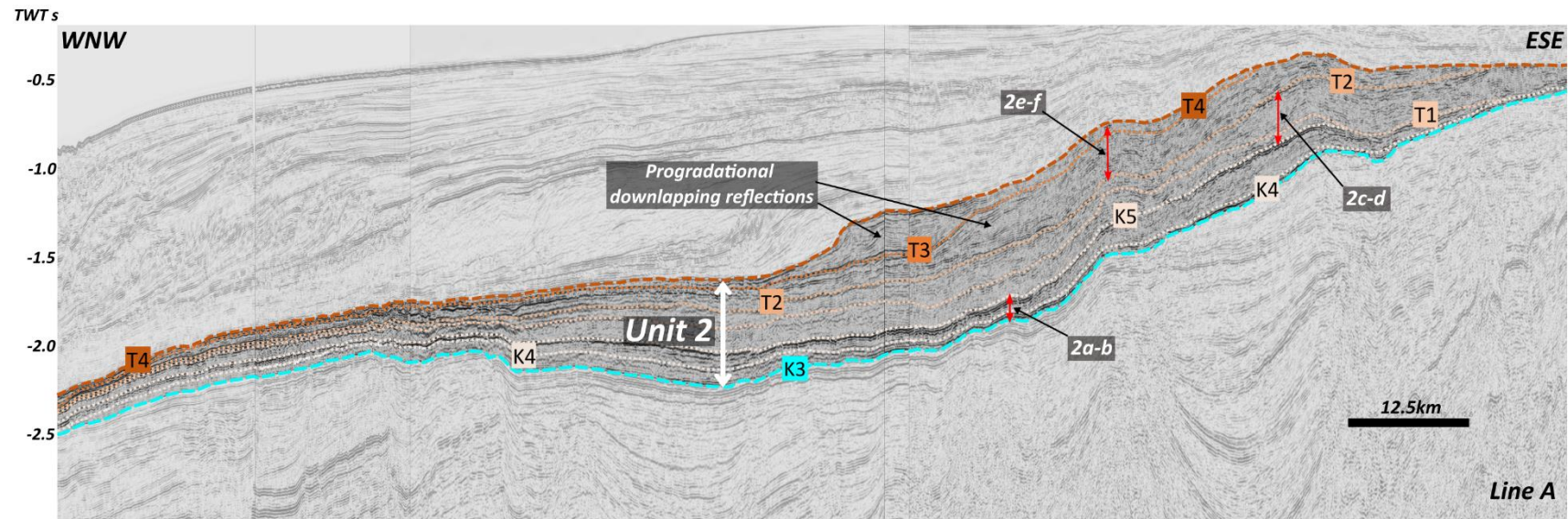


Fig. 14. Detail of regional seismic sections A and B showing major downlap surfaces corresponding to horizons T2, T3 and T4 in the northeast of the study area close to the Rankin Platform and the Dampier Sub-basin. The location of the sections is shown on the inset map).



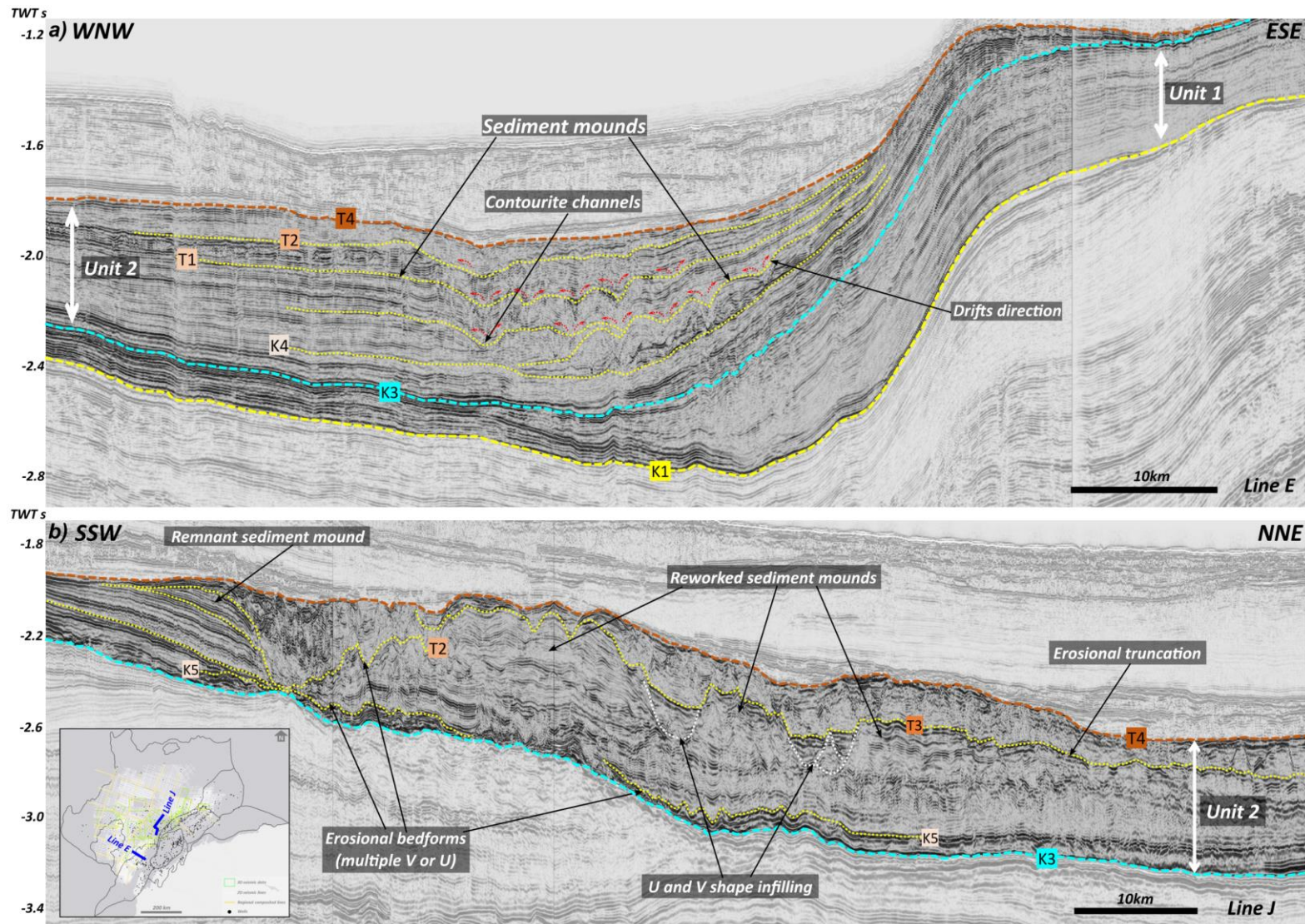
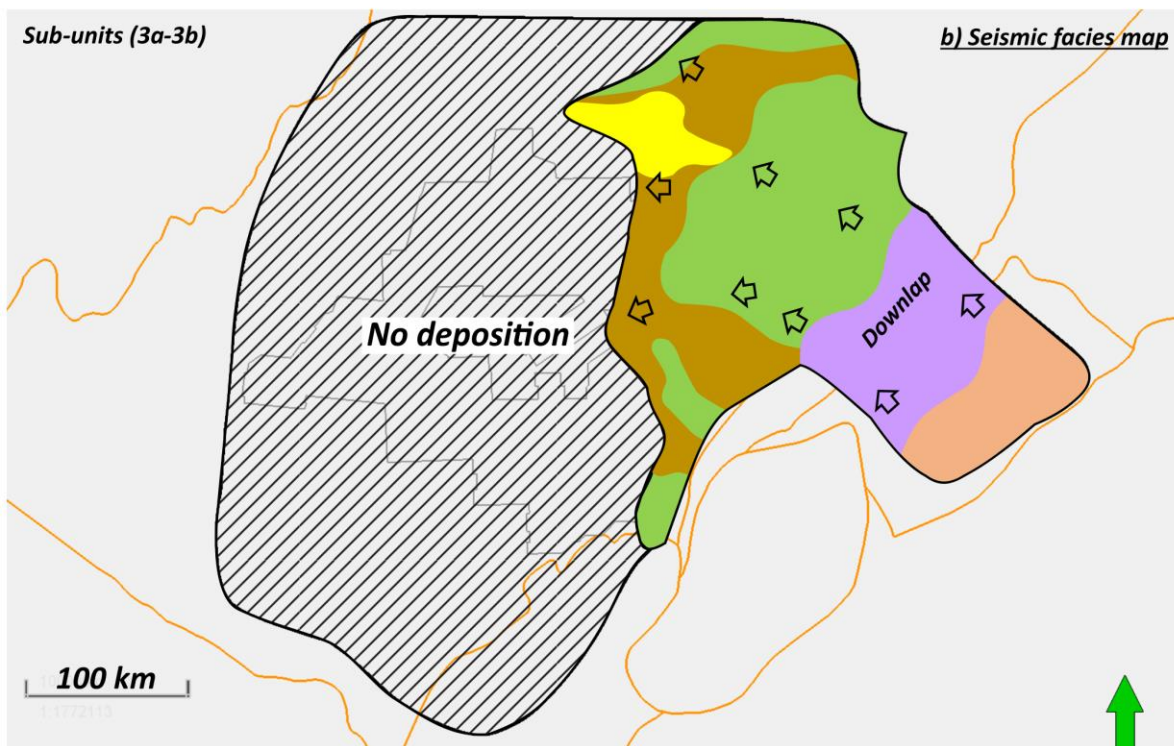
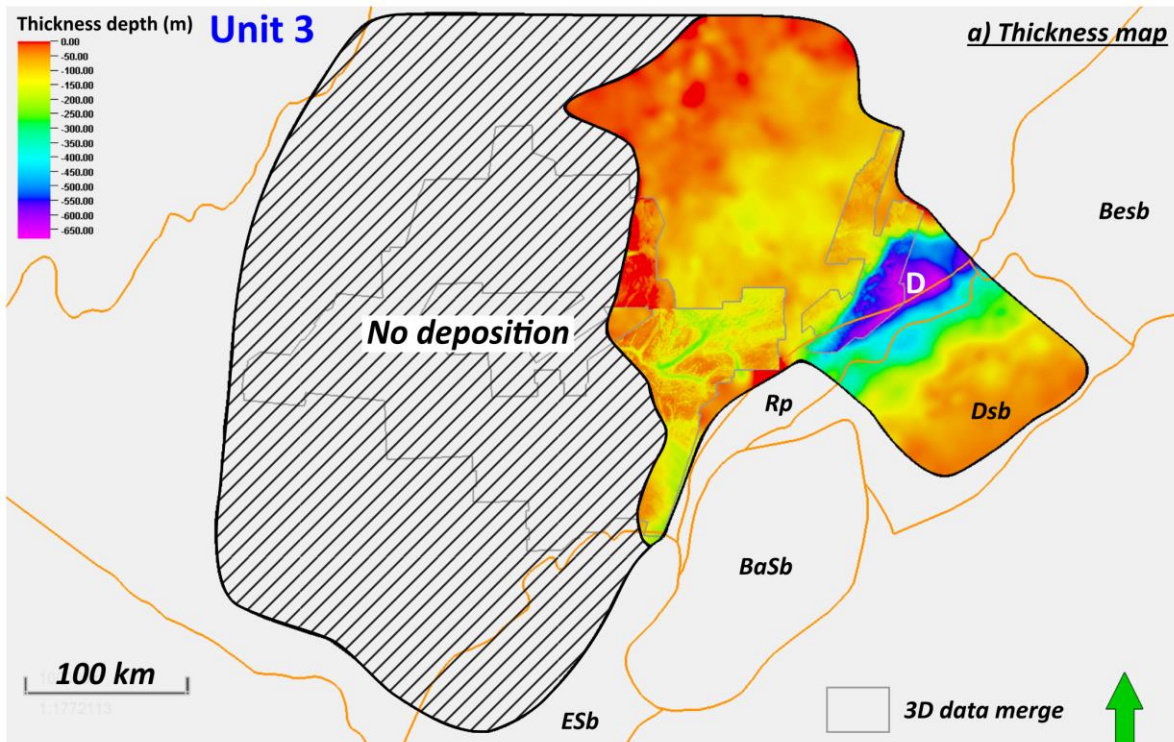


Fig. 15. Evidence for bottom current activity in Unit 2. a) Sediment drifts, sediment mounds and contourite channels on regional seismic section E. b) Highly eroded beds and simple to complex scours on regional seismic section J. The location of the sections is shown on the inset map.





Esb : Exmouth sub-basin	Basb : Barrow sub-basin	Rp : Rankin Platform	PrSp	Pf	SmCh
Dsb : Dampier sub-basin	Besb : Beagle sub-basin	D : Depocentre	Pg	SmcDc	

Fig. 16. a) Thickness map of Unit 3 with sediment depocentre D. This map was derived from horizons T6 and T5. b) Seismic facies maps of Unit 3, which contains sub-units 3a and 3b showing the distribution of PrSp (Parallel to Subparallel), Pf (Polygonal fault), SmCh (Semi Chaotic), Pg (Progradation), SmcDc (Semi- to discontinuous) seismic facies. See Table 2 for colour legend.

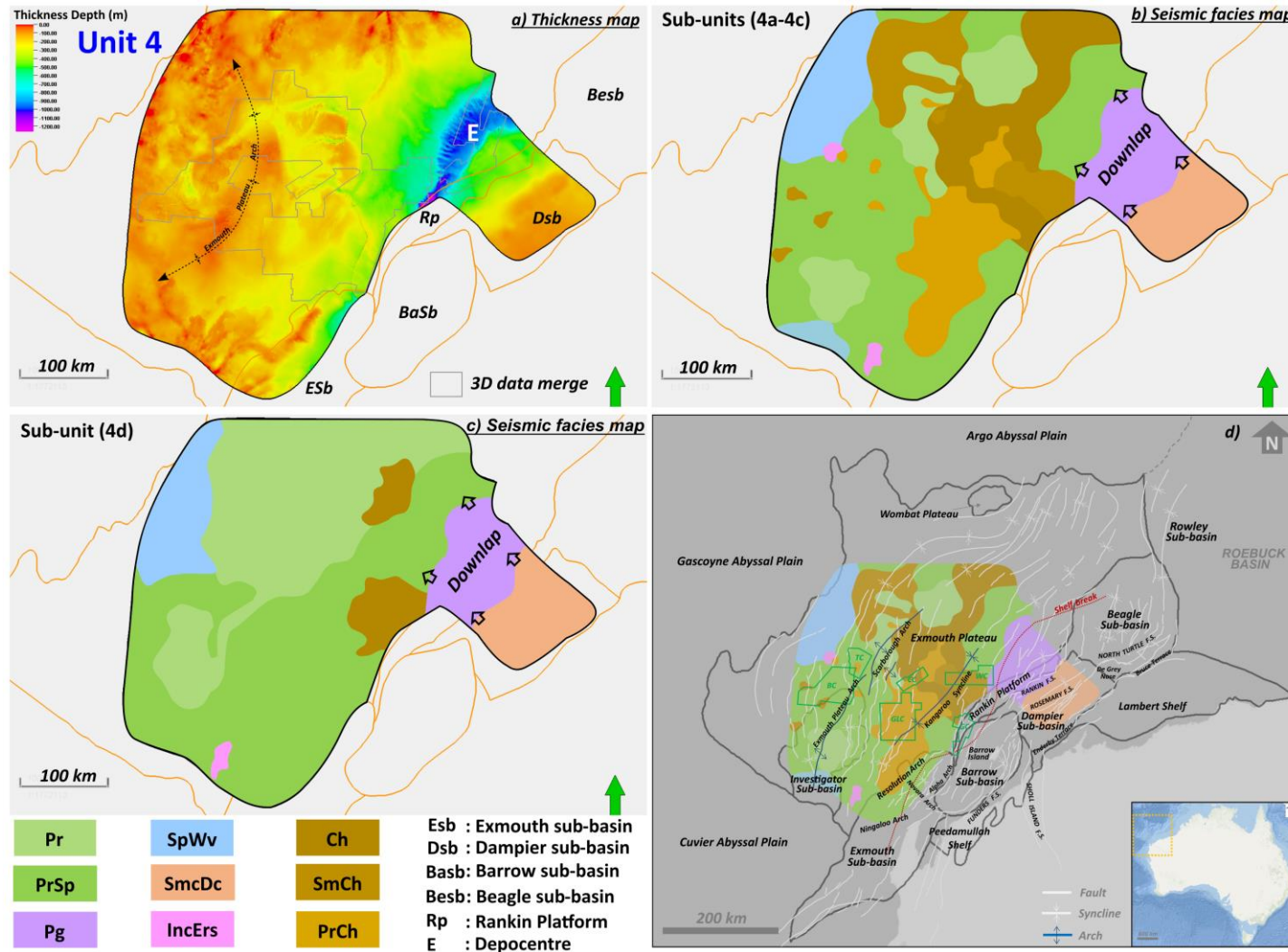


Fig. 17. a) Thickness map of Unit 4 with sediment depocentre E. This map was generated from horizon T10 and the merger of horizons T6 of Unit 3 and T4 of Unit 2. b) Seismic facies map of sub-units 4a-c showing widespread occurrence of chaotic seismic facies. c) Seismic facies map of sub-unit 4d which is mainly characterised by parallel and subparallel beds (see Table 2 for colour legend). d) MTC distribution in the NCB. The green shapes show slope failure studies from Hengesh et al. (2012) in Gorgon (GC), Willem (WC), Glencoe (GLC) and Chadon Complexes (CC), and from Scarselli et al. (2013) in Thebe (TC) and Bonaventure Complexes (BC). Pr (Parallel), PrSp (Parallel to Subparallel), Pg (Progradation), SpWv (Subparallel to Wavy), SmcDc (Semi- to discontinuous), IncErs (Incision or Erosive), Ch (Chaotic), SmCh (Semi Chaotic), PrCh (Parallel to Chaotic).



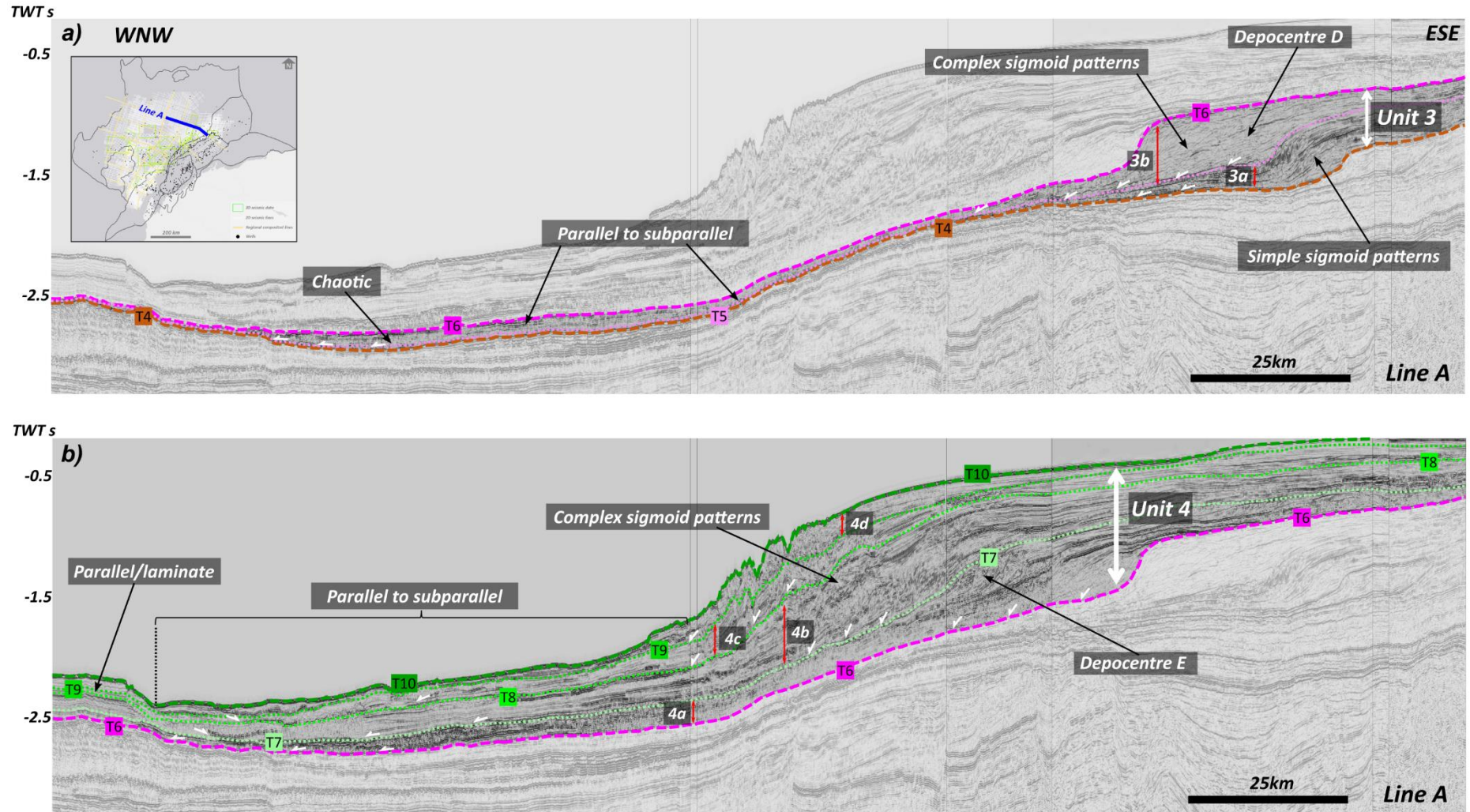


Fig. 18. a, b). Regional seismic section A illustrating the seismic facies present in Units 3 and 4. In the ESE, sub-unit 3a-3b and 4a-4d are dominated by progradational patterns that form a simple sigmoid to complex patterns. Further WNW, seismic facies pass laterally into parallel to subparallel and semi-chaotic facies, and onlap and terminate onto Horizon T4 and T6. The white arrows indicate downlapping and onlapping reflections. The location of the section is shown on the inset map.



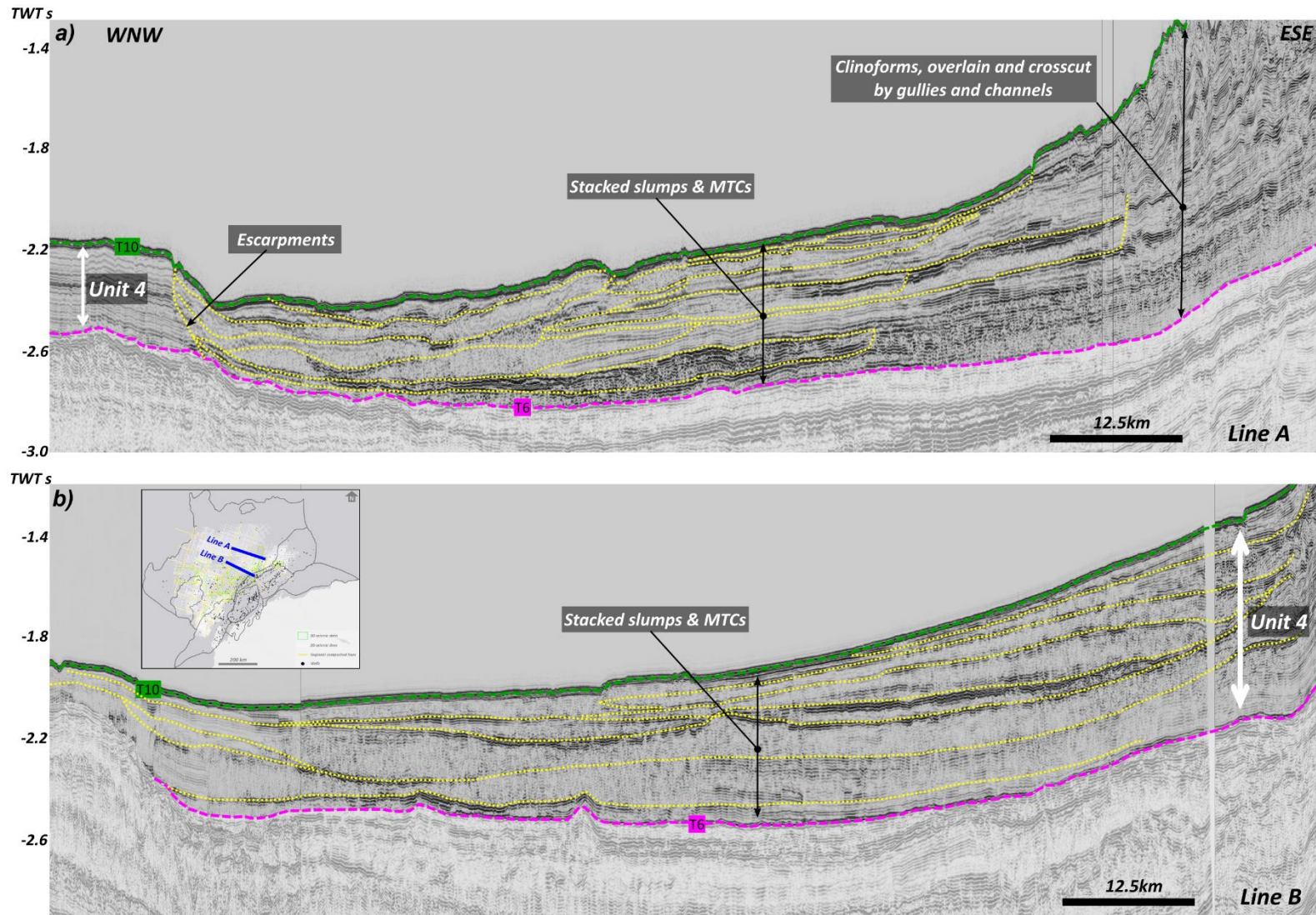


Fig. 19. a, b). Regional seismic sections A and B highlighting the presence of slumps and MTCs in Unit 4 on the NW side of the Rankin Platform. In the line A, sediment collapses mainly from a topographic high in the west, which created escarpments and sediment runoff to the east. In the line B, the slope gradient is steeper and was greatly affected by slope failure. The location of the sections is shown on the inset map.

---

*Chapter Three:*

*Cretaceous – Paleogene Evolution of  
Bottom Currents in the Northern  
Carnarvon Basin, Northwest Shelf of  
Australia*

---

# Chapter Three: Cretaceous – Paleogene Evolution of Bottom Currents in the Northern Carnarvon Basin, Northwest Shelf of Australia

---

## Research highlights

1. A detailed seismic geomorphology interpretation of Aptian – Rupelian sequences, Northern Carnarvon Basin, Australia, is reported.
2. Sedimentation is controlled by sustained bottom current activity over an 80-Myr-long period.
3. Changes in sedimentary style from mound and moat growth to subsequent filling and depocentre migration suggest waning current intensity.
4. Initiation and demise of bottom current activity correspond to paleo-geographic changes following the breakup of Gondwana.

## *Abstract*

Bottom current deposits are common features along continental margins and are typically associated with slopes, either at the continental rise or adjacent to shallow shelves. In this study, we provide a detailed characterisation of Aptian to Rupelian deposits that developed in the centre of the Exmouth Plateau of the Northern Carnarvon Basin, Northwest Shelf of Australia, on c. 500 km wide ramp-type margin, characterised by gentle slope breaks between the coastline and the deep basin. Sediment mounds and moats initially developed during the Aptian to Turonian in clastic sediments in the southwest of the study area, whereas reduced sediment accumulation characterised the north-eastern sector. During the Turonian to Lutetian, a transition to carbonate sedimentation occurred. Interestingly, these features continued to develop, with the mounds gradually establishing themselves through aggradational growth, while the moats were infilled by sediments exhibiting complex structures, including small-scale mounds and incisions with a wide variety of different morphologies. From the Danian to Rupelian, there was a notable decrease in moat infilling and mound growth, leading to significant progradation of sediment toward the northeast. This final stage of sedimentation was characterised by stacked deep incisions, ridges, and conical depressions. Initial stages of deposition correspond to a period of time when a wide and open ocean was present to the north of Australia, but only narrow seaways and

intracontinental rifts, associated with the breakup of Gondwana, were present to the west and south. The accelerated growth of mounds occurred during a period of accelerated separation of Greater Indian and Australia while cessation of bottom current activity corresponds to a period of rapid separation of Australia from Antarctica. The recognition and investigation of bottom current features provide new insights into the way in which oceanic circulation patterns may have evolved as the breakup of Gondwana progressed and can help our understanding of the processes that operate during the early stages of passive margin development and the formation of oceanic basins.

**Keywords:** *Seismic stratigraphy, morphosedimentary structures, bottom current deposits, Northern Carnarvon Basin, Exmouth Plateau, Northwest Shelf of Australia.*

## 1. Introduction

The movement of oceanic water masses driven by density and temperature gradients, winds and tides (Shanmugam, 2008), control the development of bottom (contour) currents (Rebesco et al., 2014). They shape the ocean floor by transporting, depositing, and eroding seabed sediments over time periods ranging from decades to millions of years (Roden, 1987; Shanmugam, 2008, 2014; Stow et al., 2008; Mulder et al., 2011; Hernández-Molina et al., 2016). Persistent deep water bottom currents can generate an abundance of depositional bedforms, including large sediment drifts or mounds (contourite drifts), as well as broad hiatuses and a range of erosional features (Stow et al., 2002a and b; Rebesco et al., 2014). In the last decade, Cenozoic, and particularly Quaternary, contourite systems have been widely investigated to understand their mechanisms of formation and to define key diagnostic criteria for their recognition. While it is relatively simple to relate younger deposits to contemporary oceanic circulation, it is more difficult to constrain circulation patterns in ancient oceans. Aptian to Rupelian bottom current deposits have been recognised in the Exmouth Plateau of the NCB, part of the NWS of Australia (Nugraha et al., 2019; Winata et al., 2023), a period that spans the separation of Greater India and Antarctica from Australia. This provides the opportunity to use the ancient rock record to shed light on past circulation patterns and how they have evolved during the initiation and development of ocean basins.

Most conceptual models indicate that contourite deposition primarily occurs along slopes, either at continental margins or adjacent to shallow shelves, with interactions between along-slope currents and down-slope gravity-driven processes, resulting in mixed turbidite-contourite depositional systems (Stow et al., 2011; Fonnesu et al., 2020, Rodrigues et al., 2022). In contrast, the Exmouth Plateau forms a broad, c. 500 km wide ramp-type margin (*sensu* Van Wagoner et al., 1988), with a low-angle seafloor and gentle slope breaks between the present-day coastline and the deep basin (c. 0.5 degrees). The bottom current deposits encompass a period when the margin most likely had a broadly similar geometry (Apthorpe, 1988; Bradshaw et al., 1988; Mory, 2023) and during which there was a transition from clastic to carbonate sedimentation, beginning in the Turonian (Romine and Durrant, 1996; Longley et al., 2002; Geoscience Australia, 2022). These deposits have been the subject of relatively limited investigation, mostly on the basis of 2D seismic data (Romine and Durrant, 1996), or the limited use of 3D seismic data (Nugraha et al., 2019; Winata et al., 2023). While sedimentological features characteristic of bottom current activity have been recognised, questions remain regarding the bathymetric setting in which they formed, the interaction between erosional and depositional bottom currents, how they evolve through time, their relationship to breakup of Gondwana and the early stages of oceanic basin formation. Numerous high-resolution, public domain 3D seismic datasets provide continuous coverage over large parts of the NCB, showing a wide variety of bedforms imaged in exceptional detail, allowing these questions to be addressed. In this paper we utilise mapping of merged 3D seismic datasets covering an area of  $\sim 15,000$  km<sup>2</sup> to: (1) document different geomorphological features associated with bottom current activity in the NCB, (2) describe how they change through the time, (3) consider how they fit into the broad spectrum of mixed turbidite-contourite depositional systems and (4) consider the implications of evolving bottom currents for changing oceanographic conditions from the Cretaceous to the Oligocene associated with Gondwana breakup.

## 2. Regional setting

### 2.1. Geological background

The NCB is situated on the northwest margin of Australian, covering an area of approximately 535,000 km<sup>2</sup> (Hocking, 1988). The NCB comprises several inboard sub-basins

(i.e., Exmouth, Barrow, Dampier, Beagle, and Rankin Platform; Fig. 1; Romine et al., 1997), which contain Jurassic to Lower Cretaceous syn-rift sequences. The outboard Exmouth Plateau contains thick pre-rift sequences of Triassic sediments, thin syn-rift sequences and Lower Cretaceous to Recent post-rift sediments. The inboard sub-basins are partially covered by the present-day shelf margin and have a water depth of around 200-500 m, whereas the outboard areas have greater water depths of approximately 0.8-4 km (Exon et al., 1992; Scarselli et al., 2013). The basin is bounded by three abyssal plains: the Cuvier Abyssal Plain in the south, the Gascoyne Abyssal Plain to the west, and the Argo Abyssal Plain to the north (Fig. 1). The NCB is the site of significant oil and gas production, having proven and probable reserves of about 534 MMBLS (Million Barrels) of oil and 45.33 TCF (Trillion Cubic Feet) of gas (Geoscience Australia, 2022).

The NCB has evolved in three main stages of rifting associated with Gondwana breakup (Audley-Charles et al., 1988; Driscoll and Karner, 1998; Gartrell, 2000; Borel and Stampfli, 2002; Metcalfe, 2013): from the Late Carboniferous to Late Permian (l'Anson et al., 2019; Deng et al., 2019), the Late Triassic to Middle Jurassic, and the Late Jurassic to Early Cretaceous (Bradshaw et al., 1988; Veevers et al., 1991; Baillie et al., 1994), culminating in breakup in the Valanginian. Thereafter, basin evolution was controlled by thermal subsidence (Veevers et al., 1991; Baillie et al., 1994; Driscoll and Karner, 1998; Cathro and Karner, 2006) as well as minor compression in the Late Cretaceous and Late Miocene, which resulted in the formation of broad anticlines or "arches" (Veevers et al., 1991; Baillie et al., 1994; Lee and Lawver, 1995; Romine et al., 1997; Driscoll and Karner, 1998; Hull and Griffiths, 2002; Pryer et al., 2002; Cathro and Karner, 2006). Siliciclastic sedimentation was dominant up until Turonian, after which there was a transition to carbonate sedimentation (Apthorpe, 1988; Romine et al., 1997).

## 2.2. *Oceanographic circulation*

The Aptian to Rupelian sedimentary deposits that are the focus of this study developed during two distinct phases in the post-rift tectonic evolution of the region. These can be associated with the rapid north-westwards drift of India after the Albian (Veevers, 2000), and the rapid movement of Australia northwards away from Antarctica from the Eocene (Müller et al., 2000; Seton et al., 2012). The increasing separation between continents is interpreted

to have allowed the establishment of oceanic circulation around the north-western, western, and southern margins of Australia (Miller et al., 1991; Baillie et al., 1994; Stickley et al., 2004; Houben et al., 2013). Although the precise geometry of these currents during the early stages of separation remains unclear, present-day oceanic circulation may provide insights into past events. Offshore Western Australia is affected by four surface currents, which are the Indonesian Throughflow (ITF), the South Equatorial Current (SEC), the Leeuwin Current (LC), and the Eastern Gyral Current (EGC) (Fig. 2; Holloway and Nye, 1985; Cresswell, 1991; Holloway, 1995; Gordon and Fine, 1996; Potemra et al., 2003; Gordon, 2005). To the north of Australia, the major surface currents are controlled by poleward-flow that transfers water masses from the Pacific to Indian Oceans, mainly through Eastern Indonesian islands via the ITF (Feng et al., 2018). The ITF water masses are low salinity, warm and oligotrophic, and travel along the Timor, Ombai and Lombok straits (Church et al., 1989; Molcard et al., 1996; Fieux et al., 2005; Baker et al., 2008; Gordon et al., 2005; Feng et al., 2015). They continue towards the Indo-Australian Basin, providing initial flow to the LC (Vranes et al., 2002) and generate the westward-flowing SEC (Collins et al., 2014). In addition, when the SEC traverses the Indo-Australian Basin, it also derives water mass from South Indian Ocean Current (Australian Government: DCCEEW, 2007).

To the northwest of Australia, the ITF also plays an important role in recirculating water masses offshore via the SEC and the EGC. This moves water masses across the Argo Abyssal Plain and the adjacent continental slopes, potentially due to local winds and pressure gradients (Fig. 2; Australian Government: DCCEEW, 2007). This promotes surface flows away from the shelf edge to the slope and across the abyssal area. It is assumed that ITF waters penetrate the shelf via the Holloway Current and the offshore EGC pathway (Australian Government: DCCEEW, 2007). However, at depths below the main thermocline the waters offshore of NW Australia are impacted by the Southern Antarctic Intermediate Water and Subantarctic Mode Water, as well as the Northern Banda Intermediate Water. At depths greater than ~1000 m, the water masses consist of a combination of Indian Ocean Deep Water and Lower Circumpolar Deep Water (Australian Government: DCCEEW, 2007).

West of Australia, the Leeuwin Current, as described by Cresswell and Golding (1980) and Thompson (1987), is a southward-flowing current (Fig. 2; Peter et al., 2005) primarily formed from equatorial water masses. It is relatively narrow, ranging from 50-100 km in

width, and located along the shelf edge at water depths of 200-300 m. The current is also characterised by high velocities, typically ranging from 0.1-0.4 m/s (Church et al., 1989; Smith et al., 1991; Cresswell and Peterson, 1993; James et al., 2004; Ridgway and Condie, 2004; Fieux et al., 2005; Pattiaratchi, 2006; Feng et al., 2015). On a seasonal basis, the LC can become even stronger, particularly when it is reinforced by the north-easterly Holloway Current along the shelf. The LC is connected to other currents such as the ITF or EGC to the south, which are characterised by warmer, low salinity, and cool subtropical waters further offshore. At a depth of approximately 400 m (Woo and Pattiaratchi, 2008), the subsurface Leeuwin Undercurrent (LU) flows northward (Fig. 2) and has high velocity, typically ranging from 0.32-0.4 m/s (Thompson, 1984). This current flows in the opposite direction to the LC, and its water masses originate from the denser and more saline Subantarctic Mode Waters and South Indian Central Water (Australian Government: DCCEEW, 2007). Further offshore from the LC is the equatorward-flowing Western Australian Current (WAC). This cold, high salinity current (Spooner et al., 2011) flows at great depths (~2000 m; Tchernia, 1980) in the northeastern wings of the anti-clockwise subtropical gyre of the southern Indian Ocean.

### 3. Data and methodology

#### 3.1. Dataset

This study employs six Pre-stack Time Migrated (PSTM) three-dimensional seismic cubes covering an area of ~15,000 km<sup>2</sup> situated in the central region of the Exmouth Plateau, near the Barrow sub-basin and Rankin Platform, and around the Kangaroo Syncline (Fig. 1). The seismic surveys were acquired and processed between 2004 and 2008 for hydrocarbon exploration and have a range of bin sizes and vertical sample intervals (Table. 1). The focus of most of the wells within the 3D seismic data area was on hydrocarbon targets in Jurassic and Triassic formations. Consequently, in most instances there is only limited biostratigraphic, well log and lithological information available from the shallower, non-target intervals that are the subject of this study. Seventeen wells (Fig. 1) with check-shot, sonic log and biostratigraphic data from the Cretaceous and younger sequences were selected and used to calibrate interpreted seismic horizons with age and lithological information from the Cretaceous – Paleogene intervals. All data used in this study are publicly accessible through the Western Australian Petroleum and Geothermal Information Management System



(WAPIMS) and National Offshore Petroleum Information Management System (NOPIMS) catalogues.

### 3.2. Methodology

The original 3D seismic datasets were merged using Petrel (SLB) and Blueback Toolbox (CEGAL) software to ensure data consistency, efficiency, and seismic interpretation quality. The original cubes have a full record length of 6,000 ms TWT (Two Way Time) but were cropped to an interval between 200 to 3,500 ms TWT that covers the main Cretaceous - Paleogene sequences that are the target for this study. As the individual cubes have different amplitude ranges, they were balanced to give identical amplitude distributions with a zero-centric range of  $\pm 16,000$ . The balanced seismic cubes were then merged with a vertical sample interval of 4 ms, using geometry and navigation information from the existing cubes.

Winata et al. (2023) identified four primary seismic stratigraphic units (referred to as Unit 1-4) covering the whole of the NCB that correspond to different phases in the evolution of bottom current and mass transport deposits. They were constructed from 16 horizons interpreted on a grid of regional 2D seismic sections tied to 40 wells. The ages of these horizons were determined from biostratigraphic data contained in palynological and micropaleontological reports from multiple wells and are consistent with existing markers identified by Longley et al. (2002), Marshall and Lang (2013) and Geoscience Australia (2022). An early post-rift sequence developed between the Valanginian and the early Aptian (K20.0 SB to K40.0 SB) and is succeeded by Unit 1 which spans from the early Aptian to the Cenomanian (K40.0 SB to K50.0 SB). Unit 2 covers the Turonian to early Rupelian (K50.0 SB to T30.0 SB), Unit 3 includes the Rupelian to Tortonian (T30.0 SB to T40.0 SB), and Unit 4 contains the Tortonian to Present (T40.0 SB to Recent SB) (Fig. 3 and 4).

This study focusses on Units 1 and 2 which comprise several key seismic horizons that allow them to be divided into sub-units. Horizons initially interpreted from the regional 2D grid were used to guide the interpretation of the merged 3D seismic dataset in order to create high resolution surfaces. These horizons were then used to guide the generation of additional significant stratigraphic surfaces in PaleoScan (ELIIS). In complex areas containing multiple stacked erosional and truncational surfaces and associated seismic artefacts, stratal slicing

and seismic attribute analysis were used to generate detailed seismic geomorphological maps, showing the geometries, shapes, and patterns of sedimentary bodies that form these units.

#### 4. Major morphosedimentary features

##### 4.1. *Seismic stratigraphic framework*

The base of the post-rift sequence is marked by horizon K0, regionally referred to as the Valanginian Unconformity, but which, in this part of the NCB defines a distinct shelf edge geometry at the top of a prominent sequence of clinoforms belonging to the Lower Barrow Group (Fig. 5a and 6a). The early post-rift sequence is bounded by horizons K0 and K1 in the early Aptian (Fig. 3, 4 and 5), and is dominated by fine-grained clastic deposits (Geoscience Australia, 2022). It comprises laterally conformable and continuous, moderate to high amplitude reflections cut by small polygonal faults (Fig. 5). A distinct sag is developed in the centre of the study area (Fig. 5a and 6a) and the sequence thins out to the northeast (Fig. 5a and 7a) due to a combination of onlap onto the basal K0 surface and subtle truncations at the top of the sequence by the K1 surface (Fig. 5a). Unit 1 is bounded by horizons K1 and K3 at the end of the Cenomanian (Fig. 3, 4 and 5), and is internally divided by horizon K2. In the southwest, this unit shows large, stacked gently mounded reflections with medium to high amplitude that in some areas become wavy and are incised into underlying sequences (Fig. 5). As with the underlying sequence, this sequence thins to the NE (Fig. 5a and 7b). The top of this unit marks a transition from fine-grained clastic to carbonate sediments, with carbonate sedimentation remaining dominant to the present day (Geoscience Australia, 2022).

Unit 2 represents the Turonian and Rupelian interval and is bounded by horizons K3 and T4 (Fig. 3, 4 and 5). It encompasses six main sub-units including units 2a and b between horizons K3 and K5, units 2c and d between horizons K5 and T2, and units 2e and f between horizons T2 and T4 (Fig. 4). They have varying internal characteristics, including parallel, mounded, incised and wavy seismic reflection geometries. Unit 3 corresponds to the Rupelian and Tortonian interval, bounded by horizons T4 and T6 (Fig. 3 and 5a), characterised by stacked chaotic reflections, which onlap and thin to the southwest onto a paleobathymetric

high at the top Unit 2 (Fig. 5a). As a result, it is confined to the northeast inboard area of the Exmouth Plateau. Unit 4 is marked by horizons T6 and T10, consisting of both parallel and laterally extensive stacked chaotic reflections (Fig. 3 and 4).

Depositional and erosional bedforms associated with deepwater bottom currents are recognised in Units 1 and 2, while Units 3 and 4 are characterised by mass transport complexes. Detailed descriptions of the features in Units 1 and 2 are provided in the following sections.

#### 4.2. *Unit 1: Early Aptian (~123 Ma, horizon K1) – Cenomanian (~94 Ma, horizon K3)*

Horizon K1 marks the culmination of Muderong Shale deposition, a fine-grained clastic unit deposited as a result of widespread transgression during the initial phases of post-rift subsidence (Fig. 5a, 6a-b and 7a; Romine and Durrant, 1996; Longley et al., 2002; Geoscience Australia, 2022). It is recognisable due to its prominent, consistent, and conformable reflection characteristics (Fig. 5). During the period between horizons K1 to K3, a pattern was established which divided the area into two distinct regions: an area of limited sediment accumulation to the northeast and an area of significant sediment accumulation in the southwest characterized by mounded sedimentary geometries (Fig. 5a, 6b-d and 7b). A well-defined and gently curved slope separates the two areas and is cut by broad, low relief incisions (~7 km wide, ~0.2 km deep; Fig. 6c) at horizon K3a which become narrower and more pronounced (<4 km wide, <0.1 km deep; Fig. 6d) at the top of horizon K3. There are a small number of NE-SW-oriented faults with small throws of <30 m that cut the base of the sequence. In the southwest, the K1-K3 interval contains a series of continuous parallel-stratified, large mound bodies, as well partially erosive and downlapping surfaces on the edges of the mounds which define two elongate and slightly meandering moats (Fig. 5, 6b-d and 7b). The moats can be seen throughout the sequence (Fig 5), but they are only subtly developed at K1 and become increasingly prominent up sequence. The maximum bathymetric relief between the base of the moat and the top of the mounds is approximately 300 m at horizon K3. The moats vary from about 10 to 60 km in width and are at least 30 km in length. The width of the mounds range from 25 to 60 km (Fig. 5 and 6b-d). The most westerly moat has an initial SE-NW orientation, but later shifts to an N-S orientation (Fig. 6c-d) as the mounds become more pronounced. A broader gently meandering moat in the south of the area is

particularly noticeable on horizon K3 (Fig. 6d), with the thickness maps suggesting it is narrower and more pronounced at this stage (Fig. 7b).

#### 4.3. Units 2a and b: Turonian (~94 Ma, horizon K3) – Maastrichtian (~66 Ma, horizon K5)

From horizon K3, the mounded sequences mainly consist of fine-grained carbonate sediments. The mounds continued to grow during this period, and the two prominent moats were infilled by sediment and become much narrower (Fig. 6d-f, 7c and 9a-b). The infilling of the westerly moat is mainly expressed by parallel to subparallel and multiple small to moderate scale stacked incisions, ranging from approximately 0.5 to 2 km in width (Fig. 9a-c). To the north, they transition into sequences with parallel and continuous reflections (from Fig 9b to 9a). Large scale curved, subparallel, symmetric V-shaped gullies (*sensu* Rodrigues et al., 2022) up to 2 km in width developed around the crests of the mounds between horizons K3 and K5 (T10.0 SB of Marshall and Lang, 2013) (Fig. 9a-b and 10). Further northwards, these horizons pass laterally into polygonally faulted sequences (Fig. 6d-f and 10).

The southerly moat is wider and longer than the one in the west (Fig. 6d-f), and the infilling is more complex, characterised by simple to multiple stacked mounds of small to moderate size (~6-9 km in width and ~15-25 km in length), moats, and incisions (Fig. 5a and 9d). The surface map of horizons K4a (K4 ≈ K60.0 SB of Marshall and Lang, 2013) shows segmented incisions that crosscut and are offset from one another, separated by confined mounds (Fig. 6e). RMS amplitude stratal slices between horizons K4b and K5 show that there are two types of incision - small irregular incisions (up to 1 km in width, 50-80 m in depth) that crosscut one another, trend NE-SW and are confined to the layer between K4b and K5, and larger hook-shaped incisions (~2-3 km in width, <0.1 km in depth) that cut down to the base of unit 2 (Fig. 11). The hook-shaped incisions are located on the northern margin of the moat and gradually shift from east to west. The northern boundary of the incisions merge to create a long meandering channel, which connects to and erodes the same slope as numerous smaller incisions further to the northeast (Fig. 6e).

A comparison of the thickness maps of Unit 1 (Fig. 7b) and the lower part of Unit 2 (K3 and K5; T10.0 SB of Marshall and Lang (2013); Fig. 7c) shows that more sediment began to accumulate on either flank of the deeper area to the northeast, while the centre remained

sediment starved (Fig. 5a and 9a). These sequences are characterised by parallel to subparallel and wavy reflections that are truncated by multi-stacked parallel incisions, which are particularly well developed on horizon K5 (Fig. 6f and 12). These are both perpendicular to the slope, cutting into it, and parallel to the base of the slope forming long, wide features. Downslope and in more basinal areas, the sequence is dominated by polygonal faults (Fig. 12a).

#### 4.4. Units 2c and d: Danian (~66 Ma, horizon K5) – Lutetian (~45 Ma, horizon T2)

The major mounds in the west of the area continue to grow until horizon T2, but with thinner sequences between horizons K5 and T2 (Fig. 7d-e), and with prominent gullies (sensu Rodrigues et al., 2022) present on the edges of the mounds (Fig. 9a-b). The moats continue to fill with sediment, which is generally more homogeneous and dominated by subparallel reflections (Fig. 9). However, the fill of the western moat contains gullies which follow the relief of the more elevated parts of the moat between horizons T1a and T1b (Fig. 13). Between horizon T1b (T1 ≈ T20.0 SB of Marshall and Lang, 2013) and T2, they are gradually replaced by straighter slightly incised gullies that are oriented NW-SE (Fig. 14).

In contrast to the older sequences, thickness maps show that the locus of sediment accumulation shifts to the northeast during the K5 to T2 interval (Fig. 7d-e), particularly in the region of the slope that separates the two areas. This sequence is characterised by parallel to subparallel reflections, which in part are polygonally faulted, and elsewhere are crosscut by incisions and pass laterally into multiple stacked waves (Fig. 5a, 9a and 15). The complexity in shape, orientation, and geometry of these features is exemplified by RMS stratal slices immediately above horizon T1 (Fig. 15). Sediment waves are concentrated along the slope, and they pass laterally into erosional incisions further downslope.

#### 4.5. Units 2e and f: Lutetian (~45 Ma, horizon T2) – Rupelian (~30 Ma, horizon T4)

In the T2 to T4 interval, sediment accumulation is significantly reduced in the southwest, indicating the termination of the development of the mounded and moat sequence (Fig. 8c-d). In contrast, accumulation is much greater in the northeast and exhibits seismic characteristics similar to the sequence between horizons K5 and T2 (Fig. 7f). Within this

region, there are significant incisions measuring 2-5 km in width and up to 35 km in length, running parallel and perpendicular to the underlying slope. These incisions are filled with stacked chaotic reflections (Fig. 16). Additionally, circular depressions with diameters of up to 2.5 km are observed on horizons T3 and T4 and exhibit a conical shape in cross-section. These features display a well-rounded appearance and higher relief on horizon T4 with depths reaching up to 250 m, compared to the lower relief and irregular morphologies observed on horizon T3.

## 5. Bottom current evolution

### 5.1. *Initiation and development of large-scale bathymetric relief*

During the Valanginian – Aptian, between horizons K0 and K1, the thickest deposits of the early post-rift sequence (Muderong Shale) accumulated in a depocentre defined by the front of the underlying Lower Barrow shelf edge (Fig. 6a) and a relative structural low between the Rankin Platform (the uplifted flank of the sub-basins to the southeast) and elevated rotated fault blocks of the Exmouth Plateau to the northwest (Fig. 5, 6a and 7a). While this sequence might have largely infilled remnant rift-related morphology, the contrast in Unit 1 between the mounded sediments to southwest and the dramatically thinned sequence to the NE implies the generation of bathymetric relief, with the two areas separated by a slope on which gullies develop. The marked difference in sediment thickness between these two areas and the curved nature in map view of the slope that separates them (Fig. 6b-d and 7b) suggest the presence of a persistent energetic clockwise (westward flowing) current between the Aptian and Cenomanian, which prevented sediment accumulation in the NE (Fig. 17a). The initiation of subtle sediment mounds and moats to the SW (Fig. 6b) suggest that secondary currents were most likely initiated during the Aptian and initially flowed northeastward, diverging to the northwest (Fig. 17a).

### 5.2. *Large scale mounds and moats*

The large mounded sedimentary bodies that developed in the southwest of the area are characterised by prominent laterally continuous convex seismic reflections (Fig. 5 and 9), which are largely aggradational in style. Although they are initially subtle, their relief and the

contrast with the intervening moats become more pronounced as they become established during the Aptian – Maastrichtian (Fig. 6b-f). Although the aggradational style continues into the Lutetian (horizon T2), the bathymetric expression of the mounds decreases (Fig. 8a-b) and the thickness of individual sequence gradually reduces (Fig. 5b, 9a-c). This implies persistent bottom current activity over a period of approximately 80 million years, waning gradually between the Aptian and the Lutetian (horizons K1-T2) (Fig. 17).

Two prominent moats separate the sediment mounds. Minor truncations and curvature of reflectors at the edges of the mounds, combined with reduced sediment thickness in the moats between horizons K1 and K3 (the Aptian – Turonian) indicate that they are a result of non-deposition with minor erosion. The westerly moat was initiated in the Albian (horizon K2, Fig. 5b) and became more prominent, elongated, and wider during the Cenomanian – Turonian, dissecting an originally continuous sediment mound (Fig. 6b-d). It initially had a SE-NW orientation but rotated approximately 45 degrees to a N-S trend by the Turonian (horizon K3, Fig. 6d), indicating flow towards the north (Fig. 17c). By contrast, the southerly moat maintained a consistent orientation between horizons K1 and K3, indicating continuous flow towards the northeast. The width, and to some extent the length, of both moats gradually diminished between the Coniacian and the Maastrichtian (Fig. 6e-f) as a result of sediment infill, transforming them into relatively straight channels in the west and meandering channels in the south (Fig. 17a-c). Consistent with the cessation of the growth of the mounds, the moats lost their bathymetric expression by the Lutetian (horizon T2, Fig. 8b).

### 5.3. *Moat filling processes*

Horizon K3 marks a change in sedimentary activity within the moats at the start of the Turonian. Above this, the sequence within the moats is characterised by small-scale mounds and stacked erosive features (Fig. 9). This clearly indicates both depositional and erosional current activity within the moats (Stow et al., 2008; Rebesco et al., 2014; Hernández-Molina et al., 2022). Sedimentary structures are particularly prominent between horizons K3 in the Turonian and K5 in the Maastrichtian and less pronounced between horizons K5 and T2 in the Lutetian, consistent with the waning of the currents associated with the reduced growth of the mounds.

Between horizons K3 and K5, the westerly moat is characterised by incisions in the south (Fig. 9b), which pass laterally into parallel bedded units down current to the north (Fig. 9a).



The presence of gullies on the flanks of the mounds that decrease in magnitude away from the moat suggest that as the moats filled, the currents spilled out of the moats onto the flanks of the adjacent mounds (Fig. 10). The filling also resulted in the moat becoming narrower and focussed on its eastern flank, as is particularly evident by the Paleocene (Fig. 9a-c). From the Danian to Lutetian (horizons K5 to T2), parallel bedded units dominate (Fig. 9a-c). During the Thanetian, however, gullies are developed within the moat filling sequence that are originally curved and parallel to it (horizon T1a, Fig. 13), becoming straight and parallel with a NW-SE orientation between horizons T1b and T2 (Fig. 14). This may again indicate that the currents become less confined and no longer conform to the shape of the moat.

The infilling of the southerly moat is more complex, characterised by stacked deep incisions (Fig 5b, 9), segmented incisions (Fig. 6e), irregular incisions and hook-shaped incisions (Fig. 11), suggesting fragmentation of the previous more uniform current that established the original moat. The hook-shaped incisions (Fig. 11b) show clear evidence of both deeply erosional and mounded margins (Fig. 11c). An RMS extraction between horizons K4b and K5 reveals the hook-shaped geometry of smaller scale incisions more precisely (Fig. 11a). They appear stacked and migrate from east to west. A possible explanation for this is filling of the sediment moat to the northeast (Fig. 6e-f), which may have caused the current to deflect to the south and to step back westwards. However, the incisions amalgamate on the northern margin of the moat to maintain its overall sinuous geometry. This moat also becomes progressively filled during the Lutetian (horizon T2, Fig. 8b), indicating the progressive waning of the currents.

#### 5.4. Basin floor infill

Parts of the basin floor began to fill during the Late Cretaceous with uniform parallel sequences, although large parts of the basin remain sediment starved (Fig. 7c and 12). At the end of the Cretaceous (horizon K5), a series of parallel incisions separated by ridges were developed at the base of the slope where sediment thickness was least, while in areas where thicker Cretaceous sediment had accumulated multiple stacked deep incisions and sediment waves formed (Fig. 12 and 15). Together, the orientation of these features mimics the shape of the slope. This was followed by a period of significant progradation of the slope until the middle – late Eocene (horizon T3; Fig. 5a and 7d-e), although ridges and parallel incisions continued to form along the basin margin (Fig. 12c). By this end of this period sedimentation

had almost entirely ceased in the area to the southwest, which was previously dominated by large scale mounds and moats. From the Lutetian to Rupelian (horizon T4), deposition shifted almost entirely into the basinal domain (Fig. 7f). Horizon T4 is a highly irregular surface (Fig. 16c), largely a result of conical depressions, but it is also cut by three prominent erosional incisions which also have expression at horizon T3 and in younger sequences. They are filled with chaotic sequences, characteristic of mass transport complexes, indicating the end of bottom current activity in the NCB, and a transition to gravitationally driven mass transport processes (Winata et al., 2023). The overall transition from non-deposition, through slope-parallel bedforms to sediment fill is again consistent with an overall waning of current activity.

#### 5.5. *Conical depressions*

Large circular or conical depressions formed in basin floor area during the Lutetian – Rupelian. Imbert and Ho (2012) identified similar structures, which they interpret as pockmarks, made by the successive formation and dissociation of hydrates along conical failures. Circular depressions of a similar size are identified from carbonate sediments on the Carnegie Ridge, offshore Ecuador (Michaud et al., 2005), which are interpreted as a product of deepwater dissolution, possibly enhanced by the action of bottom currents. A problem with such a hypothesis is that the Carbonate Compensation Depth (CCD), a likely trigger for deepwater dissolution, was approximately 3500-4500 m in the Indian Ocean during the Paleocene – Eocene (Bickert, 2009) and increased in depth at the end of the Eocene (Taylor et al., 2023). Given that present day water depths are less than 1400 m, and it is unlikely that they were significantly deeper during the Oligocene, a dissolution mechanism is less likely. Maestrelli et al. (2020) describe similar sized circular and elliptical depressions from the Ceará Basin, offshore Brazil, which they attribute to the up-slope migration of sediment waves and cycle steps in the associated turbidity currents. Rather than being formed by fluid escape, these then become the focus of fluid migration. However, the abrupt stratal terminations at the edges of the conical structures observed in this study are more consistent with dissolution or fluid escape.

## 6. Discussion

Our analysis shows that from the Aptian to Rupelian, large parts of the NCB, and particularly the central parts of the Exmouth Plateau, were strongly influenced by bottom current activity. These currents played a crucial role in shaping extensive sediment mounds, moats, and various other morphosedimentary structures, that developed on a ramp-style continental margin during a period that corresponded to a change from clastic to carbonate sedimentation. Current activity appears to be remarkably consistent over an 80 Myr history, although it is likely that the currents declined in intensity with time.

### 6.1. Bathymetric setting

Most conceptual models of contourite processes envisage deposition adjacent to well defined slopes, either at continental margins or adjacent to shallow shelves (e.g., Shanmugam, 2008; Stow et al., 2011; Rebesco et al., 2014), and more recently emphasise the interaction between turbidites and contourites in mixed systems (e.g., Fonnesu et al., 2020; Hernández-Molina et al., 2022; Rodrigues et al., 2022). Mounded, plastered and elongate drifts are characteristic of such settings. By contrast, from the middle of the Cretaceous to the Paleogene, the NCB was most likely characterised by a wide, gentle slope with an average dip of less than 0.5 degrees that existed between a shallow water marginal marine setting in a similar position to the present-day coastline and the deepwater setting of the outer basin margin, some 500 km to the northwest (Apthorpe, 1988; Bradshaw et al., 1988; Mory, 2023). The resulting sedimentary style is vertically accreting mounds which dominate the Cretaceous sequence, with structures analogous to laterally accreting drifts only developed during the later stages of slope migration and basin infill in during the Paleocene and Eocene. There is little direct evidence from seismic or well data for turbidity current activity during this period, although some gravitational currents may be associated with the incisions developed on the slope that marks the edge of the basin floor at the top of Unit 1 and with the mass transport complexes developed at the top of Unit 2. The sediments are entirely fine grained (Winata et al., 2023) and while there is a transition from clastic to carbonate sediments between Unit 1 (Aptian – Cenomanian, horizon K1-K3) and Units 2-4 (Turonian – Present, horizon K3-T10), it is interesting to note that there is no significant difference in the style of sediment mounds that develop during this period. Away from areas of bottom current activity, sedimentation

was likely dominated by hemipelagic processes, characterised by sequences with laterally extensive parallel reflectivity, often showing polygonal faulting (Fig. 4; Winata et al., 2023).

Given that contourite systems are often the result of the interaction between bottom currents and bathymetric barriers, this raises the question of the factors that control the restriction of bottom current activity to the central part of the Exmouth Plateau. The location of the deposits described in this paper loosely corresponds to that of the Kangaroo Syncline (Fig. 1), a poorly defined feature that started to form during Jurassic extension between the uplifted flanks of the sub-basins to the southeast (the Rankin Platform) and elevated fault blocks to the northwest (Fig. 4). While the uplifted sub-basin flanks were buried by the Early Cretaceous, uplifted fault blocks remained emergent, some at least until the Aptian (Fig. 4; Winata et al., 2023). This bathymetric control may have focussed bottom currents into the central parts of the NCB at this time. More locally, the boundary between the area dominated by the growth of mounds and moats to the southeast and the area of limited subsequent sediment accumulation to the northwest also corresponds to the change in thickness in the underlying in the Muderong Shale. It is possible that subtle bathymetric features associated with these differences in sediment accumulation may have been sufficient to localise the currents responsible for the subsequent growth of the mounds. A change from lack of deposition in the moats to the creation of bedforms resulted in their filling, which, combined with the reduction in the bathymetric expression of the mounds, suggests a waning of the flow, further expressed by the subsequent infill of the sediment starved basin floor to the northwest.

## *6.2. Plate separation and thermohaline circulation*

Our analysis shows that persistent bottom current activity occurred over an 80 Myr period corresponding to the final stages of Gondwana break up. Figure 18 shows the location of the bottom current deposits on the continental margin, the inferred currents responsible for their formation, and their tectonic context. While it is possible that bottom currents can be driven by wind and tides (Shanmugam, 2008), the location of these deposits and their consistency over a significant period of time suggests thermohaline circulation is the primary driver. Direct evidence of Cretaceous oceanic circulation patterns is limited, but inferences from our own observations, combined with knowledge of present-day currents, can be used to guide our understanding of how circulation patterns may have evolved in response to the

creation of narrow ocean gateways which developed as a result of the progressive breakup of Gondwana.

We observe that bottom current activity first occurred in the Aptian (~123 Ma). At this time, based on tectonic reconstructions of the Müller et al. (2019), a wide and open ocean, fully connected to the Pacific Ocean, existed to the north (Fig. 18a), sufficient to allow the generation of a significant clockwise current flowing to the west, comparable to the present day South Equatorial Current (SEC; Fig. 2). This may have been sufficient to drive the initial generation of sediment mounds and moats on the Exmouth Plateau. At this time, the separation between Australia and Greater India formed a narrow oceanic gateway (Fig. 18a), but in the absence of any connection to significant oceans to the south, was unlikely to generate any significant currents. However, rapid separation between Greater India and Australia between the Aptian (~123 Ma) and the Cenomanian (~94 Ma; Fig. 21b), and between India and Antarctica would allow currents to develop on the western margin, similar to the West Australian Current (WAC) and Leeuwin Undercurrent (LU; Fig. 2), connected to a growing southern ocean, with flow through a narrow gateway. This corresponds to a period of significant growth of large-scale mounds and moats, consistent with the development of such currents during this interval. The initiation of seafloor spreading between Australia and Antarctica at the end of the Maastrichtian (~66 Ma; Fig. 18c) may have allowed some of the southerly current to be diverted to the south of Australia, but the start of the rapid movement of Australia northwards away from Antarctica from the Eocene (Müller et al., 2000; Seton et al., 2012) allowed full oceanic connection on the southern margin to be established by about 30 Ma (Fig. 18d). This creates the potential for further current reorganisation and corresponds to the gradual waning of currents and the termination of bottom current activity in the NCB by the Rupelian. Increasing convergence between the Australian plate and Eastern Indonesia from this time onwards corresponds to the subsequent development of widespread mass transport complexes.

## 7. Summary and conclusions

This paper presents a comprehensive study of sediment mounds, moats, and other morphosedimentary structures that developed in the NCB as a result of persistent of bottom activity over an 80-million-year period. During the early post-rift period (Valanginian to

Aptian), a distinct sediment sag developed at the centre of the Exmouth Plateau, thinning out towards the northeast. The Aptian – Cenomanian sequence exhibits the establishment large-scale of mounded structures and moats in the southwest, which thin dramatically to the northeast. The Turonian – Lutetian interval reflects further development with aggradational mound growth and infilling of moats characterized by small-scale mounds and incisions, with a variety of different geometries. Infilling of the moats, combined with reduced bathymetric expression of the mounds, resulted in subsequent infilling of the sediment-starved basin floor to the northwest. During this time, significant progradation of the slope occurred until the Rupelian, associated with highly irregular surfaces and the development of conical depressions primarily in the basinal domain. The largest conical shapes are intersected by three prominent erosional incisions of younger age, subsequently filled with chaotic sequences indicative of mass transport complexes.

The changing patterns in sedimentation suggest initially vigorous currents that declined over time. Current activity appears to be influenced by changing ocean circulation that evolved during the progressive separation of Australia, Greater India and Antarctica. The cessation of current activity also corresponds with increasing convergence between the Australian plate and Eastern Indonesia, resulting in bottom current activity being replaced by mass transport processes. This study highlights the benefit of regional scale studies for identifying the link between sedimentary processes operating on continental margins, plate tectonics and evolving ocean circulation patterns.

#### Conflicts of Interest

The authors declare no conflict of interests.

#### Acknowledgements

We would like to express our appreciation to Geoscience Australia for providing public domain seismic and well log data used in this research. All datasets utilized in this study are openly accessible through the National Offshore Petroleum Information Management System (NOPIMS; <https://nopims.dmp.wa.gov.au/nopims>). Our gratitude also extends to Schlumberger, CEGAL, and ELIIS for granting access to the Petrel, Blueback Toolbox, and PaleoScan software, which were instrumental in our research. Furthermore, Mulky Winata

acknowledges the support of a collaborative PhD scholarship under the Aberdeen – Curtin Alliance 2018 (<http://aberdeencurtinalliance.org/>), facilitated by Curtin University (Perth, Australia) and the University of Aberdeen (Aberdeen, Scotland).

## References

- Apthorpe, M., 1988. Cenozoic depositional history of the North West shelf. In: Purcell, P.G., Purcell, R.R. (Eds.), *The North West Shelf, Australia. Proceedings of Petroleum Exploration Society of Australia Symposium*, Perth, Australia, 55–84.
- Audley-Charles, M. G., 1988. Evolution of the southern margin of Tethys (North Australian region) from early Permian to late Cretaceous. In: *Gondwana and Tethys* (Edited by Audley-Charles, M. G. and Hallam, A.). *Spec. Pubis geol. Soc. Lond.* 37, 79-100.
- Australian Government, Department of Climate Change, Energy, the Environment and Water (DCCEEW), 2007. *A Characterisation of the Marine Environment of the North-west Marine Region. A summary of an expert workshop convened in Perth, Western Australia, 5-6 September 2007.*
- Baillie, P., Powell, C.M., Li, Z., Ryall, A., 1994. The tectonic framework of Western Australia's neoproterozoic to recent sedimentary basins. *The Sedimentary Basins of Western Australia: Proceedings of Petroleum Exploration Society of Australia Symposium.*
- Baker, A. C., Glynn, P. W., Riegl, B., 2008. Climate change and coral reef bleaching: An ecological assessment of long-term impacts, recovery trends and future outlook. *Estuary, Coastal and Shelf Science*, 80(4), 435–471. <https://doi.org/10.1016/j.ecss.2008.09.003>.
- Borel, G.D., Stampfli, G.M., 2002. Geohistory of the North West Shelf: a tool to assess the Palaeozoic and Mesozoic motion of the Australian Plate. In: Keep, M., Moss, S.J. (Eds.), *The Sedimentary Basins of Western Australia 3. Proceedings of the Petroleum Exploration Society of Australia Symposium*, 119–128.
- Bradshaw, M.T., Yeates, A.N., Beynon, R.M., Brakel, A.T., Langford, R.P., Totterdell, J.M., Yeung, M., 1988. Palaeogeographic evolution of the North West Shelf region. In: Purcell, P.G., Purcell, R.R. (Eds.), *The North West Shelf, Australia. Proceedings of the Petroleum Exploration Society of Australia Symposium*, 29–54.



- Bickert, T., 2009. Carbonate Compensation Depth. In: Gornitz, V. (eds) Encyclopedia of Paleoclimatology and Ancient Environments. Encyclopedia of Earth Sciences Series. Springer, Dordrecht. [https://doi.org/10.1007/978-1-4020-4411-3\\_33](https://doi.org/10.1007/978-1-4020-4411-3_33).
- Cathro, D.L., Karner, G.D., 2006. Cretaceous-tertiary inversion history of the Dampier sub-basin, Northwest Australia: Insights from quantitative basin modelling. *Marine and Petroleum Geology*, 23, 503–526. <https://doi.org/10.1016/j.marpetgeo.2006.02.005>.
- Cresswell, G.R., Golding, T.J., 1980. Observations of a south-flowing current in the southeastern Indian Ocean. *Deep-Sea Research Part A: Oceanographic Research Papers* 27, 449–466. [https://doi.org/10.1016/0198-0149\(80\)90055-2](https://doi.org/10.1016/0198-0149(80)90055-2).
- Cresswell, G.R., 1991. The Leeuwin Current - observations and recent models. *Journal of the Royal Society of Western Australia*, 74: 1-14.
- Cresswell, G.R., Peterson, J.L., 1993. The Leeuwin Current south of Western Australia. *Marine and Freshwater Research*, 44(2), 285–303. <https://doi.org/10.1071/MF9930285>.
- Church, J.A., Cresswell, G.R., Godfrey, J.S., 1989. The Leeuwin Current. In S. J. Neshyba, C. N. K. Mooers, R. L. Smith, & R. T. Barber (Eds.), *Poleward flows along Eastern Ocean boundaries*, 230–254). Springer-Verlag. <https://doi.org/10.1007/978-1-4613-8963-716>.
- Collins, L.B., James, N.P., Bone, Y., 2014. Carbonate shelf sediments of the western continental margin of Australia. *Geological Society, London, Memoirs*, 41, 255–272. <https://doi.org/10.1144/M41.19>.
- Deng, H., McClay, K., Bilal, A., 2019. 3D structure and evolution of an extensional fault network of the eastern Dampier Sub-basin, North West Shelf of Australia. *Journal of Structural Geology*. <https://doi.org/10.1016/j.jsg.2019.103972>.
- Driscoll, N.W., Karner, G.D., 1998. Lower crustal extension across the Norther Carnarvon Basin, Australia: evidence for an eastward dipping detachment. *J. Geophys. Res.* 103, 4975–4991. <https://doi.org/10.1029/97JB03295>.
- Exon, N., Haq, B., Von Rad, U., 1992. Exmouth plateau revisited: Scientific drilling and geological framework. In U. VonRad, B. U. Haq, R. B. Kidd, S. B. O’Connell (Eds.), *Proceedings of the Ocean Drilling Program, Scientific Results*, 122, 3–20. College Station, TX: Ocean Drilling Program. <http://dx.doi.org/10.2973/odp.proc.sr.122.194.1992>.
- Feng, M., Benthuisen, J., Zhang, N., Slawinski, D., 2015. Freshening anomalies in the Indonesian Throughflow and impacts on the Leeuwin Current during 2010–2011.

- Geophysical Research Letters, 42(20), 8555–8562. <https://doi.org/10.1002/2015GL065848>.
- Feng, M., Zhang, N., Liu, Q., Wijffels, S., 2018. The Indonesian throughflow, its variability and centennial change. *Geoscience Letters*, 5(3): Article n UNSP 3. <https://doi.org/10.1186/s40562-018-0102-2>.
- Fioux, M., Molcard, R., Morrow, R., 2005. Water properties and transport of the Leeuwin Current and Eddies off Western Australia. *Deep-Sea Research Part I Oceanographic Research Papers*, 52(9), 1617–1635. <https://doi.org/10.1016/j.dsr.2005.03.013>.
- Fonnesu, M., Palermo, D., Galbiati, M., Marchesini, M., Bonamini, E., Bendias, D., 2020. A new world-class deep-water play-type, deposited by the syndepositional interaction of turbidity flows and bottom currents: The giant Eocene Coral Field in northern Mozambique, *Marine and Petroleum Geology*, Volume 111, 179-201, <https://doi.org/10.1016/j.marpetgeo.2019.07.047>.
- Gartrell, A., 2000. Rheological controls on extensional styles and the structural evolution of the Northern Carnarvon basin, North West Shelf, Australia. *Aust. J. Earth Sci.* 47 (2), 231–244. <http://dx.doi.org/10.1046/j.1440-0952.2000.00776.x>.
- Geoscience Australia, 2022. Regional Geology of the Northern Carnarvon Basin [WWW Document]. *Offshore Pet. Explor. Acreage Release*.
- Gordon, A., Fine, R., 1996. Pathways of water between the Pacific and Indian Oceans in the Indonesian Seas. *Nature*, 379: 146-149. <https://doi.org/10.1038/379146a0>.
- Gordon, A.L., 2005. Oceanography of the Indonesian Seas and their Throughflow. *Oceanography*, 18(4): 15-27. <http://dx.doi.org/10.5670/oceanog.2005.01>.
- Hernández-Molina, F.J., Paterlini, M., Somoza, L., Arecco, M.A., De Isasi, M., Rebesco, M., Uenzelmann-Neben, G., Neben, S., Marshall P., 2010. Giant mounded drift in the Argentine Continental Margin: origins and global implications in the thermohaline circulation. *Mar Petrol Geol.* 7:1508–1530. <http://dx.doi.org/10.1016/j.marpetgeo.2010.04.003>.
- Hernández-Molina, F.J., Soto, M., Piola, A.R., Tomasini, J., Preu, B., Thompson, P., Badalini, G., Creaser, A., Violante, R.A., Morales, E., Paterlini, M., 2016. A contourite depositional system along the Uruguayan continental margin: sedimentary, oceanographic and paleoceanographic implications. *Mar. Geol.* 378, 333–349. <https://doi.org/10.1016/j.marpetgeo.2015.10.008>.

- Hernández-Molina, F.J., Castro, S.d., Weger, W.d., Duarte, D., Fonnesu, M., Glazkova, T., Kirby, A., Llave, E., Ng, Z.L., Muñoz, O.M., Rodrigues, S., Rodríguez-Tovar, F. J., Thieblemont, A., Viana, A R., Yin, S., 2022. Chapter 9 - Contourites and mixed depositional systems: A paradigm for deepwater sedimentary environments, Editor(s): Jon R. Rotzien, Cindy A. Yeilding, Richard A. Sears, F. Javier Hernández-Molina, Octavian Catuneanu, Deepwater Sedimentary Systems, Elsevier, 301-360, <https://doi.org/10.1016/B978-0-323-91918-0.00004-9>.
- Hocking, R.M., 1988. Regional geology of the Northern Carnarvon Basin. In: Purcell, P.G., Purcell, R.R. (Eds.), The North West Shelf, Australia. Proceedings of the Petroleum Exploration Society of Australia Symposium, 97–114.
- Holloway, P.E., Nye, H.C., 1985. Leeuwin current and wind distributions on the southern part of the Australian North West Shelf between January 1982 and July 1983. Australian Journal of Marine and Freshwater Research, 36(2): 123-137. <https://doi.org/10.1071/MF9850123>.
- Holloway, P.E., 1995. Leeuwin current observations on the Australian North West Shelf, May-June 1993. Deep Sea Research Part I: Oceanographic Research Papers, 42(3): 285-305. [https://doi.org/10.1016/0967-0637\(95\)00004-P](https://doi.org/10.1016/0967-0637(95)00004-P).
- Houben, A.J., Bijl, P.K., Pross, J., Bohaty, S.M., Passchier, S., Stickley, C.E., Van de Flierdt, T., 2013. Reorganisation of southern ocean plankton ecosystem at the onset of Antarctic glaciation. Science, 340, 341–344. <https://doi.org/10.1126/science.1223646>.
- Hull, J.N.F., Griffiths, C.M., 2002. Sequence stratigraphic evolution of the albian to recent section of the Dampier Sub Basin, North West Shelf, Australia. In: Sedimentary Basins of Western Australia 3: Proceedings of Petroleum Exploration Society of Australia Symposium (Ed. by M. Keep & S.J. Moss), 3, 617–639. Petroleum Exploration Society of Australia Perth, Australia.
- l'Anson, A., Elders, C., McHarg, S., 2019. Marginal fault systems of the Northern Carnarvon Basin: Evidence for multiple Palaeozoic extension events, North-West Shelf, Australia, Marine and Petroleum Geology, Volume 101, Pages 211-229, ISSN 0264-8172, <https://doi.org/10.1016/j.marpetgeo.2018.11.040>.
- Imbert, P., Ho, S., 2012. Seismic-Scale Funnel-Shaped Collapse Features from the Paleocene - Eocene of the North West Shelf of Australia. Marine Geology, 332, 198-221. <https://doi.org/10.1016/j.margeo.2012.10.010>.

- James, N.P., Bone, Y., Kyser, T.K., Dix, G.R., Collins, L.B., 2004. The importance of changing oceanography in controlling late quaternary carbonate sedimentation on a high-energy, tropical, oceanic ramp: North-Western Australia. *Sedimentology*, 51, 1179–1205. <https://doi.org/10.1111/j.1365-3091.2004.00666.x>.
- Lee, T.Y., Lawver, L.A., 1995. Cenozoic plate reconstruction of Southeast Asia. *Tectonophysics*, 251, 85–138. [https://ui.adsabs.harvard.edu/link\\_gateway/1995Tectp.251...85L/doi:10.1016/0040-1951\(95\)00023-2](https://ui.adsabs.harvard.edu/link_gateway/1995Tectp.251...85L/doi:10.1016/0040-1951(95)00023-2).
- Longley, I.M., Buessenschuett, C., Clydsdale, L., Cubitt, C.J., Davis, R.C., Johnson, M.K., Marshall, N.M., Murray, A.P., Somerville, R., Spry, T.B., Thompson, N.B., 2002. The North West Shelf of Australia - a Woodside perspective. In: Keep, M., Moss, S. (Eds.), *The Sedimentary Basins of Western Australia 3. Proceedings of the Petroleum Exploration Society of Australia Symposium*, 27–88.
- Maestrelli, D., Maselli, V., Kneller, B., Chiarella, D., Scarselli, N., Vannucchi, P., Jovane, L., Iacopini, D., 2020. Characterisation of submarine depression trails driven by upslope migrating cyclic steps: Insights from the Ceará Basin (Brazil), *Marine and Petroleum Geology*, Volume 115, 104291, ISSN 0264-8172. <https://doi.org/10.1016/j.marpetgeo.2020.104291>.
- Marshall, N.G., Lang, S.C., 2013. A new sequence stratigraphic framework for the North West Shelf, Australia. In: Keep, M., Moss, S.J. (Eds.), *The Sedimentary Basins of Western Australia 4. Proceedings of the Petroleum Exploration Society of Australia Symposium*, 1–32.
- Metcalfe, I., 2013. Gondwana dispersion and Asian accretion: tectonic and palaeogeographic evolution of eastern Tethys. *J. Asian Earth Sci.* 66, 1–33. <https://doi.org/10.1016/j.jseaes.2012.12.020>.
- Michaud, F., Chabert, A., Collot, J.-Y., Sallarès, V., Flueh, E.R., Charvis, P., Graindorge, D., Gustcher, M.-A., Billas, J., 2005. Fields of multi-kilometer scale sub-circular depressions in the Carnegie Ridge sedimentary blanket: Effect of underwater carbonate dissolution: *Marine Geology*, v. 216, 205–219. <https://doi.org/10.1016/j.margeo.2005.01.003>.
- Miller, K.G., Wright, J.D., Fairbanks, R.G., 1991. Unlocking the ice house: Oligocene-miocene oxygen isotopes, eustasy, and margin erosion. *Journal of Geophysical Research: Solid Earth*, 96, 6829–6848. <https://doi.org/10.1029/90JB02015>.

- Molcard, R., Fieux, M., Syamsudin, F., 2001. The throughflow within Ombai Strait, Deep Sea Research Part I: Oceanographic Research Papers, Volume 48, Issue 5, 1237-1253, ISSN 0967-0637, [https://doi.org/10.1016/S0967-0637\(00\)00084-4](https://doi.org/10.1016/S0967-0637(00)00084-4).
- Mory, A.J., (compiler), 2023. Mesozoic transformation of Western Australia: rifting and breakup of Gondwana: Geological Survey of Western Australia, 73.
- Mulder, T., Hüneke, H., Van Loon, A.J., 2011. Progress in Deep-Sea Sedimentology. In: Hüneke, H., Mulder, T. (Eds.), Deep-Sea Sediments Developments in Sedimentology 63. Elsevier, Amsterdam, 1–22.
- Müller, D., Gaina, C., Clark, S., 2000. Seafloor Spreading Around Australia, vol. 24.
- Müller, R. D., Zahirovic, S., Williams, S. E., Cannon, J., Seton, M., Bower, D. J., Tetley, M. G., Heine, C., Le Breton, E., Liu, S., Russell, S. H. J., Yang, T., Leonard, J., Gurnis, M., 2019. A global plate model including lithospheric deformation along major rifts and orogens since the Triassic. *Tectonics*, vol. 38, <https://doi.org/10.1029/2018TC005462>.
- Nugraha, H.D., Jackson, C.A.-L., Johnson, H.D., Hodgson D.M., Reeve M.T., 2019. Tectonic and oceanographic process interactions archived in the Late Cretaceous to Present deep-marine stratigraphy on the Exmouth Plateau, offshore NW Australia. *Basin Res*, vol 31, 405–430. <https://doi-org.dbgw.lis.curtin.edu.au/10.1111/bre.12328>.
- Pattiaratchi, C., 2006. Surface and sub-surface circulation and water masses off Western Australia. *Bulletin of the Australian Meteorological and Oceanographic Society*, 19(5), 95–104.
- Peter, B.N., Sreeraji, P., Vimal Kumar, K.G., 2005. Structure and Variability of the Leeuwin Current in the south eastern Indian Ocean. *Journal of Ind. Geophysical Union*, 9(2): 107-119. <http://drs.nio.org/drs/handle/2264/451>.
- Potemra, J.T., Hautala, S.L., Sprintall, J., 2003. Vertical structure of the Indonesian Throughflow in a large scale model. *Deep Sea Research Part 2: Tropical Studies in Oceanography*, 50: 2143-2161. [https://doi.org/10.1016/S0967-0645\(03\)00050-X](https://doi.org/10.1016/S0967-0645(03)00050-X).
- Pryer, L.L., Romine, K.K., Loutit, T.S., Barnes, R.G., 2002. Carnarvon basin architecture and structure defined by the integration of mineral and petroleum exploration tools and techniques. *APPEA J.*, 42, 287–309. Australian Petroleum Production and Exploration Association, Canberra, Australia. <http://dx.doi.org/10.1071/AJ01016>.
- Rebesco, M., Hernández-Molina, F.J., Van Rooij, D., Wåhlin, A., 2014. Contourites and associated sediments controlled by deep-water circulation processes: state-of-the-art

- and future considerations. *Mar. Geol.* 352, 111–154. <https://doi.org/10.1016/j.margeo.2014.03.011>.
- Ridgway, K.R., Condie, S.A., 2004. The 5500-km-long boundary flow off western and southern Australia. *Journal of Geophysical Research—Oceans* 109 (C04017). <https://doi.org/10.1029/2003JC001921>.
- Roden, G.I., 1987. Effects of seamount chains on ocean circulation and thermohaline structure. In: Keating BH et al (eds) *Seamounts, islands and atolls*. AGU Geophy Monogr 96, 335–354. [https://ui.adsabs.harvard.edu/link\\_gateway/1987GMS....43..335R/doi:10.1029/GM043p0335](https://ui.adsabs.harvard.edu/link_gateway/1987GMS....43..335R/doi:10.1029/GM043p0335).
- Rodrigues, S., Hernández-Molina, F.J., Fonnesu, M., Miramontes, E., Rebesco, M., Campbell, D.C., 2022. A new classification system for mixed (turbidite-contourite) depositional systems: Examples, conceptual models and diagnostic criteria for modern and ancient records, *Earth-Science Reviews*, Volume 230, 104030, ISSN 0012-8252, <https://doi.org/10.1016/j.earscirev.2022.104030>.
- Romine, K.K., Durrant, J. 1996. Carnarvon Cretaceous-Tertiary Tie Report. Record 1996/036. Geoscience Australia, Canberra. <https://pid.geoscience.gov.au/dataset/ga/25187>.
- Romine, K.K., Durrant, J.M., Cathro, D.L., Bernadel, G., Apthorpe, M., 1997. Petroleum play element prediction for the Cretaceous-Tertiary basin phase, Northern Carnarvon Basin. *J. Aust. Petroleum Prod. Explor. Assoc.* 37 (1), 315–339.
- Scarselli, N., McClay, K., Elders, C., 2013. Submarine Slide and Slump Complexes, Exmouth Plateau, NW Shelf of Australia, in Keep, M. and Moss, S.J (Eds.), *Western Australian Basins Symposium 2013*, Aug 18-21 2013. Perth: Petroleum Exploration Society of Australia. <https://doi.org/10.1002/9781119500513.ch16>.
- Seton, M., Müller, R.D., Zahirovic, S., Gaina, C., Torsvik, T., Shephard, G., Talsma, A., Gurnis, M., Turner, M., Maus, S., Chandler, M., 2012. Global continental and ocean basin reconstructions since 200Ma. *Earth Sci. Rev.* 113 (3–4), 212–270. <https://doi.org/10.1016/j.earscirev.2012.03.002>.
- Shanmugam, G., 2008. Deep-water bottom currents and their deposits, in: Rebesco, M., Camerlenghi (Eds.), *Contourites*. *Dev. Sedimentol.* 60, 59–81. [http://dx.doi.org/10.1016/S0070-4571\(08\)00205-7](http://dx.doi.org/10.1016/S0070-4571(08)00205-7).



- Shanmugam, G., 2014. Modern internal waves and internal tides along oceanic pycnoclines: Challenges and implications for ancient deep-marine baroclinic sands. *AAPG Bulletin*, 98: 858–879. <http://dx.doi.org/10.1306/09111313115>.
- Smith, R.L., Huyer, A., Godfrey, J.S., Church, J.A., 1991. The Leeuwin current off Western Australia, 1986–1987. *Journal of Physical Oceanography* 21, 323–345. [http://dx.doi.org/10.1175/1520-0485\(1991\)021%3C0323:TLCOWA%3E2.0.CO;2](http://dx.doi.org/10.1175/1520-0485(1991)021%3C0323:TLCOWA%3E2.0.CO;2).
- Spooner, M.I., De Deckker, P., Barrows, T.T., Fifield, L.K., 2011. The behavior of the Leeuwin Current offshore NW Australia during the last five glacial-interglacial cycles. *Global and Planetary Change*, 75(3–4), 119–132. <https://doi.org/10.1016/j.gloplacha.2010.10.015>.
- Stickley, C. E., Brinkhuis, H., Schellenberg, S. A., Sluijs, A., Röhl, U., Fuller, M., Williams, G. L., 2004. Timing and nature of the deepening of the Tasmanian Gateway. *Paleoceanography*, 19(4), n/a–n/a. <https://doi.org/10.1029/2004PA001022>.
- Stow D.A.V., Faugères J-C, Howe J.A., Pudsey C.J., Viana A.R., 2002a. Bottom currents, contourites and deep-sea sediment drifts: current state-of-the-art. In: Stow DAV, Pudsey CJ, Howe JA, Faugères J-C, Viana AR (eds) *Deep-water contourite systems: modern drifts and ancient series, seismic and sedimentary characteristics*. *Geol Soc Lond Mem* 22, 7–20. <https://doi.org/10.1144/GSL.MEM.2002.022.01.02>.
- Stow D.A.V., Faugères J-C, Gonthier E., Cremer M., Llave E., Hernández-Molina F.J., Somoza L., Díaz-Del-Río V., 2002b. Faro-Albufeira Drift Complex, Northern Gulf of Cadiz. In: Stow DAV, Pudsey CJ, Howe JA, Faugères J-C, Viana AR (eds) *Deep-water contourite systems: modern drifts and ancient series, seismic and sedimentary characteristics*. *Geol Soc Lond Mem* 22, 7–20.
- Stow, D.A.V., Hunter, S., Wilkinson, D., Hernández-Molina, F.J., 2008. The nature of contourite deposition. In: Rebesco, M., Camerlenghi, A. (Eds.), *Contourites*. *Dev. Sedimentol.* 60, 143–156.
- Stow, D.A.V., Brackenridge, R., Hernandez-Molina, F.J., 2011. Contourite Sheet Sands: New Deepwater Exploration Target, *Search and Discovery Article #30182*.
- Taylor, V. E., Westerhold, T., Bohaty, S. M., Backman, J., Dunkley Jones, T., Edgar, K. M., 2023. Transient shoaling, over-deepening and settling of the calcite compensation depth at the Eocene-Oligocene Transition. *Paleoceanography and Paleoclimatology*, 38, e2022PA004493. <https://doi.org/10.1029/2022PA004493>.

- Thompson, R.O.R.Y., 1984. Observations of the Leeuwin current off Western Australia. *Journal of Physical Oceanography* 14, 623–628.
- Thompson, R.O.R.Y., 1987. Continental shelf scale model of the Leeuwin current off Western Australia. *Journal of Marine Research* 45, 813–827. [https://doi.org/10.1175/1520-0485\(1984\)014%3C0623:OOTLCO%3E2.0.CO;2](https://doi.org/10.1175/1520-0485(1984)014%3C0623:OOTLCO%3E2.0.CO;2).
- Tchernia, P., 1980. *Descriptive regional oceanography*. New York, NY: Pergamon Press.
- Van Wagoner, J.C., Posamentier, H., Mitchum, Jr., Vail, P.R., Sarg, J.F., Loutit, T.S., Hardenbol, J., 1988. An overview of the fundamentals of sequence stratigraphy and key definitions. *Sea Level Changes: An Integrated Approach*, SEPM Special Publication, 42, 39-46.
- Veevers, J.J., Powell, C. M., Roots, S., 1991. Review of seafloor spreading around Australia. I. Synthesis of the patterns of spreading. *Australian Journal of Earth Sciences*, 38, 373–389. <https://doi.org/10.1080/08120099108727979>.
- Veevers, J.J., 2000. Change of tectono-stratigraphic regime in the Australian plate during the 99 Ma (mid-Cretaceous) and 43 Ma (mid-Eocene) swerves of the Pacific. *Geology*, 28 (1), 47-50. [https://doi.org/10.1130/0091-7613\(2000\)28%3C47:COTRIT%3E2.0.CO;2](https://doi.org/10.1130/0091-7613(2000)28%3C47:COTRIT%3E2.0.CO;2).
- Vranes, K., Gordon, A.L., Field, A., 2002. The heat transport of the Indonesian Throughflow and implications for the Indian Ocean heat budget. *Deep Sea Research Part 2: Tropical Studies in Oceanography*, 49(7-8): 1391-1410. [http://dx.doi.org/10.1016/S0967-0645\(01\)00150-3](http://dx.doi.org/10.1016/S0967-0645(01)00150-3).
- Wijeratne, S., Pattiaratchi, C., Proctor, R., 2018. Estimates of surface and subsurface boundary current transport around Australia. *Journal of Geophysical Research: Oceans*, 123(5), 3444–3466. <https://doi.org/10.1029/2017JC013221>.
- Winata, M., Elders, C., Maselli V., Stephenson A. R., 2023. Regional seismic stratigraphic framework and depositional history of the post-Valanginian passive margin sequences in the Northern Carnarvon Basin, North West Shelf of Australia, *Marine and Petroleum Geology*, Volume 156, 106418, ISSN 0264-8172, <https://doi.org/10.1016/j.marpetgeo.2023.106418>.
- Woo, M., Pattiaratchi, C., 2008. Hydrography and water masses off the Western Australian Coast. *Deep Sea Research Part I: Oceanographic Research Papers*, 55, 1090–1104. <https://doi.org/10.1016/j.dsr.2008.05.005>.

No	3D Survey	Year	Cover Area (km <sup>2</sup> )	Bin Size (m)	Sampling Interval (ms)
1	Io-Jansz	2004	2853.47	18.75 x 12.50	2
2	Willem	2006	2665.84	25.00 x 12.50	4
3	Duyfken	2006	3806.79	18.75 x 12.50	4
4	Charon	2007	2149.39	18.75 x 12.50	4
5	Draeck	2007	1677.98	18.75 x 12.50	4
6	Glencoe	2008	4227.34	25.00 x 25.00	4

Table 1. Public domain 3D seismic datasets used in this study provided by Geoscience Australia via the National Offshore Petroleum Information Management System (NOPIMS).

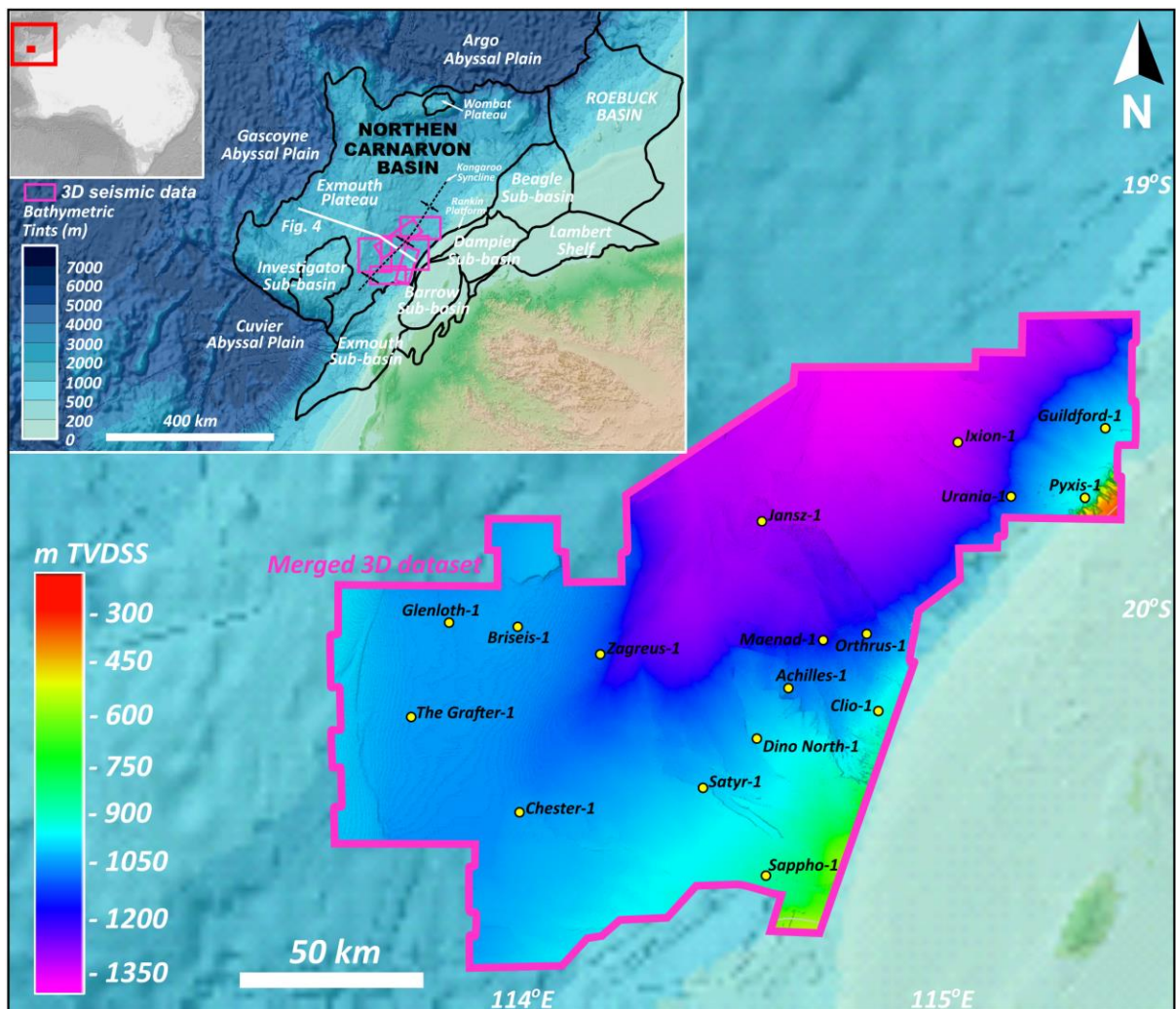


Fig. 1. Location map showing the seabed imaged by the merged 3D seismic dataset used in this study. Basin outline of the Northern Carnarvon Basin, regional present-day bathymetry, and the location of a WNW–ESE regional seismic line used to describe the regional seismic-stratigraphic scheme shown on the inset map. Wells used for stratigraphic correlation shown by yellow dots. Abbreviation for m TVDSS is metres true vertical depth subsea.



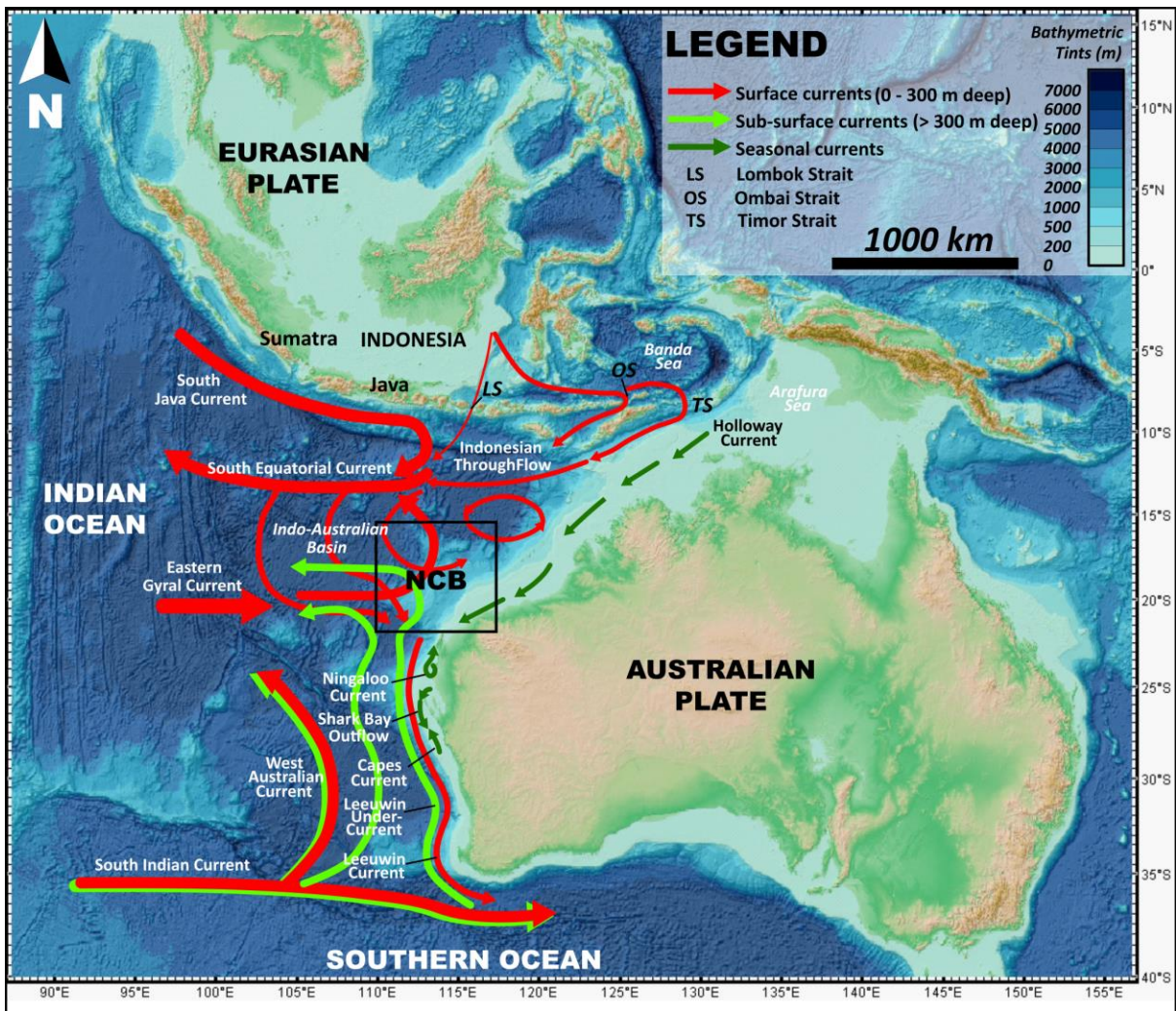


Fig. 2. Present day ocean current pathways modified from Wijeratne et al. (2018) and Australian Government - DCCEEW (2007). Shaded relief GEBCO\_2014 bathymetry map exported from GeoMapApp (data source is <https://www.gebco.net/>).

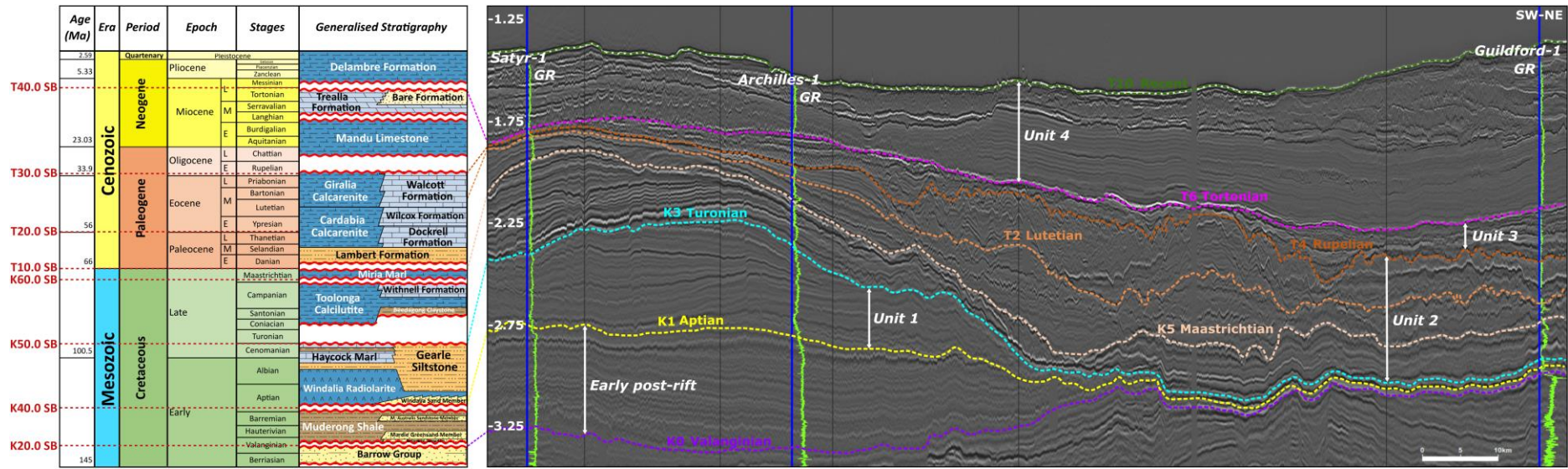
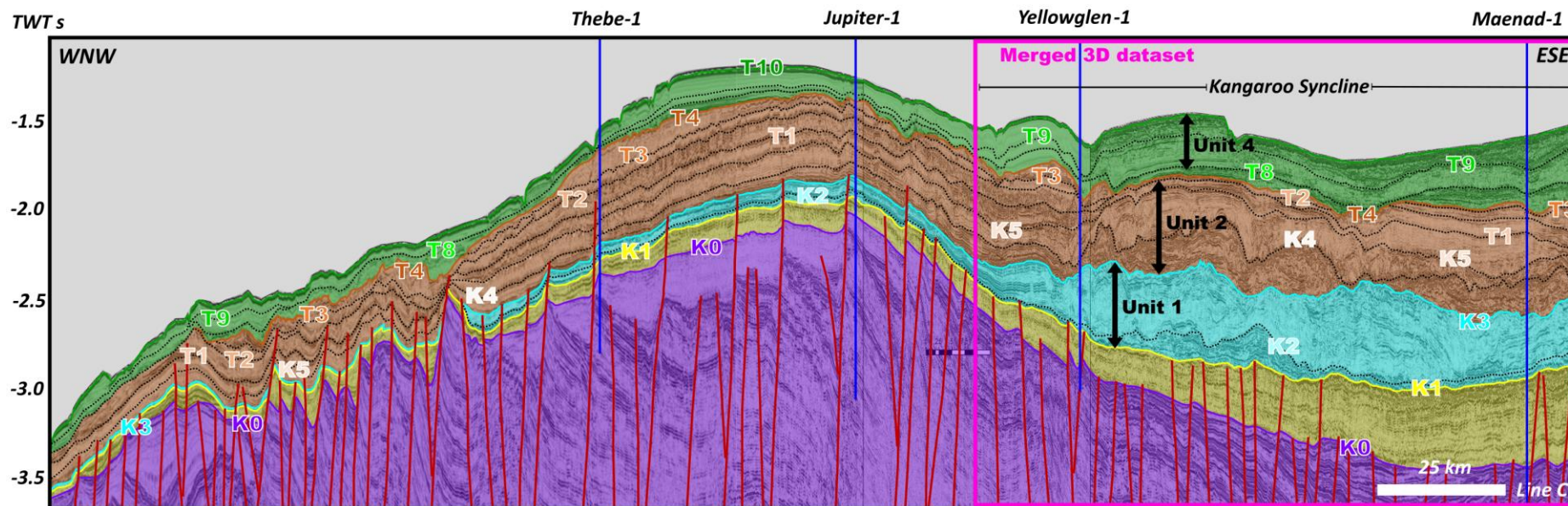


Fig. 3. Generalised stratigraphic chart for the NCB compiled from Geoscience Australia (2022), showing correlation to seismic-stratigraphy and ties to wells (Satyr-1, Archilles-1, Guildford-1, GR: Gamma-ray, see Fig. 1 wells locations). Formation names and lithostratigraphic terms are used according to the Australian Stratigraphic Units Database. Red dashed lines are boundaries given by Marshall and Lang (2013).





### TOP FORMATIONS

#### Cretaceous

- K5 ≈ Miria Marl / Withnell Formations
- K4 ≈ Upper Gearle Silstone / Toolonga Calcilutite
- K3 ≈ Lower Gearle Silstone / Haycock Marl
- K2 ≈ Windalia Radiolarite
- K1 ≈ Muderong Shale
- K0 ≈ Lower Barrow Group or Base Upper Barrow / Base Muderong Shale

Unit 2a-b  
Unit 1a-b

#### Cenozoic

- T5 ≈ Mandu Formation
- T4 ≈ Upper Walcott / Gindaria Formations
- T3 ≈ Lower Walcott / Gindaria Formations
- T2 ≈ Wilcox / Cardabia Formations
- T1 ≈ Dockrell / Lambert Formations

Unit 3a  
Unit 2e-f  
Unit 2c-d

- T10 ≈ Upper Delambre Formation (Seabed)
- T9 ≈ Middle 2 Delambre Formation
- T8 ≈ Middle 1 Delambre Formation
- T7 ≈ Lower Delambre Formation
- T6 ≈ Trealla / Bare Formation

Unit 4d  
Unit 4a-b-c  
Unit 3b

Fig. 4. A composite regional seismic cross-section oriented WNW-ESE illustrating the Triassic – Earliest Cretaceous pre- and syn-extensional sequence (purple section, horizon K0 marks the end of rifting) and Cretaceous – Recent passive margin sequences in the Exmouth Plateau (see Fig. 1 for the location of the seismic transect).



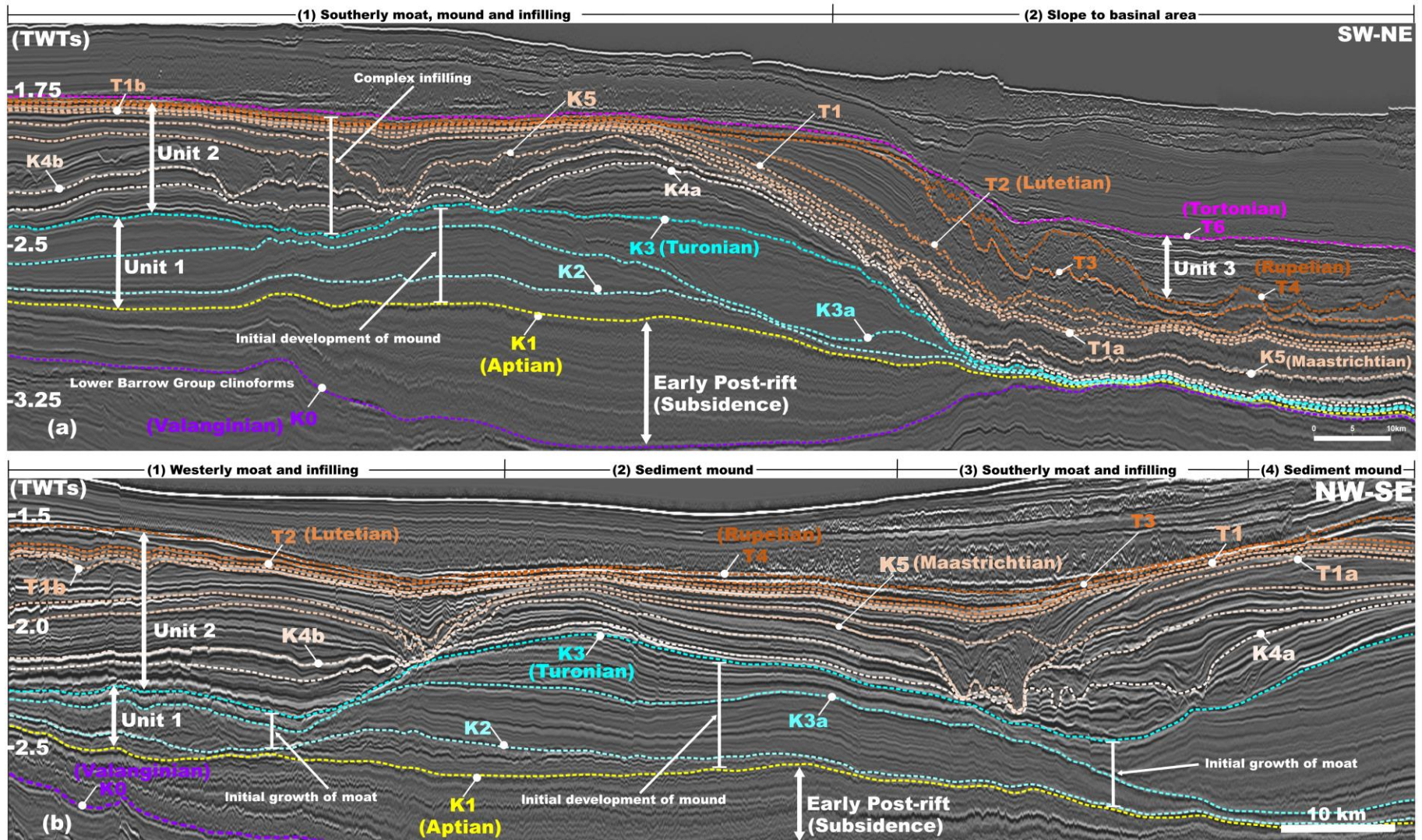


Fig. 5. a, b) Two seismic profiles oriented SW-NE and NW-SE illustrating the characteristics of Aptian – Lutetian sequences in the study area. Aggradational sediment mounds and moats are present in the southwest. In contrast, the northeast is characterised by condensed sequences from the Aptian to Maastrichtian, with more significant deposition observed from the Maastrichtian to the Rupelian (see Fig. 6d for the location of these seismic sections).



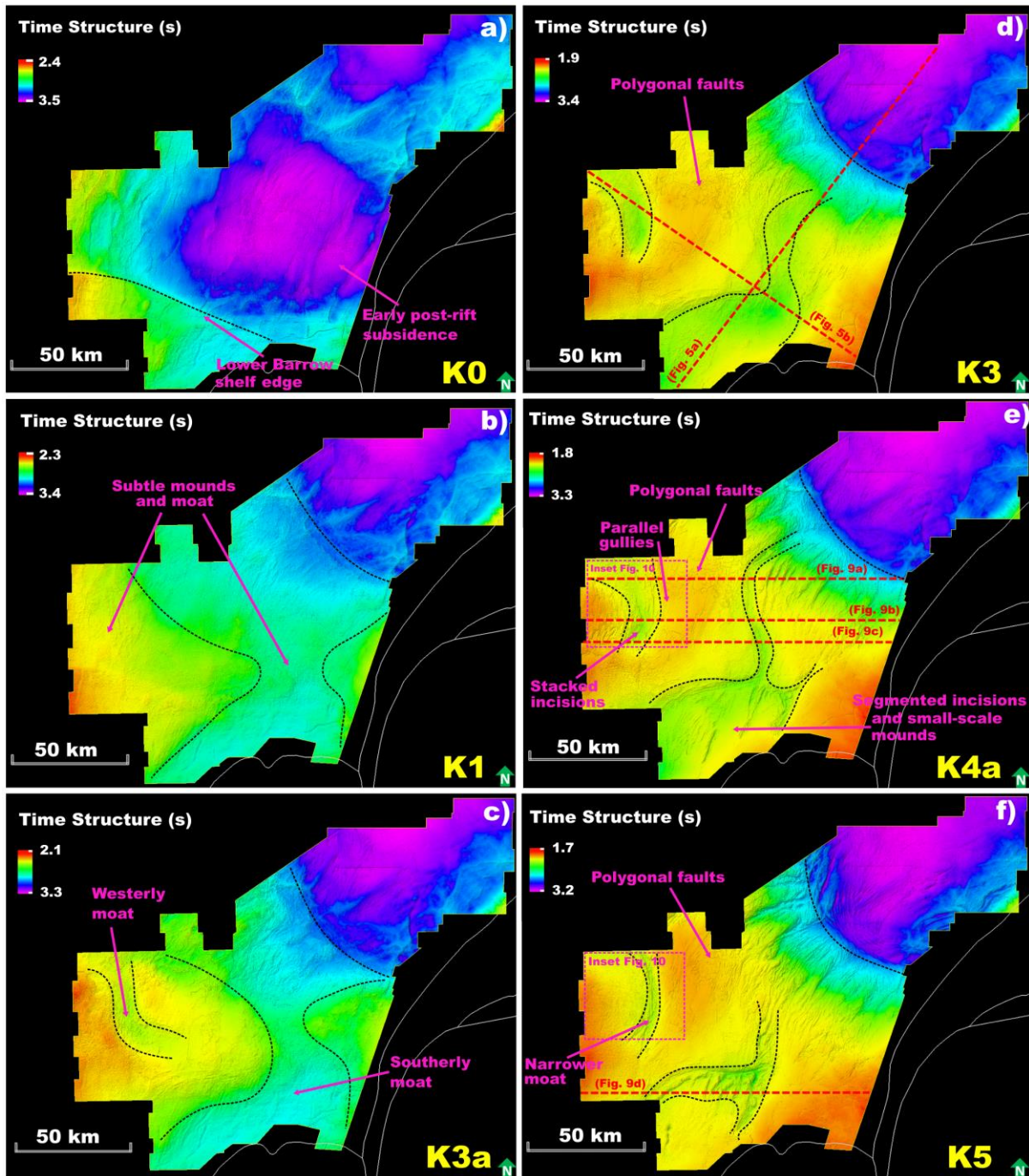


Fig. 6. a-f). Time structure maps showing the evolution of the Valanginian – Maastrichtian surfaces between horizons K0 and K5. Within this interval, the development of two southerly and westerly moats and mounds can be observed, as well as the sediment starved basin floor to the NE. The morphology of these moats changes over time, closely associated with the establishment of sediment mounds and their subsequent infilling.

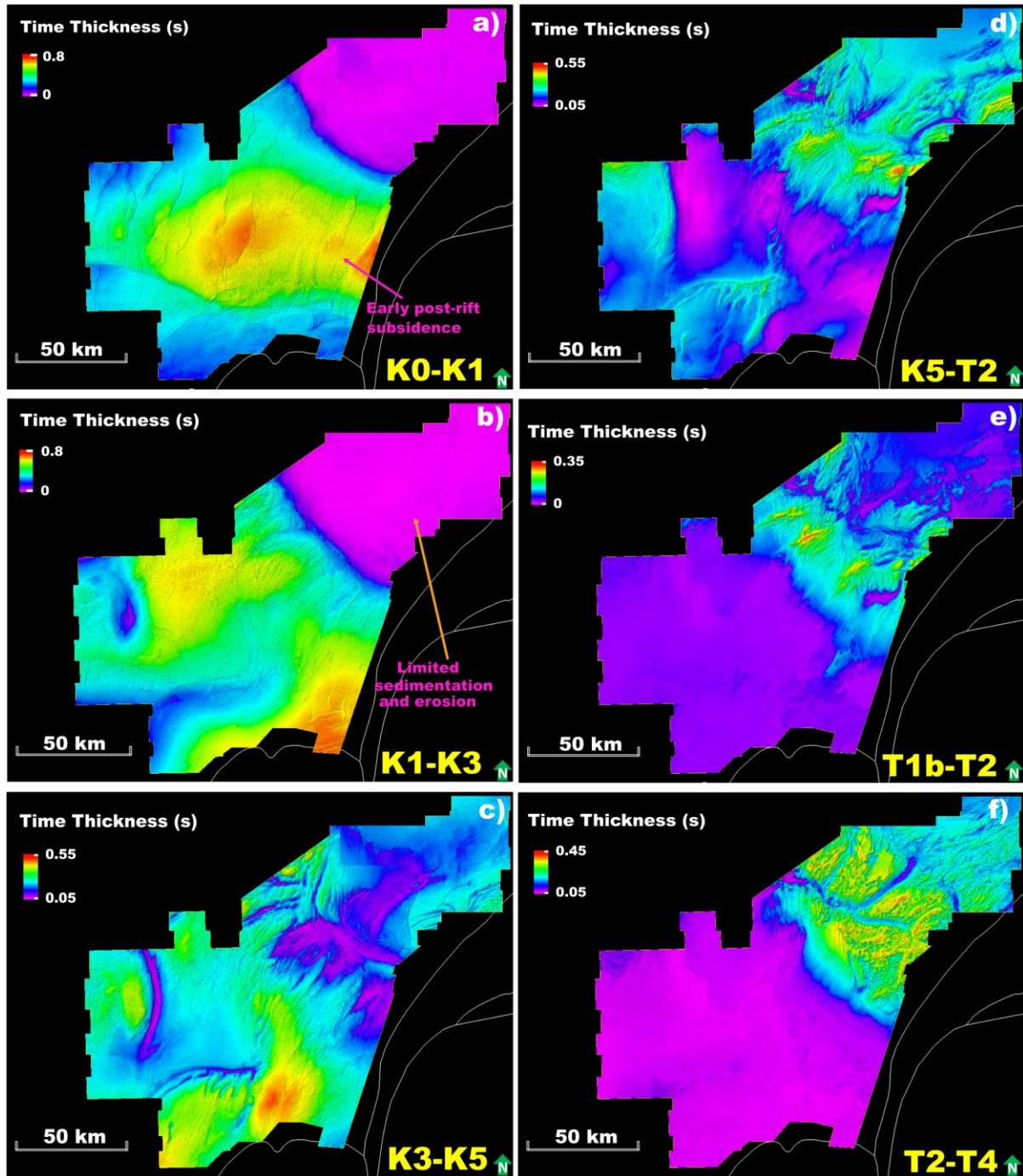


Fig. 7. a-f). Maps showing the time thickness of sediments during the post-rift phase from the Valanginian (horizon K0) to the Rupelian (horizon T4). In the southwest region, from horizons K0 to K5, significant deposition occurred compared to the northeast. However, after horizon K5, in the northeast, sedimentation significantly increases with the occurrence of multiple stacked incisions.



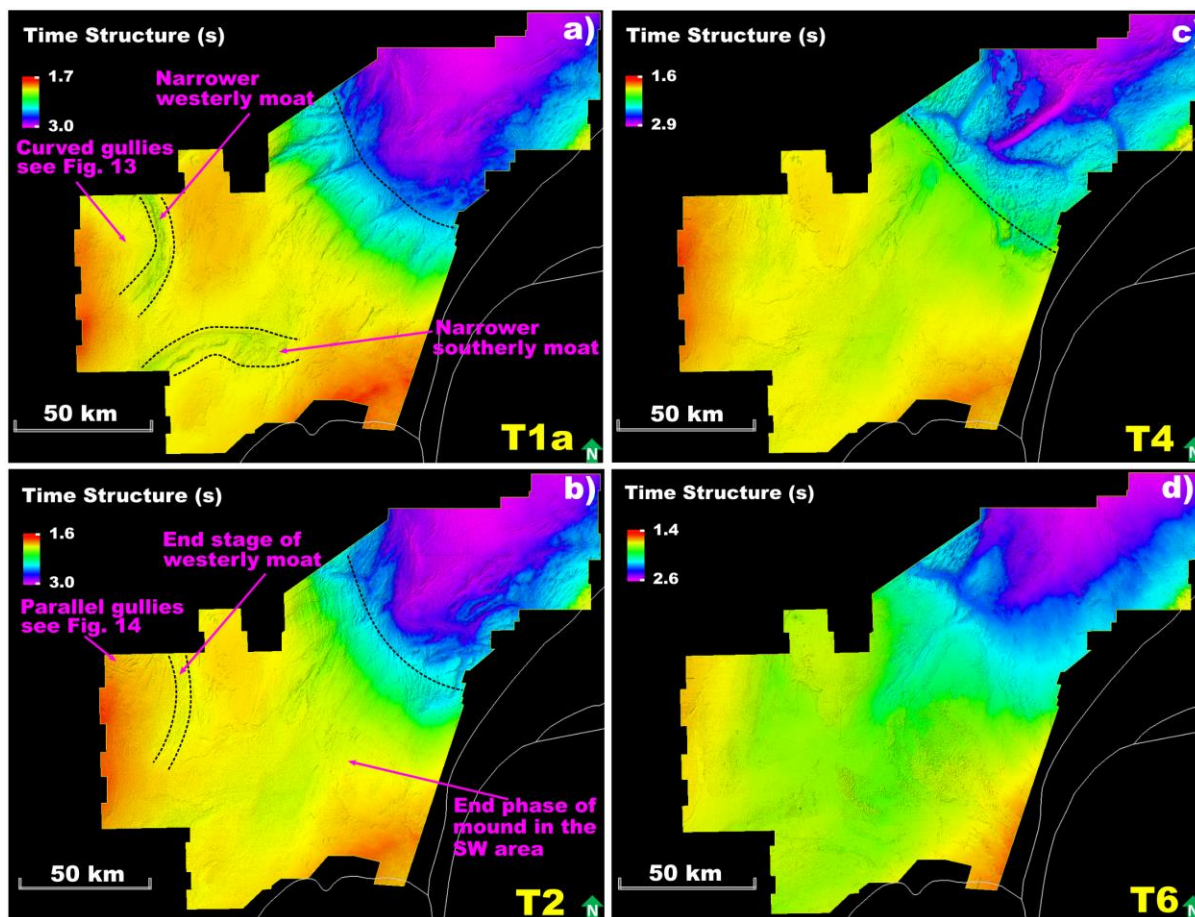


Fig. 8. a-d). Time structure maps showing the evolution of Thanetian – Tortonian (horizons T1-T6). During this interval, the two moats become narrower, which can be attributed to the continued growth of sediment mounds and the infilling by sediment. Notably, in the northeast, sedimentation progresses steadily without the formation of sediment mounds.



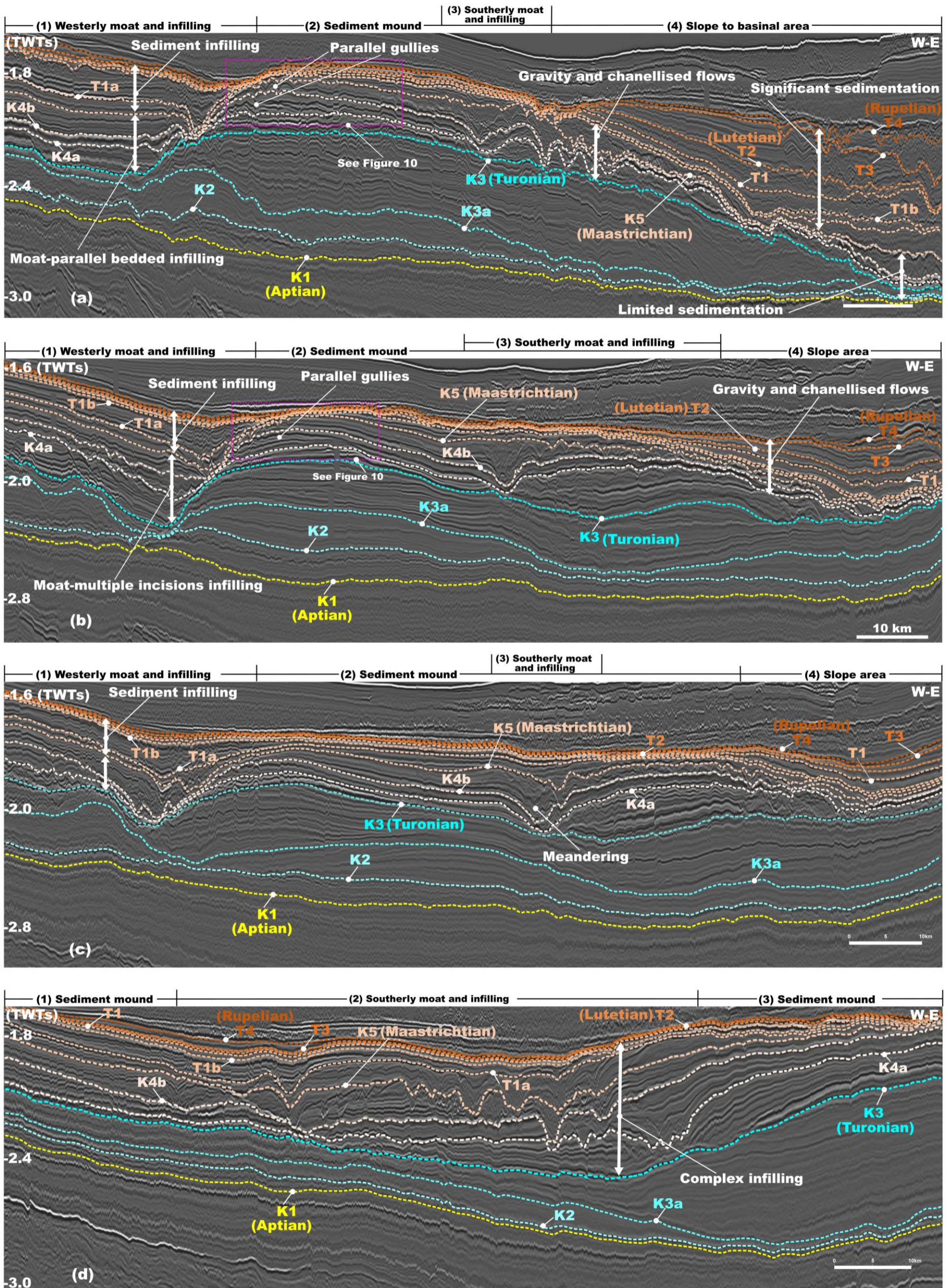


Fig. 9. a-d) Interpreted seismic profile showing the development of westerly and southerly moats as well as aggradational sediment mounds developed during Aptian – Rupelian (horizons K1-T4) in the southwest. Following the Turonian, the moats were infilled by sediment packages with a variety of sedimentary structures. In contrast, sedimentation in the northeast is limited until the Maastrichtian (horizon K5), subsequently the sediment progressively accumulated in the basinal area. Location shown in Fig. 6e.



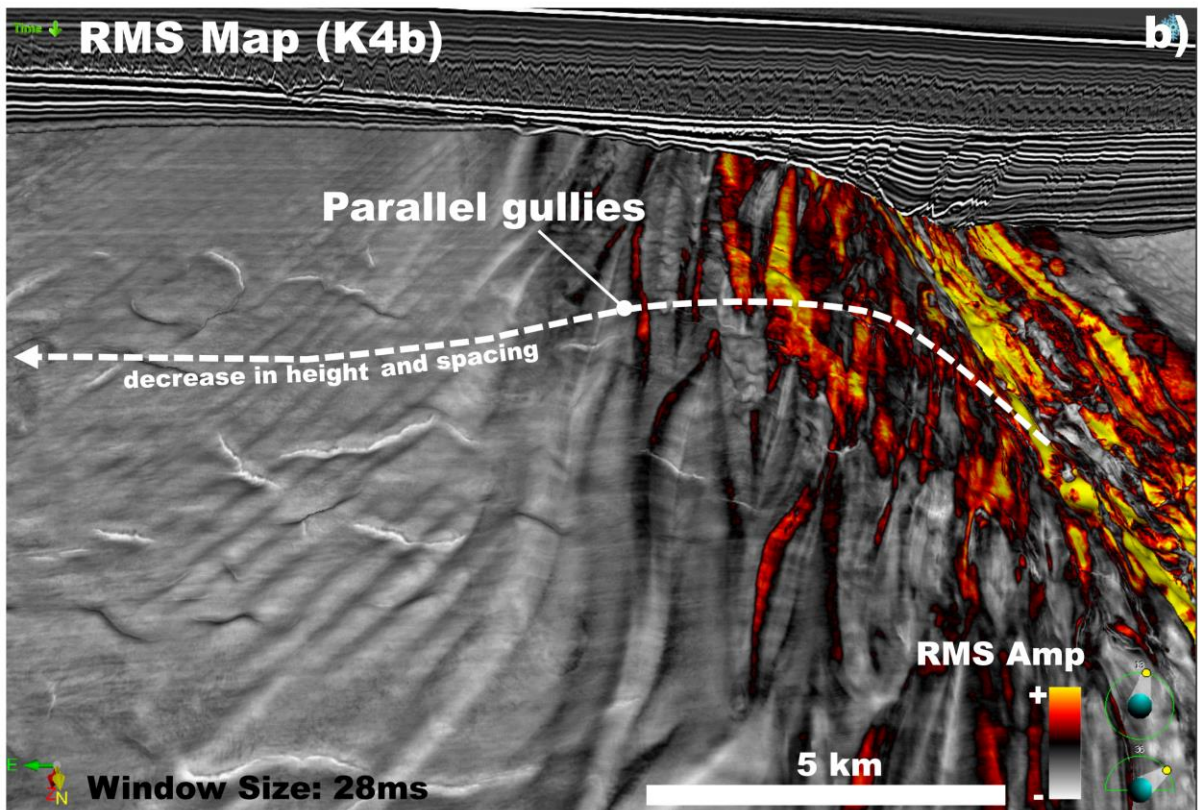
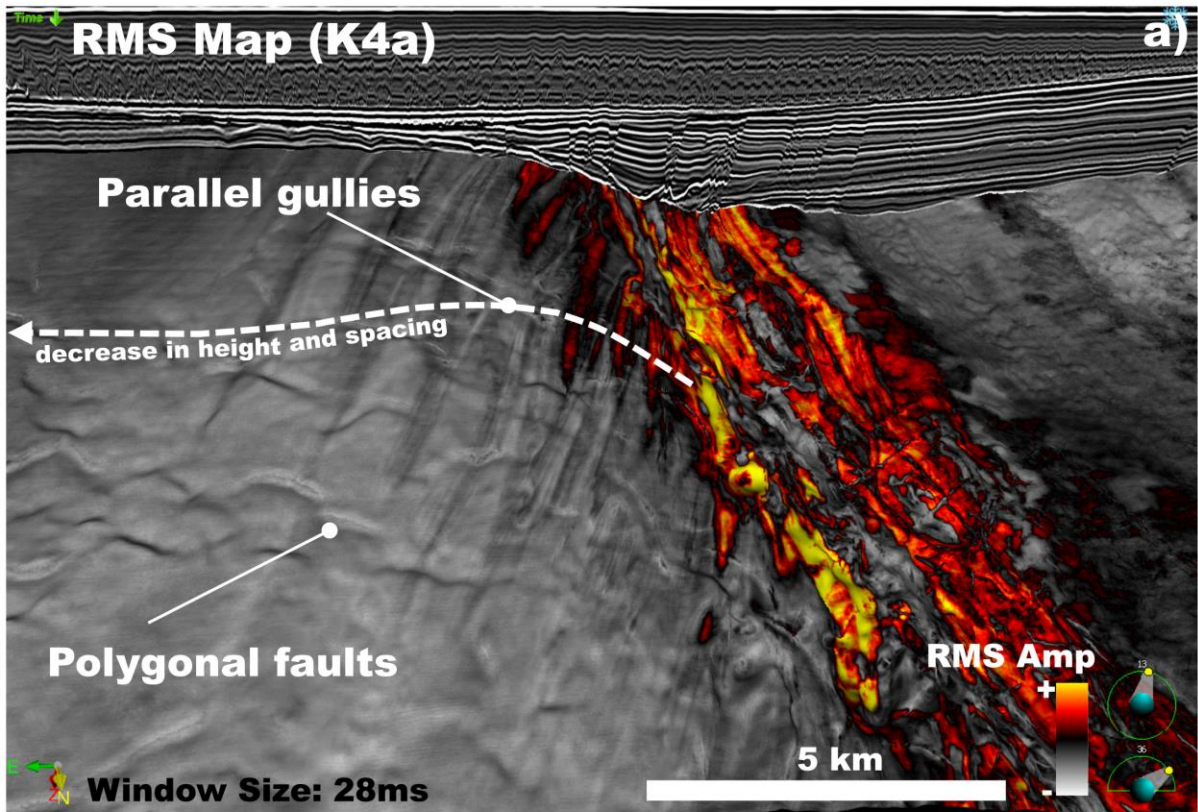


Fig. 10. a, b) RMS stratal slices illustrating the establishment of polygonal faults and parallel gullies on the crest of the westerly sediment mound between horizons K3 and K5 in the Turonian – Maastrichtian (see the location on Fig. 6e-f). The gullies reduce in size to the east, away from the moat.



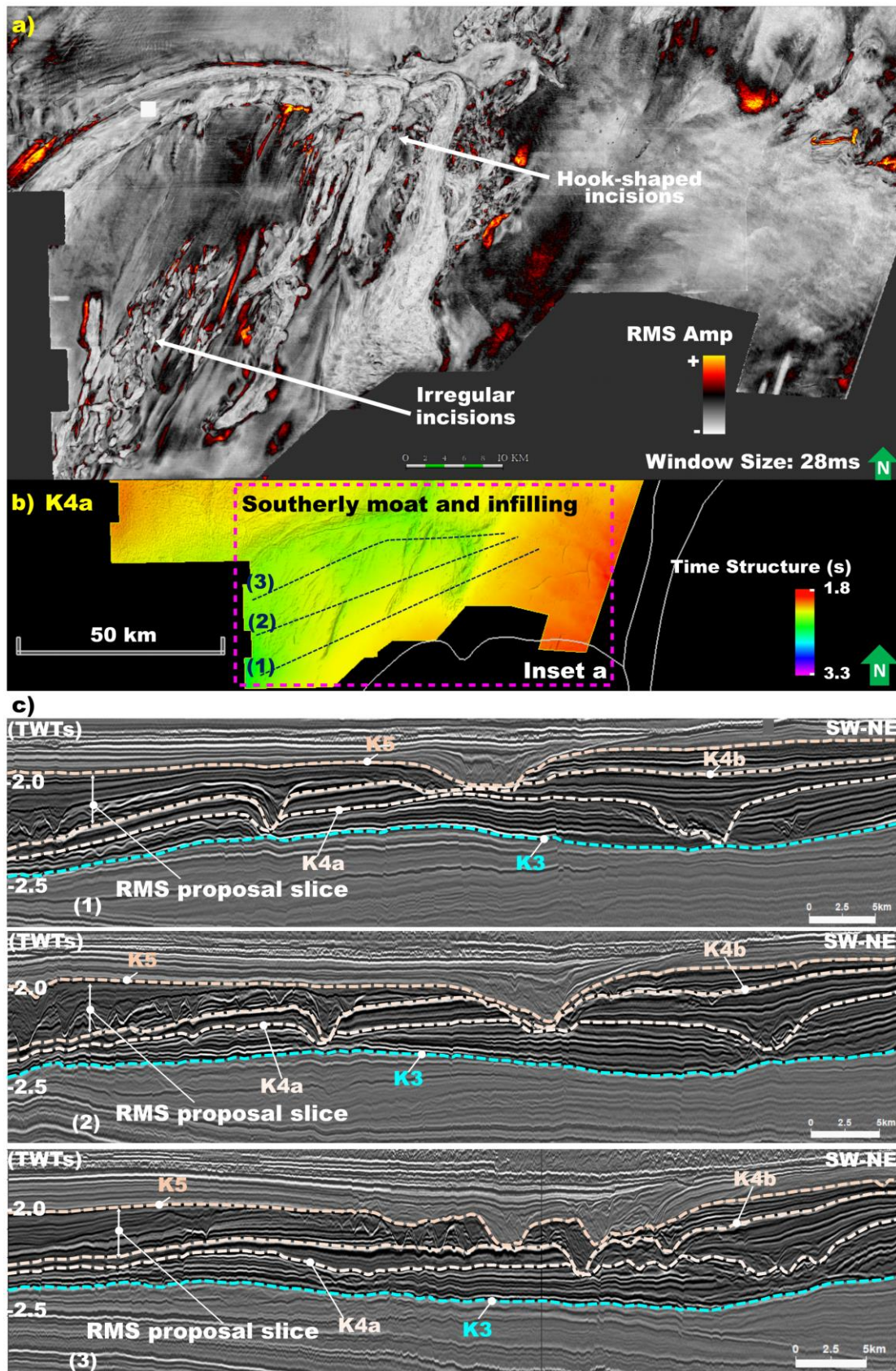


Fig. 11. a) RMS stratal slices showing the hook-shaped and irregular incisions developed between horizons K4b and K5 during infilling of the southerly moat in the Campanian – Maastrichtian. b) Time structure map of horizon K4a showing the location of southerly moat, which infilled with small-scale mounds and segmented incisions and the location of seismic lines shown below. c) Three seismic profiles showing the nature of the infill from horizons K3 to K5.



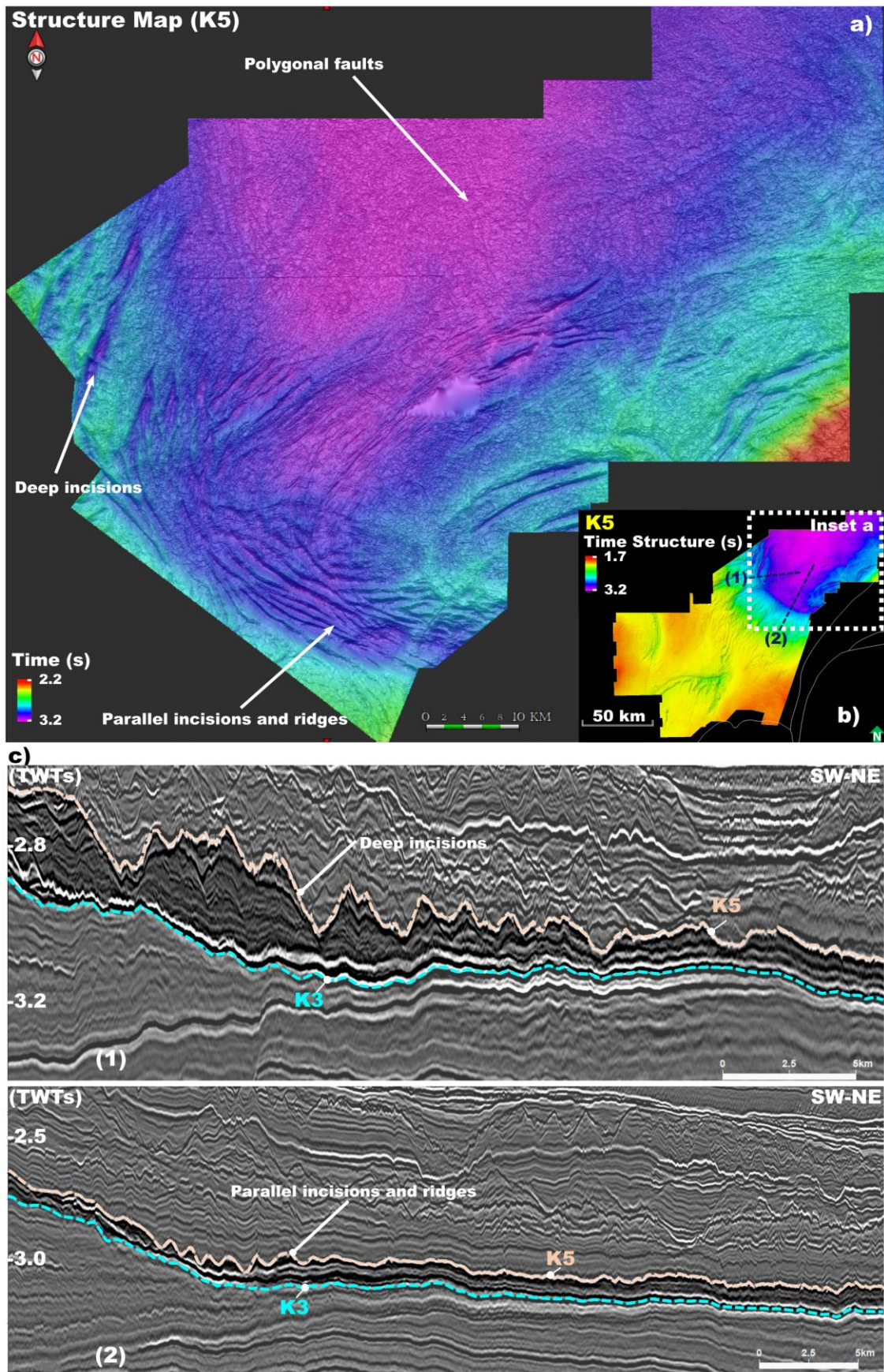


Fig. 12. a, b) Time structure map of horizon K5 illustrating widespread polygonal faults over the basin floor, large parallel incisions and deep incisions along the boundary slope. c) Two seismic profiles showing the variation in sediment thickness and sedimentary structures between horizons K3 and K5 (location shown in Fig. 12b).



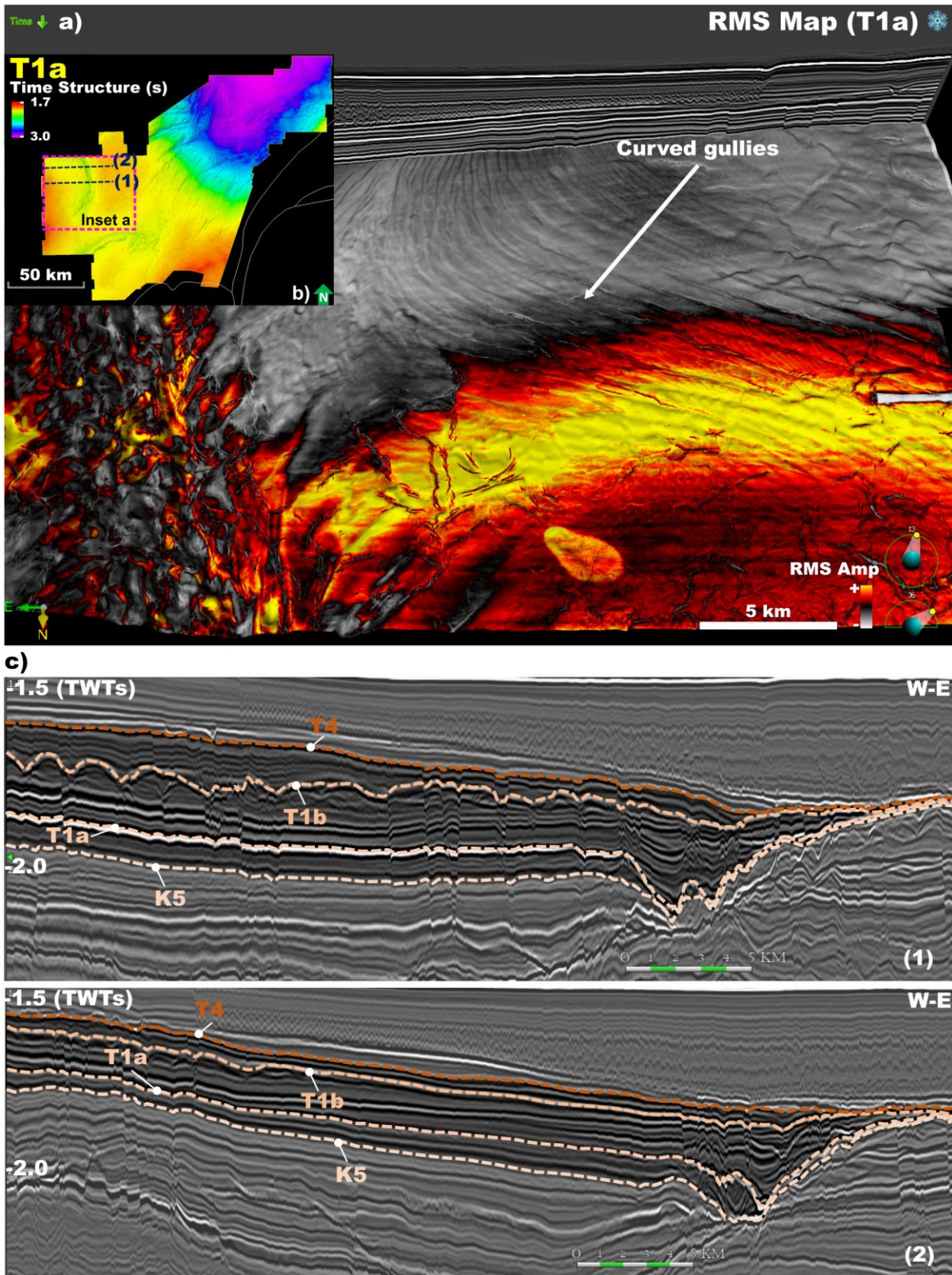


Fig. 13. a) RMS map of horizon T1a showing curved gullies in the infill of the westerly moat developed during the Paleocene. b) Time structure map of horizon T1a showing the location of the curved gullies and the location of seismic sections shown below. c) Two interpreted seismic profiles illustrating the variation in sedimentary structures between horizons T1a and T1b (time structure map of horizon T1b map shown in Fig. 14).



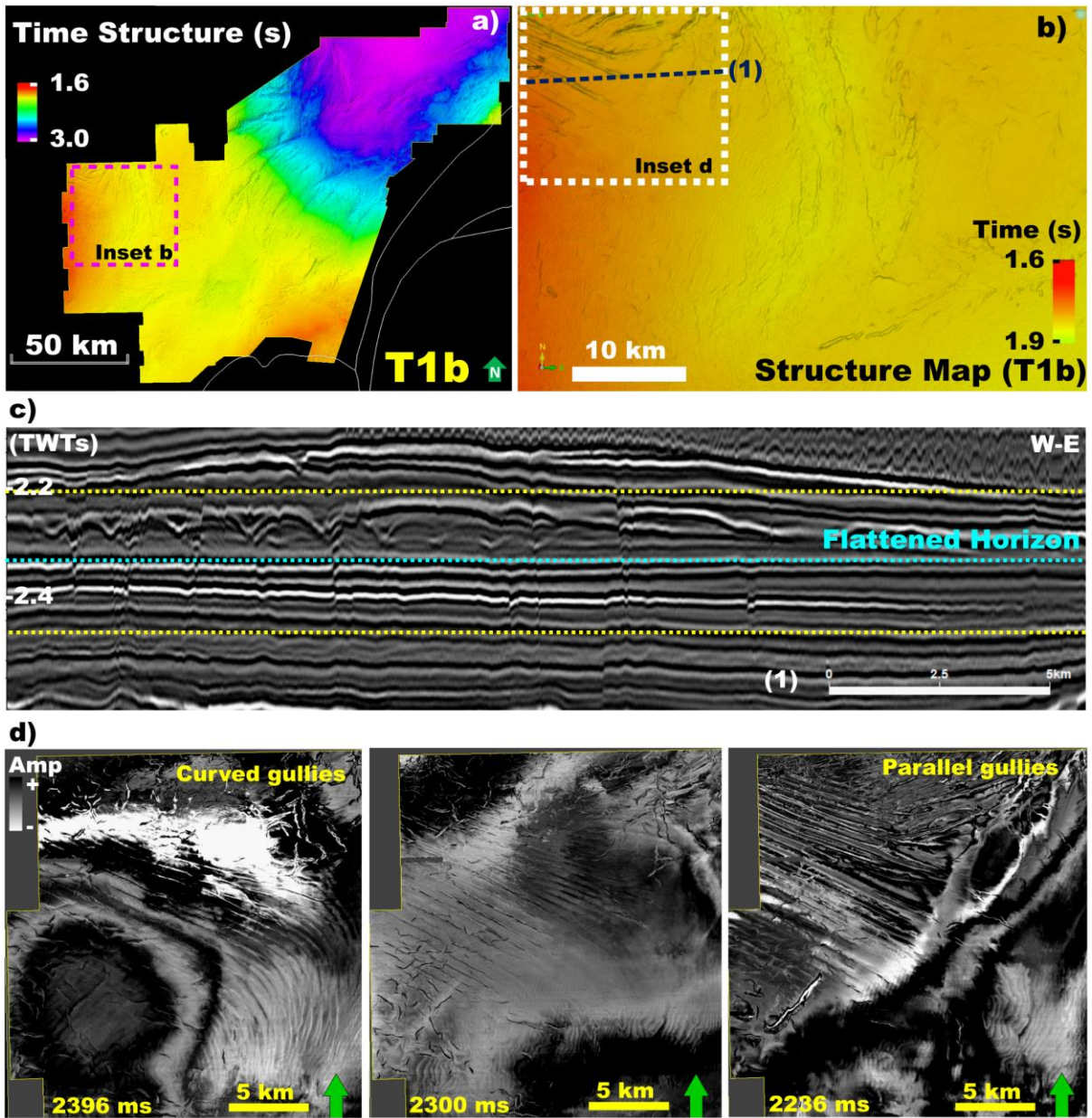


Fig. 14. a, b) Time structure map of horizon T1b illustrating parallel gullies in the infill of the westerly moat developed in the Paleocene. c) Seismic profile showing a seismic section flattened just below horizon T1b showing the contrast between curved gullies below the flattened horizon and parallel gullies above it as shown by the successive stratal slices in Fig. 14d.



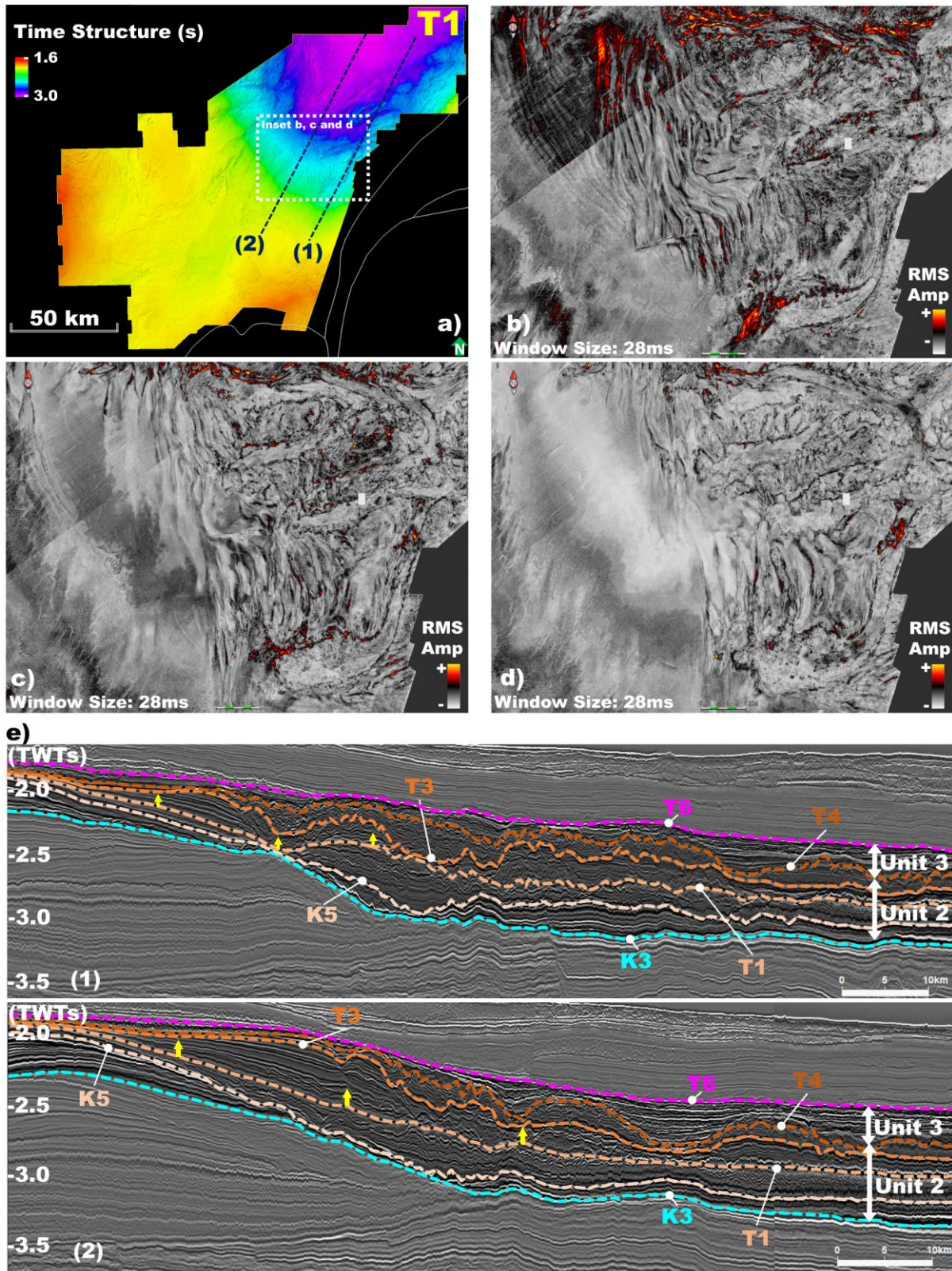


Fig. 15. a) Time structure map of horizon T1 showing the location of complex sedimentary features developed on the slope at the edge of the basin floor during the Thanetian. b, c, d) RMS maps above horizon T1 illustrating the complex interrelationship between sediment waves, parallel gullies and deep incisions. e) Two seismic profiles illustrating these sedimentary features developed at horizons T1, T3 and T4 during Thanetian – Rupelian in the northeast of the area (the location of the seismic sections shown in Fig. 15a).



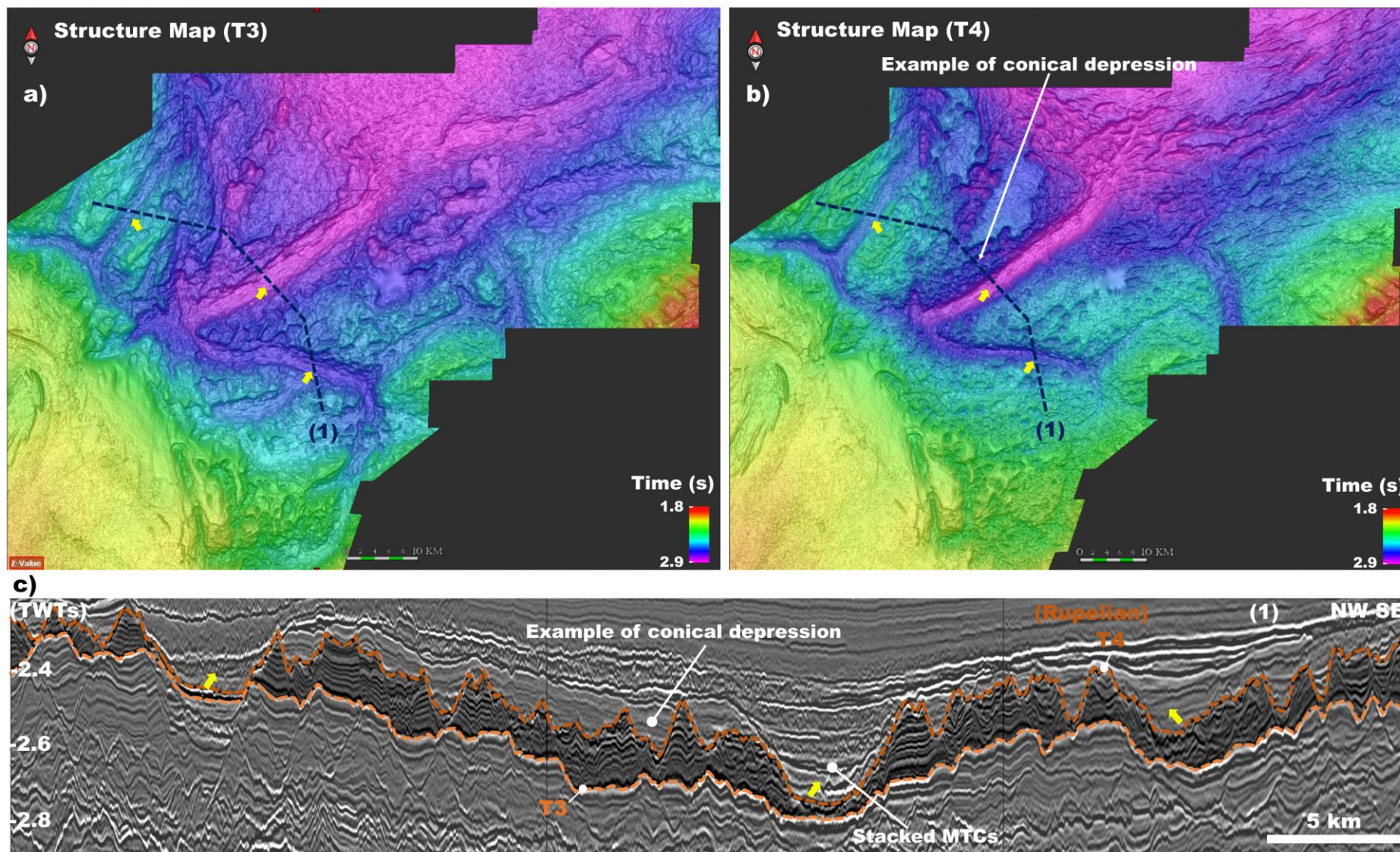


Fig. 16. a, b) Time structure maps of horizons T3 and T4 showing conical depressions indicative of large pockmarks or deepwater carbonate dissolution. c) Seismic section showing channels infilled by young MTCs (indicated by yellow arrows).



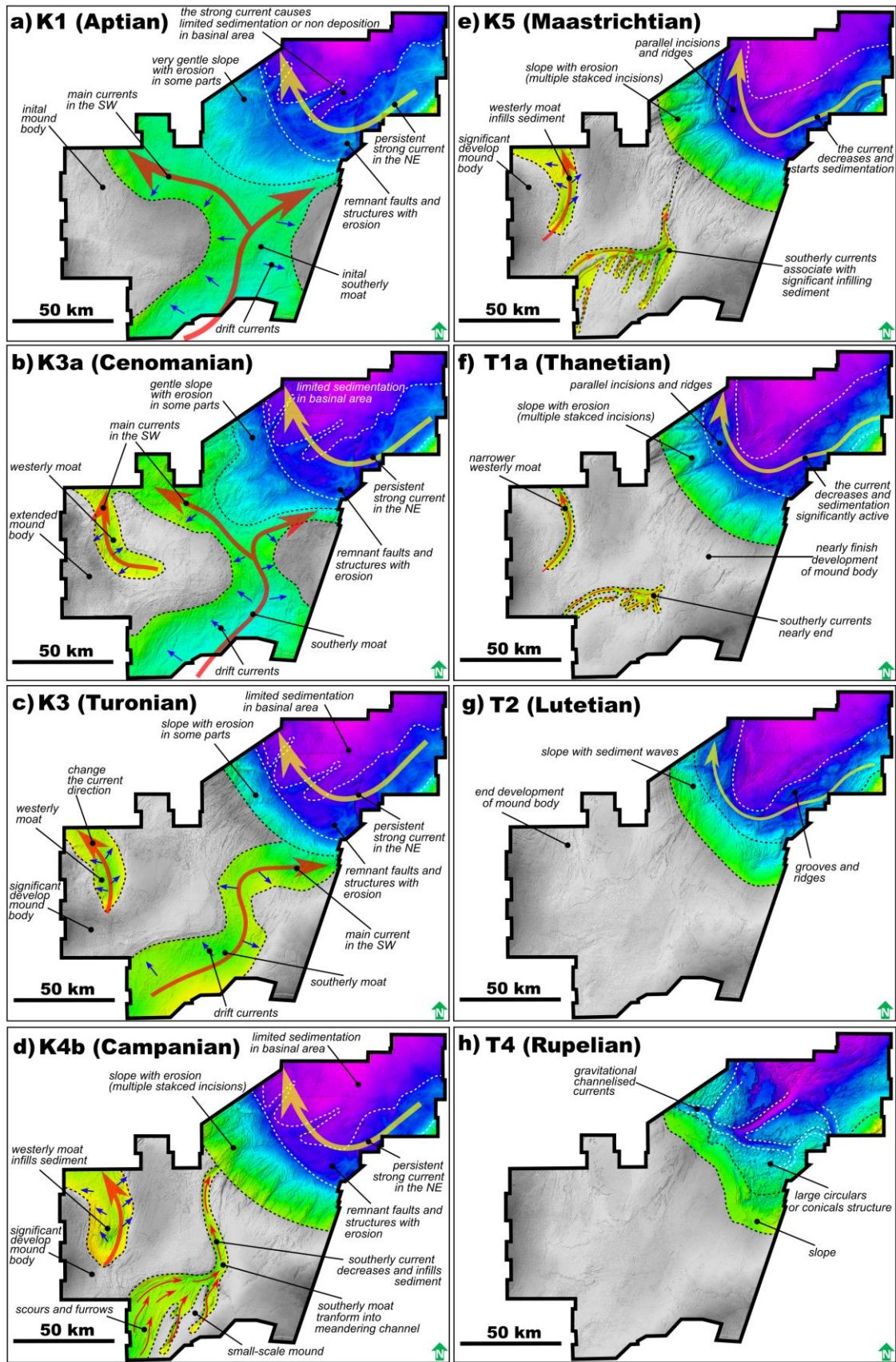


Fig. 17. a-h) Reconstruction of bottom currents activity from the Aptian to Rupelian inferred from the development of sediment mounds, moats, and complex incisions in the southwest and northeastern areas. Changes in current intensity and direction shaped these features, with a waning trend towards younger ages. The Lutetian marks the conclusion of the sediment mound and moat establishment in the southwest.



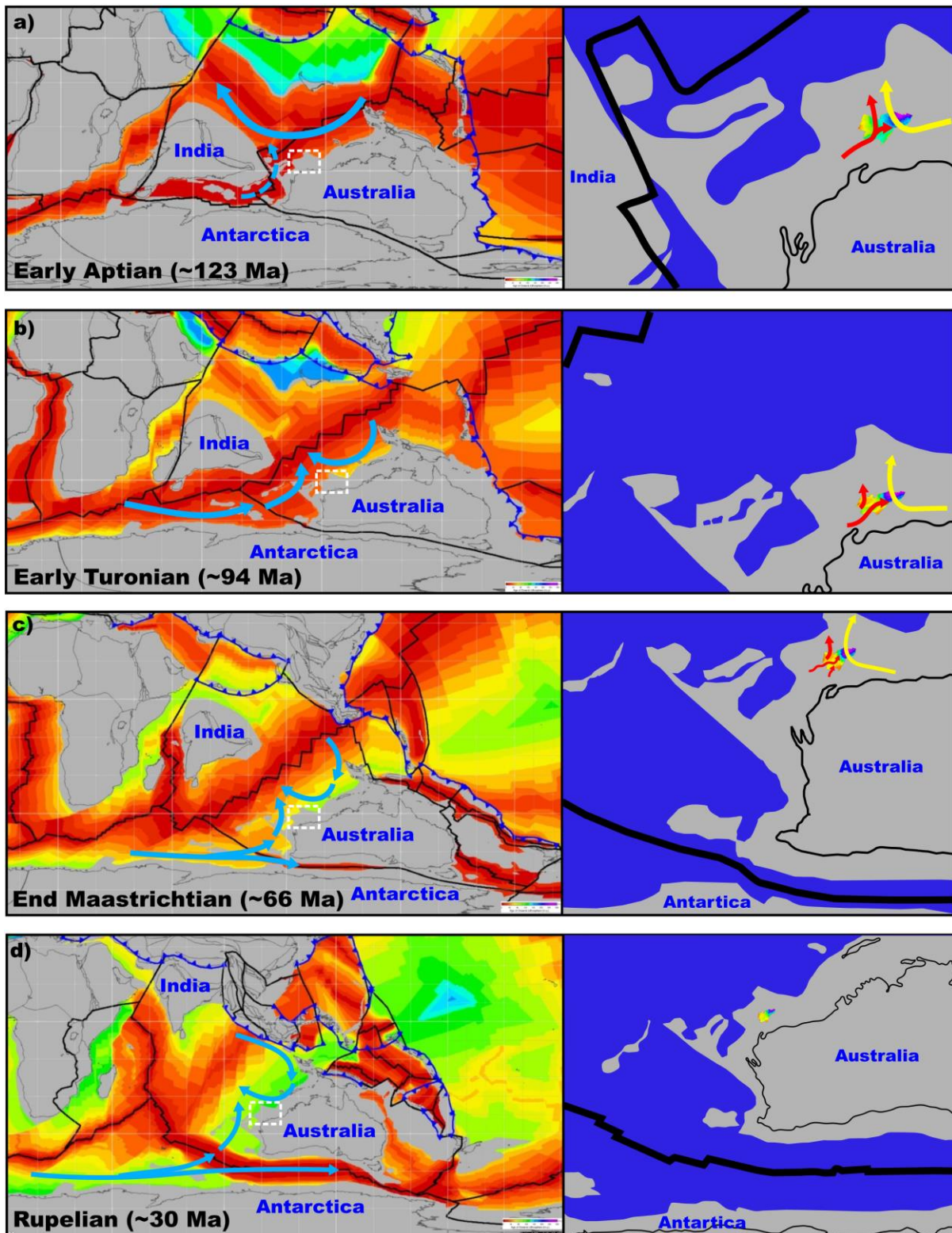


Fig. 18. a-d) Plate reconstruction compiled from Müller et al., 2019 (<http://portal.gplates.org/cesium/?view=AgeGrid>) and potential ocean circulation pathways (left hand side) with location of bottom current deposits and inferred local currents (right hand side). The opening of oceanic gateways to the west and south of Australia would have allowed reorganisation of circulation patterns which coincide with the evolution of sedimentary structures in the Northern Carnarvon Basin. See text for further explanation.

---

*Chapter Four:*

*Velocity Variations Associated with  
Seismic Facies and Seismic  
Stratigraphic in the post–Valanginian  
Passive Margin Sequences of the  
Northern Carnarvon Basin, Northwest  
Shelf of Australia*

---

# Chapter Four: Velocity Variations Associated with Seismic Facies and Seismic Stratigraphic in the post-Valanginian Passive Margin Sequences of the Northern Carnarvon Basin, Northwest Shelf of Australia

---

## Research highlights

1. The post-rift sequences in the Exmouth Plateau contain varied hemi-pelagic, bottom current and mass transport deposits.
2. Stratigraphic sequences have distinct velocity characteristics partly related to a transition of from clastic to carbonate sediments after the Turonian.
3. Lateral facies variations in Turonian and Rupelian bottom current deposits account for further velocity variations.

## *Abstract*

The post-Valanginian sequence of the passive margin in the Northern Carnarvon Basin has traditionally been regarded as a homogeneous sedimentary sequence, documenting the transition from siliciclastic to carbonate deposition. However, this simplistic interpretation can significantly misguide the prediction of velocity within complex sedimentary structures that are evident in 3D seismic data. This complexity is most apparent in the central Exmouth Plateau, marked by the presence of multiple stacked erosional and depositional structures, which are attributed to bottom current activity. Our study shows that stratigraphic sequences have distinct velocity characteristics that reflect changing depositional processes and a shift from clastic to carbonate sediments, starting in the Turonian. Additionally, lateral and vertical variations in seismic facies add to velocity complexity, especially within Aptian to Rupelian sequences dominated by bottom current activity. Slumps and mass transport complexes deposited in the Rupelian to Recent periods also have distinct velocity characteristics.

**Keywords:** *Seismic facies, seismic stratigraphy, interval velocity, Northern Carnarvon Basin, Exmouth Plateau, Northwest Shelf of Australia.*



## 1. Introduction

Understanding the velocity structure of stratigraphic sequences is of critical importance for accurate seismic imaging of subsurface geology and for establishing a reliable depth representation of subsurface structures, especially when used for well planning and precise prognoses of expected stratigraphy. Velocity structure is a function of the subsurface geology and in simple cases velocities are a predictable function of compaction and hence depth of burial. In more complex cases undercompaction / overpressure, lateral facies variations, structural complexity or differences in diagenesis may result in layers with anomalous velocities and/or lateral changes in velocity within layers. In the context of drilling operations, the association between layers with anomalous velocities and changes in lithology may also indicate changes in drilling conditions. Consequently, in areas of complex geology the accurate prediction of the depth at which such layers occur assumes heightened significance and aids in proactive planning to address drilling conditions and potential drilling challenges.

The Northern Carnarvon Basin (NCB) is a proven basin for hydrocarbon exploration and production in the westernmost part of the Northwest Shelf of Australia (Geoscience Australia, 2022). All proven hydrocarbon targets occur in pre- and syn-rift Triassic, Jurassic and lowermost Cretaceous sequences. The post-rift Aptian and younger sequences are considered non-economic hydrocarbon targets, but recent investigations show that they contain highly variable seismic facies as a consequence of bottom current activity that impinged on central parts of the basin (Winata et al., 2023). Anecdotally, accurate well prognoses in this area are challenging, as is the prediction of drilling conditions. This may in part reflect the relatively limited attention that this part of the sequence has received, and the use of relatively simple lithostratigraphic nomenclature that implies relatively uniform lithologies. The aim of this paper is to investigate the velocity characteristics of more precisely defined seismic-stratigraphic sequences which contain highly variable seismic facies (Winata et al., 2023) and hence to establish the relationship between seismic stratigraphy, seismic facies, and seismic velocities. Not only will this allow better understanding of the velocity structure of the NCB, it may also help to identify the potential for velocity anomalies on other continental margins with similar sedimentary sequences.

## 2. Geological background

The NCB developed as a result of a series of phases of rifting from the Late Carboniferous to Early Cretaceous, coinciding with the breakup of the Gondwana supercontinent (Veevers, 1988; Gartrell, 2000; Borel and Stampfli, 2002; Metcalfe, 2013). The basin covers an area of around 535,000 square kilometres (Hocking, 1988) and is bounded by the Argo Abyssal Plain, the Curvier Abyssal Plain and the Gascoyne Abyssal Plain (Fig. 1). The basin includes an outboard area of distributed extensional faulting corresponding to the Exmouth Plateau, with water depths ranging from 800 to 4,000 metres (Exon et al., 1992; Scarselli et al., 2013). The Plateau comprises three primary sequences including >10 km thick Triassic pre-rift sequences, variable thicknesses of latest Triassic to earliest Cretaceous syn-rift sequences, and post-rift Lower Cretaceous – Recent sediments. The inboard area encompasses marginal rift basins, including the Beagle sub-basin, Dampier sub-basin, Barrow sub-basin and Exmouth sub-basin, as well as the Rankin Platform, an area of uplift on the northwest flank of these basins (Fig. 1; Romine et al., 1997). The inboard sub-basins contain thick syn-rift Jurassic – Early Cretaceous sediments and in part correspond to the position of the present day shallow shelf margin with water depths ranging from 200 to 500 metres (Exon et al., 1992; Scarselli et al., 2013).

Following Valanginian breakup, the basin experienced an extended phase of subsidence as it transitioned into a passive margin (Driscoll and Karner, 1998; Cathro and Karner, 2006). During this passive margin phase, siliciclastic sediments were dominant until the Turonian. Subsequently, sedimentation shifted mainly to carbonate deposits, which continue to the present day (Apthorpe, 1988; Romine et al., 1997). However, the evolution of the NCB was punctuated by brief episodes of compression, notably in the Late Cretaceous and the Late Miocene (Veevers et al., 1991; Lee and Lawver, 1995; Romine et al., 1997; Hull and Griffiths, 2002; Pryer et al., 2002).

## 3. Data and methods

### 3.1. Dataset

This study utilises six different 3D seismic datasets and eighteen wells. The data is available in the public domain from the National Offshore Petroleum Information Management System (NOPIMS) and the Western Australian Petroleum and Geothermal

Information Management System (WAPIMS) websites. The seismic data is situated in the centre of the Exmouth Plateau and also covers part of the Rankin Platform (Fig. 1), with a total coverage of roughly 15,000 square kilometres. The seismic surveys were acquired between 2004 and 2008, primarily for hydrocarbon exploration, with a variety of bin sizes and vertical sampling intervals, as detailed in Table 1. In this research, we utilized age and lithological information, specifically from Cretaceous to Present day intervals, from wells drilled within the 3D seismic data areas to correlate key seismic horizons. As the wells primarily targeted hydrocarbon reservoirs in Jurassic and Triassic formations, there is limited lithological, well log and biostratigraphic data from the sequences that are the focus of this study.

### *3.2. Methodology*

A combination of Petrel (SLB) and Blueback Toolbox (CEGAL) software was employed to merge the 3D seismic datasets. The original data has a record length of 6 seconds in Two Way Time (TWT), but for the purposes of this study, this was trimmed to focus on the interval between 0.2 to 3.5 seconds TWT, encompassing the Cretaceous to seabed sequences. Since the original data exhibited varying amplitude values, they were standardized to achieve constant amplitude distributions within a zero-centric range of  $\pm 16,000$ . Following this amplitude balancing process, the seismic data were combined, using a vertical sampling interval of 4 milliseconds. This merging operation utilized the navigation and geometry data from the original individual surveys.

We build upon a regional seismic stratigraphic framework for the NCB established by Winata et al. (2023). This was developed from the interpretation of regional 2D seismic data integrated with several 3D seismic datasets and validated by correlation with data from 40 wells, as detailed in Winata et al. (2023). This framework identified 16 stratigraphically significant seismic horizons that were interpreted across the entire basin and were used to define the following sequences: the Valanginian – early Aptian that represents an early post-rift sequence, the early Aptian – Cenomanian (referred to as Unit 1), the Turonian – early Rupelian (Unit 2), the Rupelian – Tortonian (Unit 3), and the Tortonian – Present (Unit 4).

The regional seismic horizons were used to conduct an analysis of seismic facies and geomorphology on the merged 3D seismic dataset. These seismic surfaces were also

correlated with data from the 18 wells located within the 3D dataset. Furthermore, these surfaces were imported into PaleoScan (ELIIS) to facilitate the generation of additional stratigraphic surfaces using advanced techniques such as stratal slicing and seismic attribute analysis.

To achieve the aim of better understanding the correlation between seismic stratigraphy, seismic facies, and variations in velocity, velocity data, derived from a range of sources such as check-shot surveys, Vertical Seismic Profiling (VSP), and sonic log measurements were used to determine Time-Depth relationships between seismic data and well data and to calculate interval velocities. Interval velocities were computed over 10 metre intervals and are shown as log curves. In addition, for each stratigraphic unit, we calculated a single interval velocity value. These values were subsequently plotted against mid-point depth for each unit and were classified according to seismic stratigraphic package as well as seismic facies. V0-k functions were defined for each stratigraphic unit and for different seismic facies groups by determining best fit straight lines through interval velocity data plotted as a function of depth below the mudline in order to take into account variations in water depth.

#### 4. Seismic facies and stratigraphic framework

The final phase of syn-rift sedimentation in the NCB was marked by deposition of the Lower Barrow Group, which is thickest in the southwest. In this area it is characterised by clinoforms, which delineate a well-defined shelf edge, as demonstrated by horizon K0 (Fig. 2, 3 and 4). This corresponds to horizon K20.0 SB of Marshall and Lang (2013), and elsewhere forms an angular unconformity which is referred to as the Valanginian Unconformity (Fig. 2).

Horizons K0 and K1 mark the initial post-rift phase. The top of this sequence is early Aptian in age and corresponds to the K40.0 SB of Marshall and Lang, 2013 (Fig. 2). This sequence was dominated by the deposition of fine-grained siliciclastic sediments (Geoscience Australia, 2022) and it is characterised by laterally semi-continuous seismic reflections with moderate to high amplitudes. These sequences are extensively intersected by small offset faults, characteristic of polygonal faults (Cartwright, 1994; Watterson et al., 2000; Fig. 2, 3 and 4). A distinctive area of subsidence developed in the southwest of the study area.

Towards the northeast, the thickness of this sequence decreases significantly (Fig. 2 and 4) due to onlap on to the basal K0 surface and minor erosional truncations occurring at the top of the sequence (Fig. 2 and 4).

Unit 1 occurs between horizons K1 and K3, which corresponds to the top of the Cenomanian (K50.0 SB of Marshall and Lang, 2013; Fig. 2). The sequence is internally subdivided by horizon K2. This sequence also comprises fine-grained siliciclastic sediments (Geoscience Australia, 2022). In the southwest, Unit 1 is characterised by vertically stacked low angle and elongate mounded reflections with medium to high amplitudes, which we interpret as sediment mounds (Fig. 4). In addition, large U-shaped reflections of medium to high amplitude, which in some places show erosion or truncation are interpreted as sediment moats (Fig. 4). As with the underlying sequence, Unit 1 thins substantially towards the northeast (Fig. 2 and 4) which we interpret as an area of limited deposition, most likely due to strong bottom current activity (Chapter 3 or Winata et al., submitted).

Unit 2 corresponds to the Turonian and Rupelian time intervals, is bracketed between horizons K3 and T4 (corresponding to T30.0 SB of Marshall and Lang, 2013; Fig. 2 and 3) and the sequence shows a transition from siliciclastic to carbonate sedimentation (Geoscience Australia, 2022). Within this unit, we distinguish six primary sub-units, delineated by horizons K4, K5, T1, T2, and T3 (Fig. 3). These sub-units contain a range of seismic facies (Winata et al., 2023). In the southwest, these sequences encompass elongate mounded sediments (a continuation of the sediment mounds present in Unit 1), a variety of parallel to subparallel reflections and erosional structures, including single to multiple U, V and W-shaped incisions. These facies largely occur within the moats, and we refer to them as the "moat fills" (Fig. 4). Further to northeast, seismic facies are characterised by subparallel reflections with moderate symmetric and asymmetric U and V shaped incisions at different scales (mixed incisions) (Fig. 4), by asymmetric incisions in older sequences that are medium scale, U and V shaped, elongate and parallel, and by deep incisions and conical structures in the younger sequences (Fig. 4).

Unit 3 corresponds to the Rupelian and Tortonian interval, and is bounded by horizons T4 and T6, which corresponds to T40.0 SB of Marshall and Lang (2013) (Fig. 2). Within this unit, distinctive stacked chaotic reflections are interpreted as slumps and mass transport complexes (MTCs) (Fig. 4). This unit thins towards the southwest, where it overlaps and thins



out over a paleobathymetric high defined by the top of Unit 2 (Fig. 2 and 4). Unit 3 is restricted to the northeast inboard region of the Exmouth Plateau. Unit 4, on the other hand, covers the entire area and is defined by horizons T6 and T10, corresponding to the Tortonian to Recent. This unit exhibits a combination of parallel reflections and extensive stacked chaotic reflections, indicating that slumps and MTCs are more widespread in this unit. (Fig. 2, 3 and 4).

## 5. Velocity distribution

Interval velocities from 18 wells are plotted against depth (measured in meters below the mud line, BML). Interpreted seismic horizons were used to define 7 seismic stratigraphic sequences based on the units described above for velocity analysis purposes. They are K0-K1: Early Post-rift, K1-K3: Unit 1, K3-K5: Units 2a and b, K5-T2: Units 2c and d, T2-T4: Units 2e and f, T4T6: Unit 3, T6T10: Unit 4. We also use the 8 seismic facies described above (Polygonal Fault, Moats, Mounds, Moat Fills, Mixed Incisions, Asymmetric Incisions, Deep Incisions & Conical Depressions, and Slumps & MTCs) (Fig. 5). The interval velocities range from approximately 1500 to 3100 meters per second (m/s), covering depths up to 2100 meters (m) below seabed. Water depth varies from 745 to 1350 metres.

In general terms, three separate velocity-depth trends can be observed, with a greater rate of increase (higher K values) observed in stratigraphically younger sequences (Fig. 5a). Trend 1a reaches a maximum velocity of around 2600 m/s at a depth of 2000 meters and is mainly defined by velocities from the Early Post-rift sequence, Unit 1, Units 2a and b, and some velocities from Units 2c and d – all of Cretaceous age. Trend 2a reaches a maximum velocity of approximately 2900 m/s at depths of 1100 metres and comprises the remainder of the velocities from Units 2c and d and velocities from Units 2e and f of Upper Cretaceous and Paleogene age. Trend 3a reaches a maximum velocity of approximately 2900 m/s at depths of 820 metres and is defined by velocities from Units 3 and 4, both of Neogene age. The progressive increase in velocity gradient with decrease in stratigraphic age is also shown by Table 2, with Unit 2a and b and Unit 2c and d being the exception to this rule.

To a large extent, the velocity variation with seismic facies is linked to that of the stratigraphic units as the different units define different stages in the evolution of bottom

current activity and hence contain characteristic facies (Chapter 3 or Winata et al., submitted). As a result, the trends observed in Figure 5b bear a close resemblance to those depicted in Figure 5a. For example, the polygonal faulted sediments of the post rift sequence and the mounds and moats that are observed in Units 1, 2ab and 2cd, are characterised by lower K values. In contrast the Slumps and MTCs, which dominate in Units 3 and 4, exhibit higher K values (Figure 5b). However, it is important to note that the greatest velocity variation occurs within Unit 2, which also shows the greatest degree of seismic facies heterogeneity. Thus, the interval velocity values for the stratigraphic unit that make up Unit 2 may also mask lateral facies variations within them.

Figures 6 and 7 depict lateral and vertical variations in interval velocity within each stratigraphic unit. In the early post-rift sequence, velocity is generally uniform across most of the area, with the highest velocity observed in the southeast, associated with thinner sequence overlying sediments belonging to the Barrow Delta (Fig. 6a). Unit 1 is characterised by sediment mounds and moats, and the velocity remains relatively consistent, although some mixed incisions along the slope that marks the edge of the basinal area of thinner sediment to the northeast exhibit slightly lower velocities, while velocity increases to the east within the basinal where sediments are thinnest (Fig. 6b). Unit 2 displays the most significant variation in velocity. In Unit 2a and 2b, both mounds and slopes exhibit moderate velocity, with lower velocity near the top of the slope. The highest velocity is observed in the basinal area to the northeast, where sediment filling commenced (Fig. 6c). In Unit 2c and 2d, higher velocity is again associated with the basinal area, which began to fill significantly and contains stacked asymmetric incisions (Fig. 6d). This trend becomes more pronounced in Unit 2e and 2f, which are dominated by deep incisions and conical depressions, characterised by the highest velocity (Fig. 7a). Moving to Units 3 and 4, slumps and mass transport complexes (MTCs) begin to develop. The velocity pattern becomes more uniform, reflecting changes from proximal to distal domains (Fig. 7b and 7c).

The interval velocities for specific stratigraphic units also mask vertical velocity variations within those units. For instance, the RMS velocities calculated over 10 millisecond intervals display lower velocities in the lower sections and higher velocities in the upper sections of many of the mounds in Unit 2a and b, a phenomenon depicted in Figures 9, 10, and 12. Furthermore, mixed incisions as well as deep incisions & conical depressions in the

northeast and some moat fills in the southwest have a higher velocity (Fig. 9, 10 and 11) and higher K values (Table 2) than the mounds and moats in the southwest.

This may also be an indication of the variation of velocity with lithology. Figure 8 shows the velocity values for units that are predominantly composed of clastic sediments as compared to units that are mainly composed of carbonates. The velocities of the clastic sediments within the Early post-rift and in Unit 1 are generally lower than the velocities of the carbonate sediments in Units 2 and 4 at an equivalent depth.

## 6. Discussion

### 6.1. *Velocity trend in correlation to compaction, lithology, and sedimentary structures*

Seismic velocity within the post-Valanginian breakup sequence in the NCB is primarily stratigraphically controlled. Within individual stratigraphic units there is an increase in velocity with depth as would be expected due to the compaction and cementation of sediments as a function of burial. However, those trends are different in different stratigraphic units. Trend 1a shows the velocity variation of the Early post-rift sequence, Unit 1 (Aptian to Cenomanian) and parts of Unit 2a and b (Turonian - Maastrichtian). It is notable that the latter unit shows some higher velocities. This is attributed to the transition from clastic to carbonate sediments within this interval (Fig. 9). In contrast, Trends 2a and 3a are associated with the younger sequences and show higher velocities at shallower depths. This is linked to the ongoing deposition of carbonate sediments across the Exmouth Plateau. Overall, we suggest that clastic sediments are mainly influenced by burial and compaction, while carbonate sediments will also be affected by cementation which is less depth dependant.

Additionally, lateral variations in facies within Units 2, 3, and 4 play an important role in influencing these trends. Unit 2 in the southwest of the study area is dominated by the presence of mounds, moats, and moat fills. Although each of these features comprise fine-grained carbonate sediments, they exhibit different velocity responses. Mounded strata represent a continuous, stable process, resulting in uniform, thicker sequences, and are at a shallower level compared to moats. Most of the growth of the mounds occurs between Unit 1 and Unit 2d. They follow a lower velocity trend, but when the growth of the mounds is

reduced in Unit 2e and f, they have higher velocity values, possibly related to lower sedimentation rates and higher compaction and/or cementation. Moats are also characterised by thinner sequences and lower sedimentation rates than the equivalent sequences in the mounds. They have relatively high velocities compared to the mounds (Fig. 9 to 13), reflecting their deeper burial, greater compaction as well as greater cementation associated with lower sedimentation rates. The sediments that subsequently fill the moats generally have higher velocities than the mounds. However, the lower moat fill sequences show more evidence of erosive features (Unit 2a and b) and display higher velocities than the upper sequences that mainly contain parallel and sub-parallel reflector packages, with only minor evidence of erosion (Unit 2c and d) (Fig. 9 to 12).

In the basinal area to the northeast, the area was sediment starved during the deposition of Unit 1 and began to fill with sediments during the deposition of Unit 2, particularly during the deposition of Units 2c to f (Maastrichtian - Rupelian). These units contain a variety of sedimentary facies including mixed incisions, asymmetric incisions, and deep incisions & conical depressions. The velocities of these features are higher than those of the closest adjacent mounds and in general show a progressive increase from the mixed incisions through the asymmetric incisions (Fig. 9, 11 and 12) to the deep incisions & conical depressions (Fig. 6c-d, 7a, 9, and 10). The contrast between the mounds and moats that dominate the SW of the study area and the more basinal, sediment starved area to the NE is a result of different sedimentary processes, with greater reworking of sediments in the NE. This likely affected the nature of sediment and may also have had some effects on early cementation, through processes such as a persistent scouring and dissolution which may account for the conical depressions.

Units 3 and 4 are characterised by deposits of Slumps and MTCs, and their seismic velocities show an interesting trend related to proximity to the Neogene-Present day shelf break which is located in the east of the study area. Unit 3 contains the first evidence of clinoforms (Winata et al., 2023), implying the progradation of a carbonate shelf, with Slumps and MTCs transporting material from the base of slope, creating differences between proximal and more distal deposits. Slumps and MTCs situated closer to the shelf edge primarily consist of thicker carbonate deposits and are characterised by chaotic seismic facies, typical of the sediment reworking and rapid deposition associated with slumps and MTCs. These areas exhibit higher velocity values (Fig. 7b-c and 9 to 13). By contrast sediments

deposited farther away from the shelf break are characterised by thinner, less chaotic sequences that most likely contain a finer-grained carbonates deposited by hemipelagic deposition and turbiditic run out (Fig. 9 to 13) and are associated with lower velocity values.

## 6.2. *Implications for velocity prediction and well planning*

The post-rift sequence of the Exmouth Plateau shows a significant variation in velocity, primarily attributed to the distinct characteristics of the stratigraphic sequences and the different facies they contain. In the absence of a velocity cube, this implies that a layer-cake velocity model would be required to account for these differences. However, there are also clear lateral velocity variations within sequences, particularly between the southwest and northeast of the study area related to differences in sediment accumulation and sedimentary processes. Given the relatively small number of wells, particularly in the northeast of the area velocity maps that are contoured according to seismic facies belts, rather than simple interpolation, are more likely to produce more accurate results. Drilling conditions are also likely to be more varied in areas of heterogeneous sediments dominated by incisions, as compared to more uniform deposits represented by sediment mounds and polygonally faulted sequences, particularly where condensed sequences may be associated with harder, cemented layers.

## 7. Conclusions

In the Exmouth Plateau, the post-rift sequence, spanning from the Valanginian to the Present, is characterised by a variety of different depositional processes. This variation corresponds to eight discernible seismic facies which in turn characterise seven distinct stratigraphic units, each of which have different seismic velocity characteristics. A first order control is provided by lithology – the early post-rift sequence and Unit 1 (Valanginian to Cenomanian) are dominated clastic sediments and show lower velocity gradients, while the upper parts of Unit 2 (c/d and e/f), Unit 3 and Unit 4 (Paleocene to present) are dominated by carbonate sediments and show higher velocity gradients. Consequently, the younger sequences show higher velocities than the older sequences at the same depth due to the fact that clastic sediments reflect the effects of burial and compaction, while carbonates are additionally influenced by cementation processes. The velocity characteristics of Units 2a and



2b (Turonian - Maastrichtian) are more variable, reflecting the transition from clastic to carbonate sedimentation. In addition, lateral variation in seismic facies, which are present throughout Units 2, 3, and 4, correspond to significant lateral velocity variations. This is most pronounced in Unit 2 where bottom current activity has resulted in the greatest variety of sedimentary deposits. Mounds, moats and moat fills which occur in the southwest generally have lower velocities than asymmetric incisions and deep incisions & conical depressions which occur in the more basinal areas to the northeast. This could be due to sediment-starved conditions and greater sediment reworking in the basinal areas which may in turn promote early cementation. In Units 3 and 4 (Rupelian – Present), which are dominated by slumps and MTCs, thicker chaotic carbonate deposits near the shelf edge have with higher velocities than thinner, less chaotic finer-grained distal sediments. The significant stratigraphic and facies control on velocity variations have significant implications for seismic velocity models. In the absence of detailed seismic velocity cubes derived from 3D seismic data, velocity models that combine data from wells with stratigraphic interpretation and facies maps are likely to be more accurate. Drilling operations may also be more challenging in areas with varied sediments, especially where condensed sequences might be linked with harder, cemented layers.

#### Conflicts of Interest

The authors declare no conflict of interests.

#### Acknowledgement

We wish to express our sincere thanks to Geoscience Australia for generously providing us with access to public domain seismic and well log data that played a pivotal role in our research. All the datasets we employed in this study can be readily accessed through the National Offshore Petroleum Information Management System (NOPIMS), which is available at <https://nopims.dmp.wa.gov.au/nopims>. We would also like to extend our appreciation to Schlumberger, CEGAL, and ELIIS for granting us permission to utilize the Petrel, Blueback Toolbox, and PaleoScan software, which proved to be indispensable in our research efforts. Additionally, we would like to acknowledge the support provided to Mulky Winata through a collaborative PhD scholarship awarded under the Aberdeen – Curtin Alliance 2018. This

scholarship program is facilitated by Curtin University in Perth, Australia, and the University of Aberdeen in Aberdeen, Scotland.

## References

- Apthorpe, M., 1988. Cenozoic depositional history of the North West shelf. In: Purcell, P.G., Purcell, R.R. (Eds.), *The North West Shelf, Australia. Proceedings of Petroleum Exploration Society of Australian Symposium*, Perth, Australia, 55–84.
- Borel, G.D., Stampfli, G.M., 2002. Geohistory of the North West Shelf: a tool to assess the Palaeozoic and Mesozoic motion of the Australian Plate. In: Keep, M., Moss, S.J. (Eds.), *The Sedimentary Basins of Western Australia 3. Proceedings of the Petroleum Exploration Society of Australia Symposium*, 119–128.
- Cathro, D.L., Karner, G.D., 2006. Cretaceous-tertiary inversion history of the Dampier sub-basin, Northwest Australia: Insights from quantitative basin modelling. *Marine and Petroleum Geology*, 23, 503–526. <https://doi.org/10.1016/j.marpetgeo.2006.02.005>.
- Cartwright, J.A., 1994. Episodic basin-wide hydrofracturing of overpressured early cenozoic mudrock sequences in the North Sea Basin. *Mar. Petroleum Geol.* 11, 587–607. [https://doi.org/10.1016/0264-8172\(94\)90070-1](https://doi.org/10.1016/0264-8172(94)90070-1).
- Driscoll, N.W., Karner, G.D., 1998. Lower crustal extension across the Northern Carnarvon Basin, Australia: evidence for an eastward dipping detachment. *J. Geophys. Res.* 103, 4975–4991. <https://doi.org/10.1029/97JB03295>.
- Exon, N., Haq, B., Von Rad, U., 1992. Exmouth plateau revisited: Scientific drilling and geological framework. In U. Von Rad, B. U. Haq, R. B. Kidd, S. B. O’Connell (Eds.), *Proceedings of the Ocean Drilling Program, Scientific Results*, 122, 3–20. College Station, TX: Ocean Drilling Program. <http://dx.doi.org/10.2973/odp.proc.sr.122.194.1992>.
- Gartrell, A., 2000. Rheological controls on extensional styles and the structural evolution of the Northern Carnarvon basin, North West Shelf, Australia. *Aust. J. Earth Sci.* 47 (2), 231–244. <http://dx.doi.org/10.1046/j.1440-0952.2000.00776.x>.
- Geoscience Australia, 2022. Regional Geology of the Northern Carnarvon Basin [WWW Document]. *Offshore Pet. Explor. Acreage Release*.

- Hocking, R.M., 1988. Regional geology of the Northern Carnarvon Basin. In: Purcell, P.G., Purcell, R.R. (Eds.), *The North West Shelf, Australia*. Proceedings of the Petroleum Exploration Society of Australia Symposium, 97–114.
- Hull, J.N.F., Griffiths, C.M., 2002. Sequence stratigraphic evolution of the albian to recent section of the Dampier Sub Basin, North West Shelf, Australia. In: *Sedimentary Basins of Western Australia 3: Proceedings of Petroleum Exploration Society of Australia Symposium* (Ed. by M. Keep & S.J. Moss), 3, 617–639. Petroleum Exploration Society of Australia Perth, Australia.
- Lee, T.Y., Lawver, L.A., 1995. Cenozoic plate reconstruction of Southeast Asia. *Tectonophysics*, 251, 85–138. [https://ui.adsabs.harvard.edu/link\\_gateway/1995Tectp.251...85L/doi:10.1016/0040-1951\(95\)00023-2](https://ui.adsabs.harvard.edu/link_gateway/1995Tectp.251...85L/doi:10.1016/0040-1951(95)00023-2).
- Marshall, N.G., Lang, S.C., 2013. A new sequence stratigraphic framework for the North West Shelf, Australia. In: Keep, M., Moss, S.J. (Eds.), *The Sedimentary Basins of Western Australia 4*. Proceedings of the Petroleum Exploration Society of Australia Symposium, 1–32.
- Metcalfe, I., 2013. Gondwana dispersion and Asian accretion: tectonic and palaeogeographic evolution of eastern Tethys. *J. Asian Earth Sci.* 66, 1–33. <https://doi.org/10.1016/j.jseaes.2012.12.020>.
- Pryer, L.L., Romine, K.K., Loutit, T.S., Barnes, R.G., 2002. Carnarvon basin architecture and structure defined by the integration of mineral and petroleum exploration tools and techniques. *APPEA J.*, 42, 287–309. Australian Petroleum Production and Exploration Association, Canberra, Australia. <http://dx.doi.org/10.1071/AJ01016>.
- Romine, K.K., Durrant, J.M., Cathro, D.L., Bernadel, G., Apthorpe, M., 1997. Petroleum play element prediction for the Cretaceous-Tertiary basin phase, Northern Carnarvon Basin. *J. Aust. Petroleum Prod. Explor. Assoc.* 37 (1), 315–339.
- Scarselli, N., McClay, K., Elders, C., 2013. Submarine Slide and Slump Complexes, Exmouth Plateau, NW Shelf of Australia, in Keep, M. and Moss, S.J (Eds.), *Western Australian Basins Symposium 2013*, Aug 18-21 2013. Perth: Petroleum Exploration Society of Australia. <https://doi.org/10.1002/9781119500513.ch16>.
- Veevers, J., Powell, C. M., Roots, S., 1991. Review of seafloor spreading around Australia. I. Synthesis of the patterns of spreading. *Australian Journal of Earth Sciences*, 38, 373–389. <https://doi.org/10.1080/08120099108727979>.

- Veevers, J.J., 2000. Change of tectono-stratigraphic regime in the Australian plate during the 99 Ma (mid-Cretaceous) and 43 Ma (mid-Eocene) swerves of the Pacific. *Geology*, 28 (1), 47-50. [https://doi.org/10.1130/0091-7613\(2000\)28%3C47:COTRIT%3E2.0.CO;2](https://doi.org/10.1130/0091-7613(2000)28%3C47:COTRIT%3E2.0.CO;2).
- Watterson, J., Walsh, J.J., Nicol, A., Nell, R.R., Breatan, P.G., 2000. Geometry and origin of a polygonal fault system. *J. Geol. Soc. Lond.* 157, 151–162. <https://doi.org/10.1144/jgs.157.1.151>.
- Winata, M., Elders, C., Maselli V., Stephenson A. R., 2023. Regional seismic stratigraphic framework and depositional history of the post-Valanginian passive margin sequences in the Northern Carnarvon Basin, North West Shelf of Australia, *Marine and Petroleum Geology*, Volume 156, 106418, ISSN 0264-8172, <https://doi.org/10.1016/j.marpetgeo.2023.106418>.

No	3D Survey	Year	Cover Area (km <sup>2</sup> )	Bin Size (m)	Sampling Interval (ms)
1	Io-Jansz	2004	2853.47	18.75 x 12.50	2
2	Willem	2006	2665.84	25.00 x 12.50	4
3	Duyfken	2006	3806.79	18.75 x 12.50	4
4	Charon	2007	2149.39	18.75 x 12.50	4
5	Draeck	2007	1677.98	18.75 x 12.50	4
6	Glencoe	2008	4227.34	25.00 x 25.00	4

Table. 1. 3D seismic datasets that were used in this study. All are public domain and provided by Geoscience Australia via the National Offshore Petroleum Information Management System (NOPIMS).

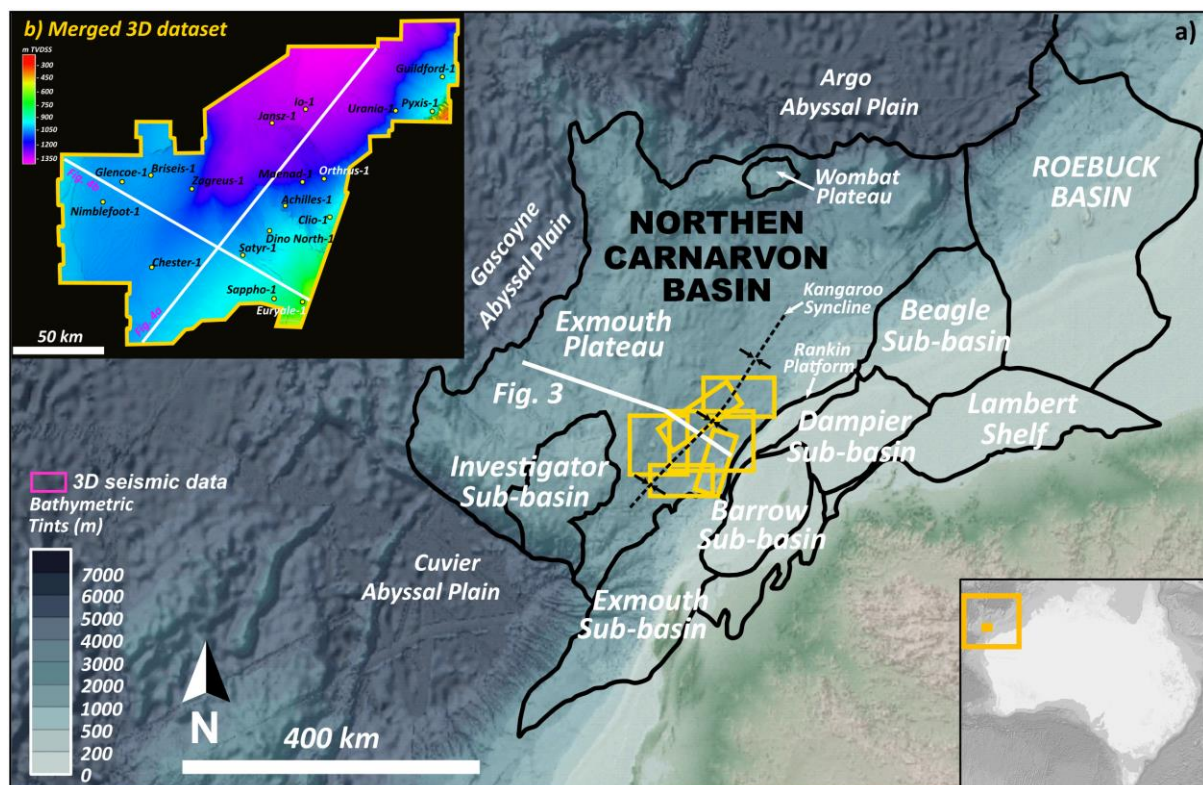


Fig. 1. Map showing the outline of the Northern Carnarvon Basin and the main structural elements within it, regional present-day bathymetry, the location of the 3D seismic datasets used in this study (yellow boxes) and the location of a WNW–ESE regional seismic line used to describe the regional seismic-stratigraphic scheme. Upper left inset map shows the seabed imaged by the merged 3D seismic data sets, the wells used for stratigraphic correlation and velocity analysis, and the location of seismic lines shown in Figure 4. m TVDSS stands for metres true vertical depth subsea.



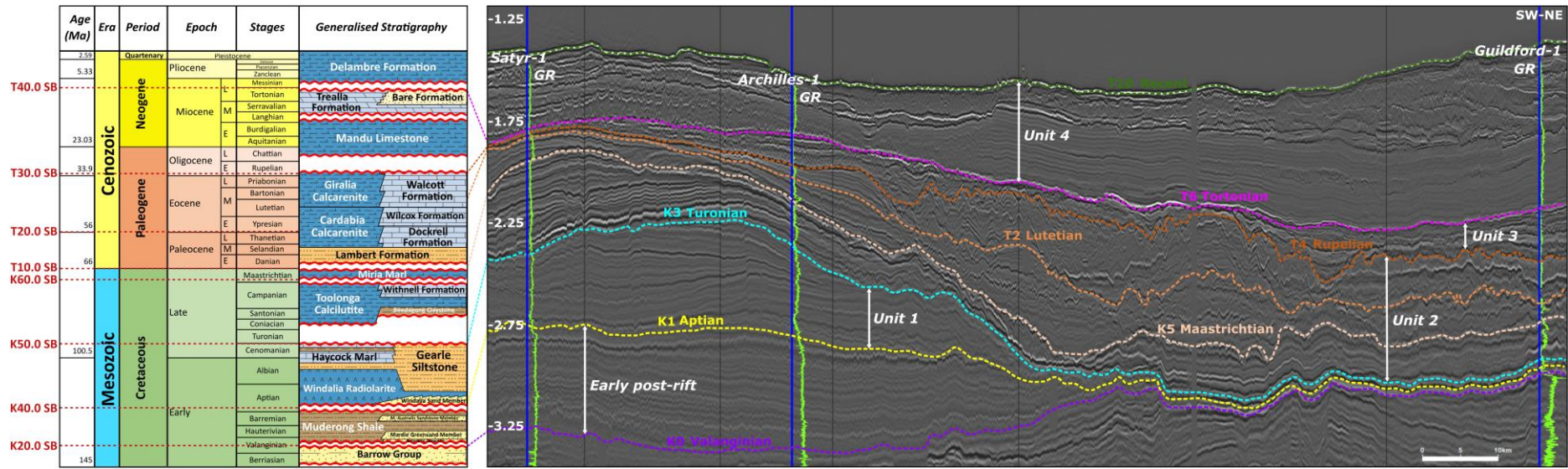
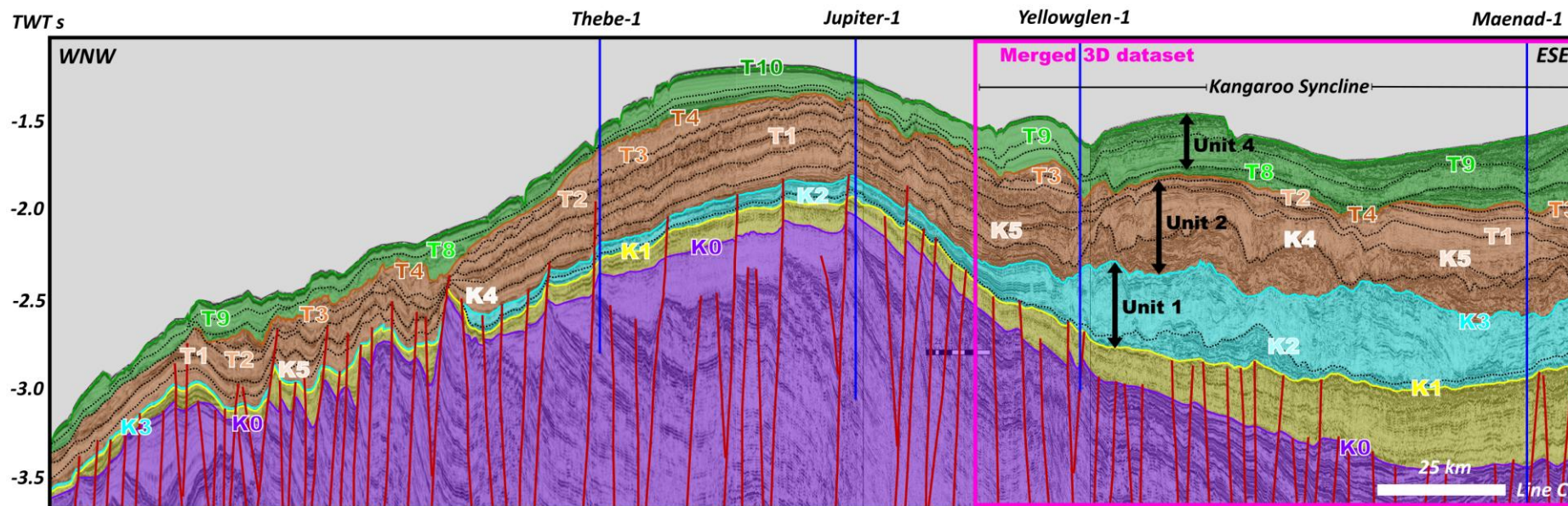


Fig. 2. Generalised stratigraphic chart for the NCB compiled from Geoscience Australia (2021) correlated to the seismic stratigraphic scheme used in this study and to formation tops in three wells (Satyr-1, Archilles-1, Guildford-1, GR: Gamma-ray, see Figure 1 for well locations). Formation names and lithostratigraphic terms are used according to the Australian Stratigraphic Units Database. Red dashed lines are boundaries given by Marshall and Lang (2013).



### TOP FORMATIONS

#### Cretaceous

- K5 ≈ Miria Marl / Withnell Formations
- K4 ≈ Upper Gearle Silstone / Toolonga Calcilutite
- K3 ≈ Lower Gearle Silstone / Haycock Marl
- K2 ≈ Windalia Radiolarite
- K1 ≈ Muderong Shale
- K0 ≈ Lower Barrow Group or Base Upper Barrow / Base Muderong Shale

Unit 2a-b  
Unit 1a-b

#### Cenozoic

- T5 ≈ Mandu Formation
- T4 ≈ Upper Walcott / Gindaria Formations
- T3 ≈ Lower Walcott / Gindaria Formations
- T2 ≈ Wilcox / Cardabia Formations
- T1 ≈ Dockrell / Lambert Formations

Unit 3a  
Unit 2e-f  
Unit 2c-d

- T10 ≈ Upper Delambre Formation (Seabed)
- T9 ≈ Middle 2 Delambre Formation
- T8 ≈ Middle 1 Delambre Formation
- T7 ≈ Lower Delambre Formation
- T6 ≈ Trealla / Bare Formation

Unit 4d  
Unit 4a-b-c  
Unit 3b

Fig. 3. A composite regional seismic cross section oriented WNW-ESE illustrating the Triassic – Earliest Cretaceous pre- and syn-extensional sequence (purple). Horizon K0 corresponds to the end of rifting and Cretaceous – Recent passive margin sequences in the Exmouth Plateau are shown in yellow, blue, brown and green. See Figure 1 for the location of the seismic transect.



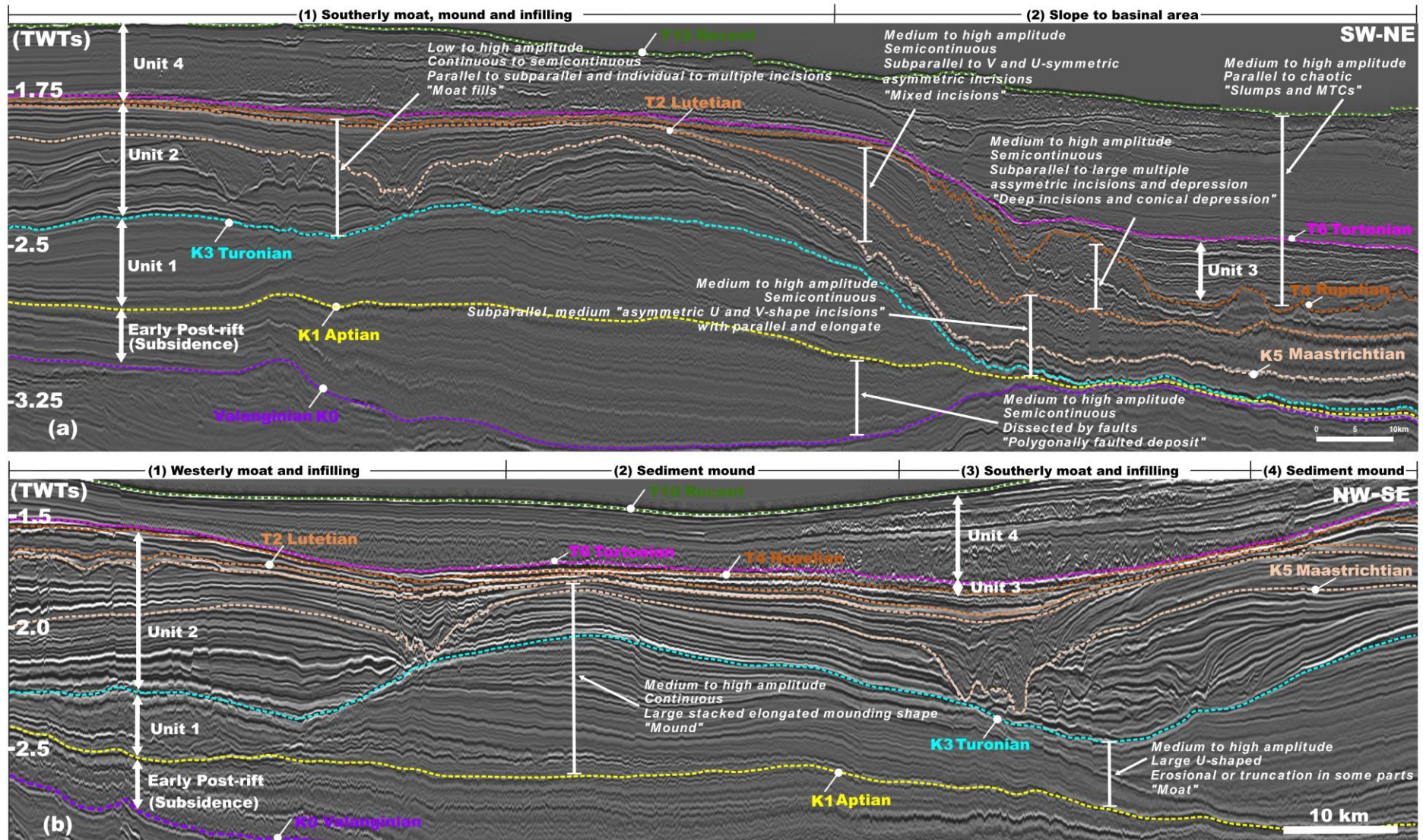


Fig. 4. SW-NE (a) and SE-NW (b) seismic sections illustrating the different seismic facies each of the seismic-stratigraphic units that comprise the Valanginian – Present day passive margin sequence. These seismic facies are correlated with velocity variations in subsequent figures. See Figure 1 on inset map b for the location of the seismic sections.

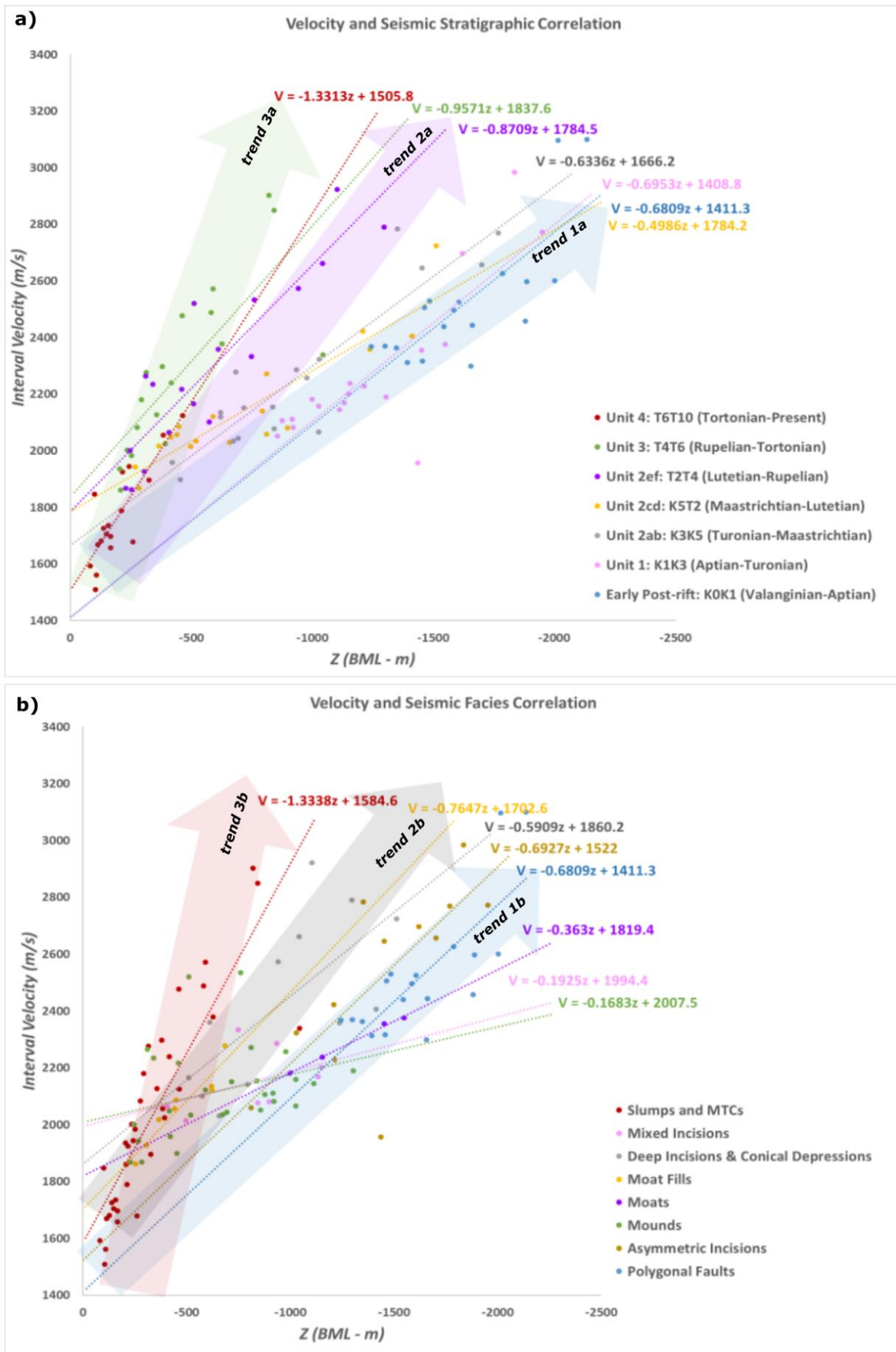


Fig. 5. a, b) Interval velocity cross plots classified according to seismic stratigraphic units (a) and seismic facies (b). Z: depth, BML: Below Mud Line.

a) No	Stratigraphic Units	$V = Kz + V_0$	b) No	Seismic Facies	$V = Kz + V_0$
1	Unit 4: T6T10 (Tortonian-Present)	$V = -1.3313z + 1505.8$	1	Slumps and MTCs (Units 3 and 4)	$V = -1.3338z + 1584.6$
2	Unit 3: T4T6 (Rupelian-Tortonian)	$V = -0.9571z + 1837.6$	2	Deep Incisions & Conical Depressions	$V = -0.5909z + 1860.2$
3	Unit 2ef: T2T4 (Lutetian-Rupelian)	$V = -0.8709z + 1784.5$	3	Asymmetric Incisions	$V = -0.6927z + 1522$
4	Unit 2cd: K5T2 (Maastrichtian-Lutetian)	$V = -0.4986z + 1784.2$	4	Mixed Incisions	Unit 2 $V = -0.1925z + 1994.4$
5	Unit 2ab: K3K5 (Turonian-Maastrichtian)	$V = -0.6336z + 1666.2$	5	Moat Fills	
6	Unit 1: K1K3 (Aptian-Turonian)	$V = -0.6953z + 1408.8$	6	Moats	Unit 1 $V = -0.363z + 1819.4$
7	Early Post-rift: KOK1 (Valanginian-Aptian)	$V = -0.6809z + 1411.3$	7	Mounds	
			8	Polygonal Faults (Early Post-rift)	$V = -0.6809z + 1411.3$

Table. 2.  $V_0$ - $K$  functions for each of the stratigraphic units (a) and seismic facies (b). Velocity gradient  $K$  increase from older to younger sequence, with a significant decrease in Unit 2cd. In terms of seismic facies, the greatest variations in  $K$  values occur in the heterogeneous seismic facies that make up Unit 2, implying significant lateral velocity variations within this unit.  $Z$ : depth in negative values, BML: Below Mud Line.



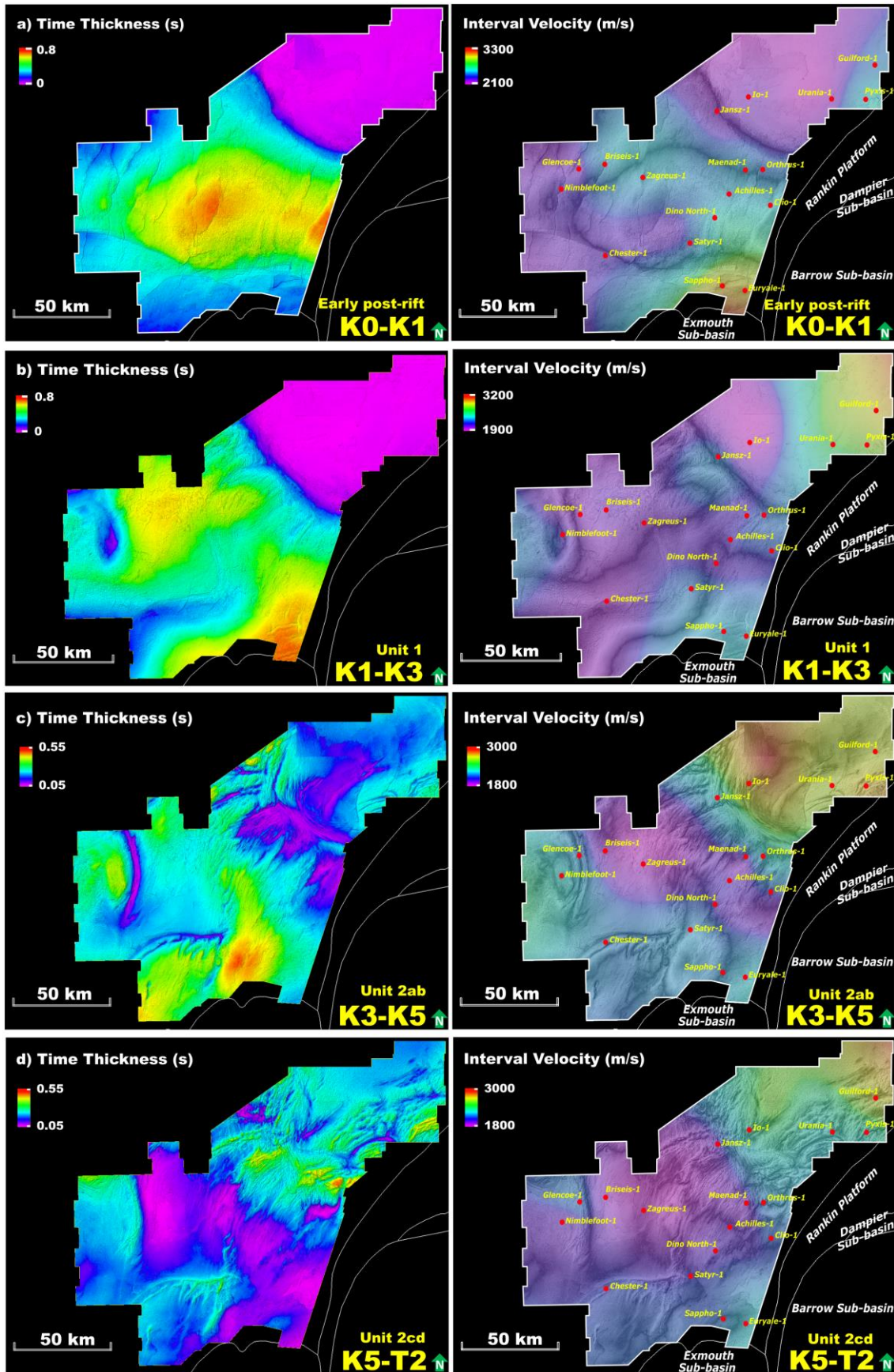


Fig. 6. Maps illustrating time thickness (left side) and interval velocity (right side) from Early Post-rift to Unit 2cd. The interval velocity maps are overlain on the thickness maps. K0K1: Early Post-rift, K1K3: Unit 1, K3K5: Unit 2ab, K5T2: Unit 2cd.

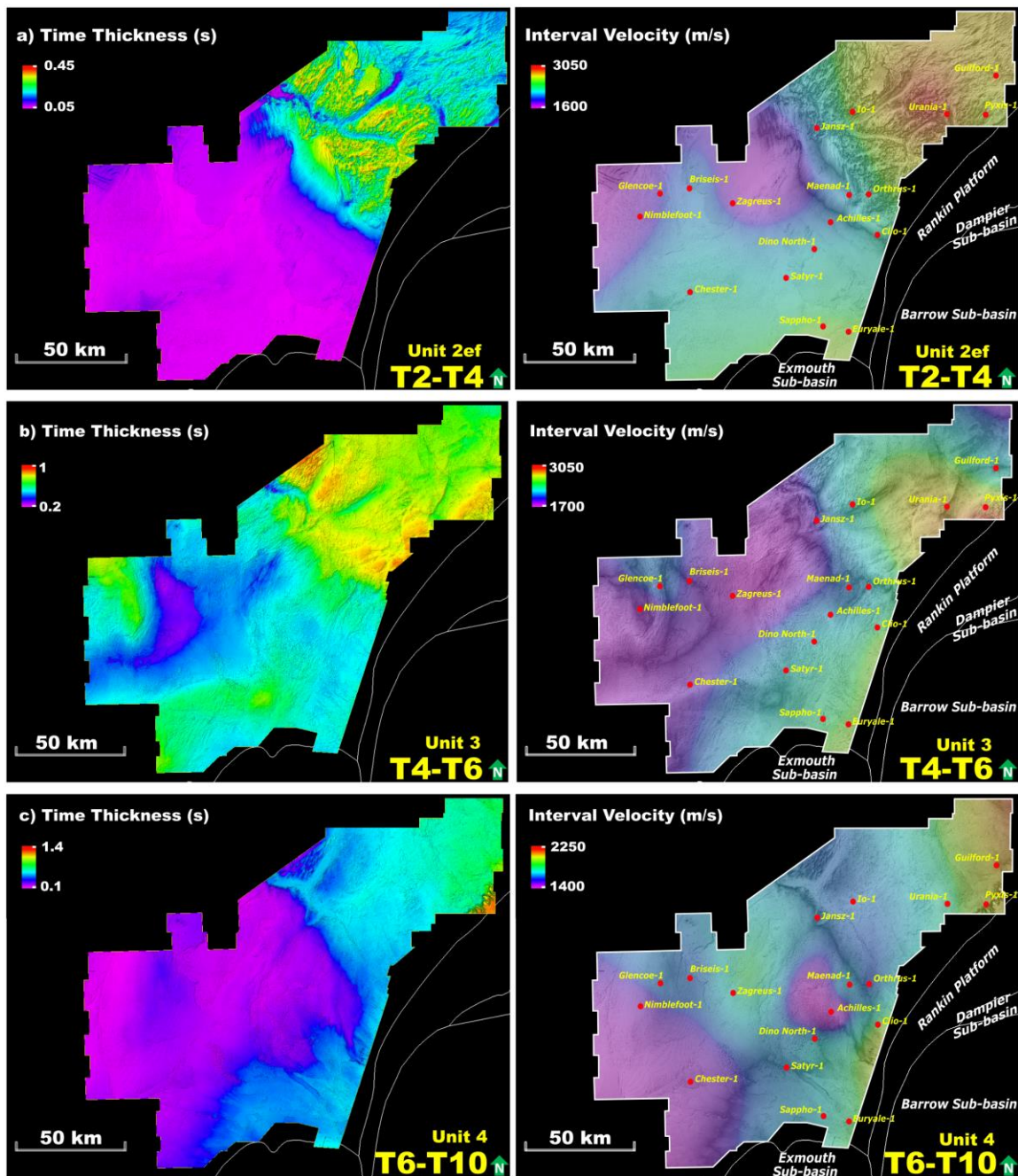


Fig. 7. Maps illustrating time thickness (left side) and interval velocity (right side) from Unit 2ef to Unit 4. The interval velocity maps are overlain on the thickness maps. T2T4: Unit 2ef, T4T6: Unit 3, T6T10: Unit 4.

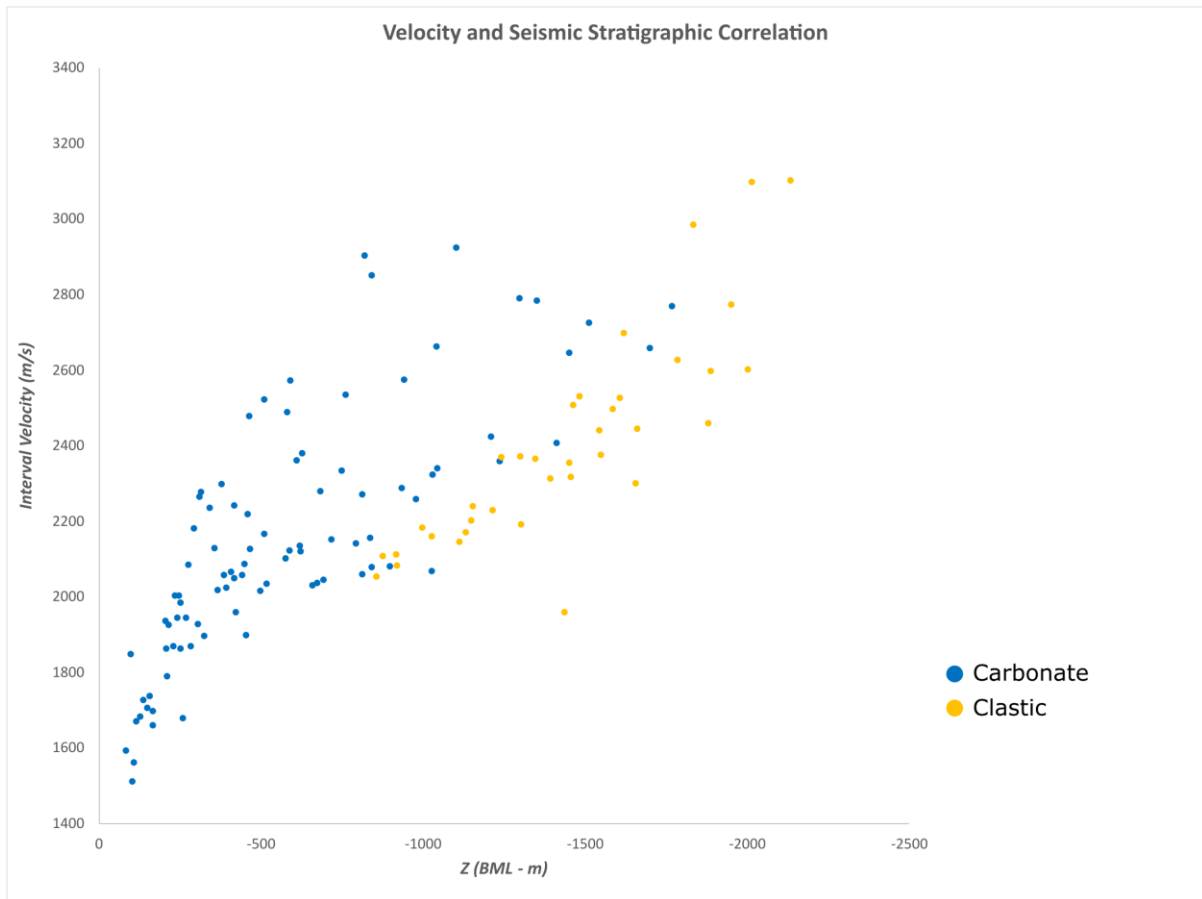


Fig. 8. Interval velocity cross plots as a function of lithology. Clastic sediments are shown in blue and carbonate sediments in yellow. Generally, the carbonate sediments have higher interval velocities than the clastic sediments. Z: depth, BML: Below Mud Line, Yellow: Clastic sediments, Blue: Carbonate sediments.



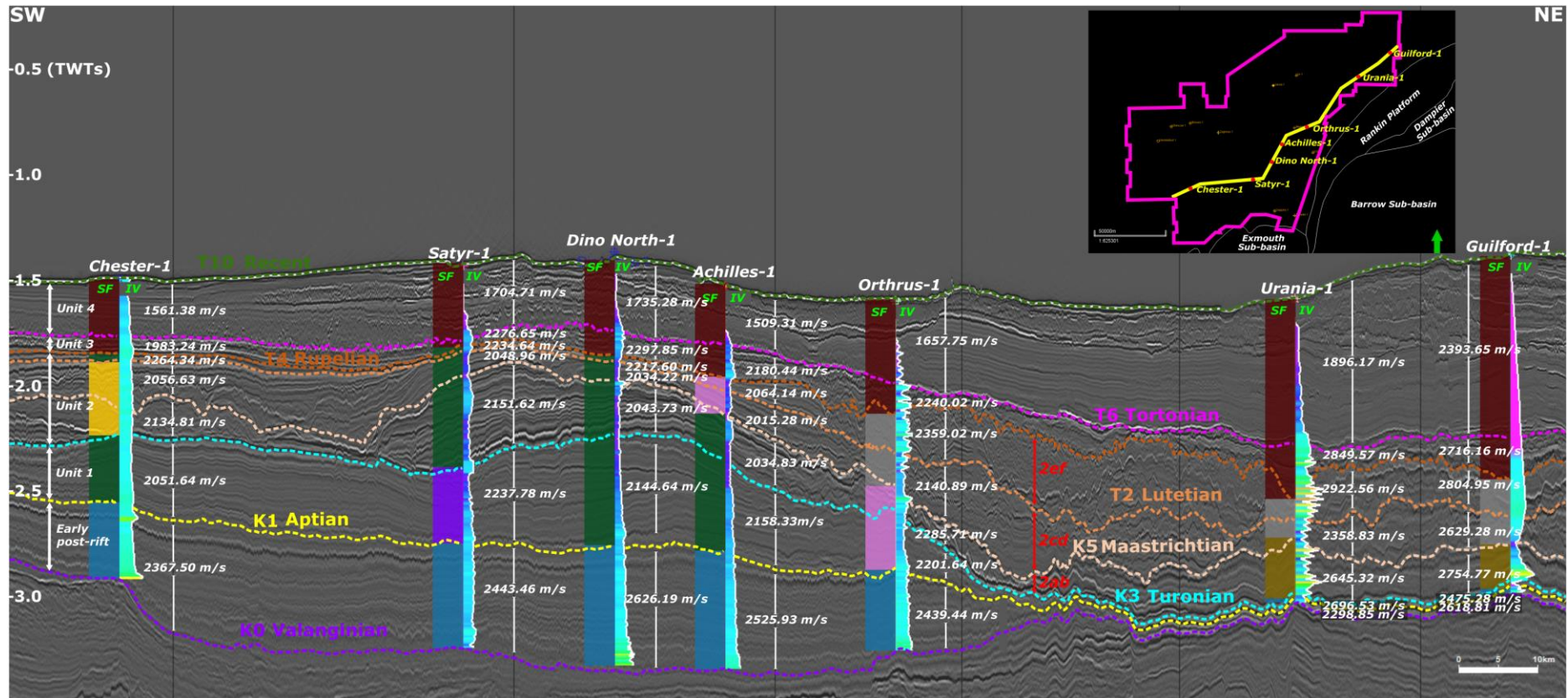


Fig. 9. Seismic profile overlies with wells section showing seismic facies (SF) and interval velocity (IV) variation between the main seismic stratigraphic boundaries. Wells location is seen on the map view. Key to seismic facies: Blue: Polygonal Fault, Purple: Moats, Green: Mounds, Yellow: Moat Fills, Pink: Mixed Incisions, Brown: Asymmetric Incisions, Grey: Deep Incisions and Conical Depressions, Red: Slumps and MTCs.

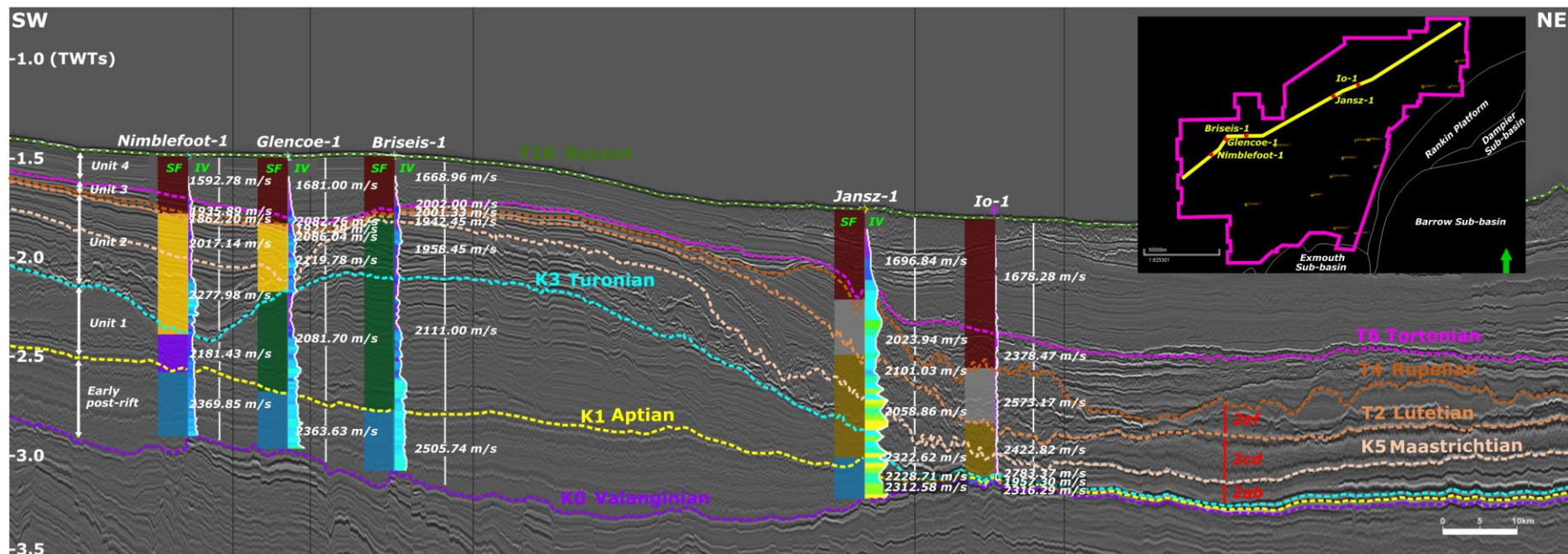


Fig. 10. NE-SW oriented seismic section showing seismic facies (SF) and interval velocity (IV) variation between wells and within the main seismic stratigraphic sequences in the SE of the study area. Line and well locations are shown on the inset map. Key to seismic facies: Blue: Polygonal Fault, Purple: Moats, Green: Mounds, Yellow: Moat Fills, Brown: Asymmetric Incisions, Grey: Deep Incisions and Conical Depressions, Red: Slumps and MTCs.



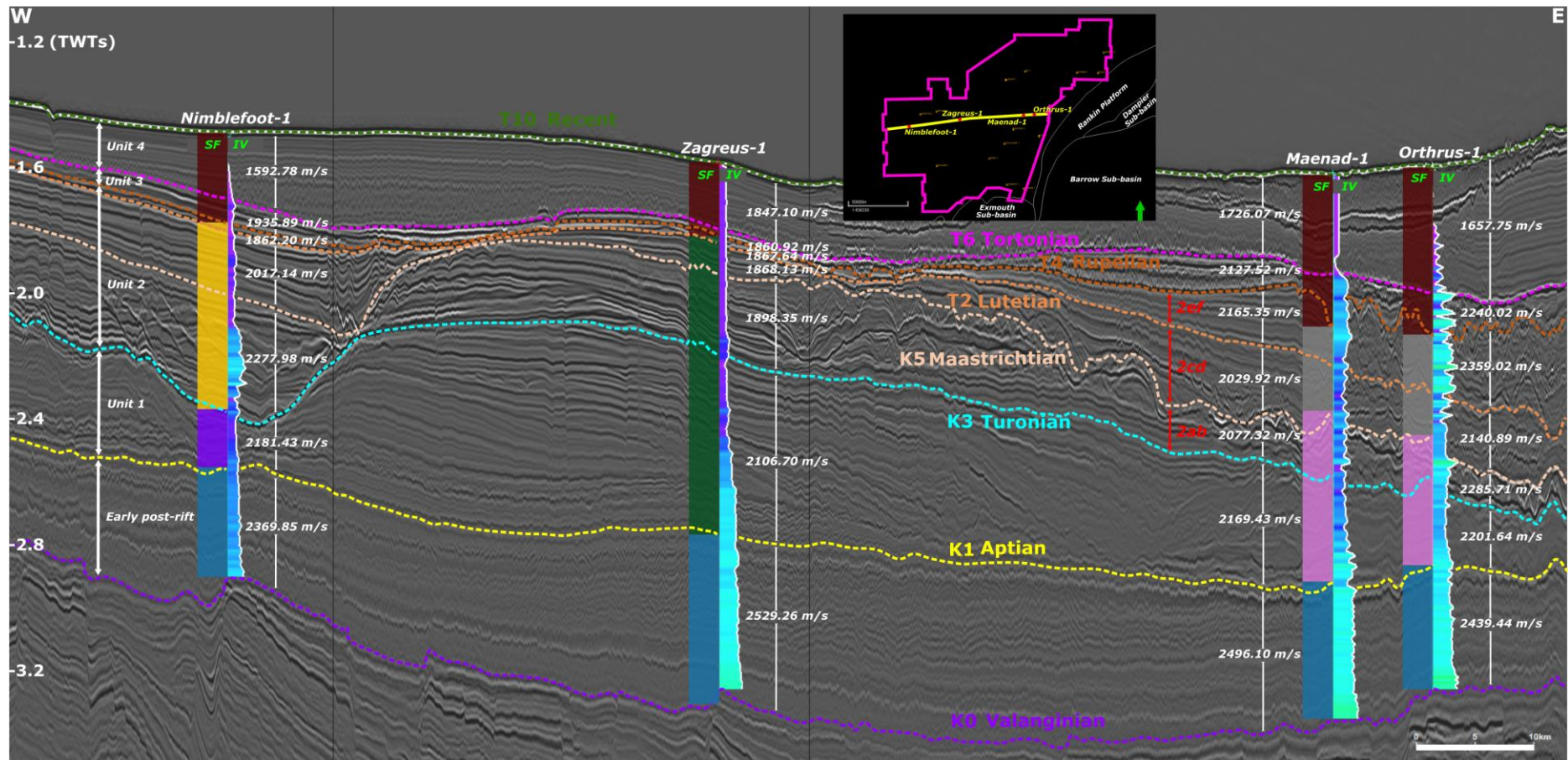


Fig. 11. NE-SW oriented seismic section showing seismic facies (SF) and interval velocity (IV) variation between wells and within the main seismic stratigraphic sequences in the NW of the study area. Line and well locations are shown on the inset map. Key to seismic facies: Blue: Polygonal Fault, Purple: Moats, Green: Mounds, Yellow: Moat Fills, Pink: Mixed Incisions, Grey: Deep Incisions and Conical Depressions, Red: Slumps and MTCs.

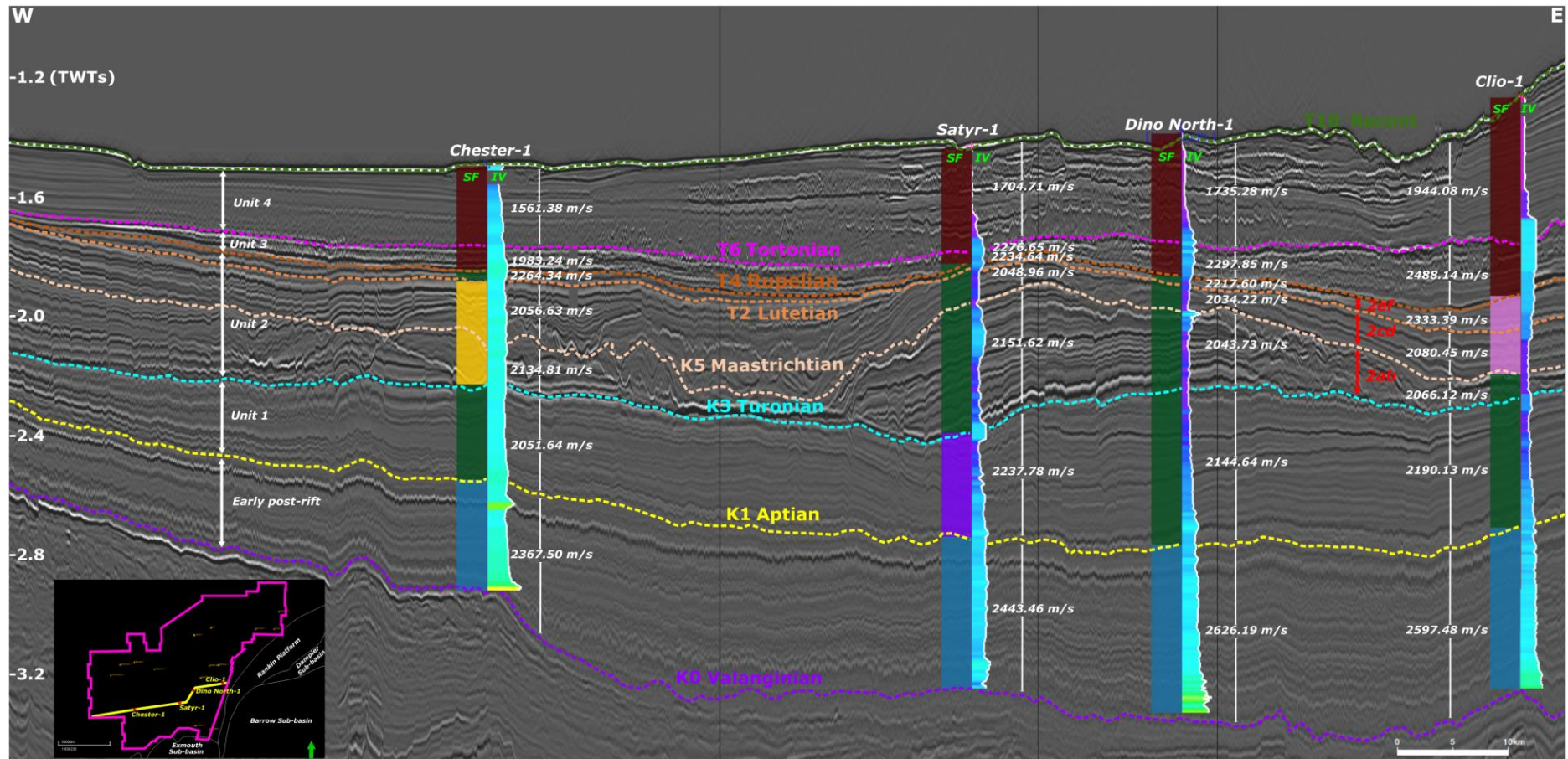


Fig. 12. E-W oriented seismic section showing seismic facies (SF) and interval velocity (IV) variation between wells and within the main seismic stratigraphic sequences in the south of the study area. Line and well locations are shown on the inset map. Key to seismic facies: Blue: Polygonal Fault, Purple: Moats, Green: Mounds, Yellow: Moat Fills, Pink: Mixed Incisions, Red: Slumps and MTCs.



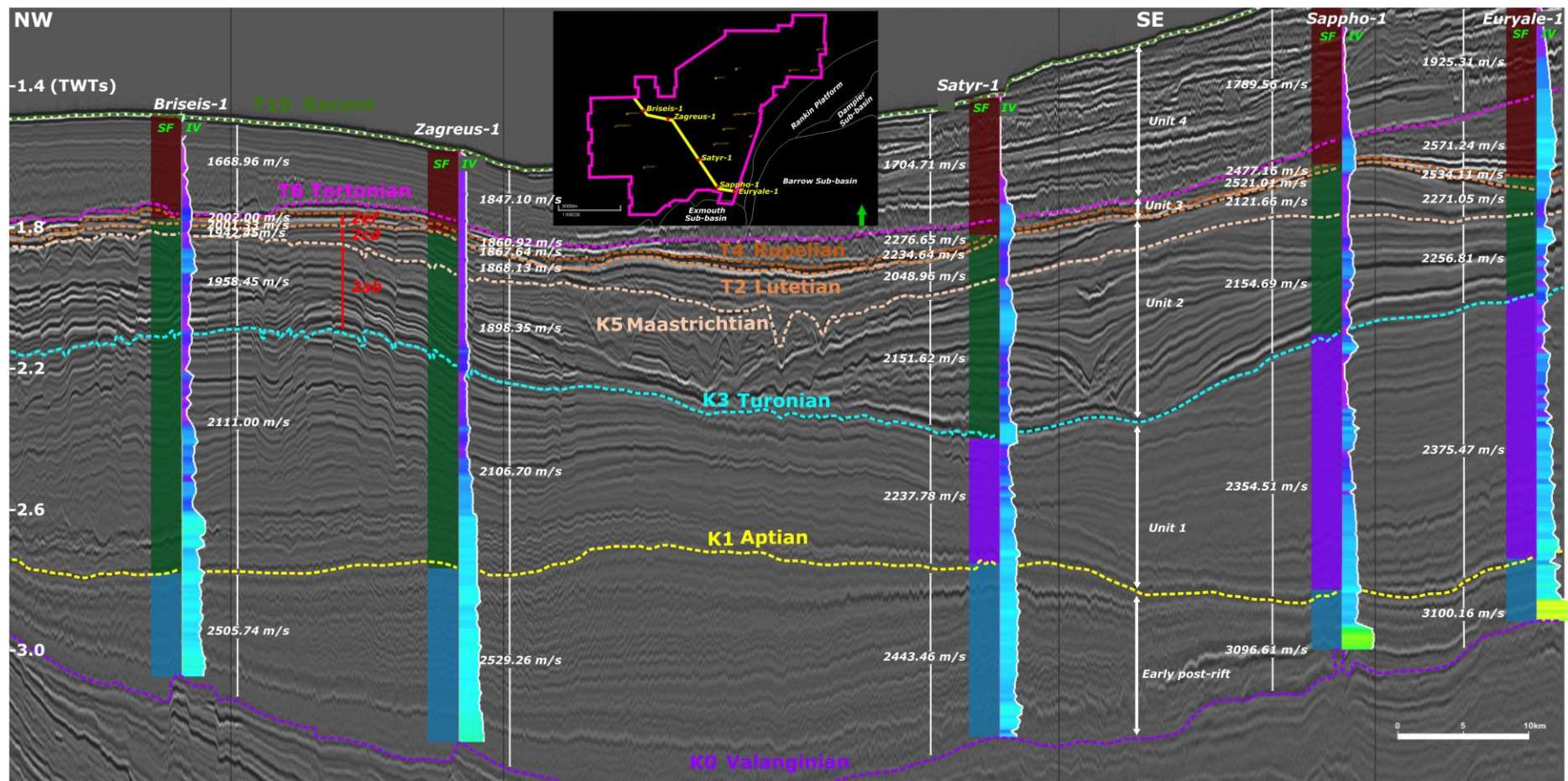


Fig. 13. NW-SE oriented seismic section showing seismic facies (SF) and interval velocity (IV) variation between wells and within the main seismic stratigraphic sequences in the south of the study area. Line and well locations are shown on the inset map. Key to seismic facies: Blue: Polygonal Fault, Purple: Moats, Green: Mounds, Red: Slumps and MTCs.

---

*Chapter Five:*  
*Summary, Discussion, and Implications*

---

## Chapter Five: Summary, Discussion, and Implications

---

### 1. Summary

This study presents a detailed seismic stratigraphic framework for the North Carnarvon Basin that sheds light on the evolution of passive margin sedimentary processes that developed following Valanginian breakup (Fig. 1). The analysis is based on 2D and 3D seismic interpretations, which have been consistently correlated with well data to establish regionally correlatable seismic stratigraphic units. This reveals the following history of the margin:

#### 1.1. *Early post-rift sequence (Valanginian – Aptian)*

After Valanginian breakup, a significant transgression occurred during the remainder of the Valanginian through to the Aptian, resulting in deposition of a relatively thin sequence (up to 150 m) across the Exmouth Plateau. This sequence onlaps onto tilted fault blocks in the west and north of the Plateau. Key depocentres are observed in the Dampier sub-basin and in the centre of the Exmouth Plateau, forming a sediment sag outboard of the underlying Lower Barrow Shelf Edge. This sequence includes a subtle lobe that formed the Upper Barrow shelf on the northwest margin of the Exmouth sub-basin. Throughout this interval, there are sequences with parallel reflectivity, polygonal faults, and low angle aggradational and progradational clinoforms (Fig. 2).

#### 1.2. *Unit 1 (Aptian – Turonian)*

Unit 1 sits conformably above the underlying sequence and is thicker than the preceding interval across most of the Exmouth Plateau. The sequence is laterally uniform, with onlaps onto rotated fault blocks in the northwest, suggesting relatively stable depositional conditions. This is correlated to further marine transgression in the NCB. However, in the southeast, particularly over the Exmouth sub-basin and the middle of the Exmouth Plateau, the sequence forms stacked gently mounded and wavy beds, indicating the impact of submarine currents and early sediment mound formation. These currents formed as the separation between Greater India and Australia (Fig. 3) increased, suggesting that they are



associated with increased ocean circulation that developed to the north in the Neo Tethys Ocean. The top of this unit marks a shift from fine-grained clastic to carbonate sediments.

### 1.3. *Unit 2 (Turonian – Rupelian)*

Unit 2 is the thickest sediment interval with polygonal faulting in the northern and western regions, indicative of a continuing low-energy depositional system on this part of the margin. However, the central Exmouth Plateau exhibits stacked incisions and bottom current deposits, suggesting energetic bottom currents, persisted in this part of the NCB. This corresponds to a significant drifting away of Greater India from Australia, as well as breakup and separation of Australia from Antarctica (Fig. 4). As the sequence evolved, these incisions transform into subparallel and parallel beds, reflecting decreased current energy. Specifically, in the central Exmouth Plateau, Unit 2 is the continuation of an 80-million-year period (beginning in the Aptian) that witnessed the significant development of sediment mounds, moats, and related structures. Large-scale mounds and moats originated in the southwest during the Aptian – Cenomanian but diminished towards the northeast. From the Turonian – Lutetian, mounds evolved into aggradational stacked formations, while moats were filled by smaller-scale mounds and multiple incisions. Subsequent infilling of moats and reduced mound expression led to basin floor filling in the northwest. Slope progradation persisted until the Rupelian, and coincided with the development of conical depressions and erosional incisions filled with chaotic slumps and MTCs that became more widespread in subsequent sequences.

### 1.4. *Unit 3 (Rupelian – Tortonian)*

Unit 3 signifies the end of bottom current activity and the beginning of progradational carbonate clinoforms, primarily in the northern Dampier sub-basin and Rankin Platform. These sequences resulted in the development of semi-chaotic deposits outboard of the clinoforms that onlap and downlap onto Unit 2, limiting the extent of this unit to the west and southeast. The chaotic sequence is associated with slumps and MTCs, resulting from slope instability in the clinoforms domain. The cessation in bottom current activity may result from further reorganisation of circulation patterns, resulting from the further drift of Australia

away from Antarctica, while the development of MTCs might have been enhanced by the onset of convergence with Eurasia (Fig. 5).

#### *1.5. Unit 4 (Tortonian – Present)*

Unit 4 sees a more pronounced development of shelf margin clinoforms, primarily progradational, but with some aggradational component. There is also an increased prevalence of chaotic sediments across the Exmouth Plateau, featuring widespread slumps and MTCs. The occurrence of slumps and MTCs is linked to slope instability, corresponding to the elevated slope gradients of the clinoforms at the shelf slope break, the formation of the Exmouth Plateau Arch, Neogene compression, and the deposition of fine-grained sediments, which provide detachment surfaces for the development of MTCs (Fig. 6).

#### *1.6. Seismic velocity in complex structures*

The complicated seismic stratigraphic framework shows lateral and vertical seismic facies variation. This reveals a complexity of velocity distribution. Velocity trends are distinguished by lithological transitions between the change from clastic to carbonate sediments after the Turonian. Clastic sediments in the early post-rift sequence and Unit 1 are characterised by parallel reflector sequences, polygonal faults and initial sediment mounds that reflect the effects of burial and compaction, while carbonates are more likely subject to cementation processes that can be more variable with depth. The greatest velocity variation occurs in Unit 2, owing to the presence of geological features such as mounds, moats and moat fills in the southwest, and asymmetric incisions as well as deep incisions and conical depressions in the northeast. These variations are further expressed by slumps and MTCs in Units 3 and 4. However, the velocity distribution between the southwest and northeast portions of Unit 2 is substantially different, with higher seismic velocities in the northeast.

## 2. Discussion

### 2.1. *Lithostratigraphic versus seismic stratigraphic correlations*

The regional seismic stratigraphic framework of the NCB presented in this thesis reveals a complex sequence of stratigraphic boundaries within the passive margin interval. Overall, 16 regional seismic horizons have been identified that are characterised by prominent and consistent seismic facies. Based on this, the sequence has been classified into four Units that reflect the evolution of sedimentary processes on the margin, revealing a period of persistent bottom current activity between the Aptian and Rupelian (Units 1 and 2), as well as a widespread development of slumps and MTCs across almost the entire area of the Exmouth Plateau from the Rupelian to the Present Day (Units 3 and 4). The sub-units that comprise each unit reflect variations in seismic facies, both laterally and vertically, and the presence of multiple unconformities, which are indicative of heterogeneous sedimentary processes. The main horizons align with the main boundaries that were identified by Longley et al. (2002) and Marshall and Lang (2013) and broadly correspond with the lithostratigraphic formation boundaries observed in well data (Fig. 1). However, the lithostratigraphic nomenclature relies heavily on descriptions of lithology from well data (mostly cuttings), which does not capture the complexity of seismic facies variations that define the seismic stratigraphic framework. This nomenclature results in inconsistent labelling of formation markers in individual wells, further complicating the correlation process. The regional seismic stratigraphic correlation provides a comprehensive correlation particularly from the Late Cretaceous (Unit 2) to Recent and includes some detail missing from Longley et al. (2002) and Marshall and Lang (2013).

This has important implications for paleoenvironmental reconstructions. Most of the focus of the studies in the NCB is on primary exploration target intervals in the Triassic – Early Cretaceous and there is very limited information from the passive margin sequences. The only published reconstructions are from Bradshaw et al. (1988) and Apthorpe (1988), with minor modifications in Longley et al. (2002) and Mory (2023). These show very simple paleoenvironmental maps based on limited well and seismic data available at that time, most of which was concentrated closer to the shore, with less constraint further offshore (Fig. 7). Bradshaw et al. (1988) suggest a gently sloping margin, with water depths increasing from less than 200 m in the study area, to greater than 200 m on the outer parts of the margin in late Early Cretaceous (equivalent to Unit 1; Fig. 7a). While the basis on which these water

depths are assigned by Bradshaw et al. (1988) are unclear, we interpret this as the initial phase of growth of sediment mounds and the early stage of bottom current activity, associated with changes in oceanic circulation brought about the separation of Greater India and Australia. This change in circulation is also recognised by Bradshaw et al. (1988), based on the widespread deposition of the Windalia Radiolarite. Apthorpe (1988) shows maps for the early Palaeocene (~Unit 2c; Fig. 7b) and early to middle Eocene (~Unit 2e and f; Fig. 7c), showing the position of outer shelf and slope settings based on palynological data immediately along strike to the NE of the study area. While the outer shelf and slope are shown as areas of uniform, fine grained sedimentation, the emergent “islands” indicated by Apthorpe (1988) may instead be places where there is an unconformity and missing sequences, as might be expected in areas where bottom current activity has caused erosion. For the Oligocene Bradshaw et al. (1988) shows a uniform deepwater environment, outboard of a narrow shelf. This map is equivalent to very top sequence of Unit 2 (~Unit 2f or the lower part of Unit 3; Fig. 7d). Again, their interpretation does not describe significant erosional structures that are shown in this research, e.g., stacked multiple deep incisions and conical depressions, erosional areas infilled by stacked slumps and MTCs. The seismic facies maps presented in Chapter 2 provide a more comprehensive picture of the depositional environments that were present on the margin at this time.

## 2.2. *The onset of bottom current activity*

The seismic stratigraphic framework presented in Chapters 2 and 3 of this thesis recognises the onset of bottom current activity in the NCB as occurring in the Aptian, in a passive margin setting. However, Mantilla et al. (2022) have re-interpreted a large Tithonian to early Valanginian, asymmetric mounded deposit on the Exmouth Plateau, associated with the Lower Barrow Group, as a deepwater sediment drift. This would imply an earlier onset of bottom current activity, during the late stages of rifting and break-up. Initially, these sediments were interpreted as a deltaic system, based on the presence of clinoforms observed on seismic data (Tait, 1985). However, Paumard et al. (2018) reinterpreted it as a progradational shelf-slope margin, taking into account the slope angle and height of the clinoform foresets. The tops of the clinoforms are interpreted as shallow water, as inferred

from the facies present in reservoirs situated on the shelf part of the system. The height of the clinoforms suggests water depths of up to 550 m on the basin floor.

Alternatively, Mantilla et al. (2022) liken the clinoforms to those formed in “delta drifts”, a somewhat confusing term adopted by Eberli and Betzler (2019) to describe laterally migrating bottom current deposits that have a superficial resemblance to deltaic clinoforms, but which form in a different (deep water) depositional environment. Mantilla et al. (2022) also base their interpretation of the Lower Barrow Group as an asymmetric mounded drift on the height and dip of the clinoform foresets, although their observations appear to overlap with typical values that they quote for shelf edge systems (evidence cited by Paumard et al. (2018) for their shelf edge interpretation). They also site subtle landward dips of the topsets as evidence for a mounded geometry, and although they rule out later tilting of the margin as an explanation for this, folding associated with the more complex inversion of the Exmouth sub-basin may be a factor. Careful structural restorations are required to determine the validity of this point. Moreover, Mantilla et al. (2022) reference a lack of evidence for fluvial systems or rivers to support a deltaic origin. However, this seems to overlook the evidence presented by Paumard et al. (2018) for shallow marine facies on the topsets and the suggestion of multiple small fluvial input systems supplying a broad shelf rather than a single large river supplying a point source delta. Rohrman (2015) argues that the primary sources of this sediment was Late Jurassic / Early Cretaceous uplift and denudation on the southwestern margin of the NCB caused by the presence of a large mantle plume. In addition, the presence of large turbidite fans in front of the Barrow shelf edge, which provide the reservoirs for fields such as the Scarborough gas field (Paumard et al., 2018), is also consistent with the shelf interpretation and provides an explanation that is more consistent with the overall paleogeographic setting than that provided by Mantilla et al. (2022).

### *2.3. Bathymetric setting of bottom current deposits*

Even if bottom current activity did initiate in the latest Jurassic / earliest Cretaceous (Mantilla et al. 2022), there was a period of 10 to 15 Myr between the Valanginian and Aptian when the newly formed passive margin was dominated by thermal subsidence, prior to the onset of bottom current activity in the Aptian recorded in this study. Paleoenvironmental maps (Apthorpe, 1988; Bradshaw et al., 1988; Mory, 2023) suggest that these bottom



currents operated on a c. 500 km wide gently sloping ramp-style margin (*sensu* Van Wagoner et al., 1988). However, these reconstructions were based on much less seismic data than is available today (Bradshaw et al., 1988) and on wells that are mainly located in proximal settings (Apthorpe, 1988). More recent tectonic reconstructions by Scotese & Wright (2018) include paleobathymetric reconstructions. As these are based present day bathymetry, modified according to published lithofacies and paleoenvironmental information for each time step, they also show a broad ramp-style margin, with water depths up to c. 3,000 m on the outer part of the margin, comparable to present day bathymetry (Fig. 8). However, this still leaves the question as to whether or not there was any bathymetric relief within this wide margin that might have influenced bottom current activity. As previously noted, the Exmouth mantle plume occurred in the Late Jurassic, causing denudation and tectonic uplift in the southwest of the NCB (Rohrman, 2015). This resulted in decompression melting, volcanic margin magmatism, and eventually in Valanginian breakup. The distribution of unconformities associated with breakup suggests that this uplift was confined to the southwest of the NCB and declined after the Hauterivian (Reeve et al., 2022), as thermal decay set in, resulting in subsidence and normal ocean spreading. Thus, by the time bottom current activity commenced, and in the area where it occurred, it is unlikely that there was any significant remnant bathymetry associated with the Exmouth Plume. This is consistent with the observation that the occurrence of igneous rocks is confined to areas west and southwest of the parts of the Exmouth Plateau subsequently dominated by bottom current activity, and that the igneous rock are almost entirely confined to the pre-Valanginian sequence (Curtis et al., 2022).

An alternative source of bathymetric relief is tectonic inversion which primarily affected the Exmouth and Dampier sub-basins to the south and south-west. (Longley et al., 2002; Norvick, 2002; Jablonski and Saitta, 2004). This is evidenced by the emergence of the Novara Arch in the early Santonian and the Resolution Arch at the start of the Campanian (Tindale et al., 1998). This post-dates the onset of bottom current activity, but the development of these structural highs may have modified current activity during the deposition of Unit 2. Mapping of these units, and the sedimentary structures that they contain from the study area towards the inverted parts of the basins will be required to establish if there is any relationship. The Exmouth Arch, which forms a prominent feature on the present-day seabed, appears not to

have formed until after the Oligocene (Chapter 2) and hence post-dates the bottom current deposits.

It should however be noted that the initial development of large-scale mounds during the Aptian did occur inboard of fault blocks that remained emergent at this time (Fig. 3c). While remnant relief was likely of the order of only a few 10's of metres by the Aptian (Rohead O'Brien, 2023), this may have been sufficient to focus current activity during the early stages of mound formation. Otherwise, there was only minor bathymetric variation on the wide gently sloping ramp-style margin on which the bottom current deposits described in this thesis formed. This contrasts with typical models of contourite deposits which describe settings adjacent to slopes that separate shallow shelves from deep basins (Stow et al., 2002; Rebesco et al., 2014; Fig. 4a-d in Chapter 1). A consequence of such a bathymetric profile is the interaction between down-slope (gravitational) currents and along-slope (contourite) currents (Shamugam, 2003; Stow, 2011; Rebesco et al., 2014; Fonesu et al., 2020). This gives rise to the concept of mixed systems in which turbidites can be reworked into deposits such as plastered drifts along slopes and elongate drifts at the base of the slopes, separated from them by moats (see Fig. 4c and d in Chapter 1).

The shelf-slope-basin models for mixed turbidite-contourite deposits are reflective of Atlantic-type margins where such geometries exist and where most studies of contourite deposits are focused. Rodrigues et al. (2022) introduced a classification system for such deposits which distinguishes between contourite-dominated systems, turbidite-dominated systems and synchronous turbidite-contourite systems, and further distinguishes between each of these systems in proximal and distal settings (see Fig. 4 in Chapter 1). Contourite-dominated systems develop where bottom current velocity and persistence dominates over turbidity current velocity and persistence. This tends to occur in proximal settings where slope gradients are gentle (e.g. Gulf of Cadiz, SE Argentina, and SW Portugal; Rodrigues et al., 2022) and distal settings where there is limited down-slope sediment supply (e.g. NE Rockall Trough, middle US Atlantic margin; Rodrigues et al., 2022).

The setting in which the NCB bottom current deposits formed is most comparable to the proximal low gradient slopes in which contourite-dominated systems develop. However, there are significant differences between the types of deposit described by Rodrigues et al. (2022) and those observed in the NCB. Based mainly on observations for the Gulf of Cadiz,

Rodrigues et al. (2022) describe elongated mounds or plastered drifts that form parallel to slopes which are cut by low sinuosity V-shaped submarine channels that change into U-shaped channels further down-slope. Material from fine-grained turbidity currents that flow down and erode these channels are redistributed by bottom currents, which also rework any accumulated turbidites. Alternatively, channels may terminate in moats adjacent to slope-parallel mounds and drifts, allowing ponded turbidites to accumulate, which may also be reworked by contourite currents. If these currents interact with the seafloor, secondary features like contourite terraces and sediment waves are formed, as seen in SE Argentina and SW Portugal (Rodrigues et al., 2022). In distal regions, contourite-dominated systems formed along the continental rise and abyssal plains are characterized by sheeted or mounded drifts with submarine channels that may form small fan lobes within the drifts or deposit further seaward, bypassing the large contourite morphologies. This has been observed in the NE Rockall Trough and the middle US Atlantic margin (Rodrigues et al., 2022). Bottom currents interact with the turbidity flows, stripping the fine-grained sediments carried in suspension or winnowing the turbidite deposits near the submarine channels.

In contrast to the types of deposit described by Rodrigues et al. (2022) (Fig. 9), there are no recorded occurrences of turbidite deposits in the Aptian to Rupelian sequence of the NCB, and no turbidite channel or canyon systems have been mapped from the extensive seismic data that covers the basin. Consequently, the type of reworked deposit described by Rodrigues et al. (2022) are not observed. Instead, sediment mounds are aggradational, rather than elongate, laterally migrating drifts. The absence of turbidites is a consequence of the laterally extensive low gradients that dominate the NCB margin and there is no bathymetric profile that allows distinction between currents flowing parallel to the slope (contour currents) and turbidity currents flowing perpendicular to the margin as depicted in the Rodrigues et al. (2022) model. Instead, the currents that impinged on floor of the NCB were most likely reworking hemipelagic deposits, rather than material from turbidity flows (Fig. 9a).

Although there is some debate about the definition and use of the term of “contourite” (Shanmugam, 2022; Rodrigues et al., 2022). Lovell and Stow (1981) describe contourite deposits as the product of persistent currents that flow consistently along a slope in relatively deep water, irrespective of the origin of the current, while the original definition of Hollister

(1967) specifically links contourite deposits to currents with a thermohaline-induced geostrophic origin. In the absence of significant bathymetric relief “bottom current deposit” appears to be a more appropriate term than “contourite” to describe the deposits in the NCB. However, Shanmugan (2022), recognises that in addition to thermohaline-induced geostrophic currents, bottom currents may also be wind-driven, driven by deep-water tides, or driven by internal waves and tides. Although Shanmugan (2022) still refers to these as currents that operate at the shelf break, this does raise the question of the origin and mechanistic link between the increasing separation of Australia, India and Antarctica, changes in thermohaline circulation patterns and the nature of the currents that impinged on the NCB, as discussed in the next section.

#### *2.4. Oceanic circulation around Australia between the Valanginian and Present Day*

The Climate Archive ([climatearchive.org](http://climatearchive.org)) presents reconstructions of ocean currents, drawing on the paleogeographic reconstructions of Scotese and Wright (2018) and the climate model simulations of Valdes et al. (2021). This provides additional information to help assess the impact of circulation patterns on the NCB developed in Chapter 3. During the Valanginian (~138 Ma), following initial separation of Greater India from Australia, there was only a narrow and restricted ocean basin to the west of Australia, but the large Neo Tethys Ocean was present to the north separating Greater India and Australia from Eurasia but connected to the Pacific Ocean to the east and restricted to the west by the position of Africa. The temperature gradient, transitioning from warm in the north to cold in the south, resulted in an anti-clockwise circulation pattern which generated significant westward currents, similar to today's South Equatorial Current (SEC; Fig. 10a) in the north of Neo Tethys Ocean and eastward flowing currents, similar to the Eastern Gyral Current (EGC) along the northern margin of Greater India and Australia. However, Scotese and Wright (2018) suggest that the Argoland terrane, which rifted from the northern margin of Australia at the start of the late Jurassic, remained emergent and relatively close to the Australian margin, sheltering it from these currents. This reduces the likely impact of bottom current activity in the NCB during this time period which was instead dominated by subsidence and transgression.

By the Aptian (~123 Ma; Fig. 10b), the EGC is shown to have intensified and moved closer to the northern margin of Australia. This, combined with the subsidence of the

Argoland terrane may have allowed currents to impinge on the NCB, corresponding to the initial creation of sediment mounds and moats at this time. Although separation of Greater India and Australia increased, creating a restricted oceanic gateway in the west, it was not until the Turonian that there was sufficient separation between Greater India and Antarctica which allowed a current equivalent to the Western Australian Current (WAC) to develop along the western margin of Australia (~94 Ma; Fig. 10c). Although this corresponds to start of Unit 2, a period of sustained bottom current activity in the NCB, the climate reconstructions also show a waning of the EGC and its migration away from the northern margin of Australia, associated with the northwards migration of the SEC, which is likely related to the northward migration of the steepest gradient in sea water surface temperatures and an intensification of this current in the narrowing gap between Greater India and Eurasia. The distribution of bottom current deposits, extending from the SW corner of the NCB, across a zone confined to the central parts of the Exmouth Plateau (Fig. 4), may be more consistent with a branch of the WAC impinging on the margin, rather than the EGC, which would more likely affect the outboard parts of the margin. The WAC may contain both surface and deep currents, including winds and tides, as well as the equivalent of the Leeuwin Undercurrent (see Fig. 2 in Chapter 3). While these currents may play a significant role in shaping the development of bottom current deposits during this stage, as the bottom currents weaken, the style of deposits changes. The growth of the mounds became more gradual and slows down, while the moats narrow. This leads to an increase in the complexity of moat filling and results in the formation of smaller, more confined mounds.

This configuration remains the same until the commencement of seafloor spreading between Australia and Antarctica at the end of the Maastrichtian (~66 Ma; Fig. 10d). This, coupled with Australia's swift northward drift from Antarctica starting from the Eocene, might have allowed a portion of the southern current to be rerouted south of Australia. This facilitated the establishment of maximum oceanic circulation along the southern edge of the continent by the Rupelian (~30 Ma; Fig. 10e). This set the stage for further weakening of the EGC and WAC, corresponding to the cessation of bottom current activity in the NCB. The growing convergence between the Australian plate and Eastern Indonesia from this point forward (Fig. 10f) correlates with the subsequent increase of extensive mass transport complexes.



### 2.5. *Bottom current deposits in clastic versus carbonate settings*

The Aptian – Rupelian bottom current deposits in the NCB straddle a significant transition from dominantly clastic to dominantly carbonate sedimentation. While most observations of contourite deposits, and models for their formation, are based on clastic settings, sediment mounds are observed in Cretaceous Chalk in the North Sea, on both seismic data (Surlyk & Lykke-Andersen, 2007) and in outcrop (Anderskov et al., 2007). Similar features have been described from a Jurassic pelagic carbonate platform in Sicily (Santantonio & Muraro, 2022). It is striking that each of these examples are morphologically similar to deposits formed in clastic environments, and similar mechanisms are proposed for their formation. Surlyk & Lykke-Andersen (2007) suggest that current velocities of 8–20 cm/s would be sufficient to allow redeposition of fine-grained carbonate mud without winnowing the coarser shelly material also present in these deposits, while Anderskov et al. (2007) argue that the current must be below the threshold of value for erosion of 23–27 cm/s, but above the velocity of 5-9 cm/s that would entrain fine grained carbonate material in suspension. Thran et al. (2018) in their study of deep water clastic contourite deposits argue that current velocity must be greater than the threshold of 10-15 cm/s required to rework clastic material, but also observe that average bottom current speed over contourite deposits of 2.2 cm/s is below this threshold. This suggests that contourite deposits may form episodically, during periods of more energetic bottom current activity (Thran et al., 2018).

Given the broadly similar current velocities required for bottom current deposits to form in both clastic and carbonate sediments, it is perhaps not surprising that the deposits are morphologically similar. In the NCB, the shift from clastic to carbonate sedimentation took place during the Turonian, following the deposition of Unit 1, and the large-scale mounds continue to grow in a very similar manner, at least until the Maastrichtian, during the deposition of Unit 2. Unit 2 does contain more varied deposits, but this represents a change from moat formation to moat fill and a change from aggradation to progradation of the main mounds, which could be more likely to related to current activity, rather than the nature of the sedimentary particles.

### 3. Conclusion

The main conclusions of this research are:

- The post-Valanginian breakup passive margin sequence of the NCB shows a complicated depositional history characterised by lateral and vertical facies variation with multiple unconformities.
- The stratigraphy records an evolution in depositional setting from hemipelagic deposition in the early post-rift sequence (Valanginian-Aptian), followed by the initiation of bottom current activity during the deposition of Unit 1 (Aptian-Turonian). This persistent bottom current activity continued during the deposition of Unit 2 (Turonian-Rupelian), particularly in the middle of the Exmouth Plateau and was terminated by the progradation of a carbonate shelf and the development of extensive slumps and MTCs across the basin in Unit 3 (Rupelian-Tortonian) and 4 (Tortonian-Recent).
- Bottom currents were present over 80 Myr, resulting in large, stacked sediment mounds, moats, moats fills and other complex erosional structures. The bottom currents developed on c. 500 km wide gently sloping ramp-style margin, an atypical setting and geometry compared to established models for bottom current deposits.
- The bottom currents in the NCB are mainly influenced by the opening and closing ocean gateways in the north, west and south during a separation of Australia, Greater India, and Antarctica.
- The complexity of the seismic stratigraphic units and seismic facies are related to variations in seismic velocity. The transition from clastic to carbonate sediments is the main control, but the greatest lateral velocity variation occurs where the greatest variation occurs as a result of bottom current activity.

#### 4. Future work

This research has highlighted the importance of bottom current activity on the Northwest Shelf of Australia. The deposits provide an interesting contrast with typical models of contourite deposition and further work is required to fully understand the conditions under which they have formed. This includes:

- Similar bottom currents deposits can be recognised in other parts of the NWS, for example in the outer parts of the Beagle and western Browse Basin. Mapping their

full extent, and relating this to tectonic reconstructions, may help constrain circulation patterns and their relationship to tectonic processes.

- Cenomanian-Santonian inversion occurred to the south, around the Exmouth sub-basin. This likely affected bathymetry and may provide further constraints on the pattern and evolution of bottom currents in the NCB. Extending mapping to the south and west will address this.
- The precise water depth in which the bottom current deposits formed is poorly constrained. Back-stripping and subsidence modelling may help to address this.
- A velocity cube derived from the processing of 3D seismic surveys would enable better calibration between seismic facies and velocity characteristics and could improve velocity prediction in the Exmouth Plateau.

## References

- Anderskov, K., Damholt, T., Surlyk, F., 2007. Late Maastrichtian chalk mounds, Stevns Klint, Denmark — Combined physical and biogenic structures, *Sedimentary Geology*, Volume 200, Issues 1–2, 57-72, ISSN 0037-0738, <https://doi.org/10.1016/j.sedgeo.2007.03.005>.
- Apthorpe, M., 1988. Cenozoic depositional history of the North West shelf. In: Purcell, P.G., Purcell, R.R. (Eds.), *The North West Shelf, Australia*. Proceedings of Petroleum Exploration Society of Australian Symposium, Perth, Australia, 55–84.
- Bradshaw, M.T., Yeates, A.N., Beynon, R.M., Brakel, A.T., Langford, R.P., Totterdell, J.M., Yeung, M., 1988. Palaeogeographic evolution of the North West Shelf region. In: Purcell, P.G., Purcell, R.R. (Eds.), *The North West Shelf, Australia*. Proceedings of the Petroleum Exploration Society of Australia Symposium, 29–54.
- Curtis, M. S., Holford, S. P., Bunch, M. A., Schofield, N. J., 2022. Seismic, petrophysical and petrological constrains on the alteration of igneous rocks in the Northern Carnarvon Basin, Western Australia: implications for petroleum exploration and drilling operations. *The APPEA Journal*, 62, 196-222. <https://doi.org/10.1071/AJ21411>.
- Eberli, G.P., and Betzler, C., 2019, Characteristics of modern carbonate contourite drifts: *Sedimentology*, v. 66, p. 1163–1191, <https://doi.org/10.1111/sed.12584>.
- Fonnesu, M., Palermo, D., Galbiati, M., Marchesini, M., Bonamini, E., Bendias, D., 2020. A new world-class deep-water play-type, deposited by the syndepositional interaction of

- turbidity flows and bottom currents: The giant Eocene Coral Field in northern Mozambique, *Marine and Petroleum Geology*, Volume 111, 179-201, <https://doi.org/10.1016/j.marpetgeo.2019.07.047>.
- Haupt, B.J., Schäfer-Neth, C., Stattegger, K., 1994. Modeling sediment drifts: a coupled oceanic circulation sedimentation model of the northern North Atlantic. *Paleoceanography* 9, 897–916. <https://doi.org/10.1029/94PA01437>.
- Hollister, C.D., 1967. Sediment Distribution and Deep Circulation in the Western North Atlantic (Unpublished Ph.D. Dissertation). Columbia University, New York, p. 467.
- Jablonski, D., Saitta, A. J., 2004. Permian to Lower Cretaceous plate tectonics and its impact on the tectono-stratigraphic development of the western Australian margin. *The APPEA Journal*, 44(1), 287–327. <https://doi.org/10.1071/AJ03011>.
- Longley, I.M., Buessenschuett, C., Clydsdale, L., Cubitt, C.J., Davis, R.C., Johnson, M.K., Marshall, N.M., Murray, A.P., Somerville, R., Spry, T.B., Thompson, N.B., 2002. The North West Shelf of Australia - a Woodside perspective. In: Keep, M., Moss, S. (Eds.), *The Sedimentary Basins of Western Australia 3. Proceedings of the Petroleum Exploration Society of Australia Symposium*, 27–88.
- Lovell, J.P.B., Stow, D.A.V., 1981. Identification of ancient sandy contourites. *Geology* 9, 347–349.
- Mantilla, O., Hernández-Molina, F.J., Scarselli, N., 2022. Can deepwater bottom currents generate clinothems? An example of a large, asymmetric mounded drift in Upper Jurassic to Lower Cretaceous sediments from northwestern Australia. *Geology* 2022; 50 (6): 741–745. <https://doi.org/10.1130/G50068.1>.
- Marshall, N.G., Lang, S.C., 2013. A new sequence stratigraphic framework for the North West Shelf, Australia. In: Keep, M., Moss, S.J. (Eds.), *The Sedimentary Basins of Western Australia 4. Proceedings of the Petroleum Exploration Society of Australia Symposium*, 1–32.
- Mory, A.J., (compiler), 2023. Mesozoic transformation of Western Australia: rifting and breakup of Gondwana: Geological Survey of Western Australia, 73.
- Norvick, M. S., 2002. Palaeogeographic maps of the northern margins of the Australian plates: initial report. Unpublished report for Geoscience Australia.
- Paumard, V., Bourget J., Payenberg T., Ainsworth R. B., George A. D., Lang S., Posamentier H. W., Peyrot D., 2018. Controls on shelf-margin architecture and sediment partitioning

- during a syn-rift to post-rift transition: Insights from the Barrow Group (Northern Carnarvon Basin, North West Shelf, Australia). *Earth-Science Reviews* Volume 177, February 2018, 643–677. <https://doi.org/10.1016/j.earscirev.2017.11.026>.
- Rebesco, M., Hernández-Molina, F.J., Van Rooij, D., Wåhlin, A., 2014. Contourites and associated sediments controlled by deep-water circulation processes: state-of-the-art and future considerations. *Mar. Geol.* 352, 111–154. <https://doi.org/10.1016/j.margeo.2014.03.011>.
- Reeve, M.T., Jackson, C.A.L., Bell, R.E., Bastow, I.D., 2022. Stratigraphic record of continental breakup, offshore NW Australia. *Basin Res*, vol 34, 1220–1243. <https://doi.org/10.1111/bre.12656>.
- Rodrigues, S., Hernández-Molina, F.J., Fonnesu, M., Miramontes, E., Rebesco, M., Campbell, D.C., 2022. A new classification system for mixed (turbidite-contourite) depositional systems: Examples, conceptual models and diagnostic criteria for modern and ancient records, *Earth-Science Reviews*, Volume 230, 104030, ISSN 0012-8252, <https://doi.org/10.1016/j.earscirev.2022.104030>.
- Rohead-O'Brien, H. R., 2023. Mesozoic Tectono-stratigraphic evolution of the Exmouth Plateau, North West Shelf Australia, School of Earth and Planetary Sciences Thesis (PhD), Curtin University.
- Rohrman, M., 2015. Delineating the Exmouth mantle plume (NW Australia) from denudation and magmatic addition estimates. *Lithosphere*, 7(5), 589-600. <https://doi.org/10.1130/L445.1>.
- Salles, T., Marchès, E., Dyt, C., Griffiths, C., Hanquiez, V., Mulder, T., 2010. Simulation of the interactions between gravity processes and contour currents on the Algarve Margin (South Portugal) using the stratigraphic forward model Sedsim. *Sediment. Geol.* 229, 95–109. <https://doi.org/10.1016/j.sedgeo.2009.05.007>.
- Santantonio, M., Muraro, C., 2022. Bottom currents on a pelagic carbonate platform: Mounds and sediment drifts in the Jurassic succession of the Sciacca Plateau, Western Sicily, *Basin Research*, Volume 34, Issue 5, 1507-1535, <https://doi.org/10.1111/bre.12669>.
- Scotese, C. R., Wright, N., 2018. PALEOMAP Paleodigital Elevation Models (PaleoDEMS) for the Phanerozoic. <https://www.earthbyte.org/paleodem-resource-scotese-and-wright-2018/>.



- Shanmugam, G., 2003. Deep-marine tidal bottom currents and their reworked sands in modern and ancient submarine canyons. *Marine and Petroleum Geology*, 20: 471–491. [https://doi.org/10.1016/S0264-8172\(03\)00063-1](https://doi.org/10.1016/S0264-8172(03)00063-1).
- Shanmugam, G., 2008. Deep-water bottom currents and their deposits, in: Rebesco, M., Camerlenghi (Eds.), *Contourites*. *Dev. Sedimentol.* 60, 59–81. [http://dx.doi.org/10.1016/S0070-4571\(08\)00205-7](http://dx.doi.org/10.1016/S0070-4571(08)00205-7).
- Shanmugam, G., 2022. Comment on “A new classification system for mixed (turbidite-contourite) depositional systems: Examples, conceptual models and diagnostic criteria for modern and ancient records” by Rodrigues, S., Hernández-Molina, F.J., Fonnesu, M., Miramontes, E., Rebesco, M., Campbell, D.C., 2022, *Earth-Science Reviews*, Volume 232, 2022, 104156, ISSN 0012-8252, <https://doi.org/10.1016/j.earscirev.2022.104156>.
- Stow D.A.V., Faugères J-C, Howe J.A., Pudsey C.J., Viana A.R., 2002. Bottom currents, contourites and deep-sea sediment drifts: current state-of-the-art. In: Stow DAV, Pudsey CJ, Howe JA, Faugères J-C, Viana AR (eds) *Deep-water contourite systems: modern drifts and ancient series, seismic and sedimentary characteristics*. *Geol Soc Lond Mem* 22, 7–20. <https://doi.org/10.1144/GSL.MEM.2002.022.01.02>.
- Stow, D.A.V., Brackenridge, R., Hernandez-Molina, F.J., 2011. Contourite Sheet Sands: New Deepwater Exploration Target, *Search and Discovery Article #30182*.
- Surlyk, F., Lykke-Andersen, H., 2007. Contourite drifts, moats and channels in the Upper Cretaceous chalk of the Danish Basin, *Sedimentology*, Volume 54, Issue 2, 405-422, <https://doi.org/10.1111/j.1365-3091.2006.00842.x>
- Tait, A.M., 1985, A depositional model for the Dupuy member and the Barrow Group in the Barrow Sub-basin, Northwestern Australia: *Journal of the Australian Petroleum Production & Exploration Association*, v. 25, 282–290, <https://doi.org/10.1071/AJ84025>.
- Tindale, K., Newell, N., Keall, J., Smith, N., 1998. Structural evolution and charge history of the Exmouth Sub-basin, Northern Carnarvon Basin, Western Australia. In: Purcell, P.G., Purcell, R.R. (Eds.), *The Sedimentary Basins of Western Australia 2*. *Proceedings of the Petroleum Exploration Society of Australia Symposium*, 447–472.
- Thran, A., Dutkiewicz, A., Spence, P., Müller, R. D., 2018. Controls on the global distribution of contourite drifts: Insights from an eddy-resolving ocean model, *Earth and Planet. Science Lett.*, 489, 228-240. <https://doi.org/10.1016/j.epsl.2018.02.044>.

Valdes, P.J., Scotese, C. R., Lunt, D. J., 2021. Deep ocean temperatures through time, *Clim. Past*, 17, 1483-1506, <https://doi.org/10.5194/cp-17-1483-2021>.

Van Wagoner, J.C., Posamentier, H., Mitchum, Jr., Vail, P.R., Sarg, J.F., Loutit, T.S., Hardenbol, J., 1988. An overview of the fundamentals of sequence stratigraphy and key definitions. *Sea Level Changes: An Integrated Approach*, SEPM Special Publication, 42, 39-46.

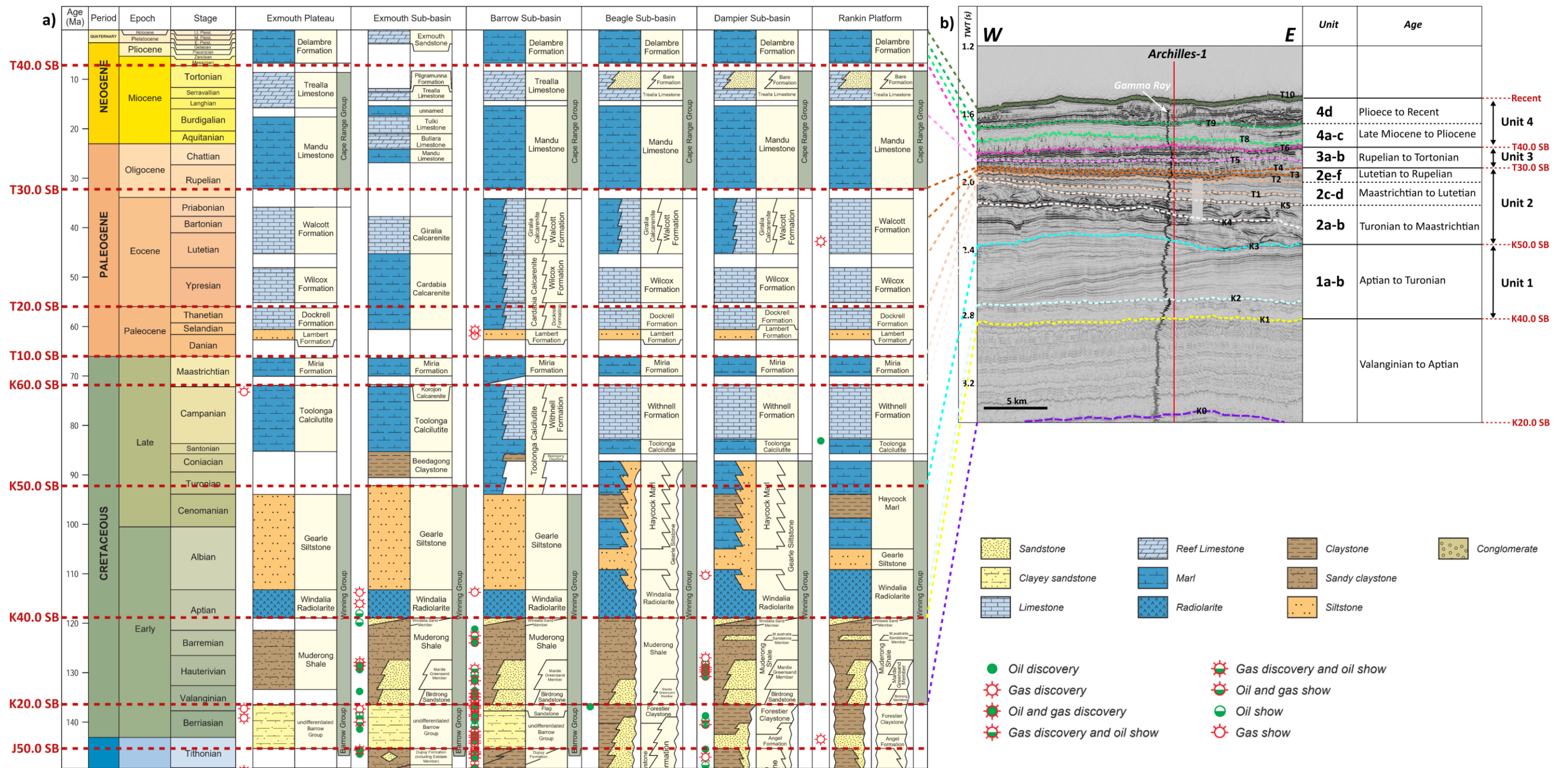


Fig. 1. Generalised lithostratigraphic chart of the NCB compiled from Geoscience Australia (2022) correlated to the seismic-stratigraphy and showing the tie with the lithostratigraphic formations in the Achilles-1 well. The link between the seismic stratigraphic picks and the main boundaries of Marshall and Lang (2013, red dashed lines) are also shown. The seismic stratigraphic interpretation shows more detail than the sedimentary sequences expressed by lithofacies.



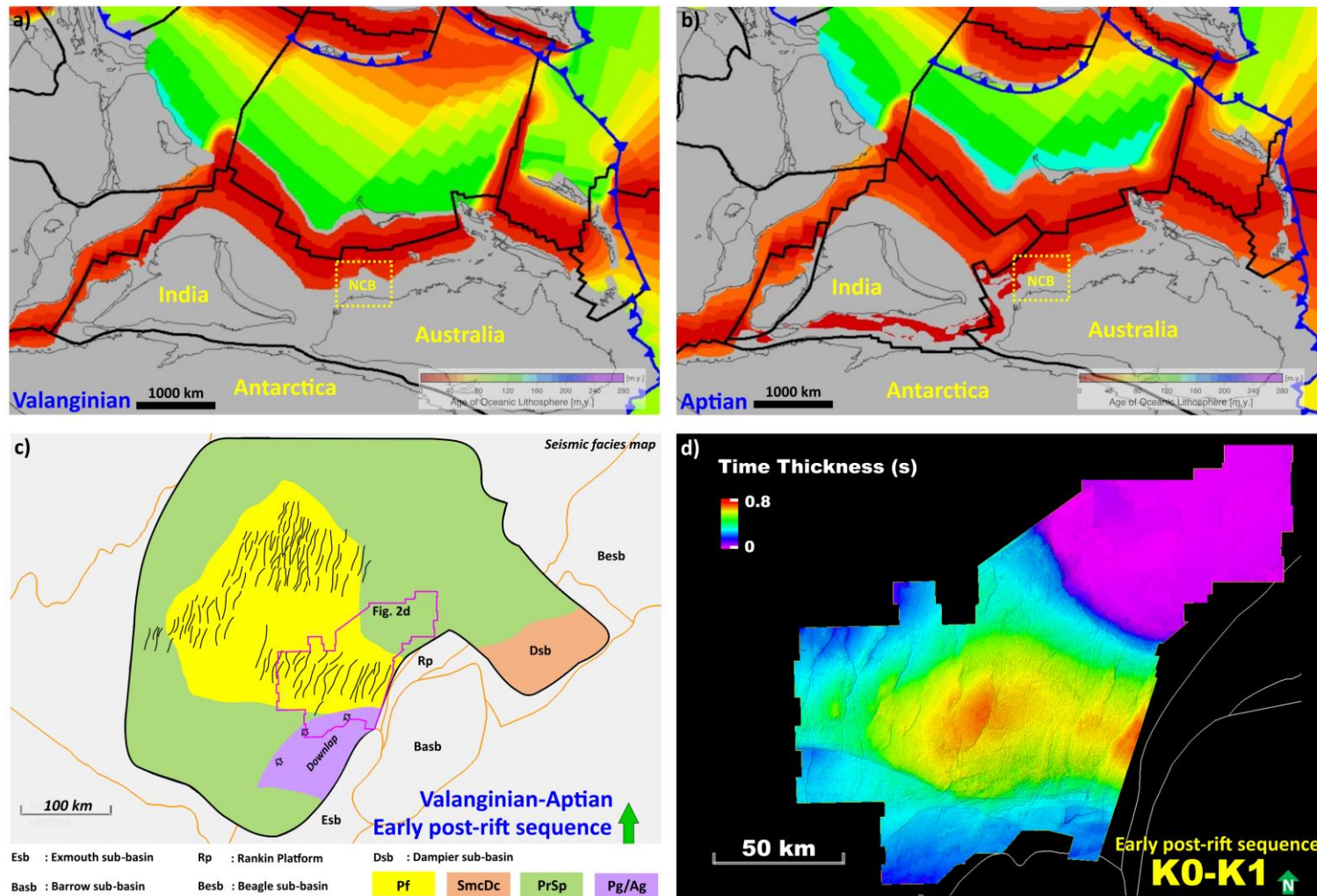


Fig. 2. a), b) Maps showing tectonic reconstructions for the Valanginian (a) and the Aptian (b), and age grids of the ocean floor for those times, taken from <https://portal.gplates.org/cesium/?view=AgeGrid> showing the development of a narrow ocean basin between Australia and Greater India. c) Seismic facies map for the Valanginian - Aptian interval. Following Valanginian breakup, the NCB subsided, and sediment was deposited during a marine transgression, infilling a sag in the early post-rift sequence. Regionally, this interval was dominated by parallel to subparallel facies (PrSp), with polygonal faults (Pf) mainly occurring in the depocentre. The depocentre can be seen in Figure 2d. SmcDc (Semi- to discontinuous), Pg/Ag (Progradation/Aggradation), black arrow: downlaps. d) Time thickness map for the Valanginian - Aptian interval.

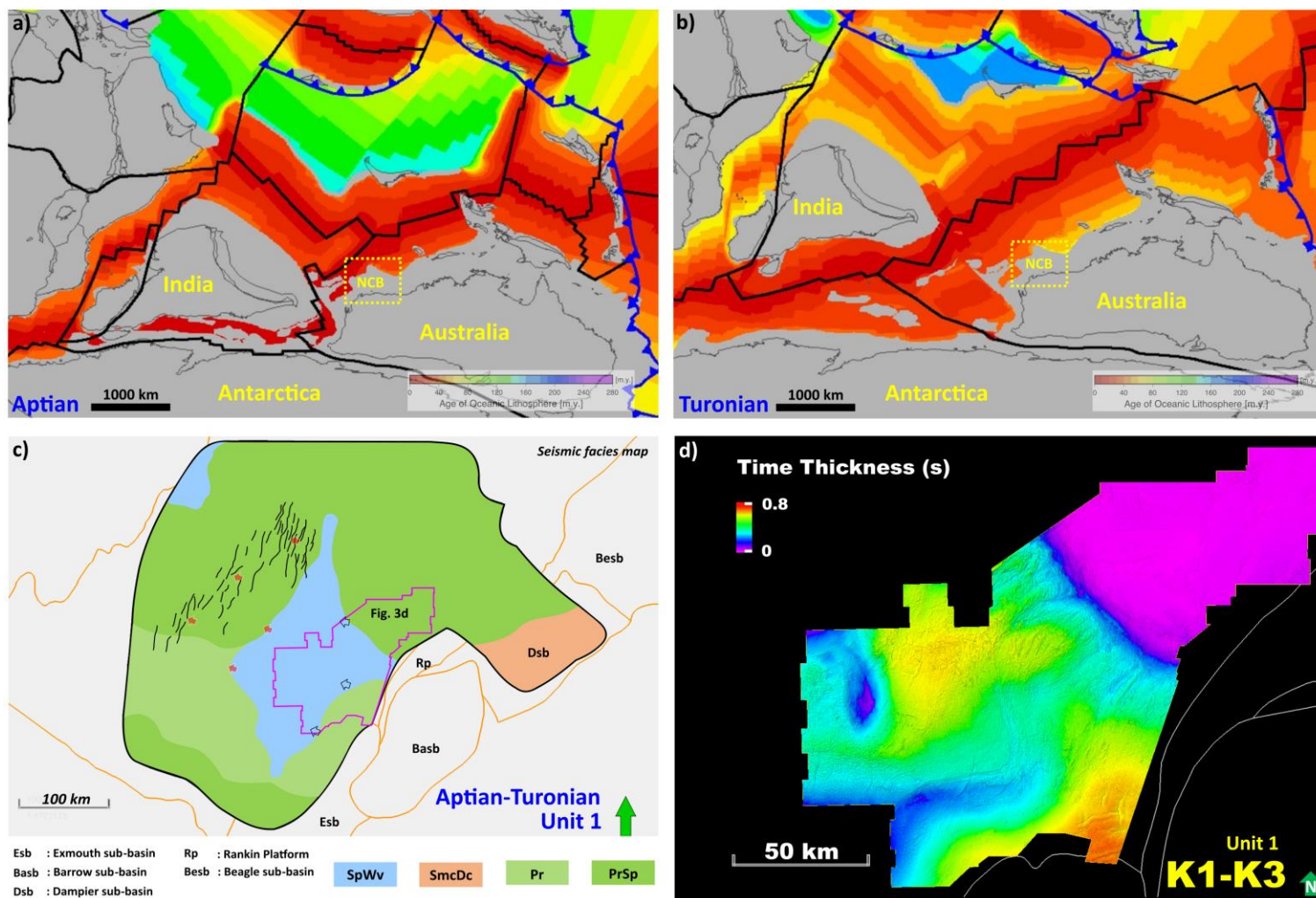


Fig. 3. a), b) Maps showing reconstructions for the Aptian (a) and Turonian (b), and age grids of the ocean floor for those times, taken from <https://portal.gplates.org/cesium/?view=AgeGrid>. During this period, Greater India continued to drift northward increasing the seaway between Indian and Australia, potentially allowing for improved ocean circulation on the western margin. c), d) Seismic facies and thickness maps showing that this is associated with the initial development of bottom current deposits in the centre Exmouth Plateau indicated by the development of SpWv (Subparallel to Wavy) seismic facies (c) and an area of significantly reduced sediment thickness (d). Red arrow: onlaps, black arrow: downlaps. Pr (Parallel), PrSp (Parallel to Subparallel), SmcDc (Semi- to discontinuous).



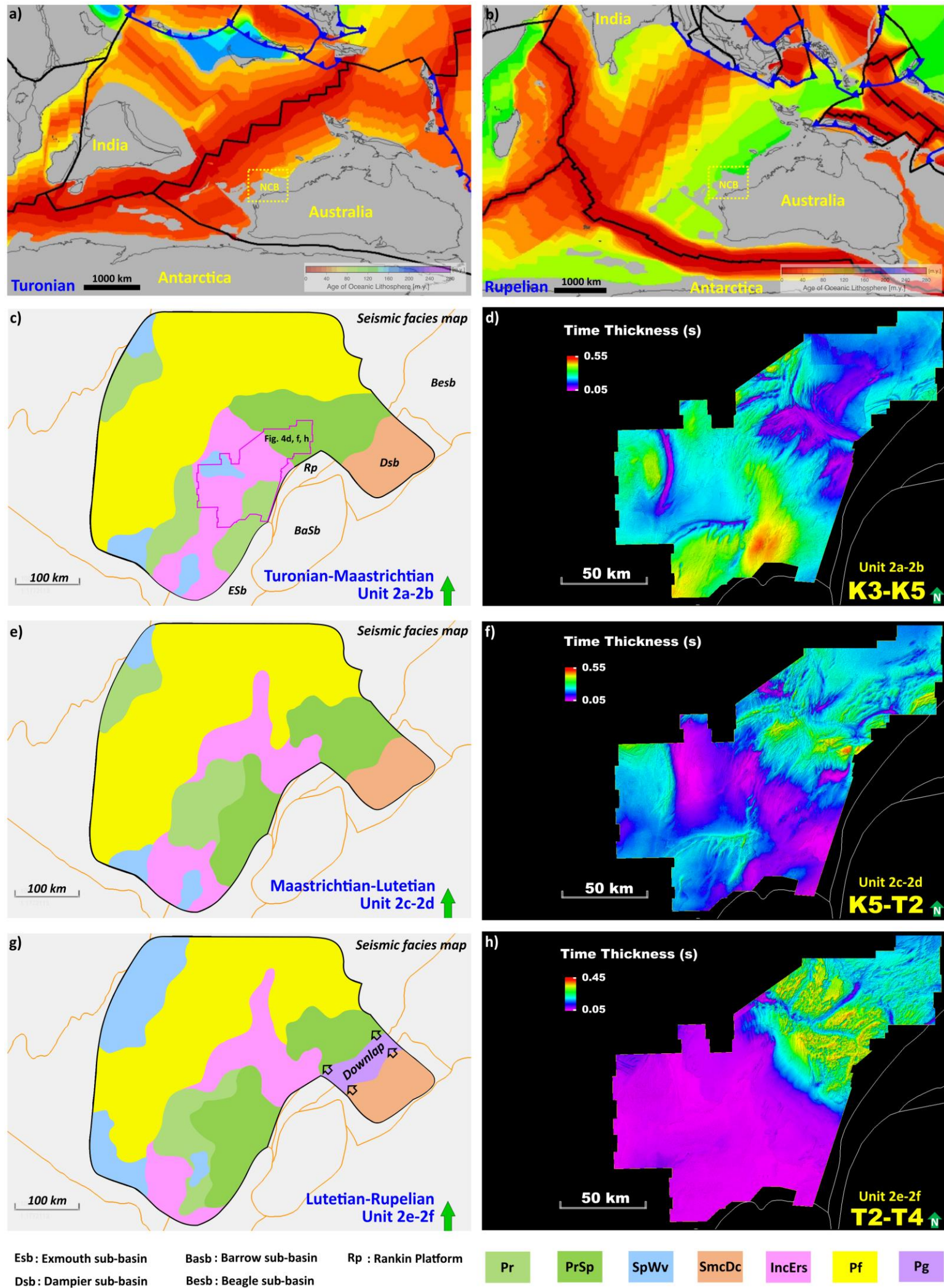


Fig. 4. a), b) Maps showing tectonic reconstructions for the Turonian (a) and Rupelian (b), and age grids of the ocean floor for those times, taken from <https://portal.gplates.org/cesium/?view=AgeGrid> showing increased separation of Greater India from Australia, the development of a wide ocean between Australia and Africa, as well as the initial stages of separation of Australia from Antarctica. c) to f) Seismic facies and thickness maps showing that this period was dominated by mounds, moats, and moat fills in the SW between the Turonian and Lutetian (c-d, e-f) and encompassed deep incisions and conical depression in the NE during Lutetian and Rupelian, as well as a shift in the location of sediment accumulation to the northeast (g-h). Pr (Parallel), PrSp (Parallel to Subparallel), SpWv (Subparallel to Wavy), SmcDc (Semi- to discontinuous), IncErs (Incision or Erosive), Pf (Polygonal fault), Pg (Progradation).



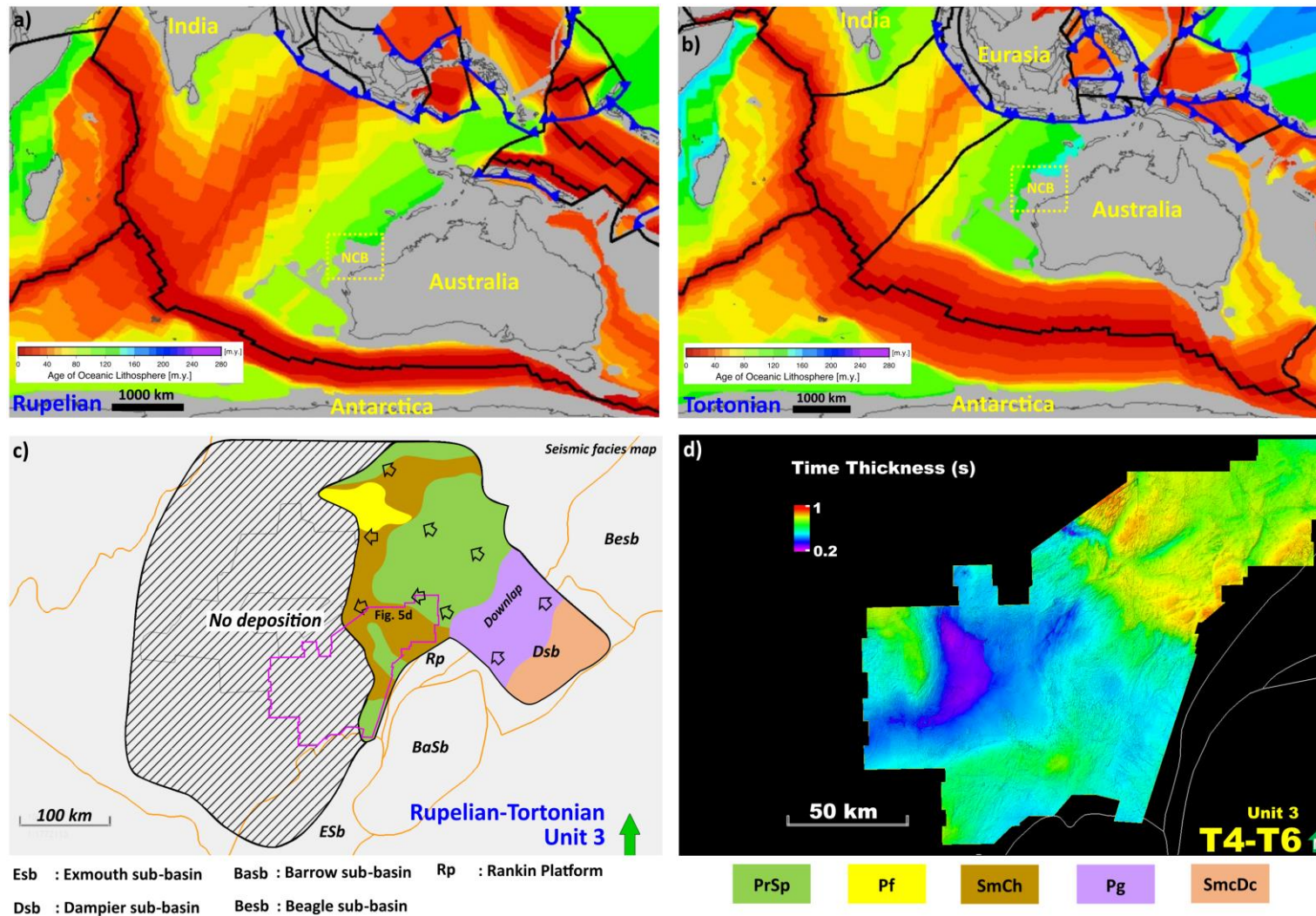


Fig. 5. a), b) Maps showing tectonic reconstructions for the Rupelian (a) and Tortonian (b), and age grids of the ocean floor for those times, taken from <https://portal.gplates.org/cesium/?view=AgeGrid> showing that Australia fully separated from Antarctica and drifted to the north, associated with subduction beneath Eurasia (from Rupelian to Tortonian). c), d) Seismic facies and thickness maps showing that this corresponds to the development of prograding carbonate ramps and the deposition of chaotic slumps and MTCs in the Exmouth Plateau. This unit is of limited extent, as well as downlaps and onlaps onto Unit 2. PrSp (Parallel to Subparallel), Pf (Polygonal fault), SmCh (Semi Chaotic), Pg (Progradation), SmcDc (Semi- to discontinuous).

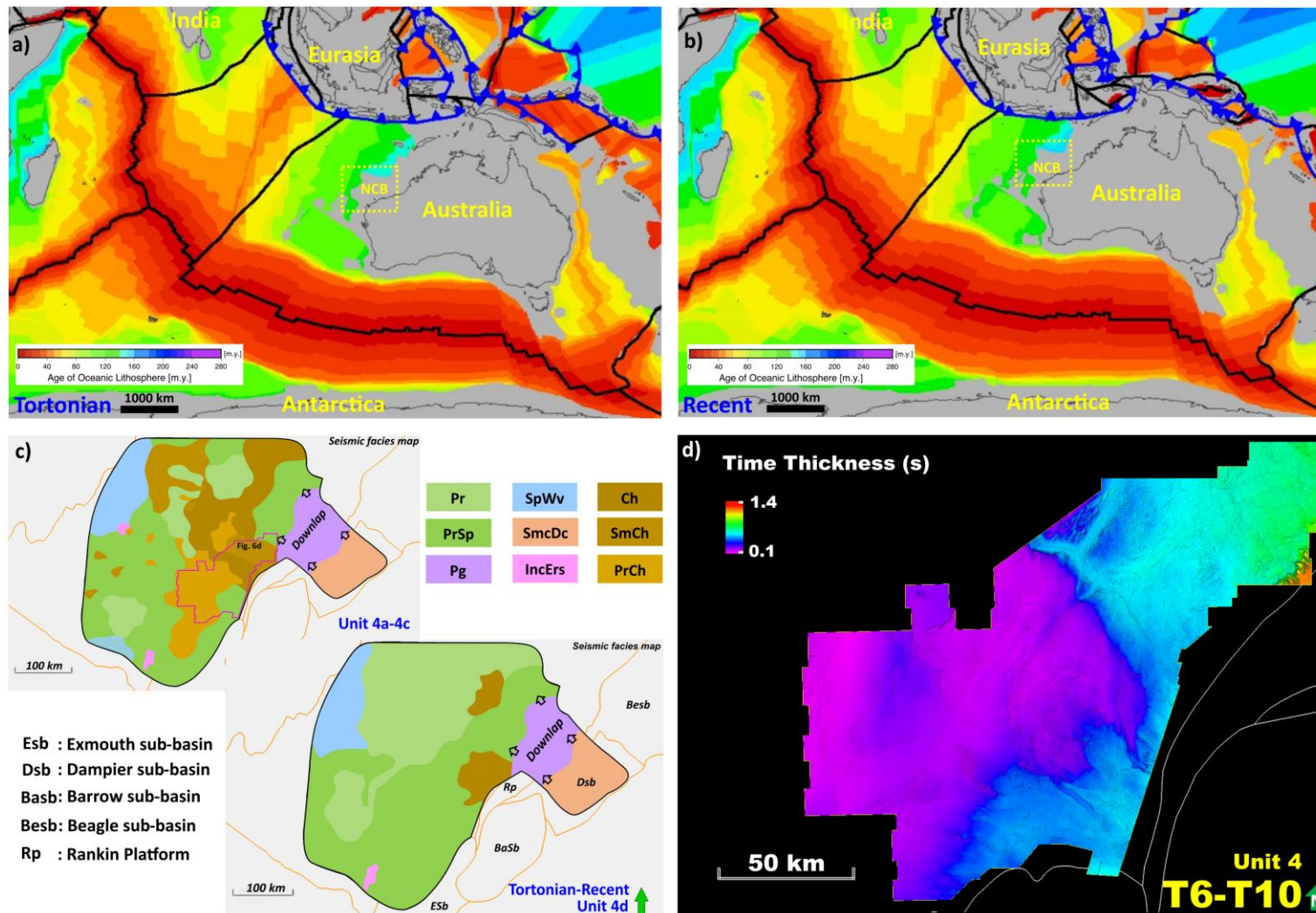


Fig. 6. a), b) Maps showing tectonic reconstructions for the Tortonian (a) and the present day (b), and age grids of the ocean floor at these times, taken from <https://portal.gplates.org/cesium/?view=AgeGrid> showing increased convergence between Australia and Eurasia. c), d) Seismic facies and thickness maps showing that this resulted in widespread slumps and MTCs in the Exmouth Plateau. The chaotic sediments (corresponding to MTCs) are less abundant in the younger sequence. Pr (Parallel), PrSp (Parallel to Subparallel), Pg (Progradation), SpWv (Subparallel to Wavy), SmcDc (Semi- to discontinuous), IncErs (Incision or Erosive), Ch (Chaotic), SmCh (Semi Chaotic), PrCh (Parallel to Chaotic).



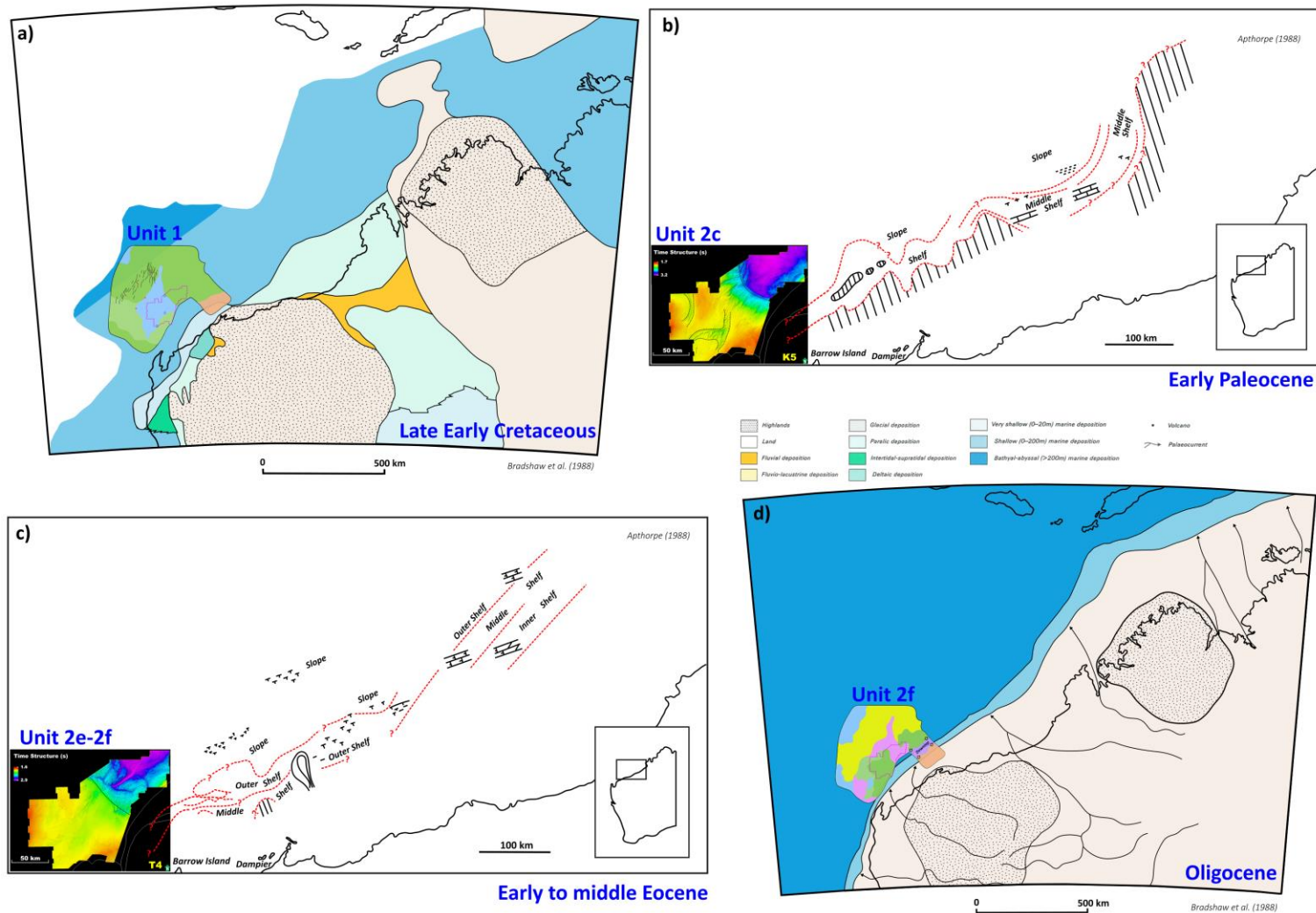
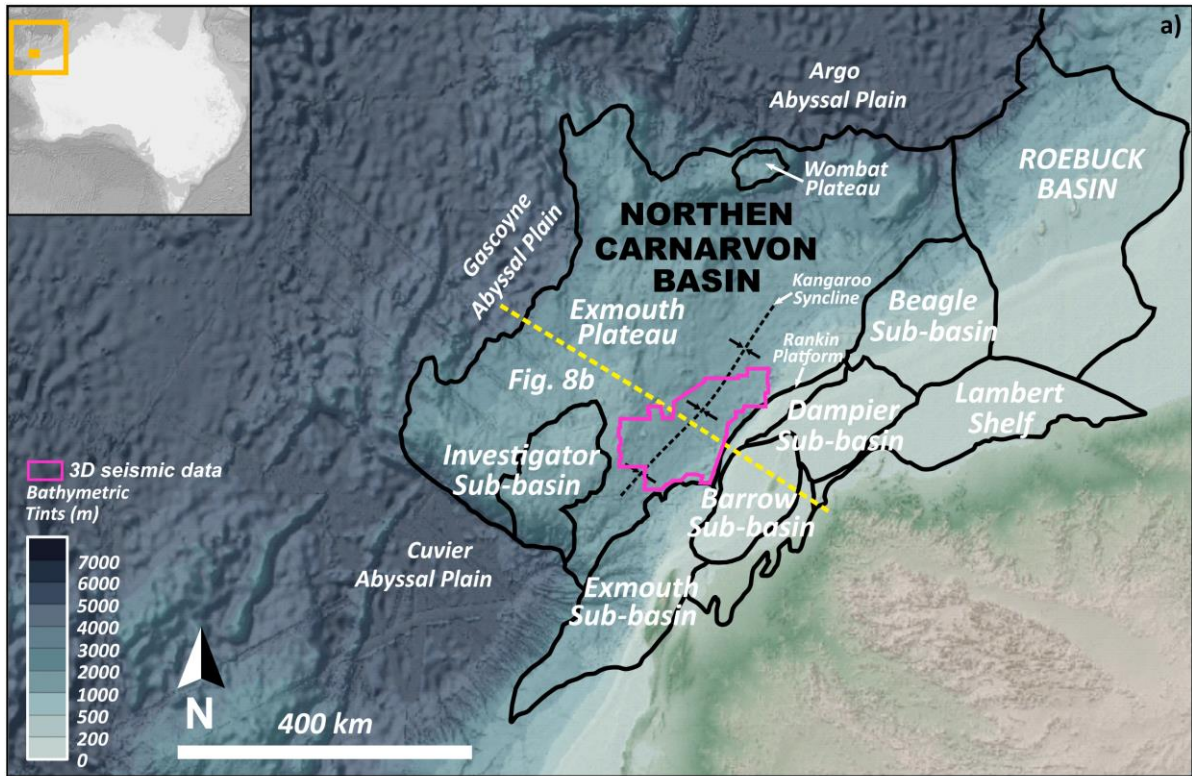
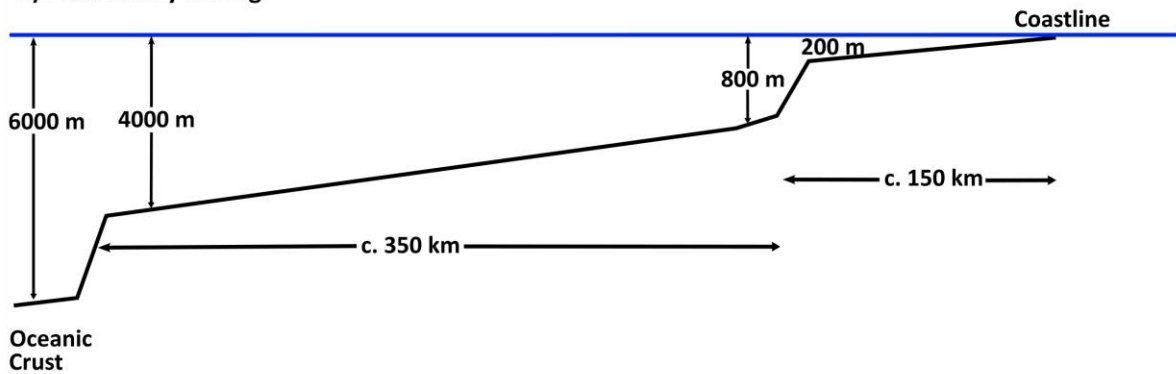


Fig. 7. a), d) Paleoenvironmental maps from Bradshaw et al. (1988) and b), c) from Apthorpe (1988) and their relationship to paleoenvironmental maps generated in this study. At the time they were created in 1988 relatively limited well and seismic data was available. Consequently, these maps are at a very regional scale and show relatively simple models, generally describing a transition from shallow marine shelf to outer shelf and slope settings between the Early Cretaceous and Oligocene. The study area of Apthorpe (1988) is to the northeast of the present study. This study shows the greater complexity of facies developed on the outboard parts of the Northwest Shelf, and the importance of bottom current activity.



b) Present day setting



c) Aptian-Rupelian setting

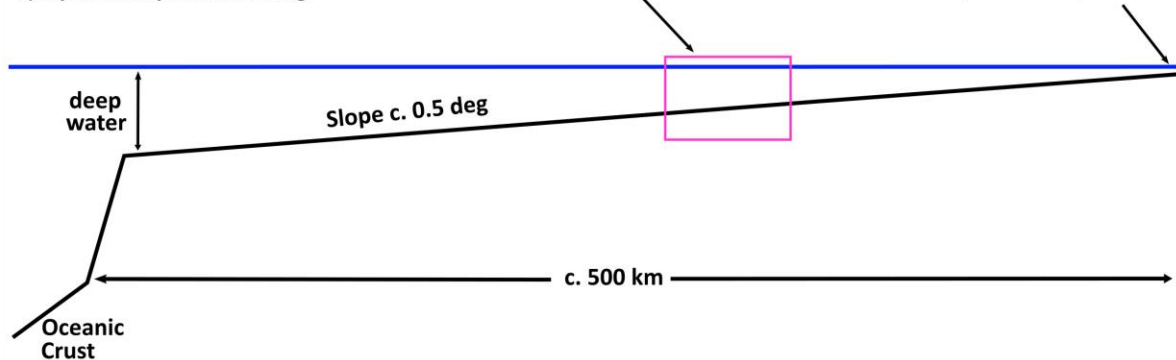
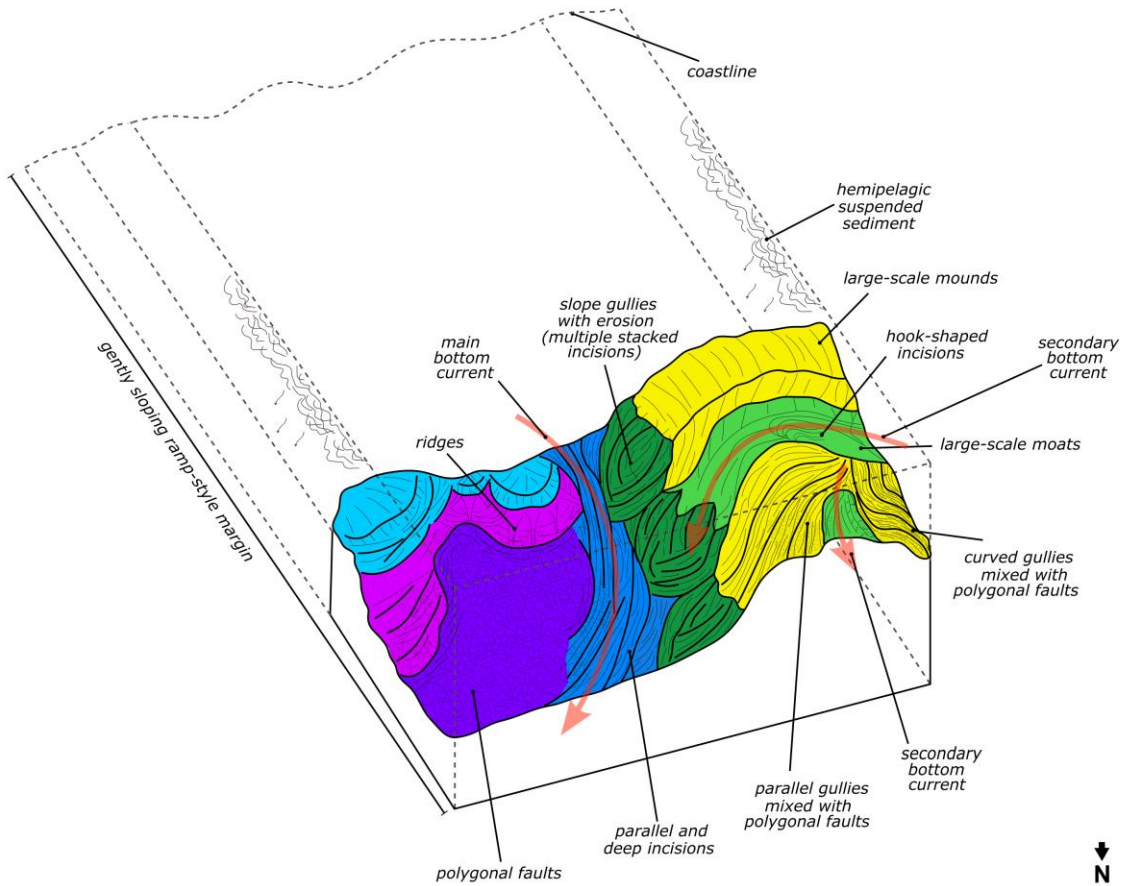


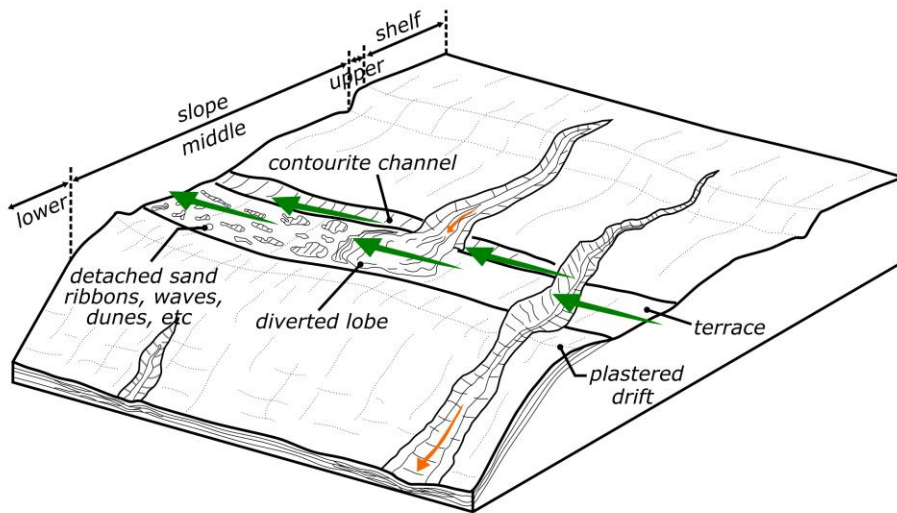
Fig. 8. a) Bathymetric map of the Northern Carnarvon Basin. b), c) A comparison of Present day and Aptian-Rupelian bathymetric profiles of the NCB. In the Aptian-Rupelian a c. 500 km wide gently sloping ramp-style margin (sensu Van Wagoner et al., 1988) was present. This is atypical of the setting for most models of contourite and mixed bottom current – turbidite deposits, which are typically developed on narrow margins with steeper slopes, such as the Atlantic margin. The location of the profile is shown in yellow dashed line.



a) Gently sloping ramp-style margin

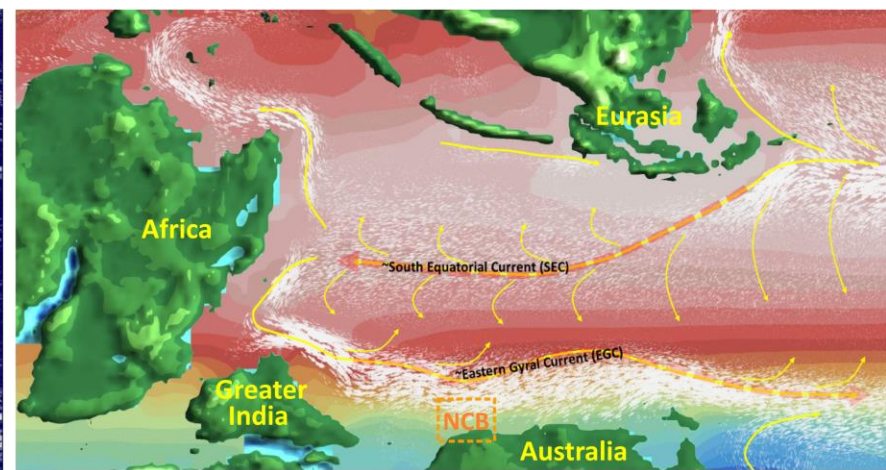
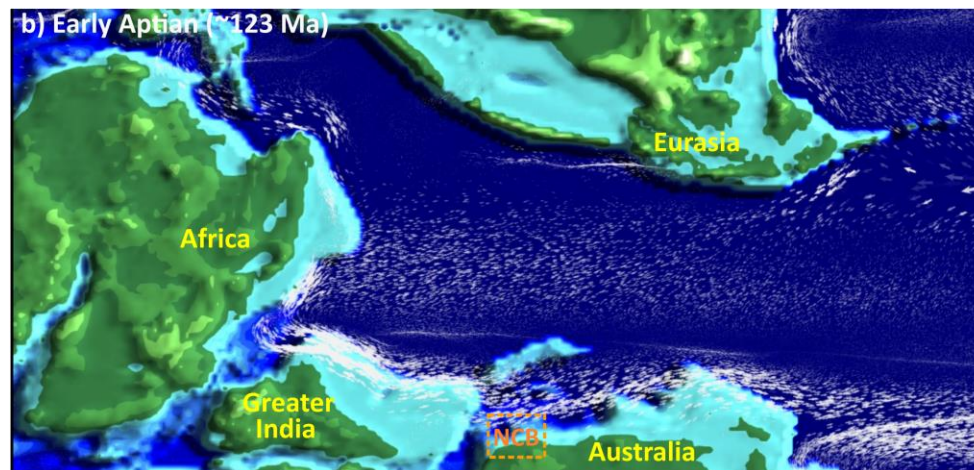
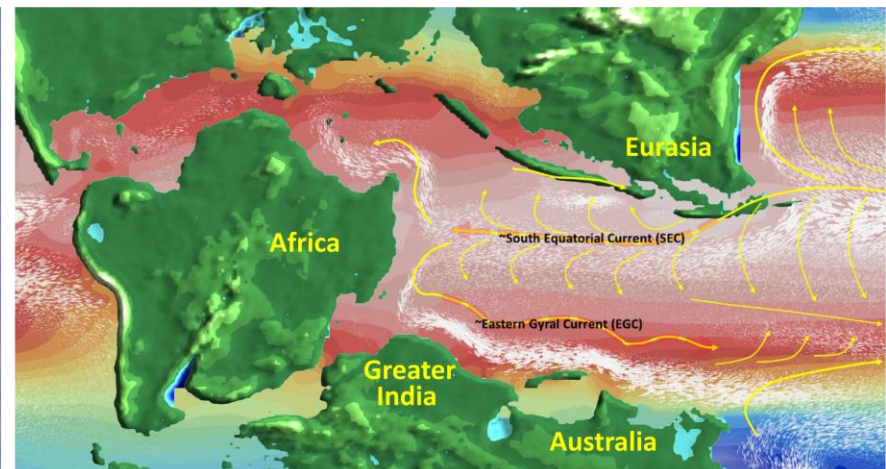
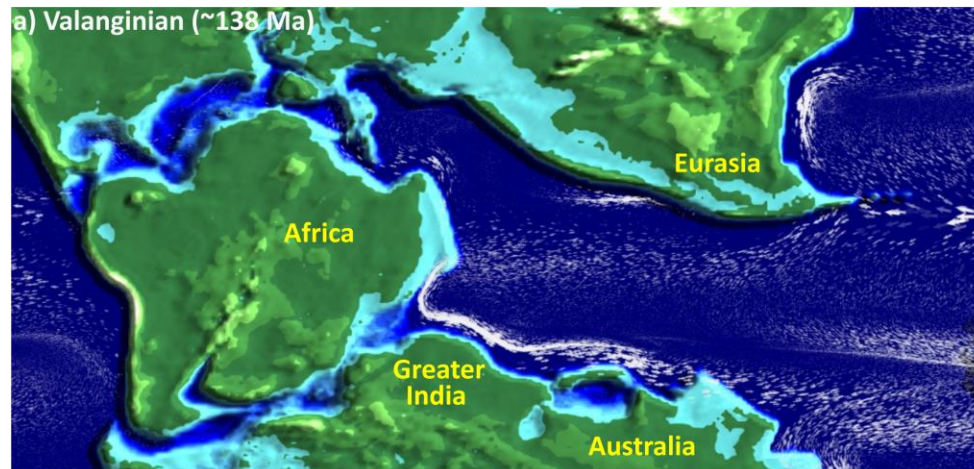


b) Rodrigues et al. (2022): Contourite-dominated system

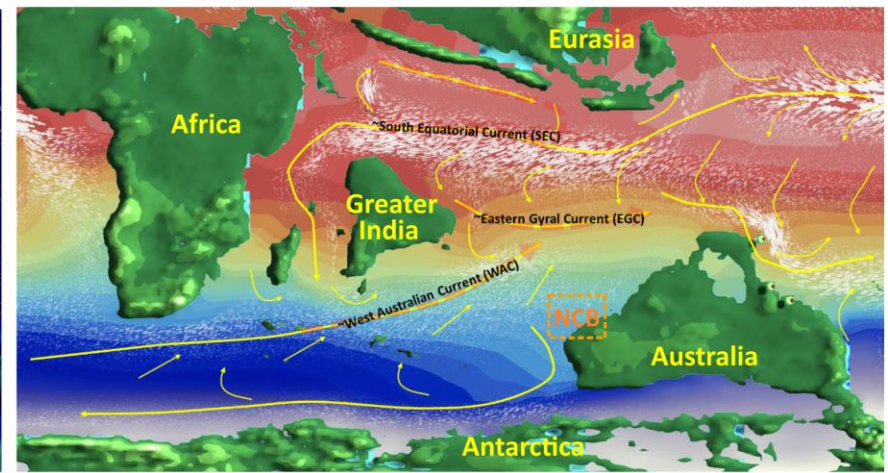
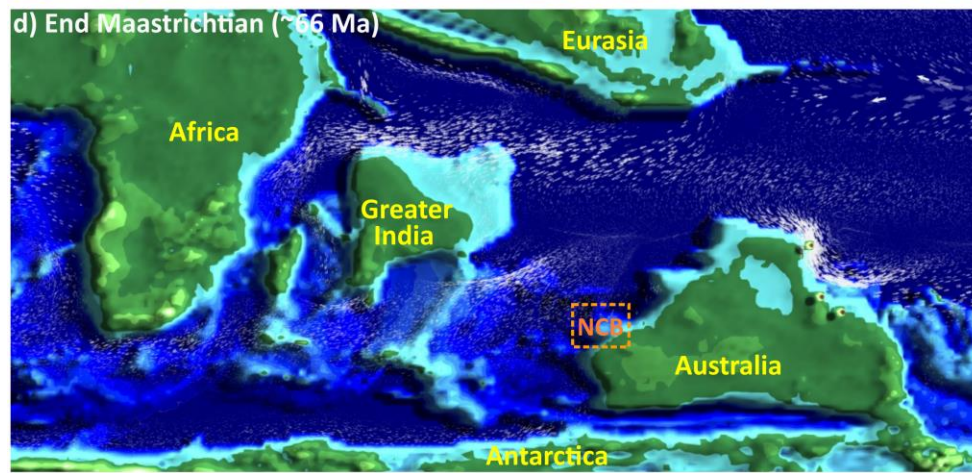
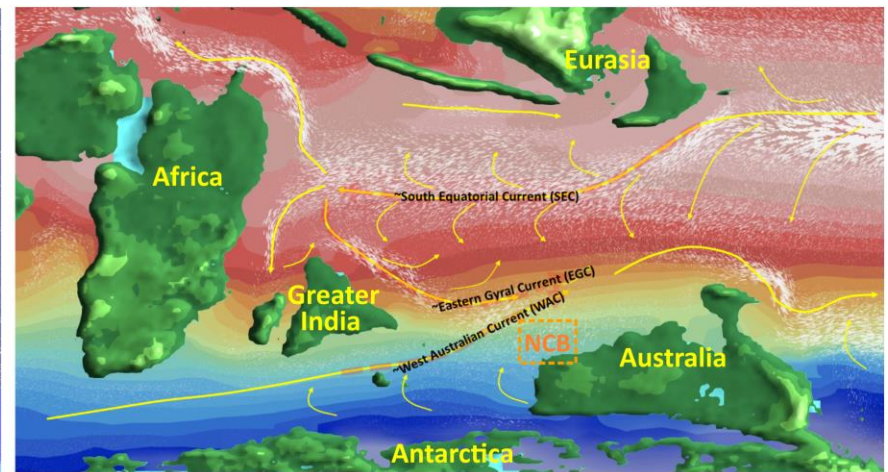
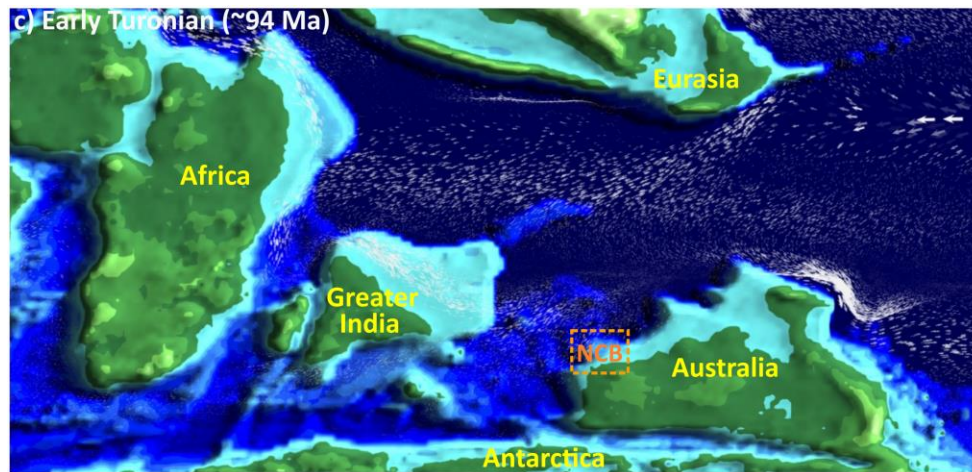


Gulf of Cadiz channel sector, Faroe-Shetland, SE Argentina, Paleogene S and SE Brazilian basins

Fig. 9. a) Schematic diagram showing interaction between currents to form different scales of sedimentary structure by reworking of hemipelagic suspended sediment on a gently sloping ramp-style margin, occurring at water depths up to 2500 m between the Aptian and the Rupelian in the middle of the Exmouth Plateau. b) The proximal low gradient slopes in contourite-dominated mixed systems (Rodrigues et al., 2022).









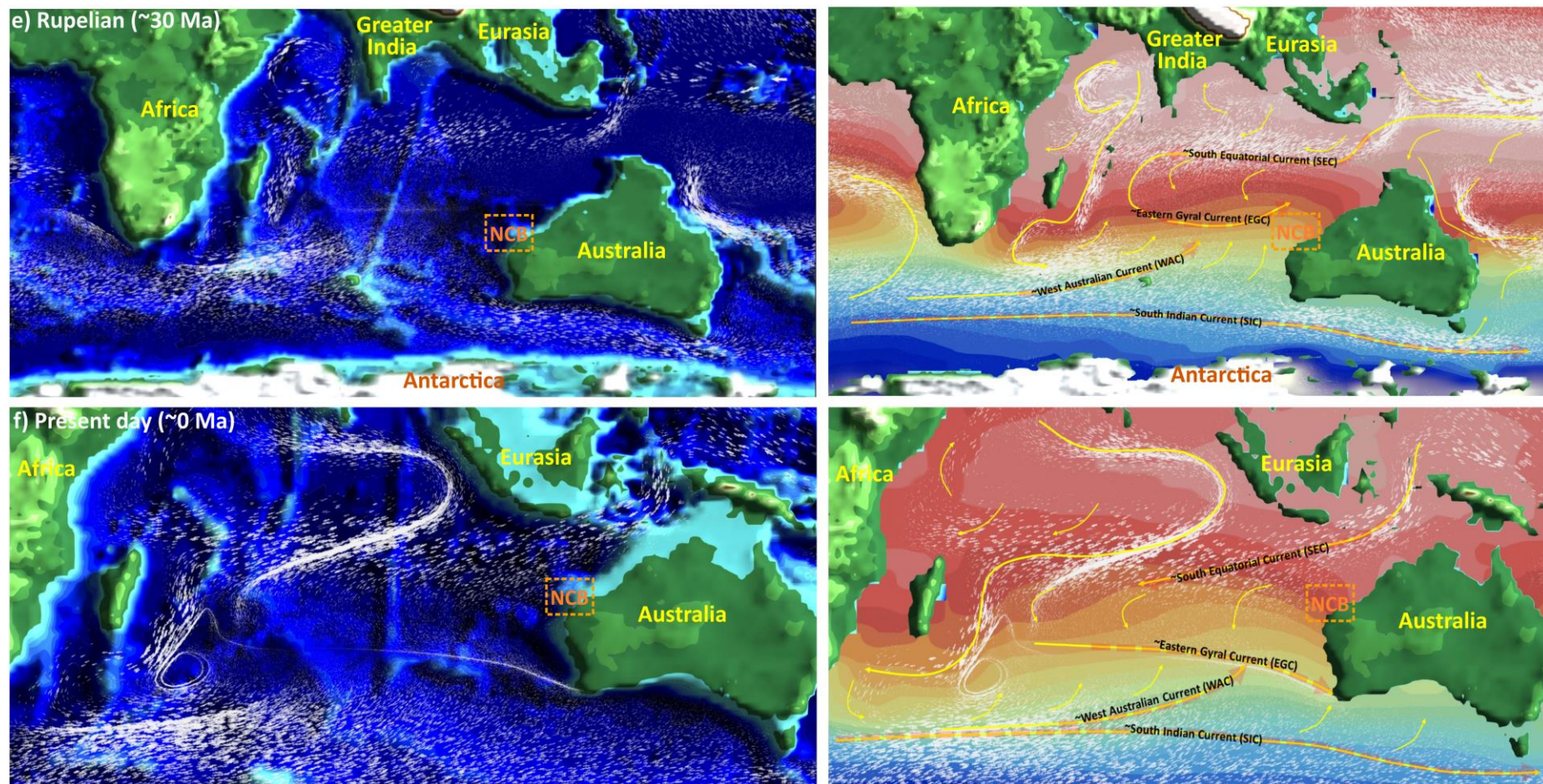


Fig. 10. a-f) Ocean currents and plate reconstructions compiled from <https://climatearchive.org/>, which refer to the paleogeographic reconstructions of Scotese and Wright (2018) and the climate model simulations of Valdes et al. (2021). The yellow arrows describe dominant currents flowing in ocean from the Valanginian to Present-day and compared to the present-day active oceanic currents. Temperature gradients is shown in the transition colours from the reddish (warm) to bluish (cold).

